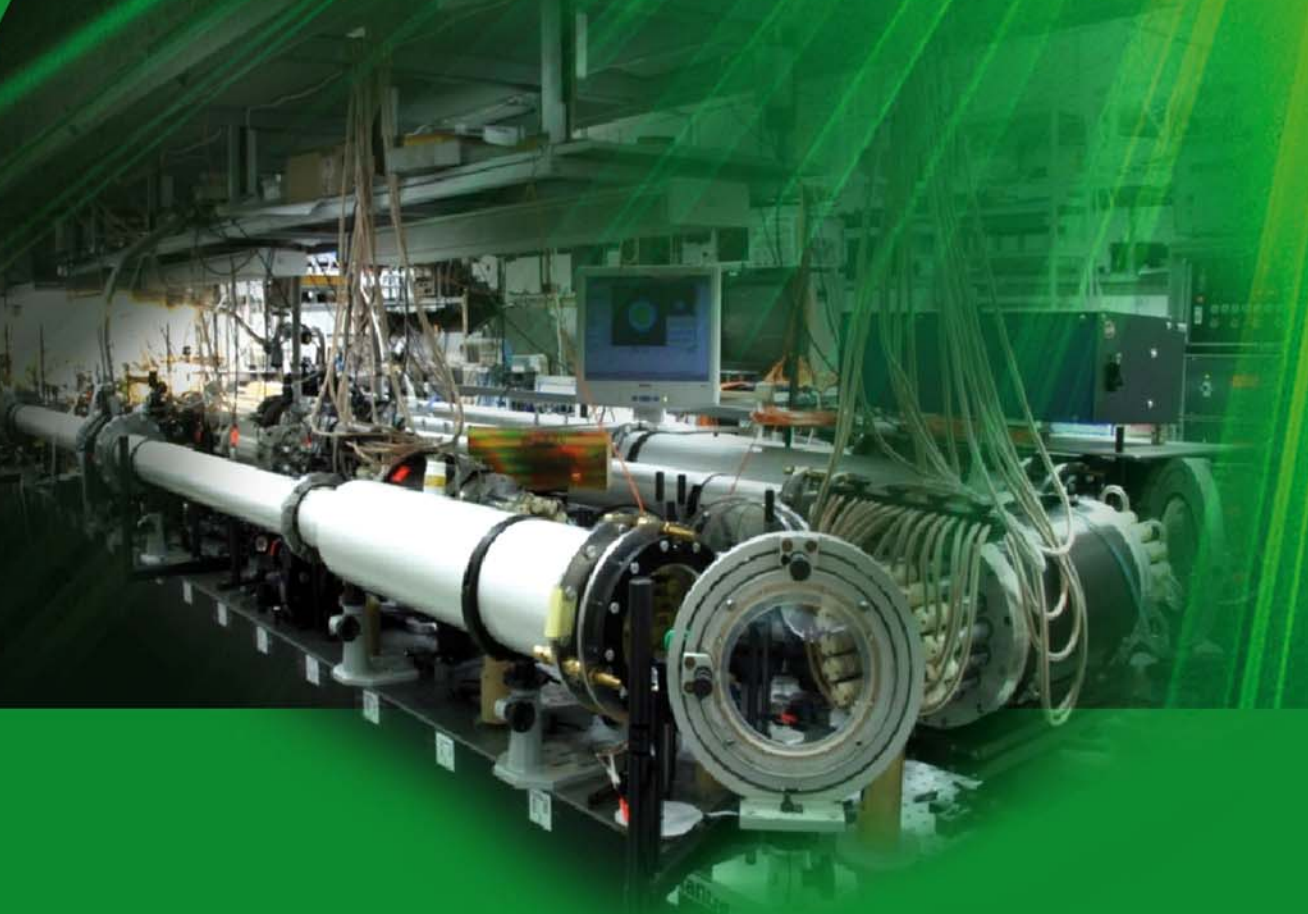




Exawatt Center for Extreme Light Studies (XCELS)





Exawatt Center for Extreme Light Studies (XCELS)

**Draft Application was prepared
by the Institute of Applied Physics RAS**

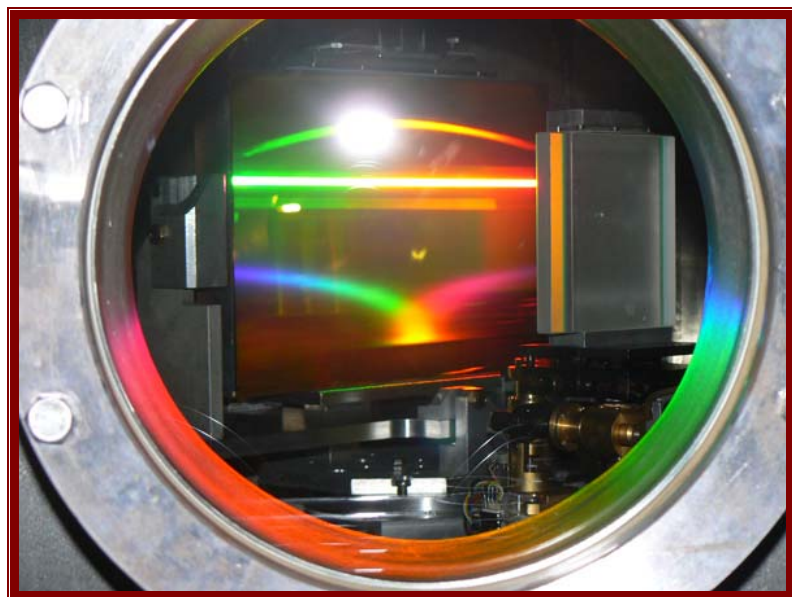


TABLE OF CONTENTS

1. Project Summary	5
Priority areas of research	5
Interest in the Project in other countries	6
Basic parameters of the XCELS infrastructure	8
Total Project budget and schedule of its implementation	11
2. XCELS: Why in Russia and why in Nizhny Novgorod	12
Major Russian scientific schools in the area of XCELS	12
Nizhny Novgorod and the Nizhny Novgorod Region – overview	14
The Nizhny Novgorod scientific-educational cluster	17
Institute of Applied Physics, the host of the XCELS Project	19
Experience of the Institute of Applied Physics in the field of the Project	23
Prospective XCELS sites	26
3. Technical Description of Project Infrastructure (Goal 1 of the Roadmap and Objectives to Achieve this Goal)	28
Objective 1. Creating two prototype 15 PW laser modules	28
Activity 1.1. Construction of the building (3000 m ²) and utilities	31
Activity 1.2. Creation of the common front end	31
<i>General scheme of the front end</i>	31
<i>Compact 200 J 527 nm Nd:glass laser for pumping final OPA</i>	33
<i>Parameters of final OPA</i>	35
Activity 1.3. Creation of the first 10 PW module prototype	37
<i>Design and creation of a pump laser</i>	37
<i>Development and fabrication of parametric amplifiers</i>	41
<i>Design and creation of a pulse compressor</i>	43
<i>Development and fabrication of devices for contrast enhancement</i>	46
<i>Design and creation of adaptive optics</i>	48
<i>Design and creation of control systems and diagnostics</i>	49
Activity 1.4. Creation of the second 10 PW module prototype	51
Activity 1.5. Phase locking of two modules	52
Activity 1.6. Enhancing module power up to 15 PW	54
Activity 1.7. Creation of electron accelerator with an energy up to 20 MeV based on a photocathode and microwave resonators	55
Activity 1.8. Creation of a prototype laser with 1 kHz pulse repetition rate	62
Activity 1.9. Establishing and equipping a laboratory for studying laser-matter interaction	63
Objective 2. Construction of buildings and utilities	64
Objective 3. Creation of 200 PW laser	65
Activity 3.1. Preparing documentation for 200 PW laser	65
Activity 3.2. Development of appropriate technologies	67
Activity 3.3. Creation of the common front end	68
Activity 3.4. Creation of twelve modules	68

Activity 3.5. Phase locking of twelve modules.....	71
Activities 3.6 and 3.7. Creation of the system for diagnostics and control of 200 PW laser.....	72
Activity 3.8. Transportation of twelve laser beams to the target chamber and to other laboratories.....	75
Objective 4. Creation of a complex of high-average-power femtosecond lasers for innovative applications	76
Activity 4.1. Developing the concept of a laser complex with high repetition rate	76
Activity 4.2. Development of production technology of diode lasers.....	79
Activity 4.3. Creating a laser with a pulse repetition rate of 10 Hz.....	81
Activity 4.4. Creating a laser pulse with a repetition rate of a few kHz	82
Activity 4.5. Transportation of laser beams to the main target chamber and to other laboratories.....	84
Objective 5. Creation of an electron source with 100 MeV energy based on a photocathode and microwave resonators	85
Objective 6. Creating the main target chamber	86
Objective 7. Establishing and equipping research laboratories	88
Objective 8. Radiation safety	89
Objective 9. Constructing a computer and communication center	93
Objective 10. Equipment of engineering and supporting workshops	94
Objective 11. Maintenance of the XCELS facility	95
References	96
4. Scientific Case & Innovative Research (Goals 2,3 and Objectives to Achieve these Goals)	98
Objective 1. Simulation of interaction of extreme light with matter and vacuum	99
Activity 1.1. Development of theoretical models of processes.....	99
Activity 1.2. Development and implementation of new computer codes	101
Objective 2. Carrying out experiments on laser-plasma acceleration of charged particles	106
Activity 2.1. Laser-plasma electron acceleration up to energies of 10-1000 GeV	106
Activity 2.2. Laser-plasma acceleration of ions to 1-10 GeV energy	111
Activity 2.3. Combined acceleration in linear and laser-plasma particle accelerators	119
Objective 3. Creating new sources of radiation in the hard X-ray and gamma-ray regions	121
Activity 3.1. Creating hard radiation sources with extremely high brightness.....	121
Activity 3.2. Creation of a compact free-electron laser and wigglers	128
Activity 3.3. Creating high-brightness narrow-band gamma-ray beams.....	130
Activity 3.4. Creating sources of electromagnetic pulses of attosecond and subattosecond duration	137
Activity 3.5. Use of sources for diagnostics of processes and structures with picometer spatial and subfemtosecond temporal resolution.....	144

Objective 4. Study of nonlinear properties of vacuum in extreme light fields	148
Activity 4.1. Study of the nonlinear optical properties of vacuum exposed to laser light with an intensity up to 10^{25} W/cm ²	148
Activity 4.2. Study of the phenomena of quantum electrodynamics in the presence of extremely strong laser fields, including processes of creating matter and antimatter by radiation	150
Activity 4.3. Study of the space-time structure of vacuum irradiated by X-rays and gamma-rays with intensity up to 10^{27} W/cm ²	155
Objective 5. Research on photonuclear physics	158
Activity 5.1. Development of diagnostic methods and tools of photonuclear physics	158
Activity 5.2. The study of intranuclear processes initiated by secondary sources of radiation	158
Activity 5.3. Studying methods for control of intranuclear processes and creation of exotic nuclear structures.....	159
Objective 6. Experimental simulation of astrophysical phenomena	160
Activity 6.1. Laboratory modeling of processes in the interiors of stars and planets	160
Activity 6.2. Laboratory modeling of gravitational effects.....	161
Activity 6.3. Laboratory modeling of early cosmological phenomena.....	164
Objective 7. Study of the feasibility of creating exawatt and zettawatt light sources	166
References	170
Innovative Research (Goal 3 and Objectives to Achieve this Goal)	173
5. Conclusion	174
6. Appendices	175
Appendix 1: Roadmap.....	175
Summary	175
Detailed Roadmap.....	176
List of Executors.....	185
Appendix 2: List of international organizations planning to participate in the mega-science project "Exawatt Center for Extreme Light Studies," and officials to address for negotiations	186
Appendix 3: Letters of Support.....	187
Appendix 4: Letters from the Ministry of Investment Policy of the Nizhny Novgorod Region and the Nizhny Novgorod State University.....	196
Appendix 5: Interview with the Chairman of the International Committee ICUIL Professor T. Tajima	200
Appendix 6: Agreement on the Establishment of the International Scientific Association (INR), "Extreme Light Fields: Sources and Applications" ELISA.....	202

1. Project Summary

The goal of the Project is establishing a large research infrastructure – the Exawatt Center for Extreme Light Studies (XCELS) using sources of laser radiation with giant (exawatt) peak power. The Project rests upon the considerable advance made in the recent years in Russia and worldwide on creating petawatt lasers (1 Petawatt = 10^{15} W) with intensity up to 10^{22} W/cm² and ultrashort pulse duration (< 100 femtoseconds = 10^{-13} s). The core of the planned infrastructure will be a new unique source of light having the power of about 0.2 Exawatt ($2 \cdot 10^{17}$ W) that exceeds the currently available ones by hundreds of times. The fundamental processes of such laser-matter interaction belong to an absolutely new branch of science that will be the principal research task of the infrastructure. There will open up opportunities for studying the space-time structure of vacuum and unknown phenomena at the interface of the high-energy physics and the physics of high fields. The envisaged applications of results of these studies will include among others development of compact charged-particle accelerators with sizes hundreds times less than the available ones, creation of sources of ultrashort pulses of hard X-ray and gamma radiation for diagnosing materials with unprecedented spatial and temporal resolution, elaboration of new sources of radiation and particles for clinical applications, and others.

Priority areas of research

The research program providing priority of XCELS functioning will include the following key areas:

1. Creation of sources of ultrashort coherent and incoherent radiation with record high brightness in the X-ray and gamma ranges based on radiation of ultrarelativistic charged particles moving in ultraintense laser fields, use of these sources for diagnosing processes and structures with picometer spatial and subfemtosecond temporal resolution.
2. Development of multicascade compact laser electron accelerators with energies above 100 GeV, use of the laser-plasma acceleration principles for developing advanced accelerator complexes with particle energies of 1-10 TeV.
3. Elaboration of compact laser ion accelerators with energies of 0.1-10 GeV and development of their applications in radiography and medicine.

4. Production and investigation of extreme states of matter arising under the action of ultrarelativistic laser fields; modeling of astrophysical and early cosmological phenomena in laboratory conditions.

5. Creation of sources of electromagnetic waves of attosecond (10^{-18} s) and subattosecond duration based on the generation of high harmonics of laser radiation and supercontinuum in a hyperwide spectral range in the course of the nonlinear interaction of powerful femtosecond laser pulses with matter, development of methods for application of such sources in the fundamental metrology and diagnostics of fast processes in matter.

6. Creation of a source of electromagnetic radiation with peak power over 1 Exawatt (10^{18} W) on the basis of the interaction of multipetawatt laser pulses with plasma in ultrarelativistic regime.

7. Study of the space-time structure of vacuum probed by radiation with intensity exceeding 10^{25} W/cm², investigation of the phenomena of quantum electrodynamics in the presence of ultraintense laser fields, including producing of matter and antimatter by means of radiation.

8. Research into a new field of science – nuclear optics – based on the use of secondary sources of gamma radiation for excitation and diagnostics of intranuclear processes.

The above program of priority research points to XCELS multifunctionality. A considerable amount of research will be carried out at the junction with other areas of knowledge – high energy physics, nuclear physics, astrophysics, and biomedicine.

Interest in the Project in other countries

XCELS's radiation source characteristics will essentially surpass the level of the most powerful available or projected laser facilities in the world, including the most advanced ones within the framework of the European infrastructure mega-project ELI (Extreme Light Infrastructure). Therefore, XCELS will naturally attract a worldwide interest in the research community by providing opportunities for international collaboration in a wide range of modern sciences and applications.

To date, the interest in participating in the creation and exploitation of XCELS was expressed by the Ministry of Education and Science of France, the Commissariat of Atomic Energy of France, the Nuclear Energy Agency of Japan, the European Centre for Nuclear Research, CERN, Los Alamos National Laboratory (USA), Fermi National Accelerator Laboratory (USA), High Energy Accelerator Research Organization KEK (Japan), Rutherford Appleton Laboratory (UK), The John Adams Institute for Accelerator

Science (UK), Center for Antiproton and Ion Research FAIR (Germany), National Research Institute of Canada. It is supposed that the main contribution of foreign partners will be supply of high-tech research equipment for the laser complex and research laboratories, totaling about 15% of the Project cost.

Currently, the most important foreign contributions to the development of the XCELS Project are made by France. In 2009, Russia and France signed the international agreement on the development of research on extreme laser fields ELISA which stimulated development of the XCELS Project. In 2011, the Ministry of Education and Science of France organized the new international institute IZEST (International Institute for Zettawatt-Exawatt Science and Technology) to provide scientific and scientific-organizational support of projects aimed at developing exawatt power lasers and their applications. XCELS is regarded by this institute as a major research project that will play a decisive role in the development of the corresponding field of knowledge in the next decade. This initiative has been supported (see the letters of support in Appendix 3) by the largest research laboratories wishing to collaborate with IZEST and XCELS.

Negotiations on cooperation under the XCELS Project are initiated with the heads of the European infrastructure project ELI and representatives of the European Commission. The ELI project, which aims at creating and using sources of extreme light fields has successfully completed the preparatory phase, in which 13 European states participated. By the results of the preparatory phase, the European Commission made a decision to build in 2011-2016 three new laser centers with sources having power of about 10 PW in Hungary, the Czech Republic and Romania with the cost of construction of each of about 280 million euros. The facility that will be built in Hungary is intended for research on the generation and use of attosecond pulses. The facility constructed in the Czech Republic will be used to develop laser-plasma accelerators and new sources of X-ray and gamma radiation. In Romania, the facility will be intended for conducting research in the field of photonuclear physics. XCELS will naturally be of interest for international cooperation with the ELI consortium on extreme laser fields, as it will have a laser source of the next generation and a research program using fields that are not available in other research centers.

Of essential importance is the support of the XCELS Project by Prof. Gerard Mourou, the initiator and head of the preparatory phase of the European ELI project and IZEST Director (France). In 2009, on the suggestion of G. Mourou, Yu.S. Osipov, President of the Russian Academy of Sciences, appealed to President D.A. Medvedev with a request to consider the proposal on full-scale participation of Russia in the international program of

extreme laser field research. The proposal was reviewed and forwarded by the Presidential Administration for approval to several ministries, including the Russian Ministry of Education and Science, which supported the proposal in general and expressed the opinion that such a participation would be preferable if a new center is constructed on the territory of our country as a subject of international cooperation in the area of extreme light fields after solving a number of issues of legal international law.

The XCELS Project is also supported by the leading international organization on the creation and use of ultra intense lasers ICUIL (International Committee on Ultra Intense Lasers), which coordinates the activities of the major laser labs around the world. The letter of support of XCELS by the ICUIL chair Prof. T. Tajima and his interview are presented in Appendix 5.

Basic parameters of the XCELS infrastructure

The subexawatt laser significantly exceeding the level of radiation power inherent in the most powerful available, constructed or Projected laser systems worldwide, will be based on the technique of optical parametric chirped pulse amplification (OPCPA) to the petawatt power developed at the Institute of Applied Physics RAS. The complex will comprise 12 identical channels, each of which will generate a pulse with the energy of 300-400 J, duration of 20-30 fs, maximum intensity at focusing more than 10^{23} W/cm² (Fig. 1.1). The channels operate by the scheme of parametric amplification in KD*P crystals with the aperture of final cascades of 30×30 cm².

It is supposed that optical pulses in laser modules of the subexawatt complex will be phased to an accuracy of hundredths fractions of a light wave period (10^{-16} s). The first phase of the Project will be creation at IAP RAS of two such modules with the power of 15 PW each based on parametric amplification in KD*P crystals. This will not only allow creating a reliable prototype of an XCELS module, but will also enable solving fundamental problems associated with phasing of channels, as well as completing diagnostic equipment for applications. In addition, final corrections will be made in the architecture and component base of the XCELS facility. Further, 12 channels of the main XCELS laser complex will be assembled by the proven technology in a newly constructed building of the international center.

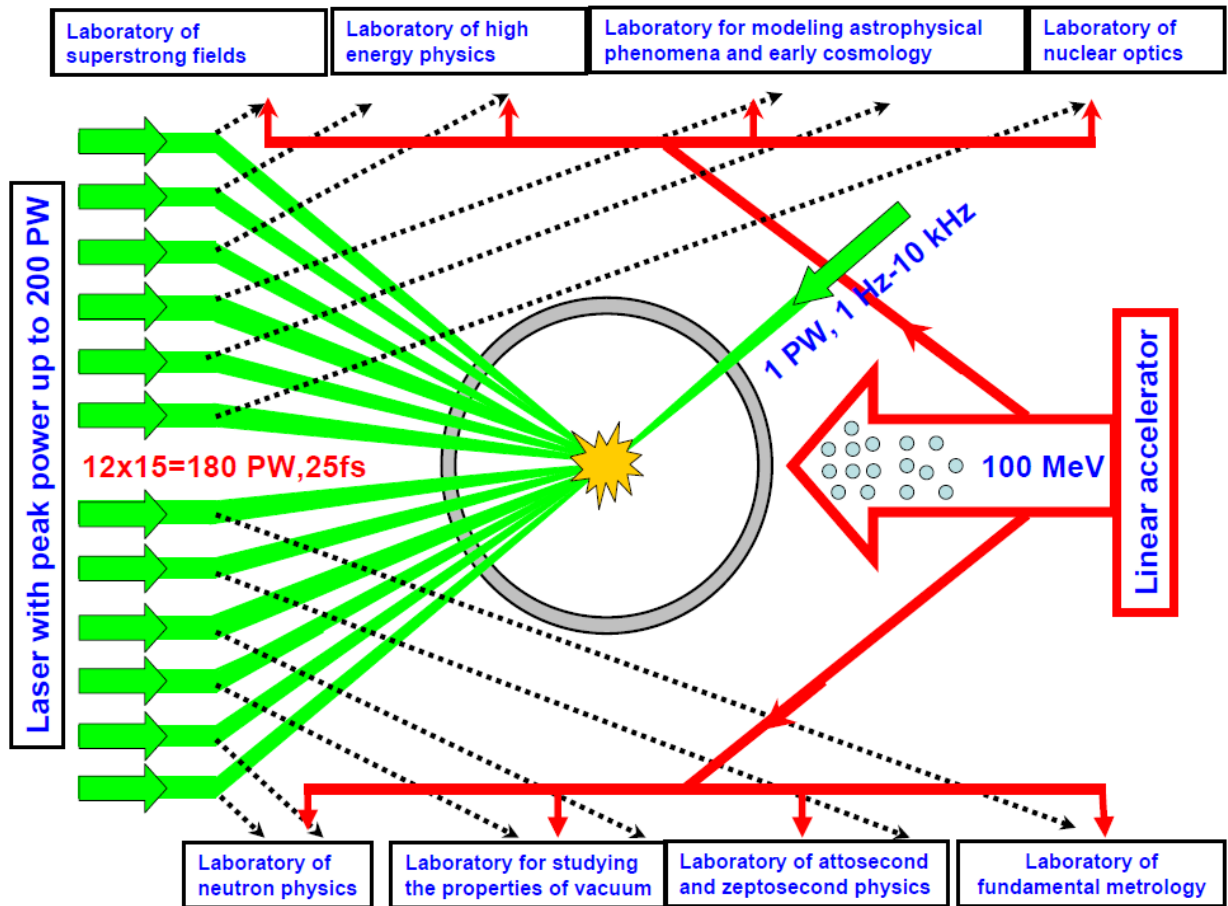


Fig. 1.1. General layout of subexawatt laser channels, the main target chamber, linear accelerator, and research laboratories

The resulting radiation at the output of the laser complex will have the following parameters: power 200 PW, pulse duration 25 fs, wavelength 910 nm, divergence not more than 3 diffraction limits.

Along with the subexawatt laser XCELS will house a 100 MeV linear accelerator of electrons and unique laboratories for experiments on the physics of strong fields, high-energy physics, laboratory astrophysics and cosmology, nuclear optics, neutron physics, laboratories for studying the properties of vacuum, attosecond and zeptosecond physics, and fundamental metrology. XCELS will also comprise a powerful center for data processing and computer modeling of the interactions of extreme light fields.

XCELS will be a unique research center of international level both in terms of the radiation source parameters and the planned research program. The period of superiority over the existing facilities and the ones constructed outside Russia intended for studies of extreme light fields will begin with the launch of the first laser prototype with the power level of 10 PW (2014) and will continue with the rise in the laser complex power (2018). The future superiority will be ensured by creation of a source of electromagnetic radiation with peak power exceeding 1 Exawatt on the basis of the interaction of multipetawatt laser

pulses with plasma in the ultrarelativistic regime (2020). The superiority of the collective program of experimental studies will be maintained from the beginning of the first experiments on the two-channel prototype (2015) and far-reaching.



Fig. 1.2. Prospective view of XCELS

From the point of view of the proposed research program, level of technological requirements to the unique laser complex, required qualification of the scientific and technical personnel, the most appropriate base for XCELS in the Russian Federation is the Institute of Applied Physics of the Russian Academy of Sciences in Nizhny Novgorod. XCELS construction and exploitation will involve collaborative efforts of a large team of Russian research and educational centers, including the Institute of Applied Physics RAS (IAP RAS), Institute on Laser and Information Technologies RAS (ILIT RAS), Russian Research Center (RRC) "Kurchatov Institute", Joint Institute for Nuclear Research (JINR), P.N.Lebedev Physics Institute RAS (LPI RAS), General Physics Institute RAS (GPI RAS), Budker Institute of Nuclear Physics (BINP), Joint Institute for High Temperatures RAS (JIHT RAS), Institute of Laser Physics of the Siberian Branch of RAS (ILP SB RAS), Russian Federal Nuclear Center (RFNC-VNIIEF), Moscow State University (MSU), National Research Nuclear University MEPhI (MEPhI), University of Nizhny Novgorod (UNN), and others.

In addition to the main base, the XCELS complex will include satellite laboratories engaged in elaborating and finalizing different critical technologies of the subexawatt laser and in developing some applications of results of the basic research obtained in XCELS. These laboratories may be organized, in the first place, in ILIT RAS, RRC "Kurchatov Institute", and MEPhI.

The average number of XCELS employees is about 300 persons, including 100 full-time engineering and technical personnel and administrative staff, 100 full-time Russian scientists, and 100 visiting Russian and foreign specialists.

Total Project budget and schedule of its implementation

The preliminary cost of the center is estimated to be 40.3 billion rubles, including 32.2 billion rubles from the state budget, 6.1 billion rubles from foreign partners, and 2 billion rubles of extra-budgetary funds from domestic sources.

Estimated annual state budget distribution

year	2012	2013	2014	2015	2016	2017	2018	2019	2020	2021
billion rubles	2.1	3.3	3.3	5.4	7.5	5.8	2.4	0.8	0.8	0.8

Detailed allocation of funds for Project tasks is presented in the Project Roadmap.

2. XCELS: Why in Russia and why in Nizhny Novgorod

Besides the essential budget investments, the feasibility of the XCELS Project in Russia is substantiated by the presence of world-renowned scientific schools and the availability of highly qualified researchers and engineers in the area of the Project.

Major Russian scientific schools in the area of XCELS

Russia has world-renowned scientific schools in the main areas of XCELS research, i.e. in the fields of laser physics, interactions of powerful electromagnetic radiation with matter, high-sensitivity optical measurements, and theoretical physics. These schools work in the major Russian academic institutions and universities.

Three scientific schools in the General Physics Institute are closely connected with the work of the prominent scientists, Nobel Prize winners Academicians A.M.Prokhorov and N.G. Basov. These are:

- «The physics of coherent laser-matter interaction, methods of controlling spatial, temporal and spectral characteristics of laser radiation" under the supervision of the Corresponding Member of RAS Pavel Pashinin.
- «The physics and technology of crystals and nanocrystalline materials for photonics," Supervisor – Academician Vyacheslav Osiko.
- «New effective optical materials and components for the near and middle infrared spectral ranges," Supervisor – Corresponding Member of RAS Ivan Shcherbakov.



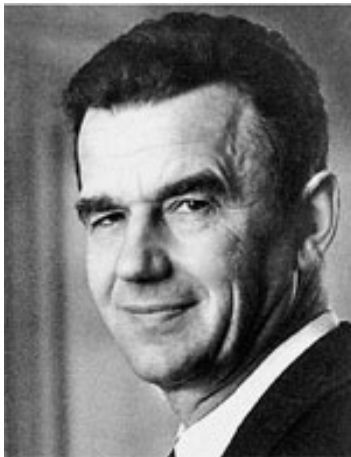
Alexander M. Prokhorov



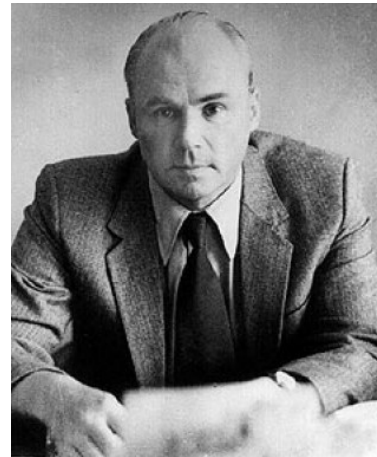
Nikolay G. Basov

At the P.N. Lebedev Physics Institute there are the scientific schools in theoretical physics headed by Academician Leonid Keldysh, in quantum radiophysics headed by Academician Oleg Krokhin, and in the theory of fundamental interactions supervised by the Corresponding Member of RAS Vladimir Ritus.

The school at the Moscow State University was formed by the outstanding Soviet scientists Academician Rem Khokhlov and Professor Sergey Akhmanov, founders of nonlinear optics. Currently, this school has the name “Femtosecond nonlinear and quantum optics” and is headed by Professor Vladimir A. Makarov.



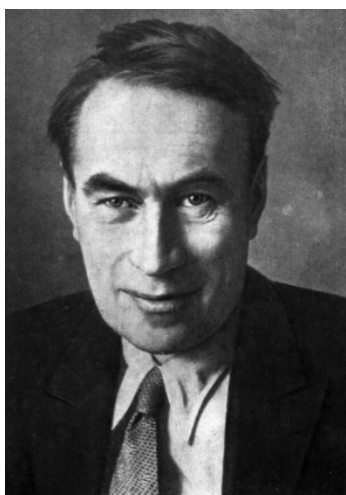
Rem V. Khokhlov



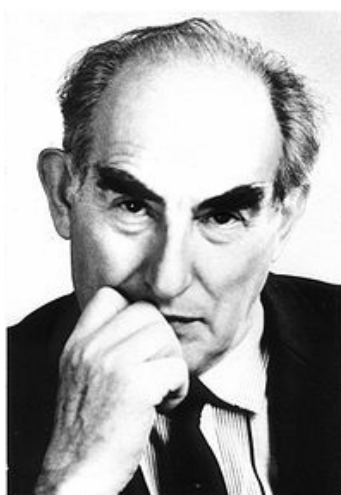
Sergey A. Akhmanov

The Institute of Applied Physics has three scientific schools, which owe their origin to the founders of the Nizhny Novgorod radio physics Academician Alexander Andronov, Nobel Prize winner Academician Vitaly Ginzburg and Academician Andrey Gaponov-Grekhov. These are:

- “The interaction of intense electromagnetic radiation with plasma” headed by Academician Alexander Litvak.
- “Femtosecond optics, nonlinear dynamics of optical systems and high-sensitivity optical measurements” supervised by the Corresponding Member of RAS Alexander Sergeev.
- “Ultraintense light fields and their interaction with matter, large aperture nonlinear optical crystals, lasers with high average and peak power, parametric conversion of laser radiation” founded by Prof. Victor Bepalov and Prof. Gennady Freidman.



Alexander A. Andronov



Vitaly L. Ginzburg



Andrey V. Gaponov-Grekhov

The Joint Institute for High Temperatures (JIHT) has the school “Investigation of the properties of condensed matter and plasma under extreme conditions at high energy densities” under the supervision of Academician Vladimir Fortov.

At the Institute of Laser Physics SB RAS there is a school in the area of XCELS that is called “Ultrahigh resolution laser spectroscopy and its applications” that is headed by Academician Sergey Bagaev.

The National Nuclear Research University MEPhI has the school “Basic problems of the behavior of quantum systems in radiation fields” supervised by Prof. Nikolay Narozhny.

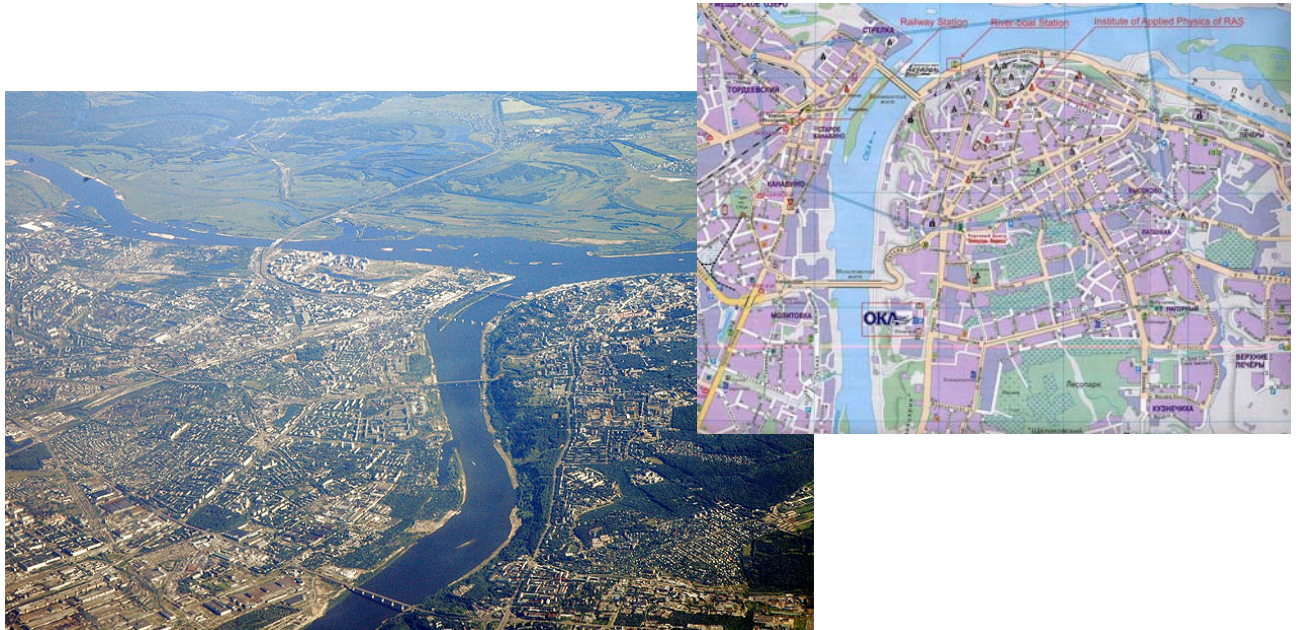
Nizhny Novgorod and the Nizhny Novgorod Region – overview



Why is Nizhny Novgorod a natural choice for the XCELS site?

Nizhny Novgorod is one of the biggest industrial, scientific, educational and cultural centers in Russia. It was founded in 1221 and recently regained its original name, having been renamed Gorky in 1932 in honor of the celebrated author Maxim Gorky, who was born in Nizhny Novgorod. Nizhny Novgorod is situated in the central European part of Russia, about 400 km east of Moscow, at the confluence of the Volga and the Oka rivers. The City has advantageous geographical location for economic and social development.

It covers an area of 41.1 thousands hectares, its population is 1370.2 thousand people, average age of inhabitants being 36.



Nizhny Novgorod is a beautiful historical and cultural center. The image of the city has preserved the multitude of historic and cultural layers that gave ground to UNESCO to include Nizhny Novgorod in the list of 100 cities constituting world historical and cultural value.



Brilliant examples of old Russian architecture are the Nizhny Novgorod Kremlin that has been preserved since the early 16-th century, the architectural ensemble of the Nizhny Novgorod Trade Fair that became a subcenter of the city in the 19th century, making the trade fair one of the biggest in Russia and Europe, and numerous churches and monasteries, more than 600 unique historic, architectural and cultural monuments.

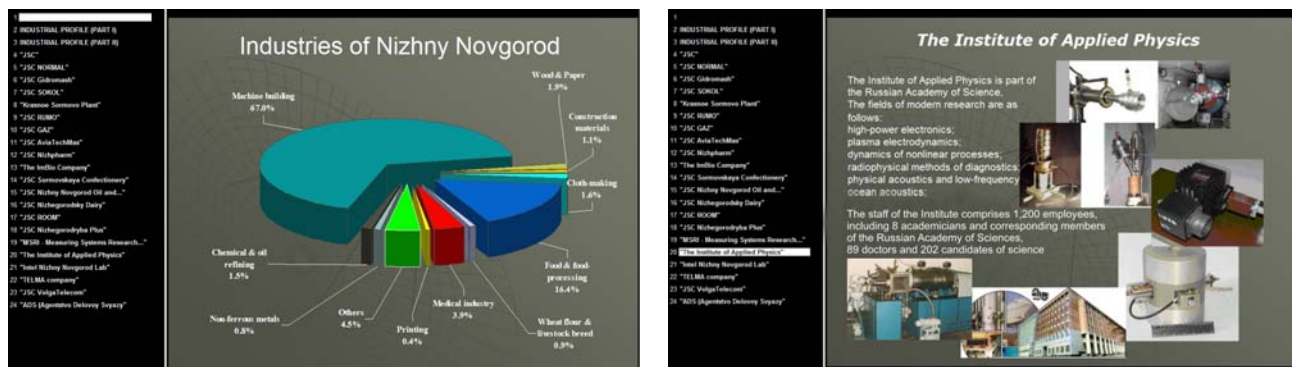
There are about 200 culture and art institutions in Nizhny Novgorod, including 8 theatres, 5 concert halls, 97 libraries, 17 cinema theaters, 25 institutions of children optional education, 16 museums, 7 beautiful parks. One of the biggest concert organizations in Russia is the Nizhny Novgorod State Academic Philharmonic Society established in 1937, now named after Mstislav Rostropovich.

The advantageous geographical location and a traditional role of Nizhny Novgorod as a trade center gave premises for creation of a comparatively high-developed transport infrastructure. Railways, motor roads, water- and airways conveniently connect Nizhny Novgorod with any Russian region, the CIS and foreign states.

The Nizhny Novgorod transport junction, which includes the international airport "Nizhny Novgorod", the railway station, and a river port is one of the most visited in Russia. Rivers and channels connect Nizhny Novgorod with 5 seas and afterwards provide an exit into the ports of the Scandinavian countries, the Eastern Europe, Africa and Asia.

Nizhny Novgorod belongs to the five most populated and industrially developed cities of Russia, is a center of the Nizhny Novgorod region and a recognized capital of the Volga economic region. It is a big business and industrial center. Business rhythm and search for new technologies guarantee its economic success in the third millennium.

Industry occupies a significant place in the City's structure. The principal branches are motor car construction, radio electronics, ship-building, atomic energy industry, metal-working industry, ferrous and non-ferrous metallurgy, wood manufacturing, food and light, medical and printing industries. Many achievements of Nizhny Novgorod have worldwide fame: the world's first commercial fast-breeder reactor, radars of the fifth generation, the world leadership in designing hydrofoils and surface effect vehicles, and others.



The advance in industries has become possible thanks to the well developed system of education.

The Nizhny Novgorod scientific-educational cluster

The Nizhny Novgorod region has all necessary conditions for effective development of scientific-educational complex and innovations.

The system of science and education comprises both fundamental and applied sciences. There are about 100 R&D facilities in the Nizhny Novgorod region, including 10 branches of federal ministries and agencies and institutes of the Russian Academy of Sciences, the Russian Federal Nuclear Center (Sarov), 18 specialized R&D institutes, 24 design, technological and survey companies, over 20 industrial companies. The number of researchers per 10 000 population in the Nizhny Novgorod region exceeds the Russian average by 4 times.

The developed defense complex, engineering industry, including aircraft manufacturing and ship-building), radio electronics, nuclear physics and power engineering, medicine, science of materials form the basis of the technological foundation of scientific and educational complex of the region.

The educational policy is based on the strategic goal to pursue innovative development and broad collaboration with national and international partners.

A strong educational system of Nizhny Novgorod provides education to 300,000 school students and 247,000 college and university students every year. Nizhny Novgorod universities are among leaders in Russia and get top positions in the rating of the Russian Ministry of Education and Science.

The number of higher educational institutions of the Nizhny Novgorod region (concentrated in Nizhny Novgorod), including branches of other universities exceeds fifty. They train tens of thousands of students, with about 5000 professors and teachers. Leading universities of the city are among the best universities of Russia. These are the Nizhny Novgorod State University, the Nizhny Novgorod State Medical Academy and the Nizhny Novgorod Linguistic University. Also worth mentioning are the State Technical University of Nizhny Novgorod and the State University Higher School of Economics.

International educational programs are continuously developing. These include the Russian-French, Russian-Italian and Russian-Danish public universities, the International Institute of Economics, Law and Management established as a result of collaborative effort of Nizhny Novgorod and European universities.

Fundamental studies are focused mainly at the academic institutes and at the Nizhny Novgorod State University. The first Radiophysics Department in the USSR was opened at UNN after World War II, and in the early 1960s the country's first department of computational mathematics and cybernetics. It is here that early research on the subject of

the Project – quantum electronics, laser physics, plasma physics, mathematical modeling of physical processes, parallel computing was conducted.

Six institutes of the Russian Academy of Sciences work in Nizhny Novgorod. These include

- Institute of Applied Physics
- Institute for Physics of Microstructures
- Institute of Chemistry of High-Purity Substances
- Institute of Organometallic Chemistry
- Nizhny Novgorod Branch of Mechanical Engineering Institute
- Nizhny Novgorod Department of the Institute of Sociology

In 2009 the Nizhny Novgorod institutes of the Russian Academy of Sciences formed the Nizhny Novgorod Scientific Center (NNSC) that is headed by Academician Alexander Litvak.



Council of the Nizhny Novgorod Scientific Center at the general meeting in 2009

The Center was established to coordinate the work of the academic institutes in the Nizhny Novgorod region, especially in interdisciplinary research, and organization of their interaction with applied research industry, industrial enterprises and regional universities. The major task of the center is also solution of infrastructural and social problems of academic science in the region, including provision of the institutes with up-to-date information and supercomputer technologies. Among the goals of the Center is interaction with local authorities, particularly aiming at their assistance in implementation of Projects in the interests of the region.

The Institute of Applied Physics is acknowledged leader of the academic science in Nizhny Novgorod.



Building of the Institute of Applied Physics

Institute of Applied Physics, the host of the XCELS Project

IAP RAS began independent activities in April 1977. The Institute was created on the basis of several divisions of the Radio Physical Research Institute of the Ministry of Higher Education of the Russian Federation. For a quarter of a century it was headed by Academician Andrey V. Gaponov-Grekhov. In 2003 Alexander G. Litvak was appointed director of the Institute and A.V. Gaponov-Grekhov became the research supervisor of IAP RAS.

IAP RAS is one of the largest and most successful institutions of the Russian Academy of Sciences. Scientific studies are provided by about 1,200 employees, about 490 of whom are scientists, including 8 academicians and corresponding members of RAS, 89 doctors and 202 candidates of science. About one third of the scientists are young people aging less than 35.

IAP RAS was conceived and created as a multipurpose institution combining fundamental and applied research in the field of plasma physics, high-power electronics, geophysics, and laser physics. The common oscillation-wave problems combining these research lines, the strong scientific foundation for applied studies, tight connections between science and the higher-education system, and high criteria for training young researchers are the main components in the model of a large academic institution implemented at IAP RAS.

Over thirty years this model proved its viability: it worked even in the nineties, which were hard times for Russian science, and its fundamental principles are, as previously, valid and important.

At present, research at IAP RAS is concentrated in three main scientific divisions: the Plasma Physics and High-Power Electronics Division, the Hydrophysics and Hydroacoustic Division, and the Nonlinear Dynamics and Optics Division.



IAP RAS structure

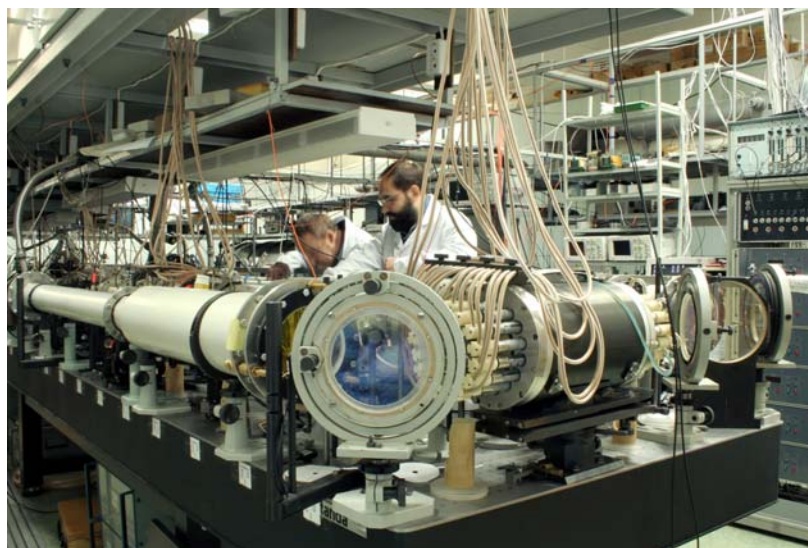
The main lines of IAP RAS research include:

- **high power electronics** (gyrotrons and their applications, relativistic electronics, microwave processing of materials),
- **plasma electrodynamics** (powerful radiation interaction with plasma, plasma astrophysics, geophysical electrodynamics),
- **radiophysical methods of diagnostics** (plasma diagnostics, millimeter and submillimeter radioastronomy, remote diagnostics of natural media, coherent seismoacoustics, vibroacoustics and spectroscopy, nonlinear acoustics, optical tomography),
- **low-frequency ocean acoustics** (long-range sound propagation in the ocean, acoustic tomography of the ocean, low-frequency radiating complexes, hardware for underwater acoustics),
- **dynamics of nonlinear processes** (nonlinear waves, dynamic chaos and structures, internal and surface waves),
- **laser physics and nonlinear optics** (femtosecond lasers and superstrong fields, processes in phase conjugation systems, laser dynamics, water-soluble crystals, biophotonics).

IAP RAS carries out over 350 scientific researches along the main directions of IAP activities annually, takes an active part in implementation of federal special, academic, interdepartmental, international and other programs and Projects.

The most prominent recent achievements of IAP RAS:

- Creation of unique gyrotron complexes for processing and creation of materials with new properties and powerful gyrotrons of the next generation for the International Thermonuclear Reactor (ITER).
- Development of the unique technology of plasma chemical deposition of diamond films from gas phase, which allows significant increase of the growth rate of diamond discs of high optical and mechanical quality.
- Development of high-rate growth and precision processing of water-soluble crystals.
- Development of the technique of optical coherence tomography for imaging internal biotissue structures and designing the corresponding devices that opened up new opportunities for nanobiophotonics and medical diagnosis, including diagnosis of cancer.
- Creation of the petawatt parametric laser complex (PEARL) that is one of most powerful laser facilities in the world; its architecture based on the technique of optical parametric amplification has been proved to be most promising for extension into the multipetawatt range.



- Creation of a multiterawatt Ti-sapphire laser complex and its use in experiments on acceleration of wake wave electrons, generation of coherent soft X-radiation, and atmospheric discharge initiation by femtosecond radiation in filamentation regime.

IAP RAS has its own pilot production equipped with modern facilities. The main task of the pilot production is timely and high-quality execution of the tasks set by the Institute's scientific divisions. The Institute possesses high-power experimental capability and modern diagnostic techniques.

A number of innovative enterprises have been established at IAP RAS. Their main task is bringing research results to operating models and prototypes and production of high-tech devices and equipment.

The IAP RAS researchers have numerous awards, including the Lenin Prize (1988) and fourteen State Prizes (1980, 1983, 1984, 1985, 1987, 1991, 1997, 1999, 2000, 2003), the Russian Federation State Prize for Young Scientists (2003), a number of RAS medals, the Medal of the European Geophysical Society, K.J. Button Medal, W. Lamb Medal, Prize of the International Thermonuclear Fusion Society, and others.

IAP RAS has wide international scientific relations. Its employees participate in major international scientific and technical programs and international projects under CRDF, NATO, ISTC, and others. Annually, about 150 employees go abroad for international scientific conferences, meetings, and sessions of different committees and societies, and approximately the same number of foreign scientists visit the Institute.



International contacts worldwide

In 2011, the institute carried out works under more than 25 international projects and grants, among which are the Projects under the international programs ITER, HiPER, LIGO, and in collaboration with big international labs like CERN, DESY, KEK and others.

Experience of the Institute of Applied Physics in the field of the Project

Confidence in the feasibility of the Project to create a subexawatt laser is based on high scientific and technological level of IAP and its collaborators. Currently, OPCPA is the only amplification technique provided by the available component base that allows IAP to be the world leader in the exploration and development of OPCPA. In 2007, this institute in collaboration with the Russian Federal Nuclear Center-VNIIEF launched the laser "PEARL" with a pulse power of 0.56 PW, pulse duration about 45 fs and energy 25 J, which is one of the most powerful lasers in the world. This laser uses parametric amplification in the KD*P crystal with the aperture of $10 \times 10 \text{ cm}^2$ which was grown at IAP RAS by the original technology of oriented high-rate crystal growth.

Construction of the laser complex "PEARL-10" with a pulse power of more than 5 PW (Fig. 2.1) was started in 2009 and is advancing successfully. Clean room with untied recessed footing with an area of 200 m^2 and special means of radiation protection from damaging factors that accompany the interaction of high-power light with matter was prepared. Optical equipment is currently installed. The first phase of the XCELS Project – the creation of two modules with the power of 15 PW – will be a natural continuation of these works that are to be completed in 2016. Further work on creation of a subexawatt laser will be associated with replication of laser channels (12 channels) and assembly of a single complex in the XCELS building.



Fig. 2.1. "PEARL-10" laser complex under construction in IAP RAS:
pump laser for parametric amplifier (left)
front end and optical compressor 110 cm in diameter and 500 cm long (right)

Another important factor for Project success is availability at IAP RAS of the unique technology of high-rate growth of nonlinear optical KDP and KD*P crystals that are key elements of the superintense parametric light amplifiers. This technology is based on the method of high-rate growth of profiled monosector crystals. It was the result of scientific research carried out at IAP RAS for several decades. This technique allows producing

optical elements with an aperture of $40 \times 40 \text{ cm}^2$ and, which is important for a unique installation containing dozens of nonlinear optical crystals, reducing the growth time by almost an order of magnitude as compared to the classical method and minimizing the waste of the crystal during processing.

IAP RAS has production capacity necessary for production of nonlinear optical components of laser systems for the XCELS Project (Fig. 2.2). It has a crystal samples machining line, including unique diamond micromilling machines and devices for controlling monocrystal billets and roughness parameters of machined surfaces with nanometer precision.



Fig. 2.2. Installations for growing large-aperture nonlinear optical crystals in IAP RAS (left) and element for frequency conversion of superintense optical radiation

For creation in the XCELS complex of channels with peak power of 15 PW, Nd-glass laser pump systems with pulse energy exceeding 1 kJ and pulse duration of about 2 ns are required. RFNC-VNIIEF has a rich experience in creating and operating such systems. VNIIEF has the laser facility "LUCH" with 4 channels of pulse energy in each channel of more than 3 kJ and duration of about 3 ns. The "LUCH" facility was used in the joint Project of VNIIEF and IAP RAS to produce pulses with energies of about 100 J in the parametric amplifier "FEMTA". This result is a world record in the power of parametric amplification of femtosecond pulses and a demonstration of one of the technologies critical for implementation of the XCELS Project (Fig. 2.3).

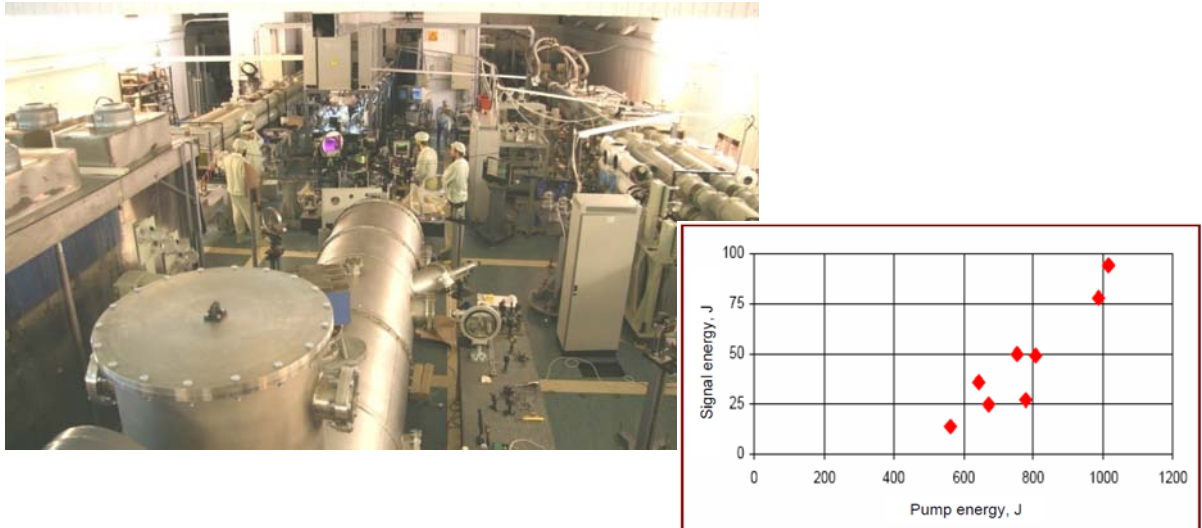


Fig. 2.3. "LUCH" facility with parametric amplifier "FEMTA" at VNIIEF (Sarov) and record characteristics of parametric amplification of femtosecond pulses

Experimental studies of fundamental scientific problems and new applications that will be implemented in XCELS are also based on solid scientific and technological reserve available to scientists in our country. For example, based on the petawatt laser "PEARL" an installation for studying laser-plasma acceleration of electrons in the interaction of powerful optical radiation with gas targets was elaborated in IAP RAS. Accelerating fields over 1 GeV/cm were produced and acceleration of electron bunches with energies up to 300 MeV, spectral width of about 10 MeV, charge of 200 pC, and angular spread of about 2 mrad was demonstrated, which is among the world's best results in laser-plasma acceleration of charged particles. These results were obtained using exclusively domestic experimental and diagnostic base (Fig. 2.4).

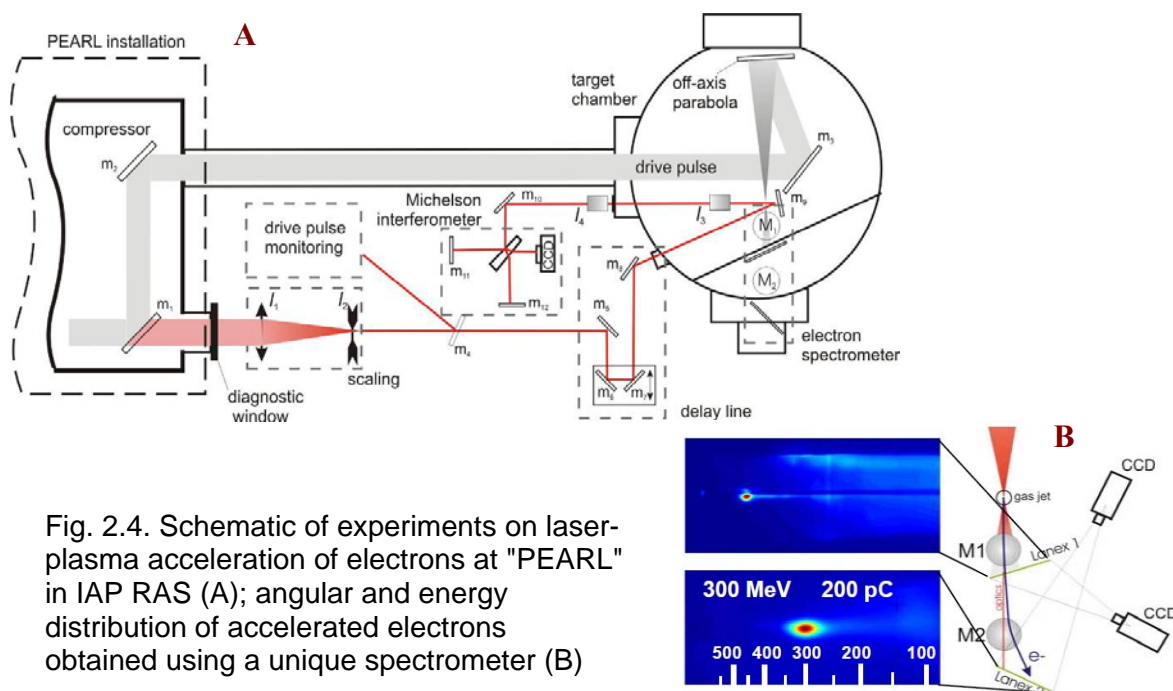


Fig. 2.4. Schematic of experiments on laser-plasma acceleration of electrons at "PEARL" in IAP RAS (A); angular and energy distribution of accelerated electrons obtained using a unique spectrometer (B)

Prospective XCELS sites

To accommodate XCELS, ground area of about 5 hectares, rather far from highways and industrial plants is required. The total area of the laboratory, administrative and ancillary facilities will be about 25 000 m², about 15 000 m² of which must have different degrees of radiation protection.

Offers of land were obtained from the Administration of Nizhny Novgorod and Nizhny Novgorod State University (see Appendix 4). Three possible XCELS locations (plots 1-3) and plot 4 owned by IAP RAS for construction of the prototype of 200 PW laser are shown in Fig. 2.5. The site for XCELS will be selected on the basis of the international Project expertise.

Prospective ground areas for XCELS construction



- 1 A plot of land offered by the Administration of the Nizhny Novgorod Region (federal property)
- 2 A plot of land offered by the Administration of the Nizhny Novgorod Region (municipal property)
- 3 A plot of land offered by the Nizhny Novgorod State University (federal property)
- 4 A plot of land to host the prototype offered by IAP RAS (federal property)

Fig. 2.5.

3 Technical Description of Project Infrastructure (Goal 1 of the Roadmap and Objectives to Achieve this Goal)

The first goal of the Project is to establish an infrastructure that will include buildings, engineering services, two prototype 15 PW laser modules, a 200 PW laser system, a high-average-power femtosecond laser facility for innovative applications, an electron source with energies of 100 MeV based on a photocathode and microwave resonators, a main target chamber, experimental laboratories, a computer and communication center, as well as engineering and supporting services. In order to fully achieve the goals set forth in this Project, it is required not only to establish this infrastructure, but also to efficiently maintain its operation, so the structure of **Goal 1** includes activities which have technical, administrative, and human resource orientation, as well as activities to ensure radiation protection of personnel.

11 objectives will be pursued to achieve **Goal 1**. See also the Project roadmap in Appendix 1.

Objective 1. Creating two prototypes of 15 PW laser modules

The key element of the XCELS Project is a laser complex with output power of 200 PW (0.2 Exawatt) , which will consist of 12 identical modules with optical pulses phased up to an accuracy better than the period of the light wave. In this regard, the first objective is to create two prototypes of such modules and to phase lock them. The prototype will be based on the technology of optical parametric amplification which has been successfully used at IAP RAS, but the power of a single laser module will be more than one order of magnitude higher than that achieved to date in Russia and worldwide. Consequently the creation and testing of the prototype prior to construction of all 12 modules is essential. In addition, despite the large number of theoretical and experimental works on phase locking laser modules, we are still unaware of any results on phase locking of pulses with enormous energy (hundreds of J) and/or pulse duration of the order of ten periods of the laser field. This is due, in our opinion, to two key physical issues: broadband light and single-pulse laser operation (one pulse per tens of minutes). The first issue makes it impossible to apply the well-developed methods of phase locking using nonlinear optics, and the second one considerably complicates the use of linear adaptive optics. All this makes it necessary to conduct experimental research on phase locking using the prototype prior to the construction of the phase locking system for all 12 modules. On the

other hand, solution of *Objective 1* will also permit starting both basic and innovative research (**Goal 2 and Goal 3**) at a level that would surpass the world level several years before the construction of the 200PW laser system and putting the entire XCELS infrastructure into operation. According to the results of activities under *Objective 1* final corrections to the architecture and components of the XCELS facility will be made.

Currently, optical parametric chirped pulse amplification (OPCPA) is the only existing technique of amplification provided by component base, allowing design and construction of laser systems with a power of 10 PW or higher. OPCPA systems use frequency modulation of short light pulses, multicascade energy amplification and subsequent recompression of the amplified pulses traditional for the generation of superintense fields. Due to a proper choice of the amplifying nonlinear medium, frequency and propagation directions of interacting waves in cascades of parametric amplifiers, broadband phase-matching conditions may be provided. Detailed description of these processes can be found in [1-15].

The most promising pumping for creation of powerful parametric amplifiers is the second harmonic of Nd:glass laser with a wavelength of 527 nm. For this pumping, the only candidates for nonlinear elements of output parametric amplification cascades are KDP and KD*P crystals whose aperture, in line with up-to-date growth technologies, may reach 30 cm or more [16]. Comparative analysis of KDP and KD*P crystals in terms of their use as nonlinear elements of powerful parametric amplifiers was undertaken in [17]. Maximum amplification bandwidth in a KD*P crystal is achieved in a noncollinear interaction scheme at a wavelength of 911 nm and a wavelength of a conjugate (idler) wave of 1250 nm. It is $\sim 2300 \text{ cm}^{-1}$, which is more than twice the maximum amplification band of 1000 cm^{-1} in a KDP crystal. Such a significant difference in the crystal amplification band is explained by the fact that the conditions of superwide phase-matching are realized in KD*P crystals.

IAP RAS is world leader in the exploration and development of OPCPA. In 2007, this institute under the joint project with RFNC-VNIIEF launched laser "PEARL" [18] with a pulse power of 0.56 PW, pulse duration about 45 fs and energy of 25 J. Parametric amplification in a KD*P crystal with the aperture of $10 \times 10 \text{ cm}^2$, which was grown at the Institute of Applied Physics by the original technology of high-rate crystal growth is used in this laser. The Institute has a technology of growing crystals with a much larger aperture, which opens up opportunities for creating on the basis of the OPCPA technology prototype laser modules with a power of 10 PW, with their subsequent upgrading to 15PW, as well as for creating a 200PW complex comprising 12 modules (*Objective 3*). The proposed OPCPA scheme with the central wavelength of 910 nm in the KD*P crystal is also used under the project of constructing 10 PW complex based on the Vulcan system [19].

The schematic diagram of a 2-channel prototype of a 200 PW laser is shown in Fig. 3.1. To achieve pulse power of 15 PW, a pulse with energy up to 400 J, duration about 25 fs, maximum intensity at focusing of more than 10^{23} W/cm², and a repetition rate of 1 shot per several hours is generated in each channel of the prototype. The aperture of the output cascades of parametric amplification in KD*P crystals is 30×30 cm². Each of the channels of parametric amplification is pumped by the second harmonic of Nd:glass laser amplifier with an aperture of 30×30 cm. The radiation energy of the fundamental and second harmonics is 3000 J and 2000 J, respectively, with pulse duration of 1.5 ns. Maximum pump radiation intensity is 1.5 GW/cm². The experience of "PEARL" demonstrates that this value does not exceed the damage threshold of a KD*P crystal.

Objective 1 includes the following nine Activities:

- Activity 1.1. Construction of the building (3000 m²) and utilities.
- Activity 1.2. Creation of a common front end.
- Activity 1.3. Creation of the first 10 PW module prototype.
- Activity 1.4. Creation of the second 10 PW module prototype.
- Activity 1.5. Phase locking of two modules.
- Activity 1.6. Enhancing module power up to 15 PW.
- Activity 1.7. Creation of 20 MeV electron accelerator based on photocathode and microwave resonators.
- Activity 1.8. Creation of a prototype laser with 1 kHz pulse repetition rate.
- Activity 1.9. Establishing and equipping laboratories for studying laser-matter interaction.

Works within the framework of these activities are described below.

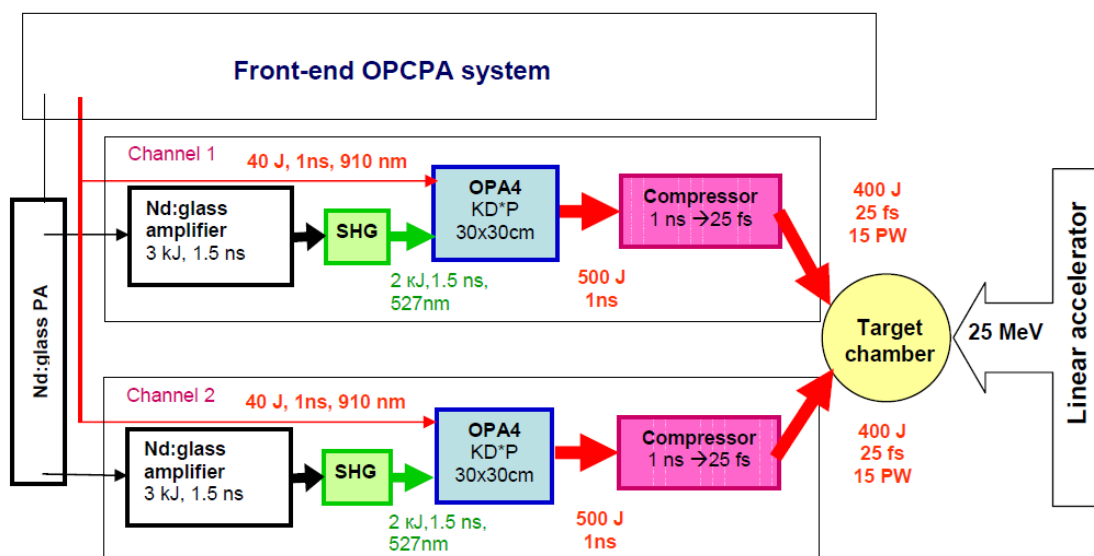


Fig. 3.1. Schematic diagram of a 2-channel prototype of subexawatt laser

Activity 1.1. Construction of the building (3000 m²) and utilities

To accommodate two prototypes of 15 PW modules a building with a total area of 3,000 square meters is required. A significant part of this area should be provided with radiation protection (see *Objective 8*). In the framework of this activity it is planned to define requirements to the building, choose construction site and construction company, build roads, carry out capital construction, provide engineering services, communications and equipment, decorating, and put the building into operation.

After that works described in *Activities 1.2-1.9* will be carried out in the building.

Activity 1.2. Creation of the common front end

General scheme of the front end

The front end of the prototype of two 15 PW laser modules is a source of broadband signal radiation (910 nm) at the input to the terminal parametric amplifier (providing formation of the space-time structure of radiation) and a source of a signal for synchronizing the Nd:glass laser amplifier with an aperture of 30×30 cm, as precise synchronization of the pump and signal is a key requirement for OPCPA.

To reduce the linear and nonlinear distortions of signal phase in the output parametric amplifiers, as well as in terms of crystal growth technology, the length of the nonlinear element should not exceed 4-5 cm. The calculations show that with the above parameters of pumping, the signal energy at the amplifier input should be in the range of 20-40 J (see Fig. 3.2). This value is close to the energy of the signal radiation at the output of the last parametric amplifier in the "PEARL" system [18]. Thus, in terms of forming broadband signal radiation, the front end of a 2-channel amplifier may be based on the proven optical design [18]. The following is a brief description of the laser "PEARL" with a few changes to be made when creating the front system.

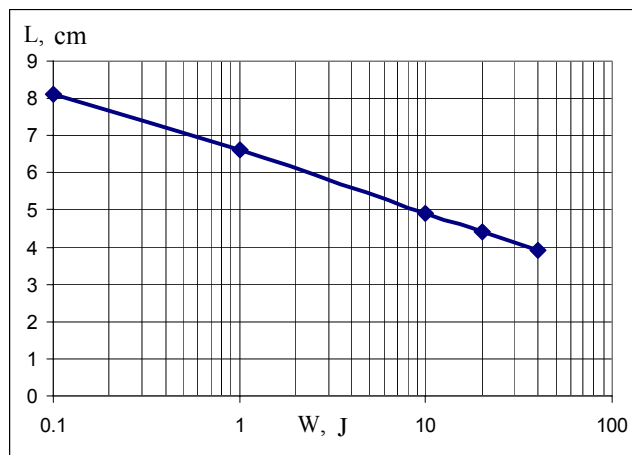


Fig. 3.2. Optimal length of the nonlinear element of the terminal parametric amplifier *versus* signal energy at the input

The front end of the prototype of two 15 PW laser modules is based on three parametric amplifiers. Its schematic diagram is shown in Fig. 3.3.

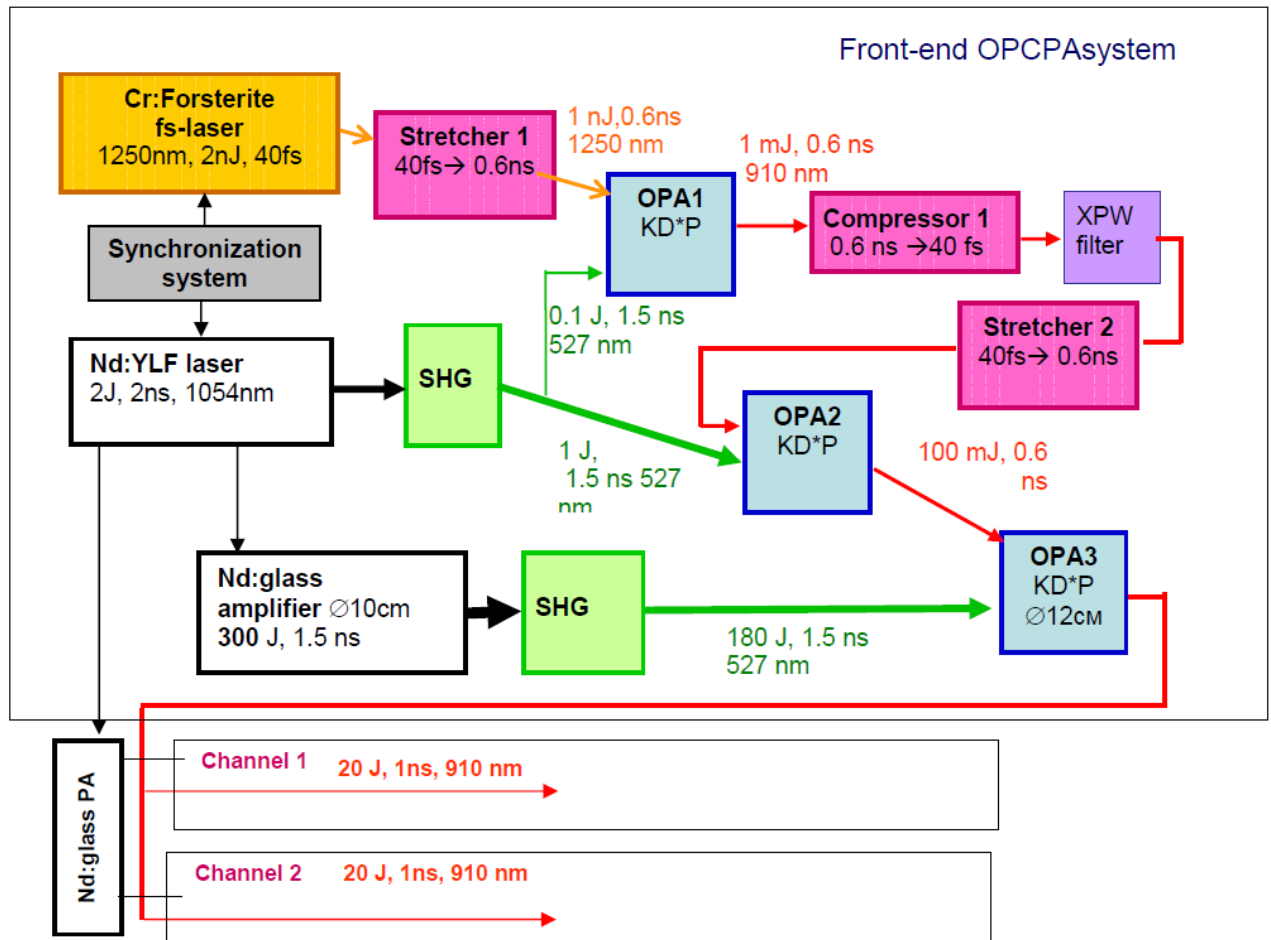


Fig. 3.3. Schematic diagram of the front end of a 2-channel prototype of 200 PW laser

The femtosecond master oscillator is a Cr:forsterite laser generating 40 fs pulses with 2 nJ energy at a central wavelength of 1250 nm. Stretcher 1 with a transmission band of 1000 cm^{-1} expands the pulse duration up to 600 ps. The first two OPAs (OPA1 and OPA2) are pumped by the second harmonic of a single-mode single-frequency Nd:YLF laser with a wavelength of 527 nm, up to 1 J energy in a 1.2 ns pulse [20]. The pump intensity at the input of the OPAs has almost uniform cross-sectional distribution and is about 1 GW/cm^2 . A two-stage synchronization scheme [21] provides simultaneous (to within ~ 50 ps) passage of the pump and amplified radiation pulses through the nonlinear OPA crystals. OPA3 is pumped by the second harmonic of a six-cascade Nd:glass amplifier [22]. The amplifier is seeded by part of the fundamental harmonic radiation of the Nd:YLF laser. The amplifier works with a period of one shot per 10 minutes and ensures output pulse energy of 300 J at the fundamental wavelength and at pulse duration of 1 ns. The second harmonic pulse energy reaches 180 J, see below for details.

OPA1 is a double-pass amplifier. During the first pass, OPA1 performs broadband conversion of chirped pulses at 1250 nm into pulses of signal radiation at 910 nm. During the second pass, the 910 nm radiation is amplified. So we call the injected radiation at 1250 nm idler and the radiation at 910 nm signal one.

The energy of the signal at the output of OPA1 is 1 mJ. To improve contrast of the compressed pulse at the output of the prototype, the signal radiation after OPA1 is compressed and passed through an XPW (Cross polarized wave) filter and is then stretched and re-amplified in OPA2.

After OPA2, the pulse energy reaches 100 mJ. After OPA2 the signal radiation passes through a spatial filter, delay line and expanding telescope and is directed to OPA3.

The requirements to the stretcher dispersion characteristic change significantly if the signal is excited by the idler wave. During the three-wave interaction chirp reversal occurs [23]. In this case, the quadratic dispersion of the stretcher-compressor system is zero if the second order dispersions of the stretcher and the compressor are identical. As for the cubic dispersion of the system, it can turn to zero only if the third derivatives of the phase incursions in the stretcher and compressor have opposite signs. We use an original stretcher, which incorporates a prism pair between the diffraction gratings [12, 17]. For a certain choice of parameters (see details in [24]) this stretcher allows efficient pulse compression at a wavelength of 910 nm after OPA using an ordinary grating compressor 1.

Stretcher 2 uses the standard scheme [25] of antiparallel arrays with image inversion telescope.

An alternative to the broadband 910 nm, ~100mJ source described above is the front end of 10PW OPCPA system based on the Vulcan laser [26].

Compact 200 J 527 nm Nd:glass laser for pumping final OPA

Radiation from a repetitively pulsed Nd:YLF laser described earlier in [20] is directed to the input of the Nd:glass amplifier. The amplifier system consists of a scheme that forms spatial beam structure, a six-cascade neodymium phosphate glass laser amplifier and a second harmonic generator. The amplifier comprises five one-pass amplifiers, one two-pass amplifier and transport telescopes. To avoid self-excitation of the amplifier, a Faraday isolator and an a-cut KDP wedge are used. The spatial beam structure is formed using an aperture line. At the output from the aperture line the radiation is formed as its eigenmode. The spatial distribution and radiation direction at the line output change insignificantly with varying direction and transverse distribution of the repetitively pulsed Nd:YLF laser beam.

The key idea of the beam forming system (described in detail in [20, 27]) is that at the output of the aperture line the field in the Fresnel diffraction region has a different configuration. We choose a plane with a large filling factor and relay its image to the plane of soft apodizing aperture based on the crystalline quartz lens with polarizer. This prevents formation of a diffraction-induced ring structure. Therefore, by selecting geometrical parameters we provide a filling factor of 0.6 at the amplifier input with a high value of transmission. An expanding Galilean telescope is added to the final stage of the line to match the beam diameter at the line output to the 10 mm diameter of the active element (AE) at the amplifier input. Achieving the maximum beam intensity at each amplifier stage requires control of small-scale self-focusing. The main contribution to the B-integral is made by a short length at the Nd:glass rods output, because the intensity increases during the propagation of radiation through the rods. That is why an increase in gain leads to a decrease in B-integral and, hence, to an increase in the output intensity.

We employ “densely packed” laser heads with a diffusive ceramic reflector (diameter 30, 60, 85, and 100 mm). A $\lambda/4$ plate before the 100 mm Nd:glass amplifier is used to provide circular polarization in order to reduce the B-integral [28, 29]. Transport telescopes (spatial filters) are required to match the beam diameter to the amplifier apertures. In addition, they relay images (by lowering the intensity variations in AEs located in the conjugate planes of Keplerian telescopes), decrease the angle of vision of the amplifiers, and limit the high-frequency component of the spatial beam spectrum. Constructively, the transport telescope is a metal cell evacuated to a pressure of 10^{-3} Torr. Lenses serve as the cell windows. At the center of the cell an aperture is mounted on a miniature three-coordinate translatable stage, which can be displaced with the help of stepper motors with a minimal step of 6 μm along the optical axis and 2 μm transversely to it. The motors are remotely controlled with an analog device or a computer. The key issues in the creation of spatial filters are lens aberrations and spatial mode filtering to suppress self-excitation of amplifiers and small-scale self-focusing. Aberration minimization determines the lens shape, while the efficiency of spatial mode filtration governs the size of the aperture, see details in [30].

Figure 3.4 shows a typical pattern of the transverse intensity distribution in the near field and far field of the beam with the energy of 300 J. The far-field intensity distribution for the fundamental harmonic is obtained with the help of a two-component objective (300 cm focus) corrected for spherical aberrations. As a second harmonic generator a 22.5 mm long KD*P crystal with type-I phase-matching (ooe) is employed. The circularly polarized first harmonic radiation is converted into linearly polarized radiation by means of a $\lambda/4$

wave plate placed after the output amplifier. The total phase-matching width for a small signal is $\pm 1000 \mu\text{rad}$. The accuracy of crystal axis alignment is $\pm 10 \mu\text{rad}$. The second harmonic pulse energy reaches 180 J with conversion efficiency of 70%.

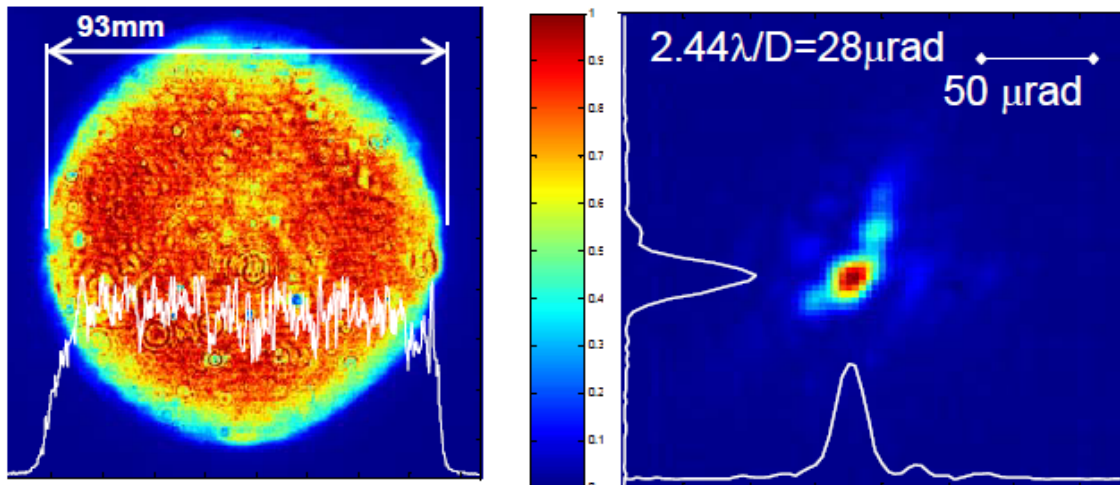


Fig. 3.4. Near and far fields of Nd:glass laser output beam (300 J, fundamental wavelength)

Parameters of final OPA

The nonlinear elements in OPA3 are uncoated KD*P crystals with a length of 80 mm and a clear aperture of 120 mm; the deuteration level is 85%. Although we have investigated the main physical characteristics of the broadband optical parametric amplification in the KD*P crystal based on the front-end system [12, 17], with the third amplifier performing only energy scaling of the system, the single-shot operation regime of the pump laser requires a special procedure to adjust OPA3. This procedure is described in [31]. The output pulse energy and efficiency of OPA3 are shown in Fig. 3.5. The curves in the figure and the temporal shape of the pump pulse passed through the OPA show deep saturation of parametric amplification. Maximum efficiency of OPA3 is 23% with respect to energy. The relatively small efficiency originates from a bell-shaped pump pulse. A flat-top pump pulse is more suitable for the final OPA stage. The chirped pulse energy at OPA3 output is up to 38 J and pretty stable from pulse to pulse (see Fig. 3.5). Due to the saturation the output spectrum is broadened up to 57 nm FWHM. Typical spectra are shown in Fig. 3.6. The good enough quality of this beam is demonstrated in Fig. 3.7. The far field distribution is measured in the focal plane of the lens with a focal length of 5 meters.

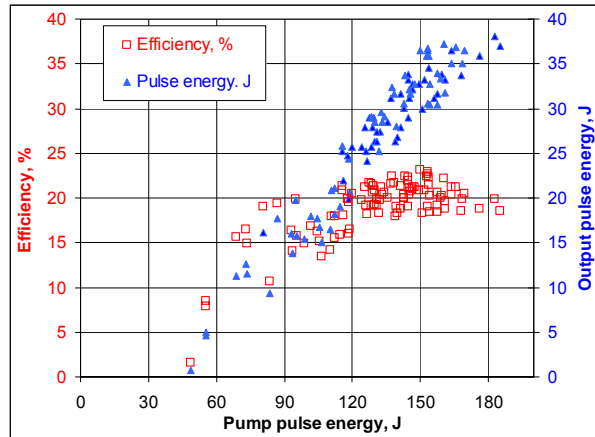


Fig. 3.5. Output OPA3 pulse energy (triangles) and OPA3 energy efficiency (squares) vs pump pulse energy

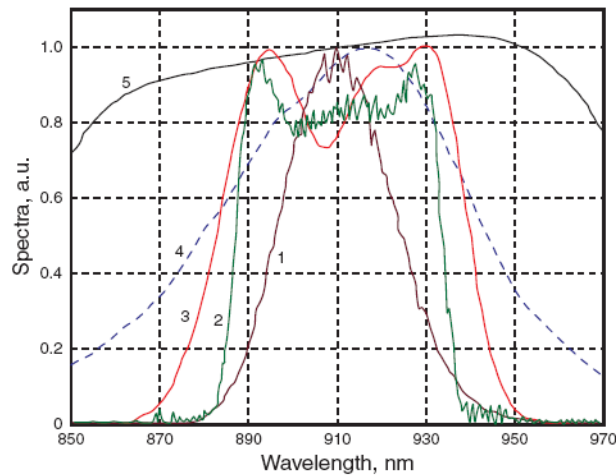


Fig. 3.6. Spectra of the injected pulse recalculated to signal wavelength (1), pulses at the output of OPA2 (2) and OPA3 (3), parametric gain in KD*P crystal (4). Dashed line (5) shows pump intensity at which the corresponding spectral components of signal are amplified

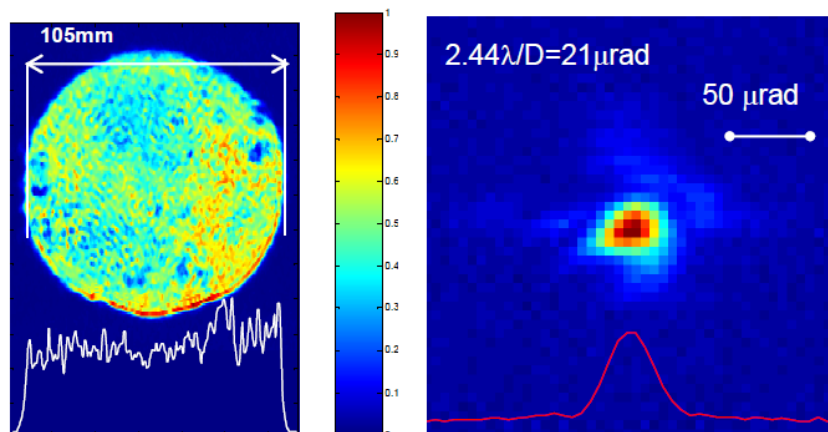


Fig. 3.7. Output OPA3 beam (38 J) intensity in the near and far fields

Activity 1.3. Creation of the first 10 PW module prototype

To obtain an output power of 10 PW pulse energy at compressor input must be 350 J. Given that the module power will be increased to 15 PW (*Activity 1.6*), the pulse energy should be increased up to 500 J. For reducing the linear and nonlinear distortions of signal phase in the output parametric amplifiers, and in terms of crystal growth technology, the length of the nonlinear element should not exceed 4-5 cm. Calculations (see *Activity 1.2*) show that for the signal energy at the amplifier input of 20-40 J, one parametric amplifier with an aperture of no more than $30 \times 30 \text{ cm}^2$ is sufficient to produce signal pulse energy of 500 J.

Creating a module based on two series parametric amplifiers reduces the requirements to the pump laser, but complicates the scheme of the module and, more importantly, greatly complicates phase locking of the modules without which it is impossible to achieve 200 PW power. At the same time, advance made in Nd:glass lasers (see below) allows the requirements to the pump pulse to be met even in the version of the module with one parametric amplifier.

Based on the said above, the module will contain only one parametric amplifier. Figure 3.8 shows the schematic diagram of the module and the radiation parameters at key points. The front end system is described in detail above (*Activity 1.2*), we proceed to description of the key elements of the module: Nd-glass pump laser, parametric amplifier, compressor, increase of laser pulse contrast, reduction of divergence by means of adaptive optics, control and diagnostic system.

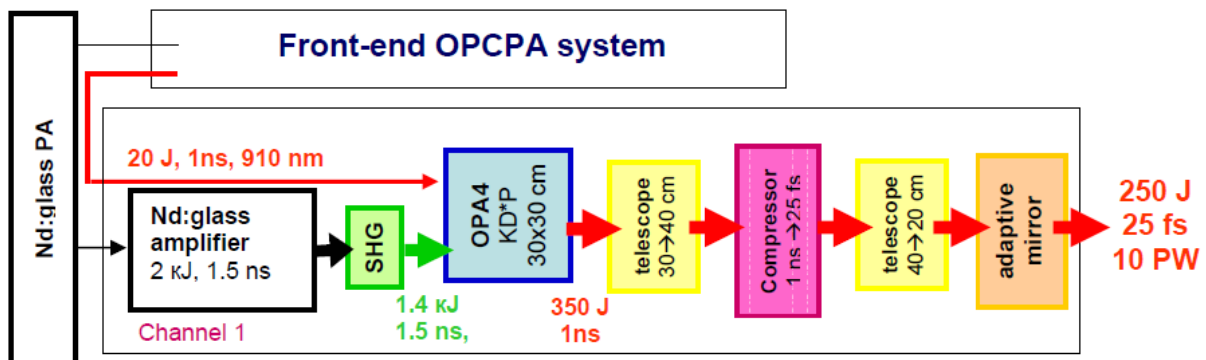


Fig. 3.8. Scheme of 10 PW module

Design and creation of a pump laser

To ensure at the output of parametric amplifier the power of 350 J, which will allow achieving after compression the laser power of 10 PW in one channel, a pump pulse with the energy of about 1.4 kJ at the wavelength of about 0.5 microns for the laser pulse duration of 1.5 ns is needed. With the current level of laser technology, it may be obtained

only in Nd:glass laser with conversion to the second harmonic. The active elements of the laser should be in the form of thin slabs, inclined in the direction of beam propagation at the Brewster angle. For more efficient use of pump lamp energy of the active laser elements, the laser beams should have a square cross-section.

Estimates based on data on the radiation resistance of Nd:phosphate glass, the magnitude of cubic nonlinearity of the glass and the experimental data on development of KJ laser systems give the aperture of light beams of order 25cm. As the pump laser is one of the most expensive parts, it is reasonable to include in the concept of the 10 PW module the possibility to increase power up to 15 PW (*Activity 1.6*). For this upgrade it is necessary to increase the pump laser pulse energy to 2 KJ at the second harmonic. Hence, the beam size of 30 cm seems to be most appropriate. Although it is slightly more than required for achieving a power of 10 PW, expensive elements need no replacement under *Activity 1.6*.

The above considerations lead us to the following concept of the pump laser. It should consist of a low-power master oscillator (MO) with pre-amplifier (PA) and power output amplifiers. The output energy of PA should not exceed the energy level of the order of 1-10 J. The MO and the PA will completely form spatial and temporal characteristics of the laser beam with allowance for subsequent distortions of the characteristics in the power laser cascades.

The 4-channel "LUCH" facility in RFNC-VNIIEF in Sarov has similar parameters but its beam aperture is 20 cm [32]. Second harmonic radiation of one of the channels is used to pump a petawatt power parametric amplifier [33].

Currently, RFNC-VNIIEF started the project of a multichannel facility UFL-2 for inertial confinement fusion with a total energy of 2 MJ and beam aperture in each channel of 40 cm. Wide, mutually beneficial collaboration between XCELS and UFL-2 is planned. Creation of a pump laser for parametric amplifiers is the most important aspect of this cooperation.

In France, near Bordeaux there is LIL laser facility with parameters close to the parameters of the pump laser of parametric amplifiers. Each channel of LIL laser with an aperture of $37 \times 37 \text{ cm}^2$ generates the energy of 15 kJ. The channels are grouped in bundles of 4 pieces each. Two bundles of LIL laser channels are forwarded to the target chamber. All 8 bundles in the chamber are directed to the target to study the conditions under which inertial confinement fusion may arise. LIL is a prototype of the megajoule laser LMJ. 240 channels total with parameters identical to LIL laser are planned in the LMJ facility.

The schematic view of one channel of LIL facility and a schematic diagram of one channel of laser in NIF (Lawrence Livermore National Laboratory, USA) that is the most detailed and approved scheme of such lasers are presented in Fig. 3.9.

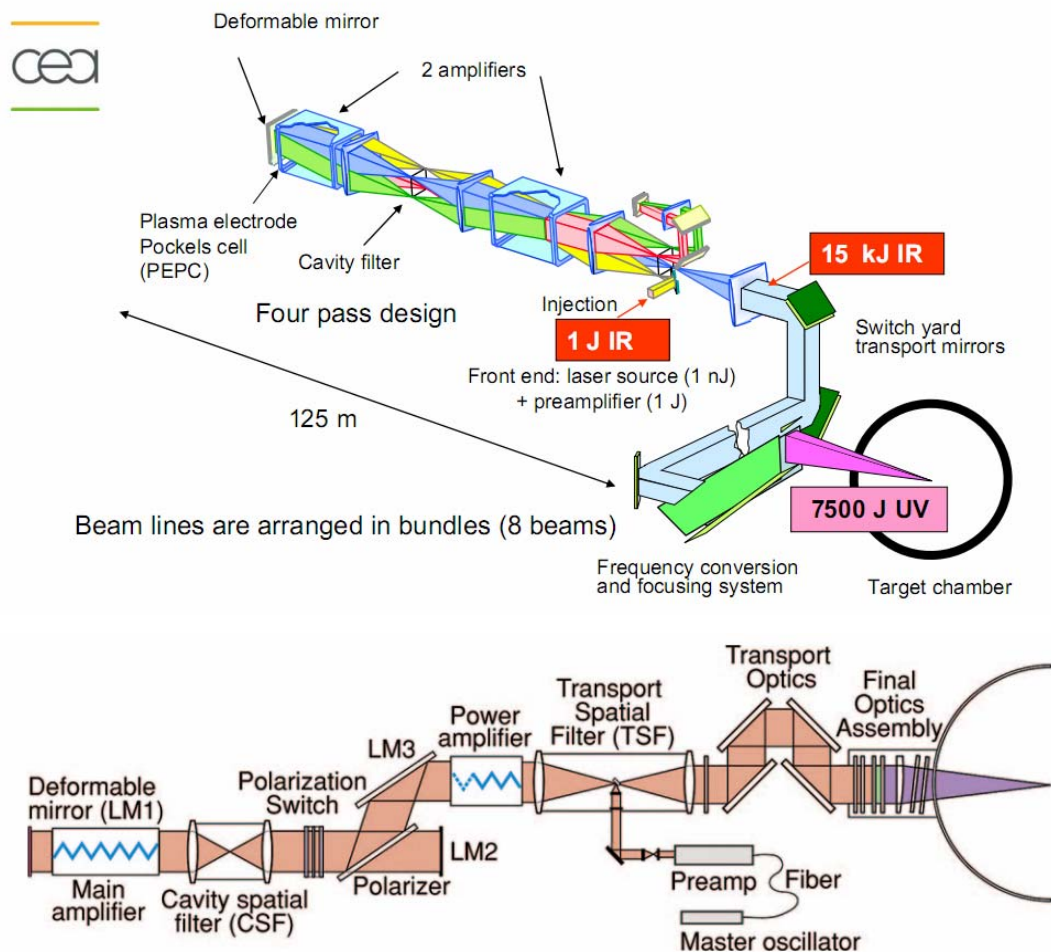


Fig. 3.9. The scheme of one channel of LIL (top) and NIF (bottom)

The main idea of a single channel of NIF laser is that, in contrast to traditional schemes of powerful laser amplifiers where the beam aperture broadens as it is propagating along the facility, a relatively low-power beam from the PA output passes to the amplifier with maximum aperture all at once. For effective extraction of the energy stored in the main amplifier, a large number of passes in the amplifier should be arranged. This is attained by placing the amplifier into the resonator which has the input and output circuits. As is seen in Fig. 3.9, the input is implemented through the spatial amplifier filter, and the output by turning polarization of the radiation by a large-aperture Pockels cell with plasma electrodes transparent to the laser beam. Further, the radiation energy in the powerful amplifier increases to the maximum value that is limited by the damage threshold of laser elements and by small-scale self-focusing of the laser beam in laser active elements.

A general view of large-aperture Pockels cells with plasma electrodes developed and manufactured in IAP RAS is shown in Fig. 3.10. The plasma electrodes transparent in the optical range enable effective feeding of high voltage to the end surfaces of the plasma Pockels cells and effective control of the laser beam polarization.

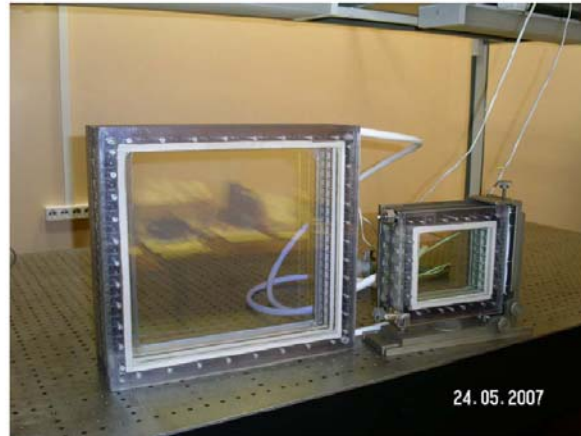


Fig. 3.10. General view of plasma Pockels cells for the aperture of 100x100 mm and 300x300 mm

A single channel of NIF laser and the pump laser of parametric amplifier have different parameters; hence, the NIF scheme can be taken as a basis, but it is necessary to finalize the parameters needed for the pump laser. In particular, in contrast to NIF, in our case an almost rectangular pulse envelope with a duration of 1.5 ns should be provided at the output of a neodymium laser [34]. Due to the high total gain of the entire multicascade amplifier (over 10^6) it is extremely difficult to calculate the time profile of the input pulse that provides its rectangular shape at the output. Therefore, preliminary experiments with a separate pump channel are needed. In the course of these experiments, the number of slabs in the main and power amplifiers should be specified more accurately.

An effective converter of radiation into the second harmonic (1055 nm to 527.5 nm) must be placed at the output of the pump laser. This will require large-aperture (30x30 cm) KD*P crystals. The same crystals should also be used in Pockels cell for polarization switch and in the half-wave plate coordinating radiation polarization of the laser fundamental harmonic and crystal orientation of the laser frequency converter.

Another issue worth mentioning is the solved but quite costly power supply of large pump flashlamps of power laser amplifiers. For effective amplification of radiation by neodymium slabs with the aperture of 30x30 cm, each slab must be illuminated by 12 lamps $\varnothing 4 \times 30$ cm in diameter. Taking into consideration the needed amount of slabs in a channel, the number of channels being 2, the total number of large lamps will be 384. If these lamps are used with 40% load, capacitor energy of 5 MJ will be needed. This battery

is a quite large-size and expensive construction. Even when using compact, self-regenerating capacitors with specific stored energy of $0.5-1 \text{ J/cm}^3$ the battery volume will be $5-10 \text{ m}^3$. Capacitors with such specific stored energy are manufactured by a number of foreign companies. In Russia, such capacitors are manufactured by the ELKOD company under the trademark K75-100.

Development and fabrication of parametric amplifiers

An output parametric amplifier for each of the two channels of the prototype will be made of a KD*P crystal with a clear aperture of $30 \times 30 \text{ cm}$ and thickness of $4-5 \text{ cm}$. The unique technology of growing large-aperture nonlinear optical KDP crystals is available at IAP RAS.

This technology is based on the method of high-rate growth of profiled single crystals. It allows producing optical elements with an aperture of $40 \times 40 \text{ cm}$, reducing growth rate by almost an order of magnitude as compared to the classical method, and minimizing crystal waste during processing.

IAP RAS has manufacturing facilities necessary for production of nonlinear optical components of laser systems for the XCELS Project (Fig. 3.11).

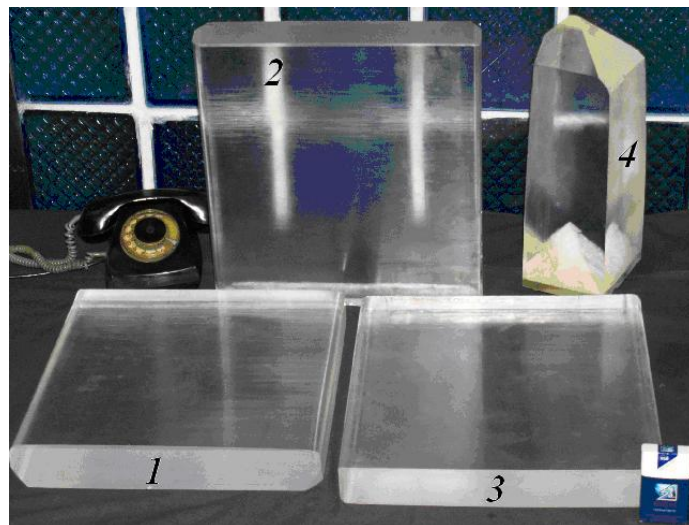


Fig. 3.11. Crystals 1-3 with $365 \times 400 \times 50 \text{ mm}$ size were grown by the high-rate growth technique for about 40 days. KDP crystal 4 with $140 \times 140 \times 300 \text{ mm}$ size was grown by a conventional technique for about a year

Second harmonic radiation of a neodymium laser with an aperture of $30 \times 30 \text{ cm}$ will be used for pumping, with the energy of the second harmonic being 2 kJ and pulse duration 1.5 ns (see Section 1.3.1). Broadband signal radiation with energy of about 20 J and duration of $\sim 0.9 \text{ ns}$ generated in the front end (*Activity 1.2*) after the expanding telescope will be injected to the amplifier input. Emission of the signal and the pump must

be synchronized in time to an accuracy of 100 ps. The synchronization will be controlled by means of fast photodiodes and a broadband oscilloscope.

To achieve broadband parametric amplification in the noncollinear geometry of three-wave interaction two phase-matching angles, namely the angle between the direction of pump radiation and the optical axis of the crystal and the angle between the propagation direction of signal and pump radiation, should be aligned. In the course of "PEARL" development a method of aligning these angles based on the spectral-angular distribution diagram of parametric luminescence was elaborated [35]. The proposed method allows independent aligning of the phase-matching angles, which was demanded for single-shot operation of the pump laser. Later this technique was used to adjust the output parametric amplifier of the "FEMTA" channel created under the joint VNIIEF and IAP RAS project [33]. This amplifier was pumped by the radiation from the "LUCH" facility working with a repetition rate of 2 shots per day. Thus, adjustment of the output parametric amplifier of a 2-channel prototype will be based on the well-developed technique.

To estimate the energy and spectral characteristics of the terminal amplifier the process of parametric amplification was simulated numerically. The computations were made for given parameters of the pump under the assumption that the energy of the signal radiation at the input of the terminal amplifier is 20 J, and its spectrum has 4th power supergaussian shape with a width of 60 nm (the pulse of the signal radiation has the same shape for a duration of 0.9 ns). This agrees well with the experimental data on the spectrum of the amplified signal obtained in the "PEARL" facility. Uniform transverse distribution of the signal and pump beams was assumed in the calculations; the reduction of the amplification efficiency associated with heterogeneity of the pump beam was taken into account by multiplying the signal energy by a factor of 0.75. The adequacy of this approach was confirmed by comparison with experimental data obtained in the simulation of operation of the parametric amplifier of the "PEARL" facility. The signal energy as a function of the length of the nonlinear element is plotted in Fig. 3.12. Gain saturation is reached for the 4.5 cm crystal length, signal energy of 500 J, and conversion efficiency of 25%. The signal pulse at the amplifier output corresponding to such a length of a nonlinear element is shown in Fig. 3.13. Thus, the results of the numerical simulation confirm the possibility of enhancing signal pulse up to the energy level required to produce peak power of 15 PW after compression.

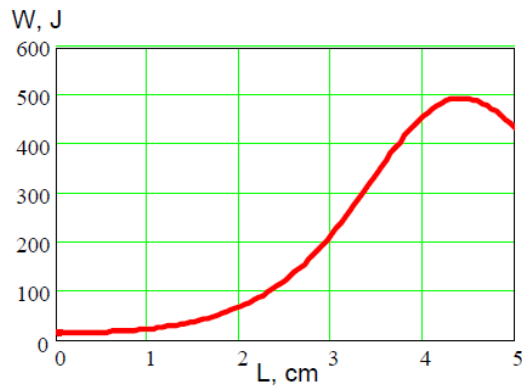


Fig. 3.12. Signal energy versus nonlinear element length

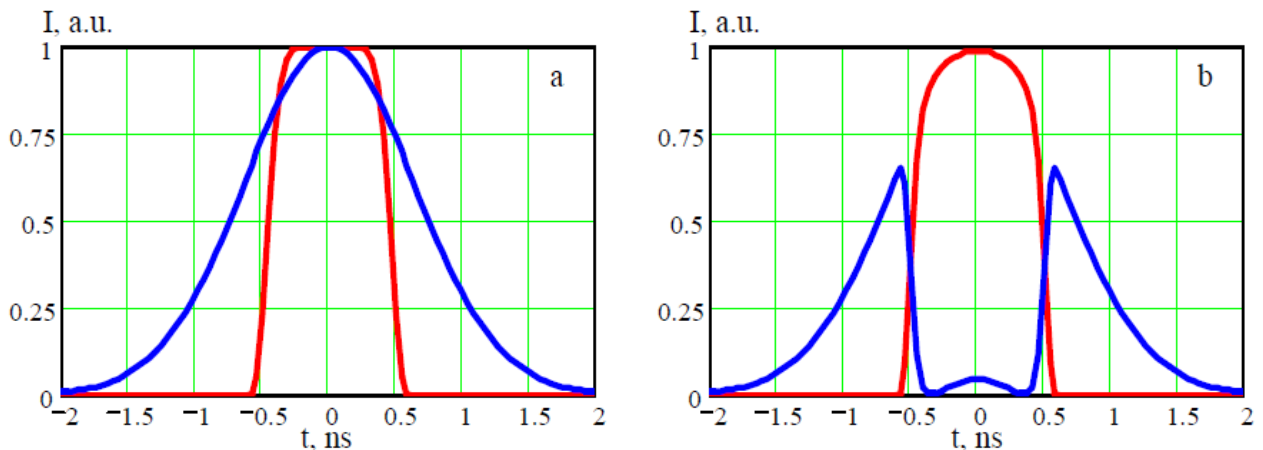


Fig. 3.13. Radiation pulses of signal (red) and pump (blue) at the input (left) and output (right) of the terminal parametric amplifier 4.5cm thick

Design and creation of a pulse compressor

According to the principal goal of the Project, the radiation at the output of each of the 12 channels of the laser complex will have the following parameters: power 15 PW, pulse duration 25 fs, wavelength 910 nm, divergence no more than 3 diffraction limits. These characteristics are formed in the compressor of ultrashort pulses.

The compressor is an essential element of a CPA system. Here the amplified laser pulse of signal radiation stretched in time is compressed to femtosecond durations. The dispersion introduced by the stretcher, when the initial ultrashort pulse produced in the master femtosecond oscillator is stretched, is compensated, so that the pulse is shortened. The peak pulse power increases in proportion to the compressed pulse. Specifically, under this Project a chirped 500 J pulse 1 ns in duration will be compressed to the pulse with a duration of about 25 fs. The inevitable losses in the compressor will reduce the pulse energy to 400 J.

The main optical elements of the compressor are diffraction gratings. Such a system has the record group velocity dispersion due to the large angular dispersion of spectral

components of the broadband pulse between two parallel gratings turned to each other by work surfaces. It is group velocity dispersion (GVD) that leads to a change in the pulse duration. The GVD signs in the stretcher and compressor are different – these devices are complementary to each other, compensating for the dispersion.

However, in addition to the fundamental difference in design, the significant difference between the stretcher and the compressor is that the stretcher is located in the front end of the system where the optical load is small, while the compressor experiences maximum load – maximum radiation intensity in the scheme (except, of course, the target). It is the reason why the power of superintense laser complexes is limited by the optical breakdown of diffraction gratings. To protect the gratings from destruction in the multipetawatt laser complex, the size of the laser beam in the compressor will be increased up to 400 mm in diameter. As the beam diameter in the amplifier will be 300 mm, an expanding telescope formed by two spherical mirrors will be located in front of the compressor. The compressor comprises four diffraction gratings (see Fig. 3.14).

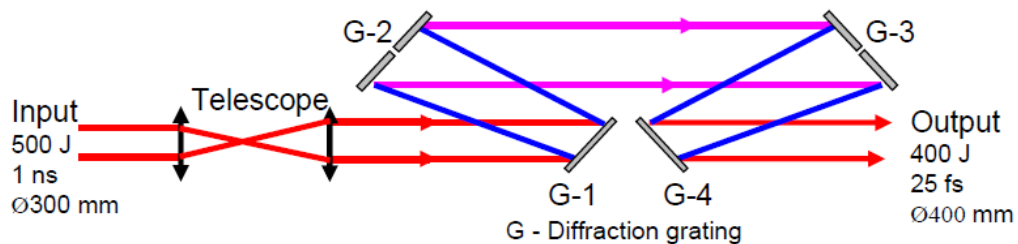


Fig. 3.14. Schematic diagram of the compressor. Gratings G-2 and G-3 are composite here

For normal operation of the 15 PW compressor diffraction gratings of appropriate size (500 mm × 800 mm) are required. For the radiation energy of a pulse arriving at the compressor of 500 J, the energy density in a 40 cm beam will be a little more than 0.4 J/cm². This value is close to the record levels for holographic gratings coated with gold operating in the long-term regime (tens and hundreds of pulses). Gratings with dielectric coating have a better resistance to optical radiation, but there may arise problems with the reflection bandwidth, which may lead to an increase in the duration of the output pulse. Tiled-grating assemblies similar to those used in the Laboratory for Laser Energetics (LLE), University of Rochester (Fig. 3.15) will most likely be used in the compressor. This scenario is favourable in the absence of the technology of producing large gratings, but significantly complicates the system of compressor adjustment.

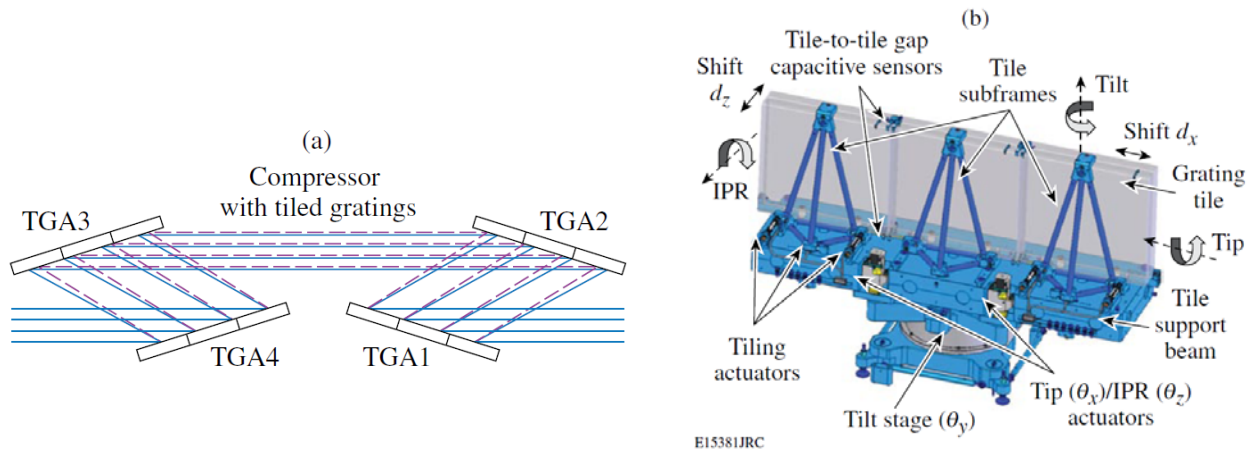


Fig. 3.15. (a) OMEGA EP compressor consists of four tiled-grating assemblies (TGA's). The size of each TGA is $1.41 \text{ m} \times 0.43 \text{ m}$.
(b) TGA assembly and tiling parameters. The picture is taken from [36]

New technologies of producing large-size diffraction gratings of different types with required damage threshold and spectral characteristics will be developed under the Project. Particular attention will be given to minimizing loss of radiant energy on lattices that inevitably reflect light to the zero – mirror order. It is expected that the reflection coefficient of the gratings to the first (operating) diffraction order will be 95%.

The output radiation intensity in the compressed pulse is so high that if such radiation propagates in air, the nonlinear self-focusing effects and beam fragmentation will be apparent in the first few centimeters, which will destroy the beam completely. Therefore, the compressor must be placed in a vacuum chamber (Fig. 3.16). All optical elements of the compressor including auxiliary optics are moved remotely by step-motors with an accuracy of a few angular seconds and microns.

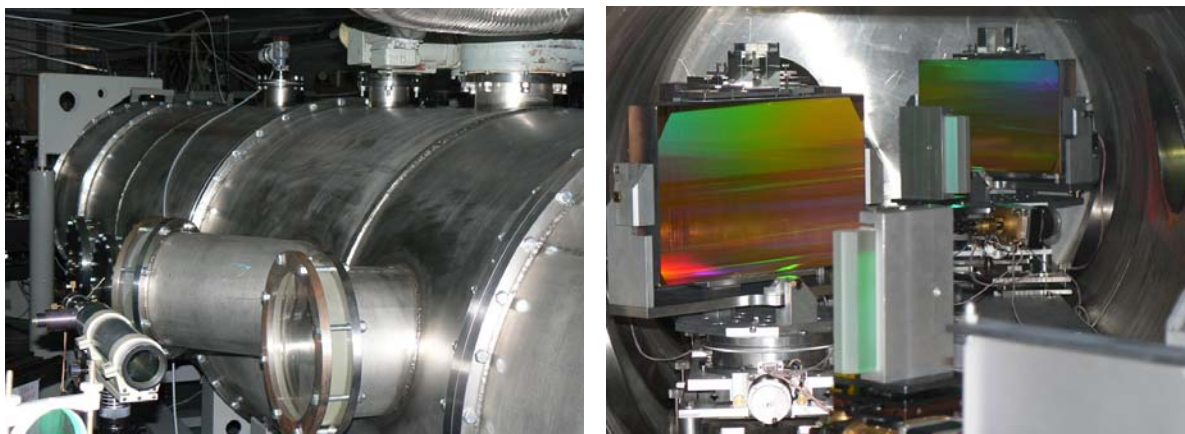


Fig. 3.16. The vacuum chamber of compressor petawatt laser pulses [33] in the parametric VNIIEF facility (Sarov), exterior (left) and inside (right) view

The vacuum chamber of the compressor will have the following dimensions: length 7 m and diameter 2 m. It is made of stainless steel or aluminum as a lightweight material. The presence of the correct size flange will provide free access to the compressor when it is set up, and the ability to remotely monitor the state of the optical element when it is under vacuum. The output window will be connected to a vacuum compressor tract from the target chamber. Thus, compressor – path – target chamber all in one volume will support the required level of vacuum (not worse than 10^{-6} Torr) by means of fore- and turbomolecular pumps.

Development and fabrication of devices for contrast enhancement

The objectives of experimental investigation of the interaction of superintense laser fields with gas and solid targets set stringent requirements to the temporal profile of optical pulse intensity. These requirements are primarily specified by the need to exclude a possibility of changing the physical characteristics of the target by precursors of superintense radiation preceding arrival of the main laser pulse.

The structure of the temporal profile of the intensity is determined by the methods of generation and amplification of laser radiation. In particular, in OPCPA laser systems the main factors are parametric superluminescence, uncompensated high-order pulse residual dispersion, incomplete spectrum reflection by the diffraction gratings of the stretcher and the compressor, as well as random phase noise produced by the inhomogeneities of the optical elements. The temporal profile may be conventionally divided into three parts: the main pulse, the interval of the near (<1 ps) and far (> 1 ps) contrast. The level of the far contrast should not exceed the plasma formation threshold; for solid targets this value is 10^{10} W/cm².

Currently, quite a number of methods for enhancing the temporal contrast of femtosecond radiation have been developed. The main of them are nonlinear filtering using rotation of ellipse polarization (NER) [37], the use of a hollow waveguide filled with noble gas [38], and the use of optical fibers with birefringence [39].

To increase the temporal contrast of the femtosecond radiation in the front end of the laser complex, the most promising means is the generation of a wave of orthogonal polarization due to the influence of cubic nonlinearity in the crystal. The interaction of intense linearly polarized laser light with a wave of cubic polarization arising in the crystal results in generation of orthogonally polarized light. The intensity of the generated wave is proportional to the third degree of input radiation intensity. The nonlinearity of the process can significantly improve the temporal contrast and reduce pulse duration. For example,

for the initial Gaussian pulse the compression ratio is equal to $\sqrt{3}$. Moreover, the incoherent noise does not convert to a wave of orthogonal polarization. A barium fluoride BaF_2 crystal may be used as a nonlinear element as it has a sufficiently high value of the anisotropic tensor of cubic nonlinearity $\chi^{(3)}$, which increases the conversion efficiency [40]. Efficiency of such a process may reach 33% [41]. The process of generating waves of orthogonal polarization aiming at increasing temporal contrast is intended to be used in the front end of the superintense femtosecond laser complex (see *Activity 1.2*).

In addition to the mentioned methods of contrast enhancement in the front end of the complex, the researchers in IAP RAS actively investigate a possibility of enhancing temporal contrast of the PW radiation. In this case, the basic physical process is generation of the second harmonic of the main radiation in ultrathin (less than 1 mm) KDP nonlinear elements with an aperture over 10 cm. Recent experimental studies have shown that the conversion efficiency to the second harmonic radiation with a power density of TW/cm^2 exceeds 70% (see Fig. 3.17). Theoretical analysis and numerical results of three-dimensional simulation revealed that due to the effects of self- and cross-action the radiation at double frequency is phase modulated, which may be corrected, thus providing significant reduction of the duration [42]. Thus, it was demonstrated that the process of doubling the frequency of superintense light will significantly increase the temporal contrast, increase peak power and intensity of the radiation received by the target.

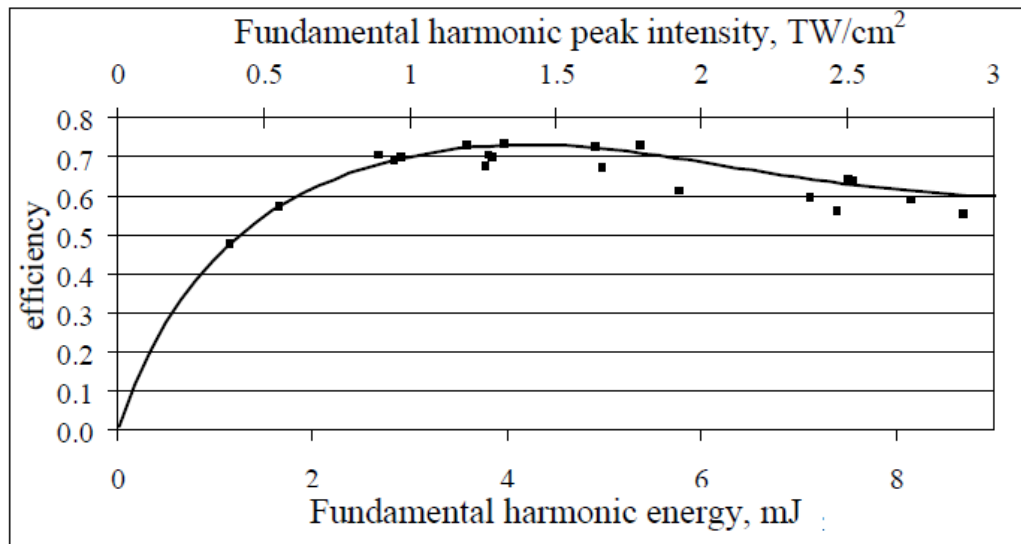


Fig. 3.17. Experimental and theoretical plots for the energy efficiency of second harmonic generation (SHG) in a 1 mm thick crystal as a function of peak intensity of the pulse at the fundamental harmonic at the crystal input

Design and creation of adaptive optics

For the majority of basic researches in the created complex, the key requirement is maximum intensity to produce which superintense pulses must be focused onto a light spot of minimum possible size. According to the diffraction laws, with a sufficiently sharp focusing a laser pulse can be focused onto a spot with the size of order wavelength. However, if the phase front is distorted, the effective focal spot size increases and the radiation intensity at the waist decreases sharply. Phase front distortions of laser radiation are inevitable at generation of pulses with a power of tens of petawatts because of nonlinear effects and the unavoidable aberrations of large-size optical elements. Thermal phase distortions arising from inhomogeneous heating of optical elements during passage of laser light may also be referred to harmful distortions.

Phase front correction is accomplished using a modern arsenal of adaptive optics. Vast experience in this area has been gained in ILIT, where the technology of deformable mirrors with distributed-action piezoelectric actuators was developed and systems of wavefront sensors controlling the shape of the mirror surface with feedback in real time were elaborated. These devices are successfully used in many major laser labs worldwide, including the Max-Planck Institute for Quantum Optics in Garching (Germany), The University of Laval (Canada), and others [43-45].

The experience in creating systems of the petawatt level demonstrates that the phase front at the output has random modulation with a spatial scale more than one centimeter and amplitude up to several wavelengths. Such phase distortions are most problematic as they cannot be filtered by spatial filters without significant loss of laser pulse energy. However, the adaptive correction system with deformable mirror can accurately compensate for the distortions of such scale and amplitude, including thermal phase distortions in optical elements [46]. The intensity of radiation after compensation can be increased by one-two orders of magnitude. An example of such correction is shown in Fig. 3.18.

For the convenience of transportation and correction, the radiation of each of the 12 channels is scaled from 40 cm at the compressor output to the aperture of 20 cm by a mirror telescope. After that, the radiation is incident on the deformable mirror which introduces phase distortions equal to the initial distortions of the wave front but with a reverse sign. Feedback may be realized either by means of a wavefront sensor that uses attenuated radiation that has passed through one of the mirrors with high reflectance, or directly by optimizing the focal spot. The latter option cannot be implemented in real time and involves a long (several thousands of iterations) procedure for optimizing the shape of

a deformable mirror. However, it is more efficient and helps further compensate for geometric aberrations in the focusing optical system. Depending on the objectives of the experiment any of these options of feedback may be used.

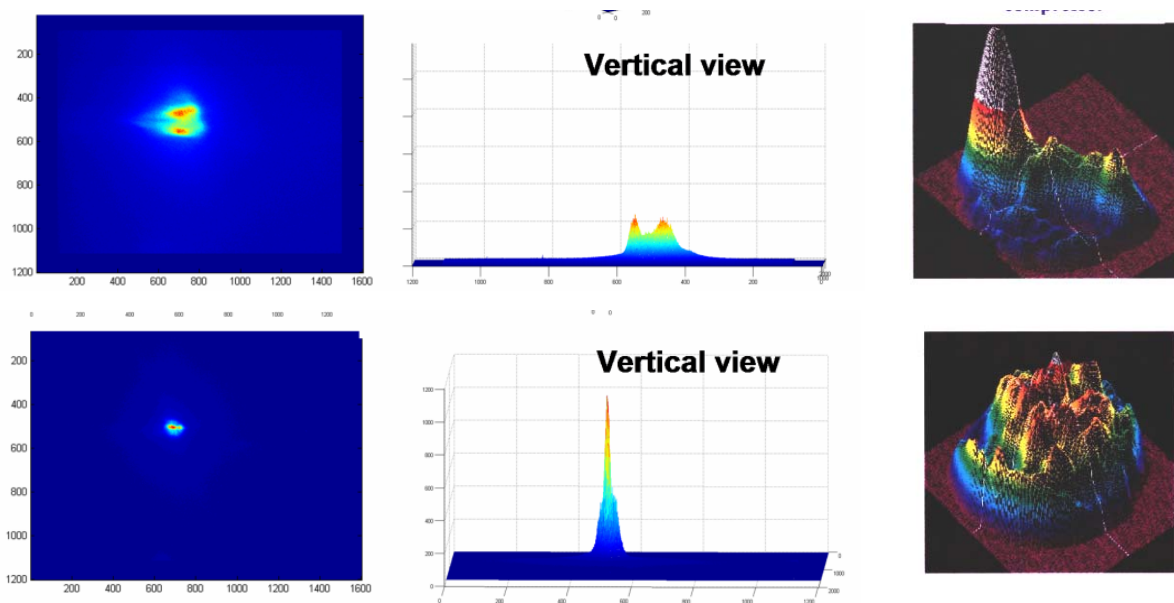


Fig. 3.18. Examples of using adaptive optics devices in ILIT: 10-fold peak intensity increase in focus with the use of adaptive system (University of Laval) – left; homogenizing intensity distribution on the surface of diffraction grating for increasing light load in the optical compressor of laser system ATLAS (Max-Planck Institute for Quantum Optics) – right

Design and creation of control systems and diagnostics

Diagnostic capabilities of a complex laser system allow assessing the state of the system at any moment of time (including immediately before the experiment): ready for operation, problems in some units, system as a whole ready to make a "shot." Moreover, the diagnostics permits effective, quick and flexible control of the experiment. The use of automation significantly increases the number of control points that may reach several thousands. For example, the NIF laser complex has 60 000 controlled elements [47].

The diagnostic and control systems are important parts of any physical installation, but they are of particular importance in the unique and large-scale facility such as a 200 PW laser. They are considered in detail in *Activities 3.6* and *3.7*. At the same time, the key elements of laser diagnostics and control will be worked out already for the 10 PW system that is a prototype of the first module of the laser complex (*Activity 1.3*).

It is convenient to consider the main objectives of the control and diagnostics of the laser complex in relation to the stages of the experiment. It is supposed that actually all the operations under the Project described below will be performed in automatic mode.

Stage I. Preparatory – to be performed before the experiment starts.

1. Quality control of optical elements (presence of breakdown in transmissive elements, mirrors, gratings, etc.), as well as of other laser elements, for example, pump lamp of laser heads.
2. Controlling the passage of the pump beams, signal light through the entire system (using the alignment laser radiation generated at appropriate wavelength). Simultaneous issuing commands, switching of a light display warning of the presence of alignment radiation.

If necessary, adjustment in automatic mode.

In case of emergency, issuing appropriate commands and warnings about the need for intervention of operations staff to align the system.

3. Quality control of beams – aperture filling, quality of image transfer, radiation collimation, beam propagation direction.
4. Controlling radiation focusing on the target.
5. Controlling the front end of the laser system.
6. Controlling compressor settings.

Automatic tuning and intervention of operations staff in case of emergency apply to items 3-6.

Stage II. Setting parameters of the experiment.

1. Setting the number of working channels.
2. Setting energy in each channel of the laser system.
3. Setting the duration of the compressed pulse.
4. Switching on the diagnostics (meters of energy, spectral and other characteristics, oscilloscopes, etc.), choosing the mode of operation of the measuring equipment.
5. Installing the necessary filters of optical radiation and beam damping.

Stage III. Experiment.

1. Controlling switching of the needed lockout (optical, electrical, etc.), light shields, disabling and lock-out of adjustment and probe lasers, and so on.
2. Checking the presence of personnel in the operation (target) room.
3. Controlling switching of measuring devices, including radiation monitors, computers, etc.
4. Testing communications (acoustic signals and commands).
5. Checking readiness of the personnel involved in the experiment.

6. Giving command – permission to conduct the experiment.
7. Charging storage batteries with needed time delays according to the scheme of the experiment, etc.
8. Start-up (automatic or manual) – "shot."
9. Automatic storage of all measured parameters of the experiment. Pre-processing. Sending data to the archives. Statistical processing of data.
10. Information about the obtained results: principal parameters, failures, etc.

Stage IV. Completion of the experiment.

1. Information about conservation of experimental parameters.
2. Express test of radiation monitoring sensors.
3. Checking the grounding, blocking and other systems.
4. Information on radiation, electrical, optical safety.
5. If possible and appropriate, allowance to enter the experimental hall.
6. Announcement of the end of the experiment.

The multipetawatt laser complex consists of the front end and 12 identical 15 PW power lasers. Each of these lasers is a system the major components of which are laser channel of the pump system of parametric amplifiers, parametric amplifier cascades, and a chirped pulse compressor.

A more detailed description of the system for control and diagnostics of these component parts is given in *Objective 3 (Activities 3.6 and 3.7)*.

[1] <https://www.llnl.gov/str/September03/Moses.html>

Activity 1.4. *Creation of the second 10 PW module prototype*

After approving the 10 PW module, recommendations for improving its operation, reliability, stability and reproducibility of the basic parameters of radiation will be prepared. Based on the gained experience the second prototype will be created. The principal goal of creating the second prototype is conducting experiments on phase locking two modules with maximum radiation power. The problem of module phase locking is a cornerstone of the entire project. It is described in more detail in *Activity 1.5*.

Activity 1.5. Phase locking of two modules

Despite the large number of theoretical and experimental researches on laser modules (channels) phase locking [48-51], there are no, to the best of our knowledge, works on phase locking pulses of enormous energy (hundreds of J) and the duration of the order of ten periods of the laser field. We believe that this is explained by two key physical issues: broadband light and a single-shot mode of laser operation (one pulse per tens of minutes). The first makes it impossible to use the broadly developed methods of phase locking by means of nonlinear optics, and the second complicates considerably the use of linear adaptive optics.

In the CW mode, the relative phase between the beams has to be carefully measured and controlled through a feedback loop to be able to coherently add the electric fields. In the femtosecond regime, the group delay and the phase delay have *a priori* different roles and should be considered independently. For pulses of duration of about 25 fs a static adjustment of the delay, along with an active correction of the phase, is sufficient to efficiently combine the pulses, because the pulse width is long compared to the optical cycle. A major difference for fs regime is also the group velocity dispersion, which has an impact on temporal pulse shapes as opposed to ns regime, and has to be matched in both arms to ensure a good time overlap to the pulses and retrieve the initial duration.

The propagation of two laser pulses relative to each other is characterized by their propagation direction, position, polarization and their temporal delay. To reach the highest intensity in the far-field when overlapping these two pulses, the propagation directions of both laser pulses have to be identical. With focusing by an ideal lens, the position of the laser pulses relative to each other is not critical and may be ignored. The polarization of the two laser pulses can be measured with conventional polarizers and adapted with wave plates. A delay between two laser pulses, however, can dramatically decrease the peak intensity and has to be aligned carefully. A change of the optical path length in one module by half wavelength will fully destroy phase locking – instead of interfering in phase and adding, the fields will interfere in antiphase and extract. To ensure that more than 90% of the maximum peak intensity has been actually reached, the deviation in the propagation direction needs to be smaller than $\pm 0.7 \mu\text{rad}$, and the delay between the two pulses smaller than $\pm 90 \text{ nm}$. In other words, time jitter must be below $\lambda/10$.

The mode of rarely (minutes) repeating pulses also imposes difficulties in phase locking. The fact is that for the linear adaptive optics (as opposed to the nonlinear one) a feedback signal is needed that allows real-time "alignment" of optical path length in different modules. Obviously, the pulse information obtained in the previous pulse (minutes

before) is hopelessly outdated. Consequently, the only possible strategy is to balance the optical path lengths in the modules immediately before the shot, but there is no guarantee that this balance will be preserved at the moment of the pulse because of the enormous energy directed in the form of the pump to the parametric amplifiers (KD*P crystals). If the amplifiers in all the modules are absolutely identical, then of course the optical lengths will change identically and their equality will not be violated. However, it is next to impossible to have in practice a large number of identical amplifiers, especially a large number of pump lasers of these amplifiers, given that the total energy of all pump lasers amounts to tens of kilojoules. The principal physical mechanisms of changing the optical path length of parametric KD*P crystal amplifiers are heat release in the crystal and nonlinear phase incursion caused by the quadratic and cubic nonlinearity.

As mentioned above, the optical path lengths in the modules must be identical to an accuracy not worse than $\lambda/10$. At the same time, it is very difficult even to formulate (the more so to experimentally verify) the demand for identity of pump lasers because the relationship between the pump energy and variation of the optical path length is very complicated and depends on many parameters. Rough estimates show that the difference in the intensities of the pump pulses should be about 1%. We intend to carry out both theoretical and experimental study of the impact of changes in optical path lengths in KD*P amplifiers during the pump. This will allow formulating final requirements for identity of phase locked modules.

Thus, phase locking of laser modules may be divided into two stages – slow and fast. At the first stage, the static optical path length difference in the channels, as well as in slow changes of these lengths is compensated using radiation from the pilot laser operating with high repetition rate. Static difference arises from the geometrical path difference, and also because of non-identity of diffraction gratings of the compressors. The latter is the most difficult, because the absolute phase of the beam can be influenced by the varying density of lines, their slope, and phase. For the precision control the gratings should be aligned over all six degrees of freedom. The experiments conducted in [52] demonstrate coherent beam combining of two femtosecond fiber chirped-pulse amplifiers seeded by a common oscillator. Using a feedback loop, a combining efficiency of 95% is obtained. The spatial and temporal qualities of the oscillator are retained, with a recombined pulse width being 230 fs.

To obtain a feedback signal it is necessary to measure the phase difference between the channels. Several methods were described in the literature, for instance [52-54]. In particular, a novel technique based on spectrally resolved far field for the coherent superposition of laser pulses was implemented in [54]. This measurement technique can

be used for coherent superposition of two or more laser pulses generated by different laser systems. The setup is able to monitor the delay and one propagation direction of the coherently added laser pulses. By doubling the setup orthogonally (e.g., by using a beam splitter) the second propagation direction can be observed. This technique was demonstrated in [55] and coherent superposition of two multiterawatt laser pulses generated in a tiled-grating compressor was implemented.

Thus, although being difficult, unsolved problem to date, phase locking of two multipetawatt modules may be implemented using available or more efficient novel techniques that will be developed as a result of new research.

Activity 1.6. Enhancing module power up to 15 PW

To date creation of a single module with an output exceeding 10 PW is problematic due to a number of limitations related primarily to the limited radiation resistance of dichroic mirrors and diffraction gratings. In addition, it is necessary to increase the pulse energy required for reliable attaining of such power. Therefore, first we plan to create (in a short time) two 10 PW prototypes (*Activities 1.3 and 1.4*) and then increase the power one and a half times.

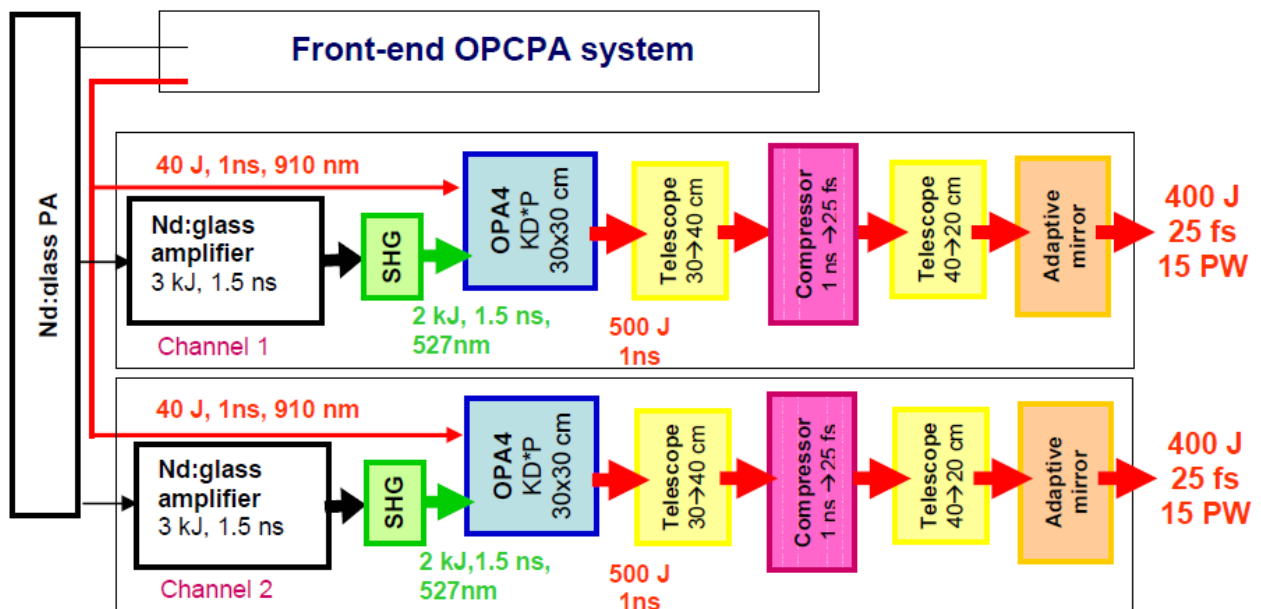


Fig. 3.19. Schematic diagram of two modules 15 PW each

This increase will be achieved by increasing the pump energy at the expense of increasing the efficiency of the output parametric amplifier, by increasing the grating damage threshold or enlarging their area (including in mosaic geometry), by shortening the pulse duration due to nonlinear broadening of its spectrum after compressor and

subsequent compression by dispersion mirrors. In the nearest years we expect substantial progress in many (if not all) of the mentioned areas, so the 1.5-fold power increase seems quite real. At the same time, rapid creation of a 10 PW module will initiate work on module phase locking (*Activity 1.5*) and research on laser-matter interaction (**Goal 2**) long before achieving the 15 PW power.

Figure 3.19 shows the schematic diagram of the two modules and the radiation parameters at key points.

Activity 1.7. Creation of electron accelerator with an energy up to 20 MeV based on a photocathode and microwave resonators

One of the directions of XCELS research is the interaction of intense laser radiation with bunches of charged particles. These bunches may be formed under the action of powerful laser radiation on the target, which ensures their synchronization with the laser pulse, but the quality of such bunches is not high and their repetition rate is limited. Using a conventional electron source based on microwave resonators it is possible to obtain electron bunches of good quality, and using a photocathode to synchronize the electron bunch with the laser pulse. The energy of the electron bunch of 100 MeV is chosen on the basis of the requirements for the parameters of electron bunch injection into a laser-plasma accelerator. Creation of such a source for the prototype is too expensive and labor consuming. At the same time, sources of electrons with the energy of 20 MeV are more accessible, but they enable unique experiments on electron injection into laser-plasma accelerator.

The basic accelerator elements are photoinjector (RF-gun with a photocathode) and a photocathode laser driver that allow synchronizing the source of e-bunches with laser pulse. These devices with parameters planned under the Project are described below.

Microwave cavity resonators with electric field component along the Z-axis operating in the 1-3 GHz range are the basic acceleration units in modern linear electron accelerators. This imposes certain requirements to the electron injector in accelerators. The injector of electrons in the accelerator must provide very short, about 1-10 ps bursts of electrons (bunches) moving strictly in one direction and with the same velocity. In the phase space of velocity coordinates, these bunches must occupy as small volume as possible. In other words, the electron bunches must have minimum emittance. Such electron bunches have maximum brightness and are in demand in today's applications, in the first place, in X-ray free-electron lasers, colliders, and others.

Photoinjectors are the most promising injectors emitting electron bunches with low and ultralow emittance. Electrons in such injectors are knocked out of the cathode by short laser pulses whose repetition rate must be accurately adjusted to the microwave radiation of the klystron feeding the injector resonator. Well known are the photocathodes that allow, with acceptable efficiency, emitting electron bunches with a charge up to several nC over a long period. The curve for a CsTe photocathode irradiated by picosecond laser pulses with wavelengths of about 0.25 microns is plotted in Fig. 3.20. It is seen from this figure that after a few days of photocathode operation, its efficiency reduces to 1%, but remains at this level for a long time.

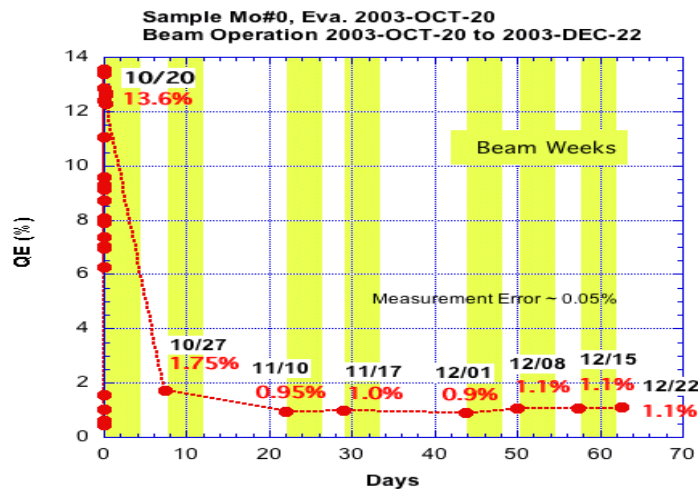


Fig. 3.20. The curve for quantum efficiency of CsTe photocathode

A CsTe photocathode is a thin (about several nm) film deposited on a metal substrate. The technology of producing such cathodes was mastered in several research centers (CERN, KEK, and others). The specific features of these photocathodes demand their storage in vacuum. Therefore, the cathodes are made either in the photoinjector or in vacuum. In the latter case, the fabricated cathodes are placed in a small vacuum container avoiding their exposure to air and transferred to the photoinjector. The container in vacuum is opened by a robot and the cathodes are installed at a fixed place in the injector.

The photoinjector schematic is presented in fig. 3.21. It can be seen in this figure that the electron bunch knocked out of the photocathode is accelerated in the sesquialteral microwave cavity to energies of 4.6 MeV.

Calculations show that for normal operation of the linear accelerator of electrons, the electron charge in each electron bunch must be 3-10 nC. This imposes requirements to the energy of each laser pulse at 1% cathode efficiency to be 1.4-4.7 μ J.

The photocathode laser driver is a laser meeting the photoinjector requirements. For efficient operation of electron accelerator, all electron bunches should be grouped into

macropulses with a repetition rate of 1-50 Hz. The number of bunches in a macropulse required in different tasks varies from a few hundred to tens of thousands. The macropulse duration is 1-1000 μs . These parameters impose requirements to the laser driver.

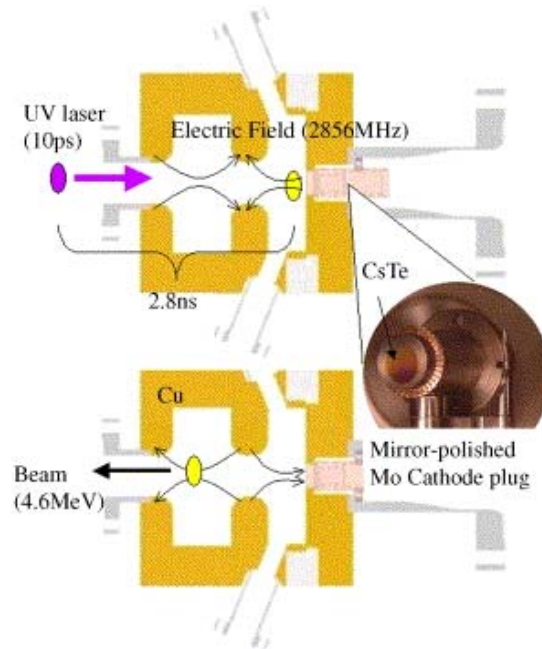


Fig. 3.21. Photoinjector schematic

Below we describe the laser driver fabricated by IAP RAS team for the photoinjector of the superconductor test facility (STF) at KEK, Tsukuba, Japan. A full list of requirements to the laser driver is given in Table 1. The driver output cascades are made on the basis of rod amplifiers with lamp pumping. The master oscillator, preamplifiers and system for forming the pulse train envelope in the laser are fiber-based.

Macropulse duration	900 μs
Macropulse fronts	0.3 μs (by the 0.1-0.9 level)
Contrast (ratio of pulse power noise to micropulse power) above 50 microseconds	1:500
Micropulse duration	8-12 ps
Standard RMS deviation of micropulse duration	1%
Repetition rate of micropulses	2.708 MHz \pm 1.3 KHz with 50-100 Hz fluctuation
Number of micropulses in the macropulse	2437
Wavelength	260-266 nm
Micropulse energy	1.4 μJ
RMS deviation of micropulse power (10 successive pulses)	3%
RMS deviation of micropulse energy (throughout the 900 ms pulse)	10%

Table 1. Requirements for laser driver of KEK-STF photoinjector

The optical scheme of the laser driver is presented in Fig. 3.22. The driver consists of the fiber part (fiber master oscillator (MO), acousto-optic modulator (AOM), and two preamplifiers), beam forming circuit (spatial filter and "soft" aperture), a two-pass two-cascade Nd-YLF rod amplifier with Faraday isolation, and generators of the second and fourth harmonics (SHG and FHG).

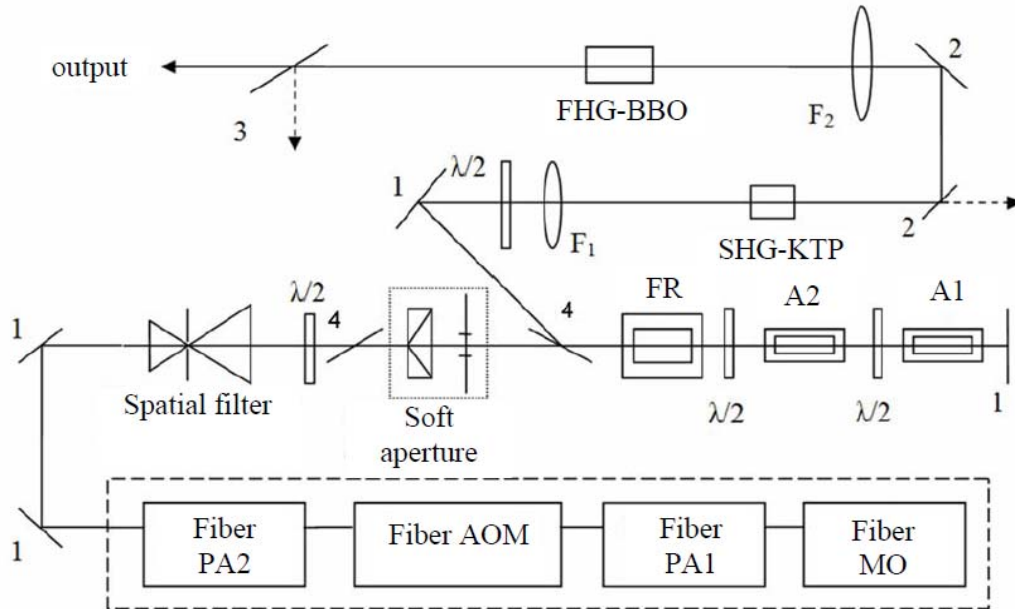


Fig. 3.22. Optical scheme of laser driver

It is clear from the Table that besides the constant micropulse energy in each macropulse, rather strict requirements are imposed to the micropulse repetition rate. This determines the choice of fiber laser for master oscillator. In a fiber oscillator with ytterbium-activated fiber operating in the self-locking mode without Q-switching, the pulse repetition rate is very stable and is determined only by the optical radiation in the cavity. It is quite convenient to match this frequency to the frequency of the RF accelerator klystron by mechanical stretching of the laser fiber cavity.

Mode locking is attained by means of a semiconductor saturable mirror SESAM. To change the pulse repetition rate, elements changing length are introduced into the linear resonator of the master oscillator. Coarse frequency change is accomplished by means of an air gap in the resonator, and fine tuning by expanding the active resonator fiber on the piezocylinder. Coarse tuning is done within the range 40.65-40.585 MHz, i.e. ± 32 kHz, while fine tuning changes the frequency within ± 230 Hz with the voltage applied to the piezocylinder being ± 200 V. The voltage of 23 V at the piezocylinder corresponds to one step of a linear translator. Both these tunings are easily incorporated into the automated cycle of frequency tuning with reference to the frequency standard or to an external signal, for example, the RF photoinjector cavity signal.

The repetition rate of laser pulses in a fiber laser fluctuates in a very narrow range of about 10 Hz. The average pulse repetition rate after a half-hour warm-up changes slightly and only if the ambient temperature changes. The average output power of MO is 2 mW, which corresponds to 50 pJ energy of micropulses. Fluctuations of the average power during 4 hours do not exceed $\pm 0.5\%$. The micropulse duration is 10 ps.

Fiber preamplifier, similarly to fiber MO is based on active ytterbium lightguide with fiber pumping. An optoacoustic modulator is placed between two amplification cascades (Fig. 3.22). The modulator has the following functions. First, it transmits every fifteenth pulse and reduces the pulse repetition rate to 2.708 MHz. Second, it forms from a continuous pulse sequence macropulses rectangular in time with the duration of 900 microseconds. Third, it is used to control the macropulse envelope (see below). At the output of pre-amplifier 2 (PU2), the power of the micropulses rises to 1600 W.

Peak laser power of fiber pre-amplifier is limited in our case by cubic self-focusing at the level of 1600 W, i.e. the micropulse energy at pre-amplifier 2 output is $W = 16$ nJ. To increase the radiation power to the desired level (Table 1), we use two rod amplifiers with active elements of Nd-YLF (diameter 5 mm, length 90 mm) with π - orientation.

To attain a rectangular shape of the output macropulse it must first be distorted so as to compensate for the time inhomogeneity of the amplification. This may be realized thanks to the capability of the control circuit of the acousto-optic modulator to control macropulse passage in time. Knowing the shape of the experimental time dependence of the gain and input radiation energy density we can calculate the time dependence of the AOM transmission coefficient such that the shape of the macropulse at the laser output should be rectangular. However, because of the inhomogeneity of radiation intensity in the amplifier section, these calculations do not give the required accuracy. Therefore, we use an iterative procedure of compensating temporal inhomogeneity of the gain. In each iteration we measure RMS deviation of macropulse power from average power. One iteration takes 10-20 macropulses. Correction is completed, if the RMS deviation from a flat-top macropulse does not exceed 2%.

The fourth harmonic of laser radiation is achieved in two stages: doubling and quadrupling of frequency generation (SHG and FHG). By the combination of three parameters characterizing the crystal: effective nonlinearity, angular phase-matching bandwidth and frequency phase-matching bandwidth, a KTP crystal is most suitable for SHG. As seen from Fig. 3.23, the maximum radiation efficiency conversion from the fundamental to the second harmonic is 55-60%.

When determining the most preferable crystal for FHG, in addition to the above mentioned criteria for effective SHG transformation, the strong influence of thermal self-radiation at the fourth harmonic must also be taken into account. Linear or two-photon absorption of fourth harmonic radiation and absorption centers formed in the crystal bulk may be used as sources of heat at thermal self-action. The latter factor may be especially important. After preliminary experiments, we chose as a radiation converter to the 4th harmonic a BBO crystal. As seen from Fig. 3.23, maximum conversion efficiency from the fundamental to the fourth harmonic is 27%, and from the second to the fourth 49%.

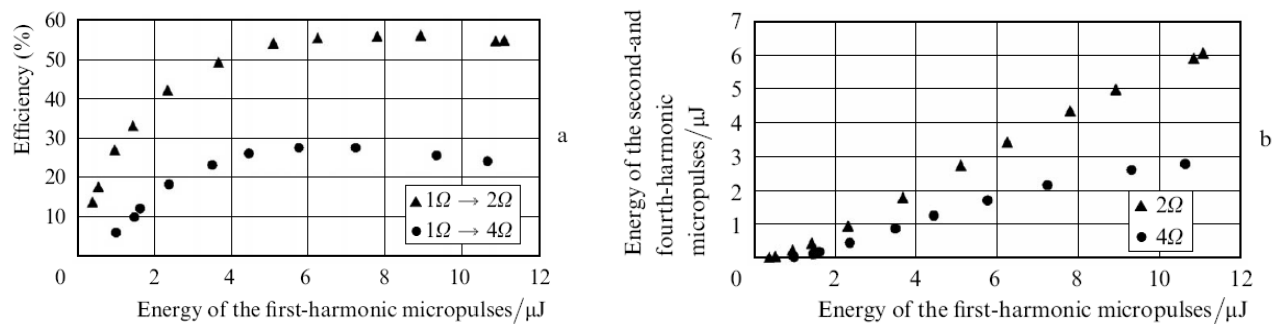


Fig. 3.23. Micropulse efficiency (a) and energy at harmonics as a function of micropulse energy at the fundamental harmonic (b)

As mentioned above, due to the temporal inhomogeneity of gain of the terminal rod amplifiers, the macropulses at the output of the fiber amplifier are two-humped. To eliminate this, a system forming a macropulse envelope was developed. Such a system controls passage of all 2437 pulses by means of AOM. Control signals are produced by the microprocessor as a result of analysis of the macropulse envelope obtained by means of the envelope photodiode – oscilloscope – PC chain. If the fundamental harmonic radiation is used for analysis, only a pulse for the fundamental harmonic is guaranteed to be rectangular, but there is no guarantee that the output radiation envelope will also remain rectangular. This occurs because the efficiency of conversion to harmonics may change during macropulse due to thermal effects. If the fundamental harmonic envelope is corrected, the pulse envelope of the second harmonic will slightly differ from the rectangle, even at full output power. This suggests small influence of thermal self-action in the KTP crystal at SHG. However, this is not the case when the second harmonic is converted to the fourth one.

Figure 3.24 shows two pairs of macropulse oscillograms: for the correction of pulses of the fundamental and fourth harmonics. The figure shows that if a good pulse shape is obtained at the fundamental harmonic, the pulse at the fourth harmonic will decay monotonically. When the correction is made by the pulse at the fourth harmonic, this pulse

will have a rectangular shape. But in this case the macropulse of the fundamental harmonic will increase in time. This reduces the efficiency of the system as a whole, but allows obtaining a rectangular macropulse.

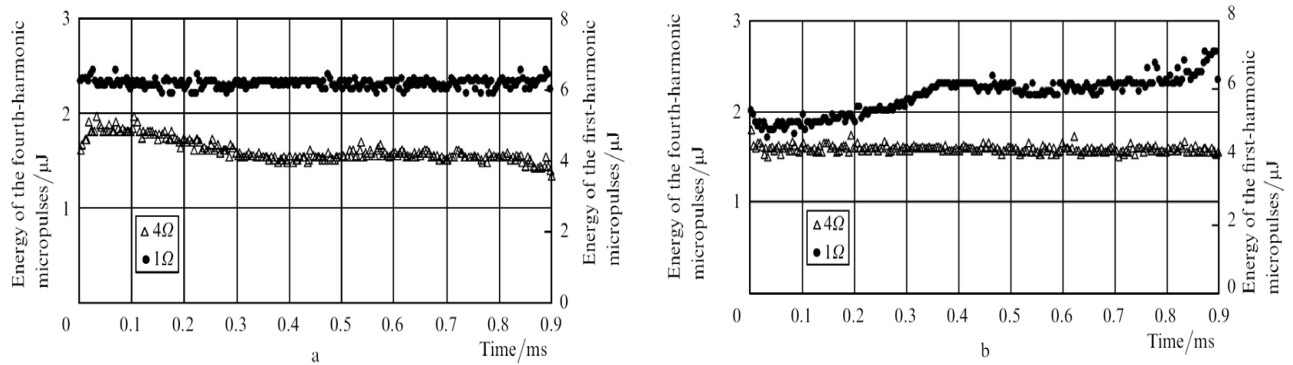


Fig. 3.24. Oscillograms of macropulse at the fundamental and fourth harmonics with correction by pulse shape of the fundamental harmonic (a) and fourth harmonic (b)

Testing the laser driver shows that the RMS deviation of power normalized to its average value is 2.5% for the fundamental harmonic, 3.6% for the second, and 2.3% for the fourth one. On a short time interval of about 3 minutes, this value is 0.5% for the fourth harmonic.

The laser system described above was manufactured and tested at IAP RAS, then disassembled and transported to KEK (Tsukuba, Japan), where it was assembled, tested and commissioned to the premises of the constructed prototype of the International Linear Collider (STF facility) [56]. The inside view of fiber MO driver is shown in Fig. 3.25. On the left one can see a piezodrum providing smooth tuning of the repetition rate of micropulses; in the right bottom corner, SESAM unit on linear translator is located that provides coarse tuning of the repetition rate of micropulses. The general view of the laser driver is demonstrated in Fig. 3.26. The laser driver is described in detail in [57, 58].



Fig. 3.25. Inside view of fiber MO of laser driver



Fig. 3.26. General view of laser driver

Activity 1.8. Creation of a prototype laser with 1 kHz pulse repetition rate

A prototype of a femtosecond (~ 20 fs) laser with kilowatt average power and peak power of tens of terawatt will have the following architecture: master oscillator, stretcher, BBO or LBO crystal parametric amplifiers, vacuum compressor, and system of radiation focusing on the target.

A block diagram of the laser is shown in Fig. 3.27. The master oscillator is an original fiber femtosecond laser developed at IAP RAS, which generates two phase-locked and frequency-shifted femtosecond pulses at the wavelengths of $\sim 1.8 \mu\text{m}$ (20 fs, 1 nJ), and $\sim 1 \mu\text{m}$ (180 fs, 100nJ) [59].

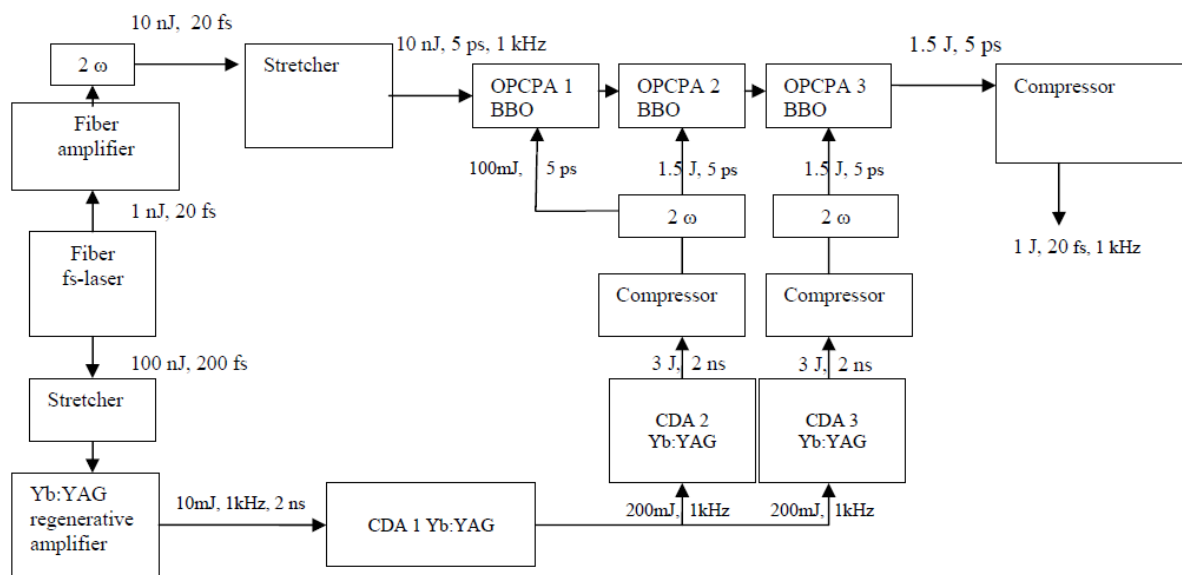


Fig. 3.27. Block diagram of the laser

The first pulse will be the signal to be amplified, the second will act as a pump for parametric amplifiers. The first pulse will be stretched to a length of ~ 5 ps in the stretcher. The second pulse after the stretcher and the regenerative amplifier will acquire an energy of ~ 10 mJ per pulse of nanosecond duration. Then, the second pulse will be amplified in the cryogenic disk amplifier CDA1 to 0.5 J and divided into two parts, each of which will be amplified to 3 J (each channel) in identical cryogenic disk amplifiers CDA2 and CDA3. After compression and frequency doubling, both parts of the second pulse will accomplish parametric pumping in three BBO crystals. As a result of parametric amplification and subsequent compression the first pulse with a duration of 20 fs will acquire the energy of 1 J.

The basic element of the prototype laser is the pump of parametric amplifier. We will address it in more detail. The parametric amplifiers are pumped by the second harmonic of the original laser on disk active elements [60] made of Yb: YAG laser ceramics and cooled to cryogenic temperatures. Inversion in the active elements is accomplished by high-efficiency diode pumping with cw fiber output.

The optical scheme of the cryogenic disk laser consists of two parts. The first of them – CDA1 preamplifier – provides a subjoule pulse and is a 4-pass 2-cascade amplifier based on active elements with a diameter of 15 mm and a thickness of ~ 1mm. The cryostat of the prototype quantum amplifier developed in IAP RAS is shown in Fig. 3.28.

The second part – two channels – are two identical cryogenic disk amplifiers CDA2 and CDA3, each of which is an 8-pass 2-cascade amplifier based on composite active elements with a diameter of 30 mm and a thickness of ~ 1 mm. Continuous power of diode pumping for each active element will be 6-8 kW. Cooling of the active element will be implemented from the edge and from the lateral surface of the active element, for which a flow cryostat with liquid nitrogen as coolant will be developed.



Fig. 3.28. A prototype cryogenic laser amplifier

Activity 1.9. Establishing and equipping a laboratory for studying laser-matter interaction

The laser-matter interaction will be studied not only on the 200 PW laser (*Objective 3*), but also on the prototype in the experimental laboratory. Towards this end, several target chambers will be created and equipped with appropriate equipment.

The goal of these experiments is modeling (for a relatively low power) of the experiments planned in the main target chamber and finishing of the diagnostic equipment. In line with these requirements, activities will be focused on developing the concept and creating in the laboratory of a system of laser beam and electron bunch delivery, as well on equipping of experimental laboratories with necessary equipment.

It is important to note that these studies will be started much earlier than it will be possible to conduct such experiments on the 200 PW laser.

Objective 2. Construction of buildings and utilities

The XCELS buildings will include the following premises:

- premises for the experimental equipment, "clean" rooms for the 200 PW laser facility and for the complex of powerful femtosecond lasers with high average power for innovative applications, tunnel for the source of electrons with an energy of 100 MeV on the basis of the photocathode and microwave resonators, room for the main target chamber, laboratories for experimental research, computer-communications center, engineering and auxiliary shops;
- engineering infrastructure: boiler room, transformer unit, parking lot, etc.;
- premises for the employees of the center: offices, conference rooms, dining room, hotel complex.

In addition to the activities aimed at design and construction, *Objective 2* includes activities involved with choosing construction site, allocation of a plot of land, and registration of relevant legal documents. These works are already underway in collaboration with the Government of the Nizhny Novgorod region.

Prospective view of the complex



Objective 3. Creation of 200 PW laser

The radiation power of 200 PW is more than two orders of magnitude higher than the world record. It will provide superiority of the created facility not only at the time of its creation, but also for many years to come. The laser complex with an output power of 200 PW is the core of the Project, its creation is the key and most expensive objective of the Project. *Objective 3* comprises two preparatory activities (3.1 and 3.2), five activities aimed at creating the laser complex proper (3.3 - 3.7), transportation of twelve laser beams to the main target chamber and other laboratories (*Activity 3.8*), and putting the complex into operation (*Activity 3.9*).

Activity 3.1. Preparing documentation for 200 PW laser

Detailed Project documentation will be developed on the basis of available experience and the experience that will be gained during construction and exploitation of the prototypes of two modules (*Objective 1*).

The general scheme is presented in Fig. 3.29.

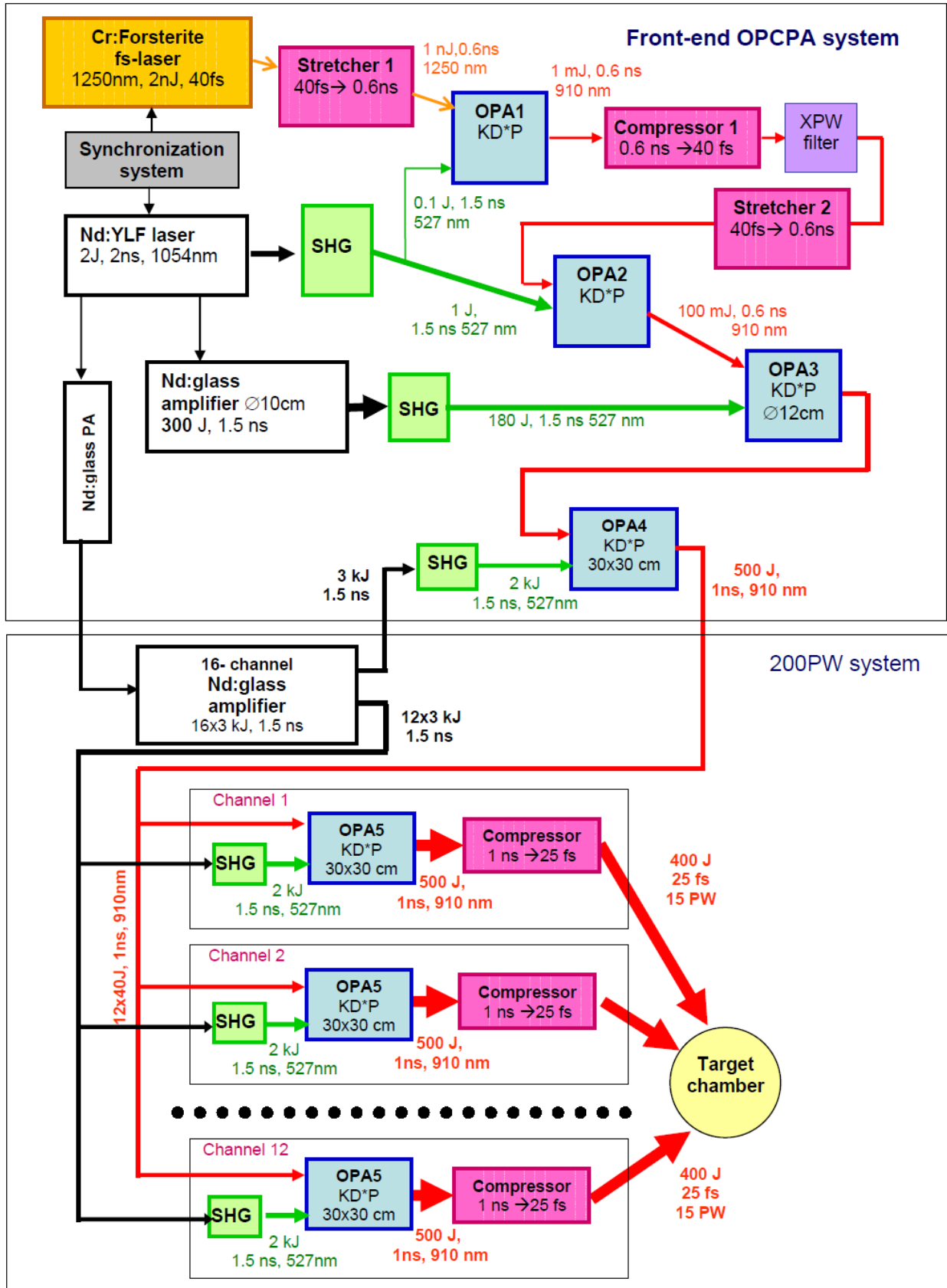


Fig. 3.29. General scheme of 200 PW laser

Activity 3.2. Development of appropriate technologies

Creation of the 200 PW laser complex will be preceded by development of the required key technologies (*Activity 3.2*):

- melting and polishing of neodymium glass,
- fabrication of pump lamps,
- production of diffraction gratings,
- growth of large-aperture nonlinear crystals,
- deposition of resistant thin-film coatings with preset dispersion properties,
- fabrication of adaptive optics.

To date, Russia has different levels of the development of these technologies in terms of achieving parameters needed for successful project implementation.

The absolute leader in melting and polishing of large-aperture neodymium glass in Russia is the Scientific Research and Technological Institute of Optical Materials. The slabs created at this Institute for beams with the aperture of 20 cm are used in the “LUCH” facility (RFNC-VNIIEF). However, the requirements to the size (beam aperture of 30 cm) and, most importantly, to the quality of the slabs under the XCELS Project are much more stringent, which will require improved technology.

Fabrication of pump lamps has a long history that began at the dawn of the laser era. Experience in building large laser facilities gained in recent years in RFNC-VNIIEF, IAP, GPI, and other centers showed that we have a technology of producing lamps, but not all parameters of the lamps meet the requirements of the Project. This refers primarily to the stability of parameters from sample to sample, and to the lifetime of lamps with a large number of flashes. In addition, the size of the lamps used even in the “LUCH” facility is much less than that to be used in the Project. Note that the pump lamps are broadly employed in laser technology and have a large market both in Russia and abroad.

The diffraction gratings used in the petawatt facilities “PEARL” (IAP RAS) and “FEMTA” (RFNC-VNIIEF) were produced by the St. Petersburg company “Holograte”. They can serve as prototype gratings for the 200 PW laser, but their size, damage threshold, efficiency, and spectral band should be increased substantially. The French company Horiba, for example, may be an alternative supplier of gratings.

The growth technology of large-aperture nonlinear crystals for second harmonic generation, the Pockels cell and for parametric amplification is available at IAP RAS. The size of the grown crystals (40 cm aperture) even exceeds the requirements of the Project

(30 cm), but the damage threshold and optical quality should be improved. In addition, the technology of growing thin crystals required for frequency doubling of femtosecond radiation (diameter 30 cm, thickness 400 μm) is at its first stages so far.

Resistant thin film coatings with preset dispersion properties are not produced in Russia, to the best of our knowledge. At the same time, a vast experience of work with deposited thin films is a promising sign of a possibility of developing such a technology.

ILIT RAS has gained rich experience in fabricating adaptive optics. However, their technology needs further development, taking into consideration the high requirements of the Project to the transverse resolution of adaptive optics and to the depth of phase modulation.

It is important to note that this activity will be completed before completion of the construction of the buildings of the complex (*Objective 2*).

Activity 3.3. Creation of the common front end

Creation of the common front end will also be started prior to completion of the construction of buildings for the two prototypes. Later on the front end will be moved and put into operation in the main building of the center.

Despite the general principles of construction, the front end of the 200 PW laser differs significantly from the front end of the prototype of two modules, as the energy of the output pulse of signal radiation must be an order of magnitude higher. The required energy level ($500 \text{ J} \approx 12 \times 40 \text{ J}$) corresponds to the output energy of one of the channels of the prototype. Thus, for creation of the front end of the 12-channel 200 PW laser, the front end of the prototype must be supplemented with one more cascade of parametric amplification with an aperture of $30 \times 30 \text{ cm}$. This cascade will be pumped by the 2nd harmonic radiation of one of the channels of a 16-channel Nd:glass amplifier (see Fig. 3.29). 12 more channels of the amplifier will be used to pump the output parametric amplifiers in 12 modules. The remaining 3 channels will be reserve ones or will be used to create subpicosecond multipetawatt channels based on CPA at wavelength of 1054 nm.

Activity 3.4. Creation of twelve modules

Creation of twelve modules (*Activity 3.4*) will start with collecting a set of basic components immediately after launching the prototype of the first module (*Activity 1.3*). Upon completion of the construction (*Activities 1.3* and *1.4*) and phase-locking (*Activity 1.5*) of two prototypes, final details of the scheme will be determined, which will enable completing collecting components and further assembly, aligning, debugging,

synchronization, and testing simultaneous operation of 12 modules that have not been phase locked.

To ensure pumping of the parametric amplifiers of the 200 PW laser 13 identical channels will be required (12 channels for twelve 15 PW modules and 1 for the front end system) that were described earlier in *Activity 1.3* (creation of the prototype). However, despite the fact that the optical system of the channels should repeat that of the prototype channels, structurally they must differ greatly.

The total of 16 channels are planned, in groups of 8 channels. Simultaneously 13 channels will operate in the 200 PW laser. Radiation of the remaining 3 channels can be used either as an independent source of light in other applications, or as a reserve in case of repair of some of the main channels. Grouping of channels into a matrix of 8 pieces each (as is done in the NIF and LMJ facilities and is planned in UFL-2M) imposes severe structural changes in the pump laser.

The general view of one half of the matrix of 2×4 amplifiers is shown in Fig. 3.30. As is clear from the figure, laser beams collected in the matrix of 2×4 pieces can make the whole facility more compact and the amplifiers may be illuminated by fewer lamps. Instead of $384 \times 8 = 3072$ lamps with simple scaling of single channels, 640 longer lamps will be sufficient with grouping of channels in matrices of 2×4 pieces.

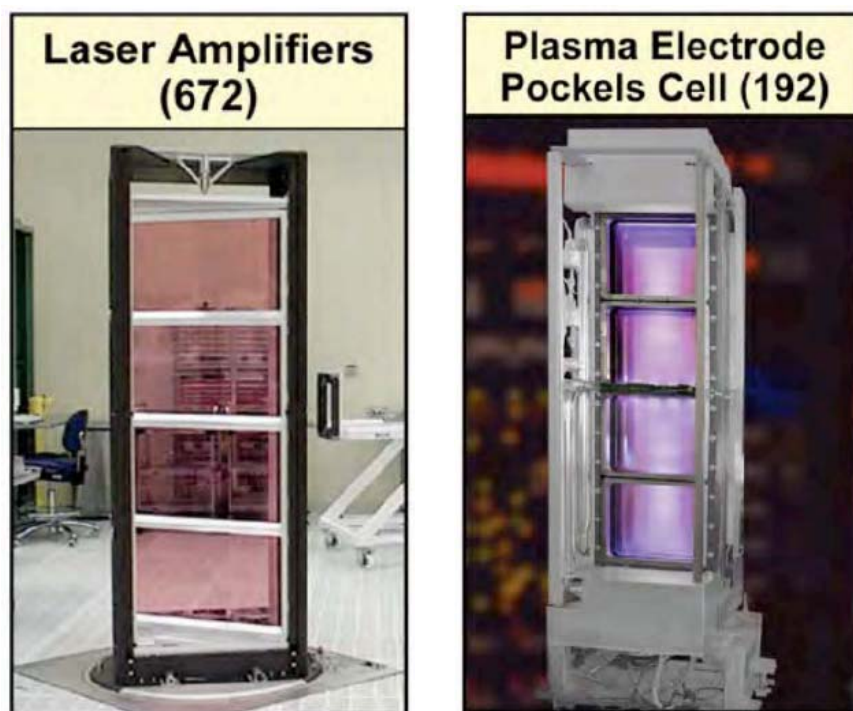


Fig. 3.30. General view of one half of the matrix of 2×4 amplifiers (left) and large-aperture Pockels cells with plasma electrodes (right) of NIF

Pockels cells must also be grouped in matrices. A general view of one half of the matrix of large-aperture Pockels cells with plasma electrodes in the NIF facility is presented in Fig. 3.30 (left). The plasma electrodes that are transparent in the optical range enable supplying high voltage to the end surfaces of the plasma Pockels cell and controlling laser beam polarization.

An effective radiation converter to the second harmonic (1055 nm to 527.5 nm) must be placed at the pump laser output. Towards this end, large-aperture (30×30 cm) KD*P crystals are required. They must also be grouped in matrices of 2×4 pieces.

The spectral and energy characteristics are assessed as described in *Activity 1.3*. It is assumed that the signal energy at the input of the last cascade of parametric amplification of the front end of OPA4 is 40 J and 1/12 of the signal amplified in it is injected to the input of each of the 12 terminal OPA5 amplifiers. The calculations show that the optimal length of nonlinear amplifier elements is 4 cm (see Fig. 3.31). Pulse shape (and hence spectrum shape) of signal radiation at the OPA4 input and output and at the OPA5 output is shown in Fig. 3.32. The signal energy at the OPA5 output is 530 J.

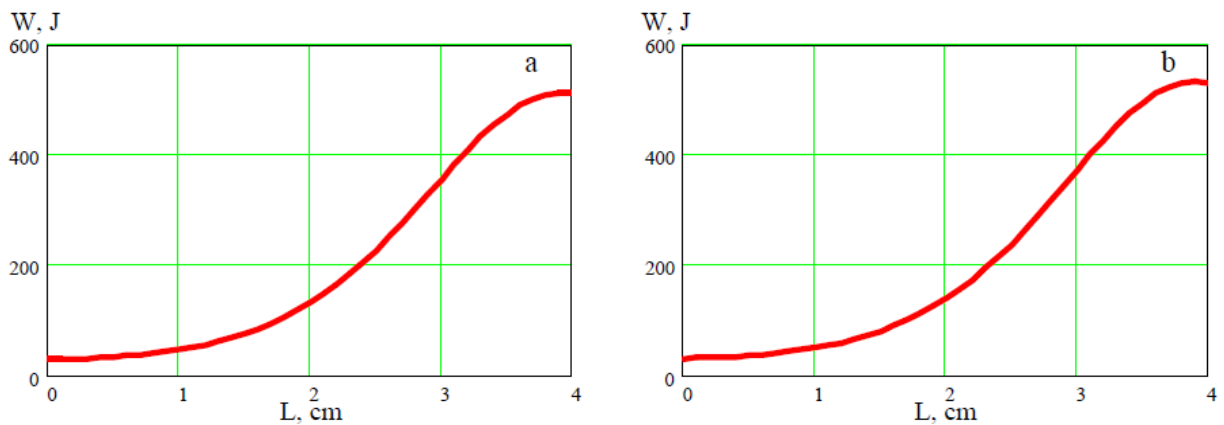


Fig. 3.31. Signal energy versus length of the nonlinear element in OPA4 (a) and OPA5 (b) amplifiers

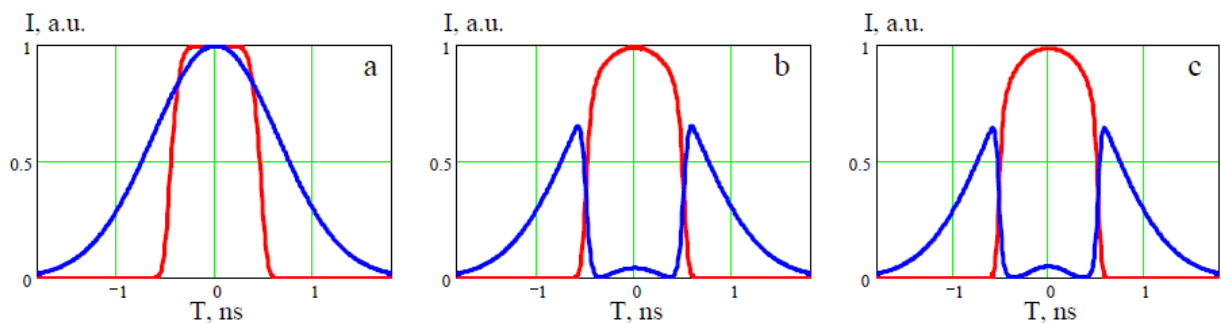


Fig. 3.32. Signal pulse (red) and pump pulse (blue) at the OPA4 input (a), output (b) and the output of terminal parametric amplifier OPA5 (c)

Activity 3.5. Phase locking of twelve modules

Activity 3.5 begins immediately after creation of the front end (*Activity 3.3*). Experiments of phase locking of 12 modules without laser beam enhancement in the modules will be carried out. They will enable testing the majority of the functional parameters of the system of phase locking before creation of the 12 modules. Debugging and refinement of phase locking of power modules will start on completion of *Activity 3.4*.

Phase locking of twelve multipetawatt modules is undoubtedly a more complicated task than phase locking of two modules in terms of technological and technical aspects. At the same time, the physical basis detailed in *Activity 1.5* remains unchanged.

Note that phase locking of twelve modules is closely linked to the performance of adaptive optics. On the one hand, it is difficult to phase lock beams with large aberrations, as the phase measurement process is difficult (strictly speaking, this refers to phase locking of two beams also, but restrictions on maximum amount of aberrations are much more stringent for twelve beams). On the other hand, the adaptive mirror is the most simple and elegant way to adjust the absolute phase in each module. At the same time, correction of aberrations in each channel (adaptive optics) and adjustment of the absolute phase of each channel (phase locking) are two processes controlling the radiation phase, each of which requires a feedback loop. For stable operation these feedback loops must work independently, without cross influencing each other. From this point of view the use of a single optical element (adaptive mirror) to control aberrations as well as absolute phase may prove to be unreliable. In this case, the absolute phase of each module will be controlled by a conventional mirror moved across its surface by a mechanical motor (actuator).

Thus, being a complex, unsolved yet problem, phase locking of twelve multipetawatt modules may be solved either using already developed methods, or even more effective new techniques that will emerge as a result of the research.

Activities 3.6 and 3.7. Creation of the system for diagnostics and control of 200 PW laser

The diagnostics and control units are important parts of the complex laser system that allow quick and flexible control of operation in automatic mode. The use of automation significantly increases the number of control points that may reach several thousands. The key elements of the system for diagnostics and laser control will be worked out already for the 10 PW system (see Activity 1.3).

Each channel of the pump laser will comprise in addition to the amplifiers a great amount of optical elements: mirrors, lenses, apertures, and a system of optical pumping of active elements with flash lamps. The length of each channel is of the order of 150 m, some elements of the scheme (main amplifier) will be assembled based of a multi-pass scheme. Thus, for the control of normal (standard) operation of the pumping system diagnostics of laser radiation along its propagation path should be provided. It is necessary to enable automatic adjustment of the key optical elements of the pump laser.

Some elements of the diagnostics and control of the NIF experiment described in [61] are shown in Fig. 3.33. We plan to use a similar architecture.

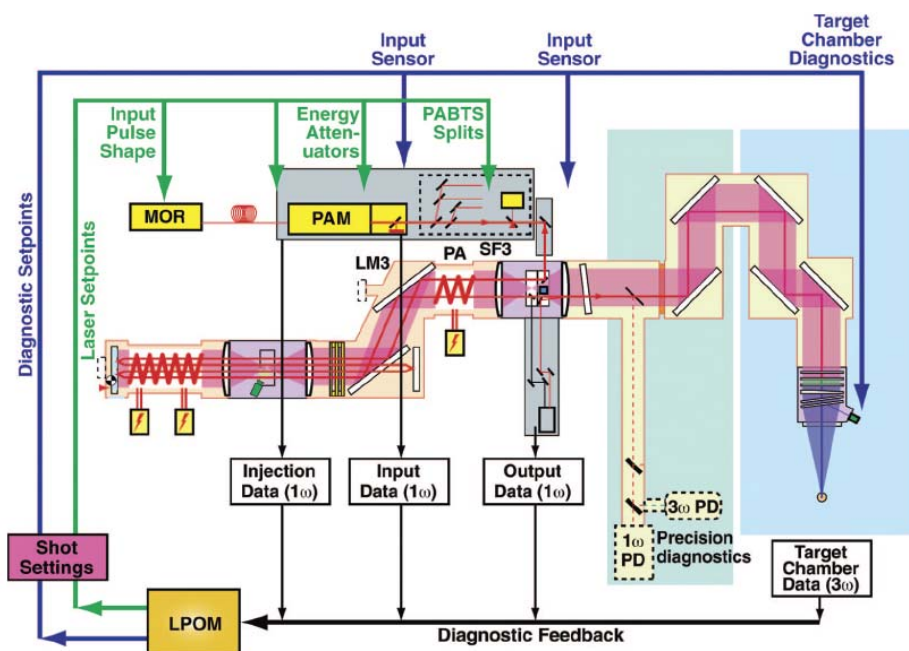


Fig. 3.33. Illustration of laser performance operations model (LPOM) shot setup process [61]. High-level shot goals and laser configuration data are read by the LPOM and used to generate shot set points for the injection laser system and for diagnostic systems. Shot data is fed back to the LPOM for postshot analysis and for optimization of laser models

A large number of optical elements, including spatial filters will be located between the parametric amplifier cascades, as well as in the pump system. To control the quality of surface and bulk of nonlinear crystals that are the main elements of the parametric amplifier, the quality of mirrors and other optical elements of the scheme, the position of all

the optics, the complex will have a system for adjusting the optical units that will be based on stepper motors with remote control.

For the convenience of automatic adjustment of the optical elements the entire laser tract will be illuminated by low-power radiation from additional alignment (pilot) lasers. The lasers must have a wavelength and polarization of the radiation close to the corresponding characteristics of the pump or signal.

Measurement of the alignment laser beam position will allow adjusting different optical components of the laser system. For this, sensors of the near and far fields of the beam will be installed behind the main folding mirrors of the system. On receiving information from the sensors of alignment of the laser beam position special software will send control signals to the stepper motor of the translators and rotatory devices of optical elements.

The radiation of the alignment laser of the pump system in time consists of short (about 1 ps) pulses with high repetition rate. The ideal candidate for this is radiation of a fiber laser operating in CW Mode Locking. The pulse 1 ps radiation mode allows time synchronizing to high accuracy (0.1 mm) pulses from different channels. This is achieved by means of streak cameras measuring temporal mismatch between different channels of the pump laser.

The diffraction gratings inside the vacuum compressor will be controlled analogously, i.e., by means of translators and rotatory devices. The system for controlling and adjusting chirped pulse compressor also includes telescopes and autocollimators equipped with CCD-cameras, and additional sources of laser radiation. The controls of the diffraction grating of the subpetawatt facility "PEARL" in IAP RAS can be visualized in Fig. 3.34.

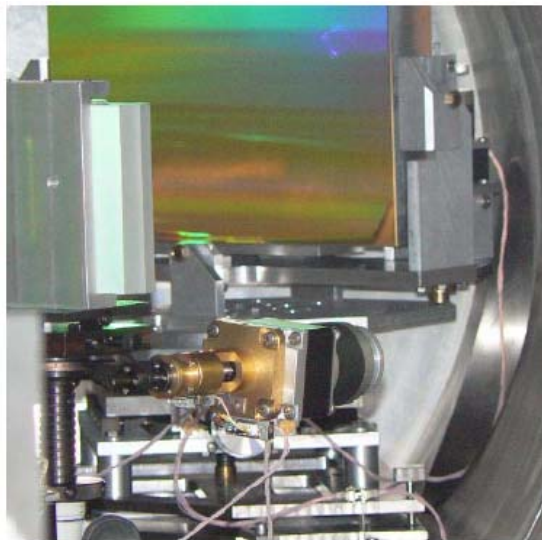


Fig. 3.34. Control elements of the diffraction grating of the subpetawatt facility "PEARL" in IAP RAS

Another important element of controlling the laser system is measurement of the spatial, temporal and energy characteristics of radiation at key points of the laser scheme. Such monitoring is necessary in connection with the requirements for laser beam pumping: uniform intensity over the cross-section and high energy parameters close to the damage threshold for optical elements of the laser.

For the diagnostics of spatial, temporal and energy parameters of the primary emission of the laser, diagnostic stations will be developed that measure the energy, near and far zones of the beam, radiation depolarization, and temporal parameters of laser radiation at each flash. These stations will be installed at the inputs of the main and start-up amplifiers, at the output of the main amplifier after each passage, and at the output of the entire pump system. They will also measure the characteristics of the signal radiation on its path between the cascades of the parametric amplifier at the compressor input and output.

In addition to the diagnostics of optical elements, electrical circuits are to be controlled. Sensors that measure the time dependence of the discharge current of the lamps will be installed in the power supply circuit of flash lamps pumping the active elements of the amplifiers. 640 lamps must be monitored. Therefore, 640 current pulses must be registered in every shot. It is also important to have information on the energy in the capacitor battery before and after the shot, information on the characteristics of the discharge circuit, for example, on the preionization pulse in the lamps, the voltage in the lamps, etc.

Thus, within the framework of the objective of creating a system for diagnostics and control of the laser complex, the equipment enumerated above must be created and put into operation, that will provide information on functioning of individual components and the whole system. Preliminary estimates show that at least 3000 parameters must be monitored simultaneously in the proposed complex. Software and hardware will be developed for collecting and storing the information. In addition to primary processing of the results of measurement of various parameters in the experiment, the software should also provide information on the operation of the facility as a whole, so as to prevent any unexpected situations in the operation of the complex.

Activity 3.8. *Transportation of twelve laser beams to the target chamber and to other laboratories*

For using the radiation of the 200 PW laser in physical experiments all the 12 beams must be delivered to the main target chamber and to other laboratories. The main difficulties in creating a system of transportation are a large diameter of laser beams (not less than 20 cm), the need to provide vacuum on the entire route from the laser pulse compressor to the target, and precision focusing and control of the optical path with an error much less than the wavelength.

The geometry of feeding 12 beams is determined by the geometry of focusing at which the focus field intensity is maximum. A detailed theoretical analysis of this problem (see *Objective 6*) shows that the optimal configuration is that with the laser most closely describing the directivity pattern of the dipole located at the center of the focus. In this respect, the double-circle geometry shown in Fig. 3.35 is most effective. The focus intensity obtained by numerical solution of Maxwell's equations is more than twice the intensity at focusing one beam with a power of 200 PW.

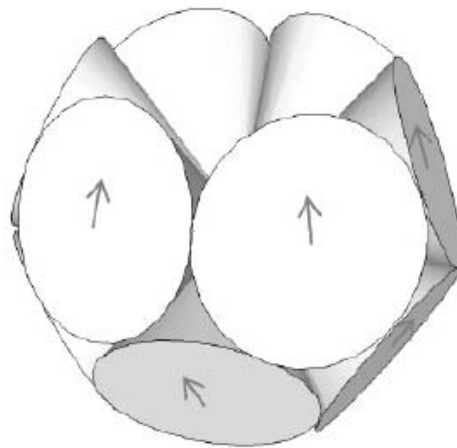


Fig. 3.35. The double-circle geometry

Objective 4. Creation of a complex of high-average-power femtosecond lasers for innovative applications

The 200 PW laser (*Objective 3*) is undoubtedly the key XCELS element, but not the only one. This record power is attained at the expense of a small pulse repetition (once in a few hours). For a number of applications, especially innovative ones, such a low repetition rate is unacceptable, but such enormous power is not needed either. In this regard, an important component of the XCELS Project is creation of a complex of high-intensity femtosecond lasers with high repetition rate (1 Hz to 10 kHz) and relatively small power up to 1 PW. This complex, being complementary to the 200 PW laser, will use the same engineering and technical infrastructure for physical applications (*Objective 2, Activities 5 - 10*). In addition, the synchronization of the 200 PW laser with the lasers operating with a high repetition rate will open up wide opportunities for their application for the diagnostics of the interaction of 200 PW radiation with matter.

The OPCPA technique has several advantages permitting its use not only for achieving a power of 200 PW, but also for the development of petawatt power lasers operating with high repetition rate (from a few Hertz to kiloHertz). First of all, it should be noted that in contrast to the CPA, in OPCPA the difference in the quantum energy of the pump and the signal is not released in the crystal in the form of heat, because it is extracted by the idle wave. This opens up opportunities to work with a high repetition rate, with low thermal loads and, consequently, a diffraction-limited beam. Moreover, the amplification band provided by nonlinear LBO crystals exceeds the amplification band even of the Ti:sapphire crystal that is the champion among the CPA lasers. Thus, it becomes possible to achieve not a record, but a fairly high power and high repetition rates at relatively low pulse energy, and therefore at low pump energy [62].

Activity 4.1. Developing the concept of a laser complex with high repetition rate

Several laser projects with high peak and average power are available worldwide today. These include "Lucia" [63], "Halna" [64], "Mercury", "Polaris" [65], and "Genbu" [66] projects. Some of them have not been completed yet; it is expected that they will achieve the maximum energy of 10-30 J in the near future.

All these laser systems use diode pumping, some of them use cryogenic cooling of active elements. For example, a cryostat (Fig. 3.36) is currently developed under the "Lucia" project [67] in which an active element is blown by gaseous helium, which in turn is cooled by liquid nitrogen (Fig. 3.37).

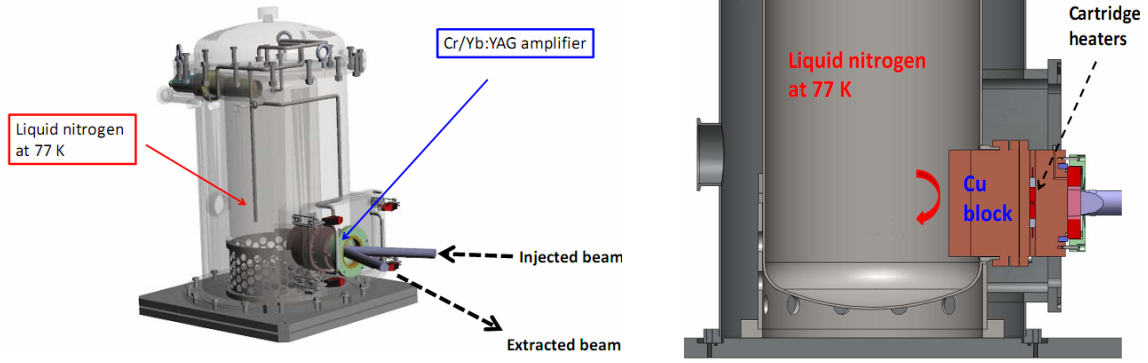


Fig. 3.36. Cryostat in the "Lucia" project

Composite Cr⁴⁺/Yb³⁺:YAG Lucia disk

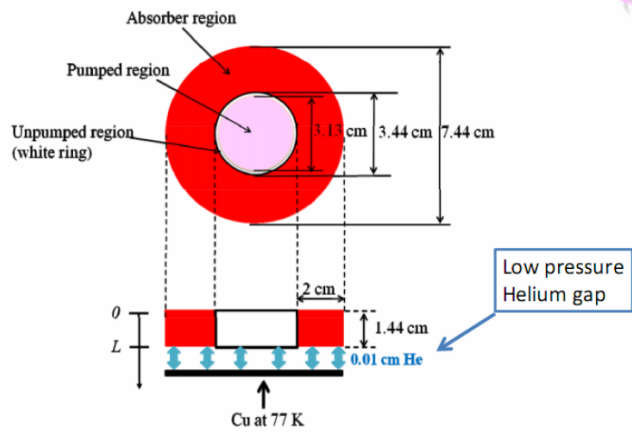


Fig. 3.37. Cooling the active element in the "Lucia" project

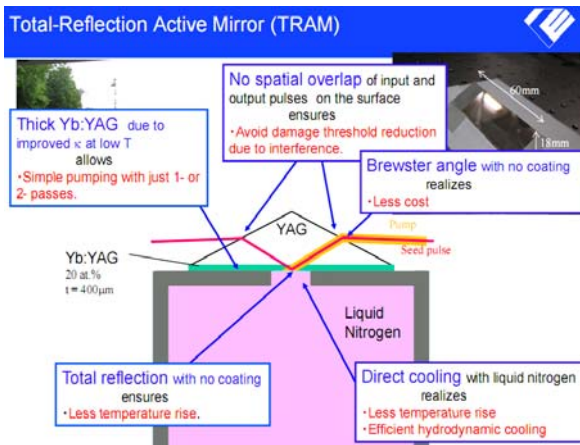


Fig. 3.38. Cooling the active element in the "GENBU" project

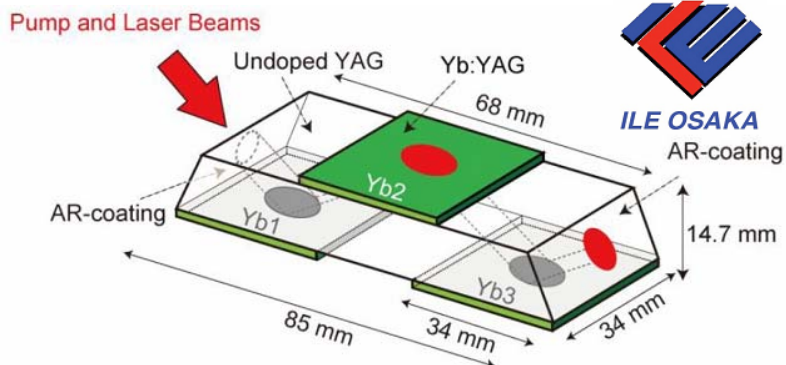


Fig. 3.39. Total-reflection active-mirror (TRAM) in the "GENBU" project

Under the "Genbu" project, disk active elements are cryogenically cooled directly by liquid nitrogen (Fig. 3.38). The shape and appearance of the active elements were changed several times. Today, they are slab-shaped composite elements (Fig. 3.39) with three doped activator regions – active mirrors. The original geometry “cryogenic Yb: YAG composite ceramic with a total-reflection active-mirror” is called TRAM.

In Russia, there are practically no works in the field of lasers with high average and peak power based on the technologies using diode pumping, cryogenic cooling, slab or disk geometry. A laser system with pulse energy of 0.1 J and repetition rates up to 200 Hz was developed in IAP RAS. This system was built using diode pumping and cryogenic cooling of disk active elements [60]. The next step is increasing the pulse repetition frequency to 1 kHz and pulse energy enhancement to 1 J. The pulse of this laser will be used to pump ultra-broadband parametric amplifiers on LBO and BBO crystals providing the duration of compressed pulse up to 5 fs (*Activity 1.8*) in the developed petawatt laser system.

Currently, a large number of active media for disk lasers are studied: Nd:YAG, Yb:GGG, Yb:LuVO, Yb:YVO, Yb:NaGd(WO₄)₂, and others. The appearance and development of optical laser ceramics is expected to stimulate rapid advance of disk lasers to a higher power range. Ceramic elements have optical properties similar to crystal properties but they are much stronger [68] and their diameter may reach tens (!) centimeters [69].

Besides the large aperture, an extremely important advantage of optical ceramics is the possibility of producing active media, which cannot be grown as a single crystal. Examples are oxides of rear earth elements doped with neodymium and ytterbium: Nd:Y₂O₃, Nd:Lu₂O₃, (Nd,Yb):Sc₂O₃, Yb:Y₂O₃, etc. Pulses with durations of 65 fs and 70 fs were generated in Yb:Lu₂O₃ and Yb:Sc₂O₃ crystals, respectively, in [70]. These media are excellent candidates for creating sources of superintense fields operating with high repetition rate. One of the options for constructing a multipetawatt laser is developed at the Institute of Applied Physics: a CPA laser on large-aperture ceramics (Nd,Yb):Lu₂O₃ or (Nd,Yb):Sc₂O₃ with lamp pumping similar to Nd-glass lasers. The excitation from the neodymium ions is transferred to the ions of ytterbium, which provide a broad band (direct pumping of ytterbium is possible only in diode lasers, which makes scaling difficult). A still broader bandwidth may be obtained by simultaneous use of several oxide crystals (Sc₂O₃, Y₂O₃, Lu₂O₃, etc.), similarly to the use of several brands of neodymium glasses.

The technique of thermo-optical constant calculation by measuring thermal depolarization developed at IAP RAS [71] allowed registering for the first time the optical

quality of the ceramics produced in Russia [72] (see the photo in Fig. 3.40) and confirming in experiment the effect of random small-scale modulation of thermal depolarization in optical ceramics predicted earlier [71].



Fig. 3.40. Ceramic sample of domestic production

Activity 4.2. Development of production technology of diode lasers

Powerful diode lasers are now frequently used for high-efficiency optical pumping of solid-state lasers with different active elements. Diode lasers must satisfy a large number of requirements and must be optimized for each application in terms of spectral and structural characteristics, electro-optical efficiency, pulse repetition rate, and cost.

Diode lasers have long found a "niche" in material processing. Currently, a number of organizations in Russia are involved in the development of diode lasers, including JSC "Semiconductor Devices", Federal State Unitary Enterprise (FSUE) "POLUS", Joint Stock Company «Research-and-Production Enterprise "Inject"», General Nano Optics. The General Nano Optics company has recently received support of ~ 2 billion rubles for the organization of production and innovations under support of "Rosnano" [73]. The above organizations specialize primarily in manufacturing diode laser modules with a wavelength of 800 - 810 nm, pulse duration of 0.5 ms and repetition rate up to 30 Hz (Fig. 3.41). The brightness of these modules is up to 2 kW/cm², and cost per 1 kW of no less than 30 thousand rubles with mass production. In addition, none of the domestic producers specializes in manufacturing ready-to-work diode lasers.

The media doped with ytterbium (Yb:YAG, Yb:CaF₂, Yb:GGG, etc.) are the most promising for lasers with high average and peak power. The absorption maxima of these media are in the region of 940 nm and 975 nm with absorption bandwidth from 2 to 20 nm, depending on the medium.

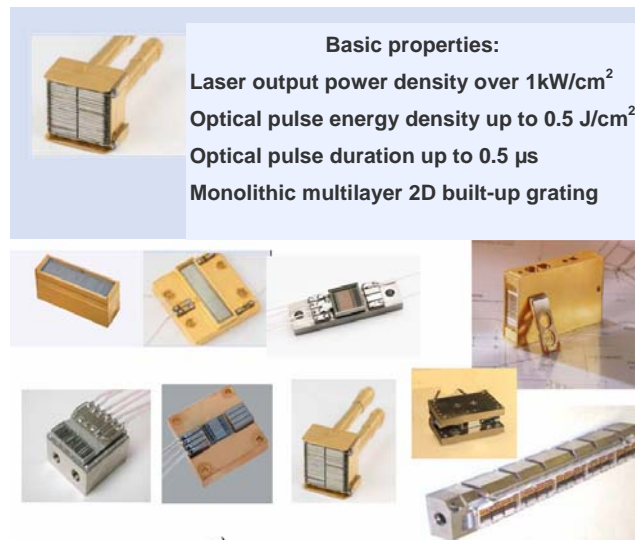


Fig. 3.41. Typical products of JSC "Inject"

Also worth mentioning are two modes of diode laser operation as a pump: pulse mode for lasers with repetition rate of less than 1 kHz and CW operation with repetition rate 1 kHz and more. The international experience demonstrates that electro-optical efficiency above 60% may be attained in both modes. Pump radiation may be fed into the active element in two ways: by longitudinal pumping (which demands collimating optics and fiber output at the diode module) or by transverse pumping (which requires focusing optics). Given these requirements, and based on the technologies available in Russia, it is necessary to solve several problems for creating diode lasers that would provide high efficiency optical pumping of lasers with high average and peak power:

1) Optimization of the spectral characteristics of diode lasers: development of diode lasers with a wavelength of 940 nm and 975 nm, development of diode laser arrays with spectrum width no more than 2 nm, stabilization of radiation wavelength by means of Peltier elements thermal stabilization.

2) Development of diode laser arrays with high brightness and high electro-optical efficiency in pulsed and cw modes of operation: improving the quality of materials and manufacturing, development of effective cooling diode arrays, the use of new production technologies of diode lasers (for example, cryogenic cooling of the diode arrays).

3) Fabrication of optical elements for supplying radiation to the active element of the laser: development of fiber radiation output from a diode laser, development of microlenses for radiation collimation, development of optical systems for feeding the pump to the active element (fabrication of laser heads with longitudinal and transverse diode pumping).

4) Reducing production cost of diode laser arrays: organization of small-scale production using robotic equipment.

Note that the applications, including commercial ones, of diode lasers are far beyond the scope of the Project. Market demand for diode lasers is quite high now and it will grow in the coming years.

Activity 4.3. Creating a laser with a pulse repetition rate of 10 Hz

The laser with average power of 2 kW, peak power over 1 PW, and pulse repetition rate of 10 Hz will have the following architecture: master oscillator, stretcher, BBO (LBO) crystal parametric amplifiers, and vacuum compressor.

The block diagram of the laser is shown in Fig. 3.42. The Ti:sapphire master oscillator generates two pulses, the first of which will be a signal to be amplified, and the second will act as a pump in parametric amplifiers. The first pulse is stretched to a length of ~ 5 ps in the stretcher (or dispersion mirrors). The second pulse is spectrally cut (or shifted by photonic crystals) at a wavelength of 1.3 microns and after the stretcher and regenerative amplifier acquires an energy of ~ 10 mJ per pulse of nanosecond duration. Then, the second pulse is amplified in disk amplifier DA1 up to 0.5 J and is split into two parts, each of which is amplified to 3 J (each channel) in identical disk amplifiers DA2 and DA3. After DA3 the radiation is again split into two parts and amplified in identical disk amplifiers DA4 and DA5 to the pulse energy of 30 J (each channel). After compression and frequency doubling the four parts of the second pulse (see Fig. 3.42) act as parametric pump in four BBO crystals. As a result of parametric amplification and subsequent compression the first 5 fs pulse acquires the energy of 8 J.

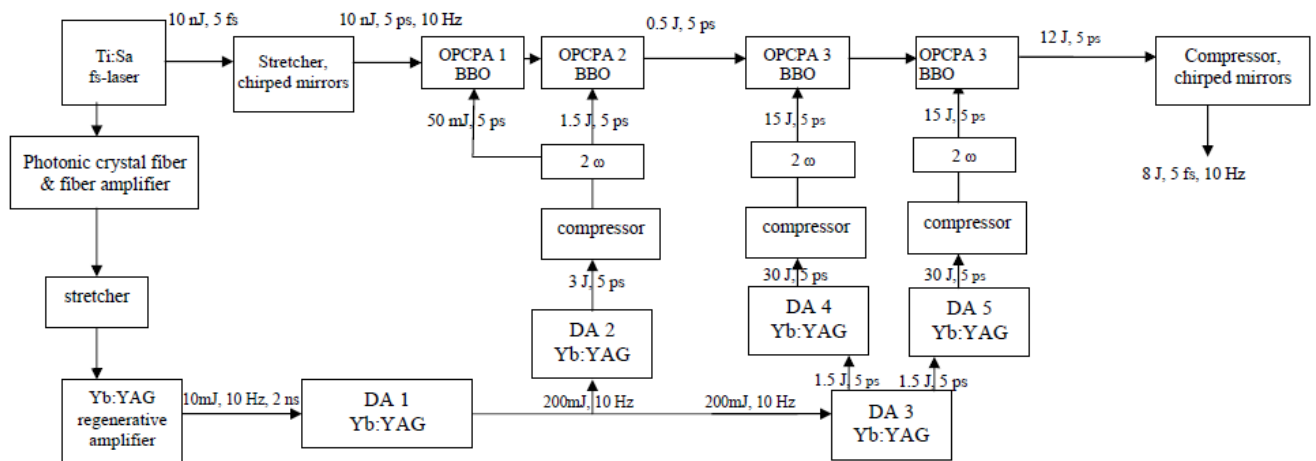


Fig. 3.42. Block diagram of the laser

The optical scheme of the cryogenic disk laser consists of three parts. The first of them – CDA1 preamplifier – provides a subjoule pulse and is a 12-pass 2-cascade amplifier based on active elements with a diameter of 15 mm and a thickness of ~ 1 mm.

The second part, that is an amplifying one, consists of two identical cryogenic disk amplifiers CDA2 and CDA3 and provides pulse amplification to 3 J. It is an 8-pass 2-cascade amplifier based on composite active elements with a diameter of 30 mm and a thickness of ~ 5 mm. The third part of the output amplification also consists of two identical amplifiers CDA4 and CDA5 and provides pulse amplification up to 30 J. It is an 8-pass 2-cascade amplifier on active elements having diameter ~ 80 mm and thickness ~ 2 cm.

Activity 4.4. Creating a laser pulse with a repetition rate of a few kHz

A kilohertz laser with kilowatt average power (pulse energy of 1 J) and peak power of hundreds of terawatts (5 fs pulse duration) will have the following architecture: Ti: sapphire master oscillator, stretcher, BBO (LBO) crystal parametric amplifiers that allow enhancing broadband ($\sim 2000 \text{ cm}^{-1}$) radiation, providing pulse durations up to ~ 5 fs, and vacuum compressor. The scheme slightly differs from the architecture of the laser described in *Activity 1.8*, so we will discuss it in more detail.

The block diagram of the laser is shown in Fig. 3.43.

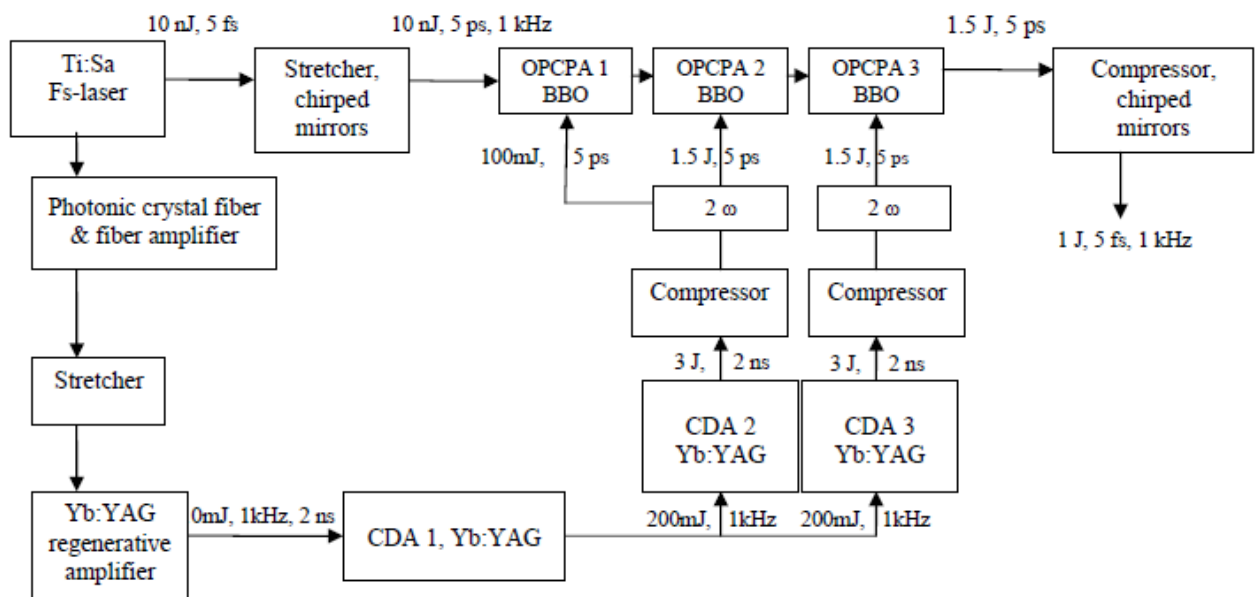


Fig. 3.43. Block diagram of the laser

Two pulses generated by the Ti:sapphire master oscillator are extracted. The first of them is a signal that will be amplified, the second will act as a pump in parametric amplifiers. The first pulse passes to the stretcher (or dispersive mirrors) where it is stretched to a length of ~ 5 ps. The second pulse is spectrally cut (or shifted by photonic crystals) at a wavelength of 1.03 microns and after the stretcher and regenerative amplifier acquires an energy of ~ 10 mJ per pulse of nanosecond duration. Then, the second pulse

is amplified in cryogenic disk amplifier CDA1 up to 0.5 J and is divided into two parts, each of which is amplified to 3 J (each channel) in identical cryogenic disk amplifiers CDA2 and CDA3. On compression and frequency doubling, both parts of the second pulse act as a parametric pump in three BBO crystals. As a result of parametric amplification and subsequent compression the first pulse with a duration of 5 fs acquires the energy of 1 J.

The main element of the laser prototype is parametric pumping. The parametric amplifiers are pumped by SHG of the original disk laser with active elements made of Yb:YAG laser ceramics and cooled to cryogenic temperatures. Inversion in the active elements is accomplished by high-efficiency cw diode pumping with fiber output. The optical scheme of the cryogenic disk laser consists of two parts. The first, preamplifying part CDA1 provides a subexawatt pulse. It is a 4-pass 2-cascade amplifier based on active elements 15 mm in diameter ~ 1 mm thick.

The second part is similar to that described in *Activity 1.8*. It should be noted, however, that with the increase of pulse repetition rate up to several kilohertz (while maintaining pulse energy), problems associated with the accumulation of heat due to the parasitic effects in laser optical elements, such as thermal depolarization and thermal lens, increase too. Therefore, the available material base must be improved as follows:

1. For efficient cooling of active elements of the pump laser, the system of cryogenic heat sink should be modernized. A fill-in cryostat must be replaced by a continuous flow cryostat in which cooling is performed by a liquid nitrogen flow through the radiator of the active element.

2. Each active element must be made of composite material, which is a sandwich structure: a thin (less than 1 mm) Yb:YAG disk and pure YAG 10 mm thick connected by diffusion welding, optical contact or otherwise. This change in the design of the amplifying part of the pump laser will allow maintaining high quality of the laser beam and high efficiency of conversion of pump radiation to the energy of the laser pulse.

3. The same methods for reducing thermal effects can also be used for frequency doubling of pump laser radiation and at the cascades of parametric amplification, as a small crystal thickness compared to the diameter will provide effective heat removal from the ends of these elements and will ensure the lowest temperature gradients.

4. When a laser pulse with repetition rate of 1 kHz or more is compressed, thermal effects may also occur in the diffraction gratings. To reduce these effects gratings with a dielectric rather than gold coating may be required. Compression may also be achieved by means of dispersion dielectric mirrors. Such mirrors almost do not introduce thermal distortion; in addition, they allow short laser pulses to be compressed without energy loss.

Activity 4.5. Transportation of laser beams to the main target chamber and to the other laboratories

High average power laser radiation will be used both in the main target chamber (*Objective 6*) together with the radiation of the 200 PW laser and electron bunch and in the other laboratories (*Objective 7*). Delivery of laser beams to all experimental areas and routine switching from one laboratory to another will be provided for under the Project. This ensures flexibility in preparing and conducting experiments but will require development of a system of beam transport.

Taking into consideration high peak power, it is necessary to create a vacuum path that does not present great difficulties, the more so that the beam diameter is much smaller than in the 200 PW laser. A more difficult task is to transfer the image from the laser output to the interaction region in laboratory. Without this, beam distribution in the experimental laboratories and in the main target chamber will be inhomogeneous. For this reflecting telescopes are required, which will increase the diameter of the vacuum channel.

In addition, the system for synchronizing each high average power laser with the 200 PW laser must take into account the time of passage of light to the main target chamber and its possible changes in the course of exploitation, such as those associated with a change in the geometry of the transportation system.

Objective 5. Creation of an electron source with 100 MeV energy based on a photocathode and microwave resonators

One of XCELS's research directions is the interaction of intense laser radiation with bunches of charged particles. These bunches may be formed under the action of powerful laser radiation on the target, which ensures their synchronization with the laser pulse, but the quality of such bunches is not high and repetition rate is limited. The use of a conventional electron source based on microwave resonators will provide good quality of electron bunches, while a photocathode will help to synchronize an electron bunch with a laser pulse. The electron bunch energy of 100 MeV is chosen based on the requirements for the parameters of electron bunch injection in a laser plasma accelerator. This opens up the opportunity for conducting unique experiments on accelerating electrons to energies above 10 GeV (**Goal 2, Objective 2, Activity 2.1**).

The main elements of the accelerator are a photoinjector (a photocathode RF-gun) and a photocathode laser driver which enable synchronization of an electron bunch source with a laser pulse, and accelerator sections. The description of the first two devices with parameters envisioned for the project is given in *Activity 1.7*, so there is no point to repeat it here.

In the accelerator sections, standard microwave resonators powered by high-power (several MW) klystrons will be used. The record-breaking acceleration rates in such accelerators are 20-30MeV/m, and the 10 MeV/m value is achieved routinely. With this (routine) acceleration rate, the length of the whole electron source (including a photoinjector) with energy 100 MeV will be 100-150 m, which fits well into the Project infrastructure.

For accelerator construction, we will use the rich experience gained by research teams at the Institute of Nuclear Physics SB RAS, Joint Institute for Nuclear Research (Dubna), and DESY (Deutsches Elektronen-Synchrotron). IAP RAS is now collaborating with the latter two institutions to create and study photoinjectors with unique parameters. A photograph of the photocathode RF-gun at DESY is shown in Fig. 3.44.



Fig. 3.44. The photocathode RF-gun at DESY

Objective 6. Creating the main target chamber

At XCELS, the interaction of laser radiation with matter will be studied in the main target chamber and in the experimental laboratories. All 12 beams of the 200 PW laser, an electron bunch and highly repetitive laser radiation will be directed to this chamber. The chamber will have all necessary engineering and diagnostic equipment. The chamber size will be determined later; however, experience of other large-scale laser facilities (e.g., NIF at Lawrence Livermore National Laboratory, USA) shows that the chamber should be installed during construction of the building (*Activity 2.7*), as is foreseen in the roadmap below.

An important aspect in the design and construction of the main target chamber is the focusing geometry of the 12 laser beams. The task of achieving the maximum intensity at a fixed total power of several laser pulses includes, besides the technical aspects, finding optimal focusing geometry, i.e., an optimal spatial arrangement of the focusing pulses. If we assume that the pulses can be synchronized to within the phase of a wavelength and focused in an arbitrary manner, the problem of finding the optimum can be formulated mathematically, and consists in the analysis of appropriate solutions of Maxwell's equations.

The peak amplitude in the focus is proportional to the square root of intensity. Therefore, at a coherent focusing onto one point of two counter-propagating pulses, the peak intensity is two times higher than in the case of focusing of a single pulse with the same total power. Thus, in order to achieve maximum intensity it is reasonable to divide the total power into several channels, which is also due to technical issues. On the other hand, when the number of channels increases, the focusing angle decreases, and, consequently, so does the intensity in the center due to the increase in the focal spot size. Thus, it is clear that there is an optimal number of channels.

Another important factor is the need to orient the propagation direction of laser pulses and their polarization so as to get the maximum field intensity at linear addition of fields of all pulses at the focal point. Obviously, from this point of view it is advisable to orient the laser pulses in the single-circle geometry, as shown in Fig. 3.45 on the left. However, in this case the focusing angle decreases rapidly with increasing number of pulses, whereas part of the space near the circle remains idle. A detailed theoretical treatment of this problem shows that optimal is the configuration at which the laser pulses most closely follow the directivity pattern of the dipole located at the center of the focus. From this point of view, besides the single-circle geometry, a double-circle geometry appears to be efficient, as shown in Fig. 3.45 on the right.

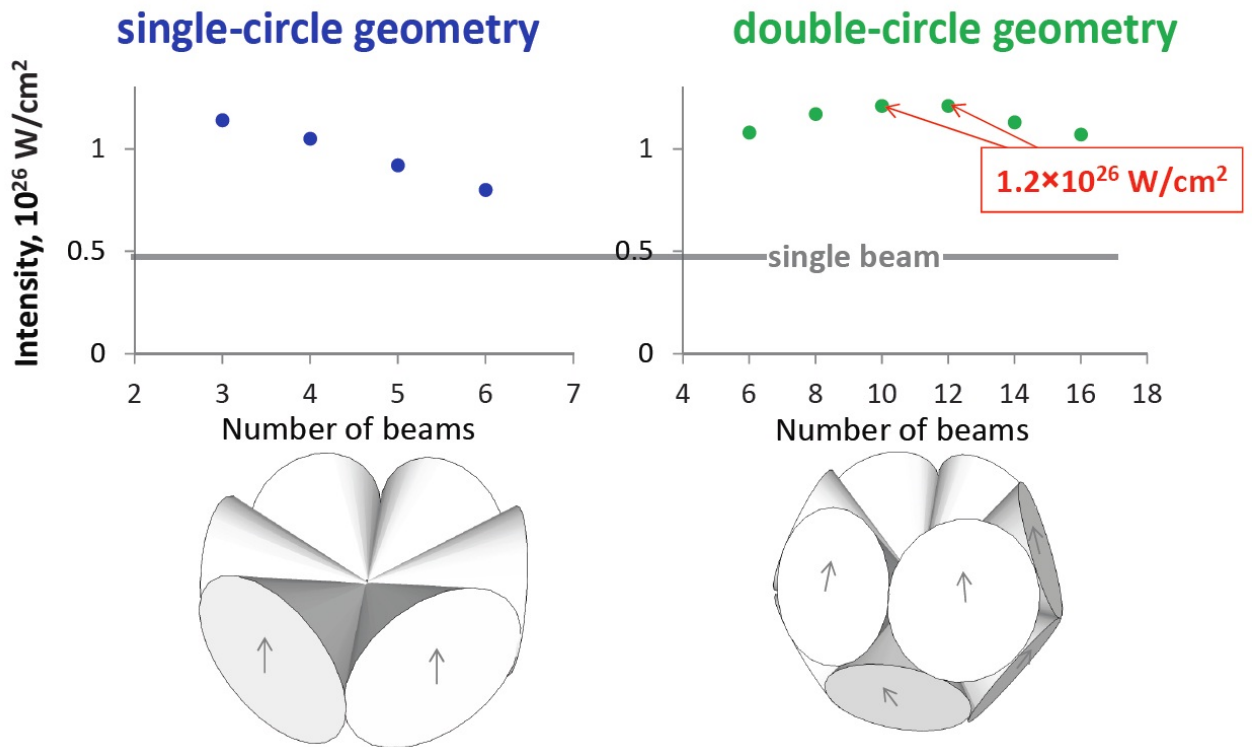


Fig. 3.45. The intensity in the focal plane vs the number of laser pulses at coherent addition in a single-circle geometry (left) and a double-circle geometry (right) at total pulse intensity 180 PW

The intensity in the focus, obtained by numerical solution of Maxwell's equations, is shown in the upper part of Fig. 3.45 for both geometries, as a function of the number of laser beams. It was assumed that each laser pulse has a uniform intensity distribution within the focusing angle, and their total power is 180 PW. From these results it is evident that in this formulation most optimal are 10 or 12 beams oriented in the double-circle geometry. Thus, for a total power of 180 PW the intensity in the focus is approximately 1.2×10^{26} W/cm², which is estimated to be sufficient for the study of such effects as avalanches of electron-positron pairs.

Objective 7. Establishing and equipping research laboratories

The laser-matter interaction will be investigated not only in the main target chamber (*Objective 6*), but also in experimental laboratories, which will be about ten. The exact number and purpose of each laboratory will be defined later. One function of these laboratories is to conduct specific experiments, and the other is to model (at relatively low powers) experiments to be carried out in the main target chamber, to test and to adjust diagnostic equipment. In accordance with these requirements, activities will be held to develop the concept and to create a system for delivery of laser beams and an electron bunch to the labs, as well as to fully equip the experimental laboratories.

It is planned to establish the following laboratories: Laboratory of Ultraintense Fields, Laboratory of High Energy Physics, Laboratory for modeling astrophysical phenomena and early cosmology, Laboratory of Nuclear Optics, Laboratory of Neutron Physics, Laboratory to study the properties of vacuum, Laboratory of Attosecond and Zeptosecond Physics, Laboratory of Fundamental Metrology. This list may be completed in the course of the project.

This Objective includes four Activities:

- Activity 7.1. Developing the concept of delivering laser beams and an electron bunch to the laboratories.
- Activity 7.2. Creating a system of delivery of laser beams and an electron bunch to the laboratories.
- Activity 7.3. Equipping the research laboratories.
- Activity 7.4. Establishing and equipping the satellite laboratories.

Within the framework of *Activity 7.4* it is planned to establish and equip satellite laboratories at the Institute on Laser and Information Technologies of the Russian Academy of Sciences, National Research Centre (NRC "Kurchatov Institute") and the Moscow Engineering Physics Institute, involved in the development of different critical subexawatt laser technologies and a number of fundamental research applications with the XCELS.

Objective 8. Radiation safety

During the interaction of intense laser light with matter, charged particles are accelerated to ultrarelativistic speeds. At deceleration, bremsstrahlung inevitably occurs in the X-ray and gamma-ray ranges. In some cases, this radiation has unique properties and may be the immediate aim of experiments, in other cases, however, this radiation is parasitic. Anyway, radiation protection and radiation monitoring is absolutely necessary. The time scope for this objective coincides with the time of the whole Project. The implementation of this objective will be concurrent with the beginning of the Project, since calculations for the system of radiation protection of the personnel and equipment should be considered when designing all structural elements of the main building of the facility, the accelerator tunnel and other buildings in proximity.

In the framework of this *Objective*, seven *Activities* are planned, including defining a set of requirements for the radiation protection system; working out a draft project for the radiation protection of personnel from radiation sources in the target chamber, in experimental laboratories and in the accelerator tunnel; establishing the radiation protection system of personnel, fabrication and testing of safety means, providing dosimetric monitoring during operation of the laser facility.

Carrying out large-scale experiments using high-intensity laser radiation makes the task of protecting personnel from radiation hazards (all kinds of electromagnetic radiation, in the first place) especially important for the design and construction of such laser systems.

Calculations show that even for the subpetawatt operation of the laser facility it is necessary to provide personnel protection against radiation from relativistic plasma. For example, in [74] detailed radiological studies were performed in the vicinity of a 100 TW laser facility in LULI at Ecole Polytechnique, France. Radiological characterization of the experimental chamber and the other areas of the ultraintense laser facility revealed significant levels of X-ray, gamma and neutron radiation. Different techniques were used to detect and measure this radiation: TLD, photofilms, bubble detectors and germanium spectrometry. A test series of radiological measurements was made for 150 laser shots (300 femtoseconds) with energies in the 1 to 20 J range and a target illuminance of 10^{19} W/cm². Gamma dose equivalents in the vicinity of the chamber varied between 0.7 and 73 mSv. The dose equivalent due to the neutron component was assessed to be 1% of the gamma dose equivalent.

The results of the work on the Vulcan petawatt laser system at the CCLRC Rutherford Appleton Laboratory, UK, where photon doses of up to 43 mSv at 1 m per shot were measured during commissioning studies are described in detail in the paper [75]. It

also overviews the safety and shielding system of the target chamber in order to comply with the Ionising Radiation Regulations 1999 (IRR99), maintaining a limiting dose to personnel of less than 1 mSv/yr.

Figure 3.46 shows a photograph of a protective shielding surrounding the target chamber at the Vulcan petawatt laser system in the UK.



Fig. 3.46. The Vulcan petawatt laser system at the CCLRC Rutherford Appleton Laboratory. Petawatt target chamber with primary photon and neutron shielding [75]

Thus, in multipetawatt and exawatt laser systems, it is of primary importance to provide radiation monitoring and radiation protection of personnel, including personnel working with the laser system and the accelerator, and all the auxiliary and support personnel working in the area adjacent to the target hall.

Calculations of radiation protection for personnel and equipment will precede the design of all structural elements of the main building of the facility. In paper [76] on Radiation Protection at the Large Hadron Collider, the importance and necessity of such preliminary calculations is clearly stated:

"For the first stage, the maximum intensities and losses that form the basis of the shield design must be agreed upon by laboratory management *before* shield specification begins. The second stage, which has to have the agreement of the appropriate regulatory authorities, is illustrated by considering the design constraints chosen for the CERN Large Hadron Collider (LHC)".

The sources of penetrating radiation are elementary particles (electrons, protons) emerging at the time of the laser pulse and accelerated by the laser field to ultrarelativistic velocities, neutral and ionized atoms, secondary particles arising from cascade processes and knocked out of the target material, walls of the target chamber, etc. Various isotopes formed in the material of the facility construction also can be a source of radiation with a long half-life-decay.

Special attention in calculations of the protection system should be given to the bremsstrahlung produced by braking of electrons as they interact with the absorber (protection), and with the walls of the target chamber. Another most hazardous radiation is the flux of neutrons knocked out by heavy particles from the material surrounding the target. Directivity patterns of particle spread and of ionizing radiation depend strongly on the specific features of the experiments, the geometry of the target material (the object of research), and the radiation intensity. Thus, it is necessary to consider both the 4π -divergence radiation and the low-divergence radiation.

Works on X-ray diagnostics of Petawatt laser interactions with underdense plasmas formed from the ionization of a helium gas jet are being performed at the Vulcan facility in the United Kingdom. It was shown [77] that at focused intensities of $> 2 \cdot 10^{20} \text{W/cm}^2$ electrons can be accelerated in cavitated channels to energies in excess of 300 MeV, travelling with highly nonlinear trajectories which will give rise to X-ray radiation. The goal was to fully characterize the angular and spectral X-ray emission pattern as well as the emission source size and consequently determine the dynamics of the energetic electrons.

Various methods are used to assess and calculate the irradiation dose from the area of the interaction between a target and a short pulse high power laser for personnel protection from radiation exposure. In particular, in [78] the authors obtained some simple equation to estimate the forward component of a photon dose. The dose estimated with this method is roughly consistent with the result of Monte Carlo simulation. With some assumptions and corrections, it can reproduce experimental results obtained and the dose result calculated at other laboratories.

Protective shieldings may have quite an impressive scale. Figure 3.47 shows one of the forty-four shield doors in the target hall at NIF [79].

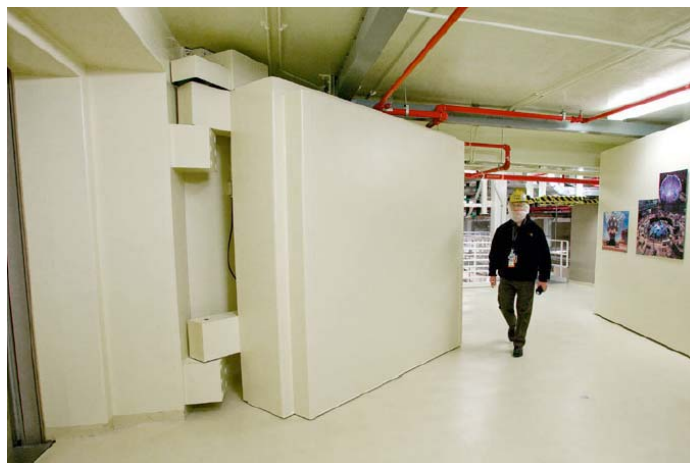


Fig. 3.47. NIF. Forty-four shield doors that were assembled, mounted, and filled with concrete; these doors, some weighing as much as five tons, provide neutron and radiation shielding for high-yield ignition experiments in and around the Target Bay [79]

Numerous safety systems are being incorporated into NIF to assure that all experiments can be safely carried out [80]. The neutrons, X-rays, and gamma rays generated in a shot can be harmful if not properly controlled. Two-meter-thick concrete walls and doors encase the target bay in a protective shield and absorb most of the emitted radiation energy. Walls of adjacent areas further reduce the energy to safe levels for workers. Throughout construction and commissioning, safety has been the number one priority.

Thus, taking into account the world experience in constructing largest-scale laser and accelerator facilities, the task of ensuring radiation safety of personnel will be addressed in the first place – as one of high priority tasks. To do this, a number of measures will be taken to comply with Russian and international safety standards. In particular, we plan the following:

- the target chamber will be placed in a separate room – the target hall, which will be remote from laboratories and offices with the personnel not directly involved in experiments,

- the target hall will have large size, which ensures additional protection since the intensity of radioactive radiation of a point source is inversely proportional to the square of the distance to the object,

- walls of the target hall will have a layered structure consisting of a moderator and an absorber of secondary neutrons and including special concretes of sufficient thickness,

- the target hall will have labyrinth-like exits with massive shielding doors,

- the target chamber and its "stuffing" will be made primarily of materials in which there are no activation processes,

- shielding will cover the target chamber all over and will be in the immediate vicinity to the chamber,

- there will be local extra shielding at places of most probable exit direction of hazardous radiation and particles,

- each employee will be provided with personal dosimeters; dosimetric readings will be controlled both by the employee and by a special control service,

- the target hall will be equipped with dosimetric equipment and a blocking protection system which will ensure that no employee is present in the target hall during the experiment,

- special activities will be undertaken to study the intensity and directivity patterns of hazardous emissions from the target chamber,

- measurements and control of ionizing radiation scattering inside and on the surface of the target chamber will be necessarily included in plans of experiments as a high-priority and obligatory issue.

Objective 9. Constructing a computer and communication center

It is impossible to imagine a modern research center without its own powerful computer and communication center, which provides necessary computing power for all kinds of work performed at this center. In particular, the computer-communications center should have the following functions. First, this includes processing, classification and archiving of experimental data obtained at XCELS. Second, this involves remote control of scientific and engineering equipment. Third, numerical simulations of conducted experiments will be made both at the stage of planning these experiments (prediction of results and optimization of experiments), and at the stage of interpretation of the results obtained. Fourth, numerical study of new phenomena and effects will be carried out. Fifth, data obtained in the course of experiments and numerical simulations will be visualized. Sixth, connections of the XCELS with other scientific centers in Russia and abroad will be maintained.

To effectively accomplish the full range of available tasks, it is required to construct a powerful computer cluster with the computing power of several Pflops (10^{15} floating point operations per second). As of October 2011, the world's most powerful supercomputer, the K computer at the Institute of Physical and Chemical Research, Kobe, Japan, has the maximum computing power of about 8 Pflops [81]. The maximum performance of computing systems increases exponentially with time, increasing every three years by 10 times (see Fig. 3.48).

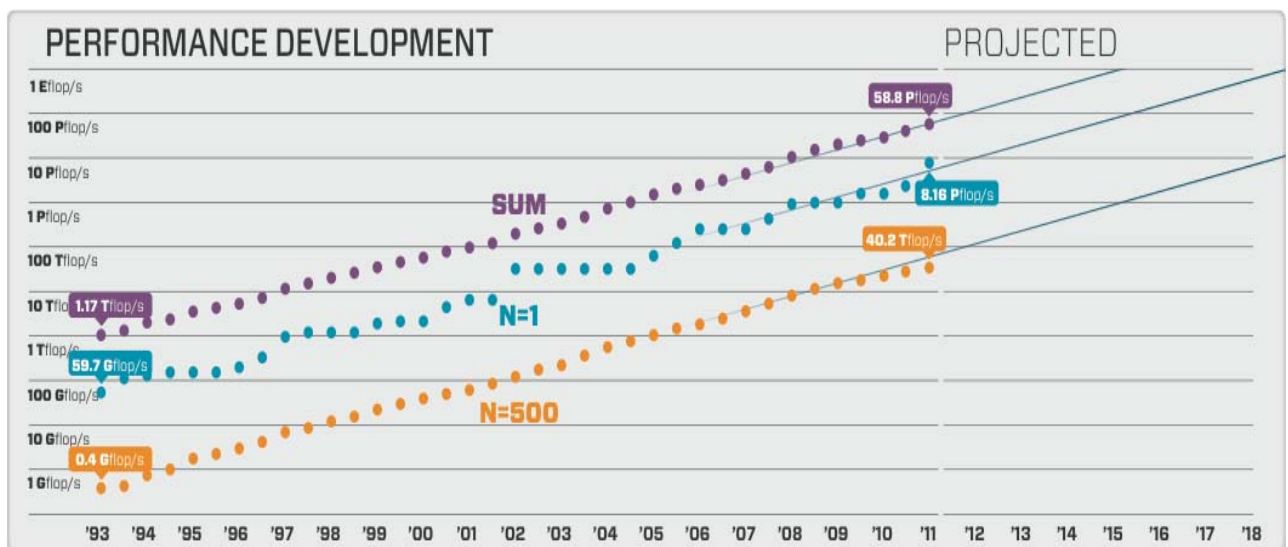


Fig. 3.48. Statistics of 500 most powerful supercomputers in the world [81]. The upper (purple) line – the total performance of 500 most powerful supercomputers. The average (blue) line – performance of the most powerful supercomputer. The bottom (orange) line – performance of the last supercomputer on the 500 list

One of the promising directions in technology is to create supercomputer systems based on GPUs (GPGPU). Their advantage over conventional systems is their lower cost per unit of performance and lower power consumption (about 1 MW per 1 Pflops). Such systems are already available in a number of centers worldwide, in particular, in China and Japan, and occupy three positions in the top 5 of the TOP 500 list. At the same time, the GPU-based systems, due to specific hardware, imply a more complex process of software development, in particular, basically new numerical methods and schemes. The development of such methods will be one of the tasks to be addressed within the XCELS project (see also **Goal 2**).

Objective 10. Equipment of engineering and supporting workshops

For efficient operation of XCELS, it is required to promptly execute all works connected with the creation of the facility and carrying out planned experiments. For this purpose, an optical section (polishing and applying of thin film coatings), a radio-electronics laboratory (design and development of power supplies, data acquisition boards, phase switching circuits, etc.), a vacuum equipment laboratory (testing of vacuum tract and all elements before placing them into the vacuum tract), mechanical workshops (manufacture, assembly and testing of optical mounts, and other mechanical parts), and a cryogenic station (providing liquid nitrogen, and, if necessary, liquid helium) will be established and equipped with appropriately.

Objective 11. Maintenance of the XCELS facility

Efficient functioning of the facility both at the stage of creation and at the stage of experiments will require efforts in the areas of management (*Activity 11.1*), human resources (*Activity 11.2*), infrastructure maintenance (*Activity 11.3*), and international cooperation (*Activity 11.4*). The activities under *Objective 11* will begin either simultaneously with or shortly after the start of the project. Completion of all activities coincides with the end of the project.

Activity 11.1. (effective management) involves organizing and introducing a management structure at the construction stage and at the stage of experiments, setting up rules for internal documents management, organizing an international relations management structure, organization of recording and registration of scientific results.

Activity 11.2. (human resources) includes the dissemination of information about the Project, attracting talented high school students to educational and research work, development and establishment in universities of special teaching courses on project-related topics, supervising bachelor's and master's degree theses on project-related topics, supervising PhD theses on project-related topics, organizing traineeships for Russian specialists abroad.

Activity 11.3 (efficient operation of infrastructure) is aimed at maintaining buildings and utilities, two prototypes of 15 PW modules, 200 PW laser, high average power lasers, 100 MeV electron source, experimental laboratories, the main target chamber, computer and communication center, engineering and supporting workshops.

Activity 11.4 (effective international cooperation) includes the establishment and operation of an international supervisory board, attracting foreign scientists to installation works and research at the facility, attracting foreign technologies, organizing scientific conferences on project-related topics, and creation and updating of the XCELS web-site.

References to Section 3

1. Piskarskas, A., et al., *Sov. Phys. Usp.*, **29**, 969, 1986.
2. Dubietis, A., et al., *Optics Communications*, **88**, 437, 1992.
3. Ross, I.N., et al., *Optics Communications*, **144**, 125, 1997.
4. Matousek, P., et al., *IEEE Journal of Quantum Electronics*, **36**, 158, 2000.
5. Collier, J., et al., *Applied Optics*, **38**, 7486, 1999.
6. Ross, I.N., et al., *Applied Optics*, **39**, 2422, 2000.
7. Jovanovic, I., et al., in *Conference on Lasers and Electro-Optics* Baltimore, MD, 2001.
8. Yoshida, H., et al., in *Conference on Lasers and Electro-Optics* Baltimore, MD, 2001.
9. Ross, I.N., et al., in *Conference on Lasers and Electro-Optics* Baltimore, MD, 2001.
10. Zhang, S.K., et al., in *Conference on Lasers and Electro-Optics* Baltimore, MD, 2001.
11. Yang, X., et al., *Applied Physics B*, **73**, 219, 2001.
12. Andreev, N.F., et al., *JETP Letters*, **79**, 144, 2004.
13. Freidman, G., et al., in *Conference on Lasers and Electro-Optics* Long Beach, CA, 2002.
14. Bepalov, V.I., et al., in *Conference on Lasers and Electro-Optics* San Francisco, CA, 2004.
15. Dvorkin, K.L., et al., in *Modern Problems of Laser Physics*. Novosibirsk, Russia, 2004.
16. <http://www.clevelandcrystals.com/news.shtml>.
17. Lozhkarev, V.V., et al., *Laser Physics*, **15**, 1319, 2005.
18. Lozhkarev, V.V., et al., *Laser Physics Letters*, **4**, 421, 2007.
19. Hernandez-Gomez, C., et al., CLF Annual Report, http://www.clf.rl.ac.uk/resources/PDF/ar06-07_s7vulcan_10pwproject.pdf, 2006-2007.
20. Poteomkin, A.K., et al., *Quantum Electronics*, **35**, 302, 2005.
21. Katin, E.V., et al., *Quantum Electronics*, **33**, 836, 2003.
22. Poteomkin, A.K., et al., *IEEE Journal of Quantum Electronics*, **45**, 854, 2009.
23. Danelius, R., et al., *JETP Letters*, **42**, 122, 1985.
24. Freidman, G.I., et al., *Quantum Electronics*, **37**, 147, 2007.
25. Martinez, O.E., *IEEE J. Quantum Electron.*, **QE-23**, 59, 1987.
26. Lyachev, A., et al., *Opt. Express*, **19**, 15824, 2011.
27. Martyanov, M.A., et al., *Quantum Electronics*, **38**, 354, 2008.
28. Bunkenberg, J., et al., *IEEE Journal of Quantum Electronics*, **QE-17**, 1620, 1981.
29. Vlasov, S.N., et al., *Soviet Journal of Quantum Electronics*, **12**, 7, 1982.
30. Poteomkin, A.K., et al., *Applied Optics*, **46**, 4423, 2007.
31. Lozhkarev, V.V., et al., *Optics Express*, **14**, 446, 2006.
32. Garanin, S.G., et al., *Quantum Electronics*, **35**, 299, 2005.
33. Belov, I.A., et al., in *Laser Optics - 2010*, 2010.
34. Haynam, A., et al., *Appl. Opt.*, **48**, 3276, 2007.
35. Khazanov, E.A., et al., in *International Conference on High Power Laser Beams*. Nizhny Novgorod - Yaroslavl - Nizhny Novgorod, 2006.
36. Review, L., *Quarterly Report*, **115**, 2008.
37. Jullien, A., et al., *Optics Letters*, **29**, 2184, 2004.
38. Homoelle, D., et al., *Opt. Lett.*, **27**, 1646, 2002.
39. Stolen, R.H., et al., *Opt. Lett.*, **7**, 512, 1982.
40. Jullien, A., *Opt. Lett.*, **30**, 8, 2005.
41. Ramirez, L.P., et al., *OSA/HILAS*, 2011.
42. Mironov, S.Y., et al., *Applied Optics*, **48**, 2051, 2009.
43. Druon, F., et al., *Opt. Lett.*, **23**, 1043, 1998.
44. Wattellier, B., et al., *Rev. Sci. Instrum.*, **75**, 5186, 2004.
45. Fourmaux, S., et al., *Optics Express*, **16**, 11987, 2008.
46. Fourmaux, S., et al., *Optics Express*, **17**, 178, 2009.
47. <https://www.llnl.gov/str/September03/Moses.html>.
48. Fan, T.Y., *IEEE J. Sel. Top. Quantum Electron.*, **11**, 567, 2005.
49. Leger, J.R., *External methods of phase locking and coherent beam addition of diode lasers, in Surface Emitting Semiconductor Lasers and Arrays*, ed. G.A. Evans and J.M. Hammer. 1993: Academic.
50. Kapon, E., et al., *Opt. Lett.*, **9**, 125, 1984.
51. Andreev, N., et al., *IEEE Journal of Quantum Electronics*, **27**, 135, 1991.

52. Daniault, L., et al., in *In Proc. 8th ultrafast conference Ultrafast Optics*. Monterey, 2011.
53. Shay, T.M., et al., *Opt. Express*, **14**, 12015, 2006.
54. Hornung, M., et al., *Optics Letters*, **35**, 2073, 2010.
55. Horung, M., et al., in *In Proc. 8th ultrafast conference Ultrafast Optics*. Monterey, 2011.
56. *International Linear Collider reference design report ILC global design effort and world wide study. Executive Summary*. Executive Summary ed. J. Brau, Y. Okada, and N. Walker. Vol. XXIV. 2007, ILC.
57. Potemkin, A.K., et al., *Quantum Electronics*, **40**, 1123, 2010
58. Kuriki, M., et al., in *Annual meeting of Particle accelerator society of Japan*. Himeji, Japan, 2010.
59. Andrianov, A.V., et al., *Optics Letters*, **35**, 3805, 2010.
60. Palashov, O., et al., in *SPIE Optics + Optoelectronics*, Prague, Czech Republic, 2011.
61. Haynam, C.A., et al., *Applied Optics*, **46**, 3276, 2007.
62. Butkus, R., et al., *Applied Physics B*, **79**, 693, 2004.
63. Chanteloup, J.F., et al., in *Conference on Lasers and Electro-Optics, Technical Digest (CD) (OSA, 2006)*, 2006.
64. Kawashima, T., et al., *J. Phys. IV, France* **133**, 615, 2006.
65. Hein, J., et al., in *Frontiers in Optics, OSA Technical Digest (CD) (OSA, 2003)*, 2003.
66. Tokita, S., et al., *Optics Express*, **15**, 3955, 2007.
67. Lucianetti, A., et al., *Beyond 10 J/2 Hz LUSIA current status with cryogenic amplifier*, in *SPIE Optics and Optoelectronics*. 2011: Prague.
68. Kaminskii, A., et al., *Optics Letters*, **32**, 1890, 2007.
69. Lu, J., et al., *Applied Physics*, **39**, 1048, 2000.
70. Tokurakawa, M., et al., in *Advanced Solid-State Photonics*. Nara, Japan, 2008.
71. Mukhin, I.B., et al., *Optics Express*, **13**, 5983, 2005.
72. Palashov, O.V., et al., *Quantum Electronics*, **37**, 27, 2007.
73. http://rusnanonet.ru/rosnano/project_diode-laser.
74. Borne, F., et al., *Radiation Protection Dosimetry*, **102**, 61, 2002.
75. Clarke, R.J., et al., *J. Radiol. Prot.*, **26**, 277, 2006.
76. Stevenson, G.R., *Radiation Protection Dosimetry*, **96**, 359, 2001.
77. Kneip, S., et al., *Central Laser Facility Annual Report*, 34 2005/2006.
78. Hayashi, Y., et al., *Radiation Protection Dosimetry*, **121**, 99, 2006.
79. Moses, E.I., in *23rd IAEA Fusion Energy Conference*. Daejeon, Korea Rep., 2010.
80. https://lasers.llnl.gov/about/nif/how_nif_works/target_chamber.php.
81. <http://top500.org/lists/2011/06>.

4. Scientific Case & Innovative Research

(Goals 2, 3 and Objectives to Achieve these Goals)

The second objective of our Project is to conduct fundamental research on the basis of the established infrastructure. The experimental studies will be performed in four main areas, which are now called the "four pillars of physics of extreme light," including the establishment of secondary sources of accelerated particles and hard photons based on the interaction of extremely strong fields with matter, and the development of attosecond and zeptosecond sources of electromagnetic radiation, photonuclear physics and the study of nonlinear properties of vacuum in superstrong fields. An additional experimental direction based, to a certain extent, on the results of the previous ones, is a laboratory simulation of astrophysical and early cosmological phenomena. To set up experiments and interpret their results, we will perform theoretical modeling of the interaction of radiation with matter in the range of intensities of 10^{23} - 10^{27} W/cm², which are several orders of magnitude superior to the intensities obtained to date at the world's most advanced laser facilities. Along with this, concepts of the development of light sources at the exawatt and zettawatt power levels based on the interaction of multipetawatt pulses with plasma will be worked out. The development of these concepts will be accompanied by the development of appropriate components.

A project with closest to the XCELS scientific objectives is the European ELI project (Extreme Light Infrastructure, <http://www.extreme-light-infrastructure.eu/>), currently under development. The Project involves research on physics of strong fields by means of intense laser radiation. The intensity of the laser field at the focus with all laser rays combined is supposed to reach 10^{23} W/cm². The Project consists of three "pillars", dedicated to the research on charged particle acceleration, attosecond physics and photonuclear physics, respectively. Under the XCELS Project, the estimated laser field intensity should be 2 orders of magnitude higher than at ELI, allowing, for the first time, to investigate in laboratory environment the quantum electrodynamic effects, such as breakdown of vacuum, generation of electromagnetic cascades, etc. Thus, the XCELS Project can be viewed upon as the fourth "pillar" of ELI, dedicated to the physics of superintense fields. Moreover, due to the higher laser intensity at the XCELS, one may expect higher energies of charged particles and gamma rays. In this sense, the ELI and XCELS projects can be considered complementary to each other and their synergy will benefit both the projects.

Objective 1. Simulation of interaction of extreme light with matter and vacuum

Activities under this objective include the development, analysis and calculation of laser-plasma particle acceleration models, new light sources in the X-ray and gamma-ray ranges, including light sources of attosecond and zeptosecond durations, models of quantum electrodynamics in superstrong laser fields, models of extreme states of matter under extremely high temperatures and pressures. To perform this simulation, new computer codes, including those intended for calculations on high performance computers of the XCELS computer and communication center, will be created and implemented. Based on the analytical and numerical calculations, experiments on the observation of new phenomena will be planned and experimental results will be interpreted.

Activity 1.1. Development of theoretical models of processes

Focusing of intense laser light on matter leads to energy concentration in a small space-time region and the generation of high-speed particles. Much progress has now been made in laser-plasma acceleration of electrons. In the laboratory, quasimonoenergetic electron bunches with energy 1 GeV have been obtained [1]. The acceleration of plasma electrons can be divided into three stages: (i) scattering by a laser pulse, (ii) electron self-injection (electron capture) into a plasma cavity, (iii) electron acceleration in the plasma bubble. First, the plasma electrons involved in the interaction are scattered in the field of the laser pulse, forming a plasma cavity. Only a small fraction of the scattered electrons are captured into the formed cavity and are accelerated to high energies. Currently, there are no reliable theoretical models describing these three stages and the dynamics of the laser pulse during its propagation in plasma. In addition, it is required to analyze various ways to control the self-injection and various schemes of the injection of an external electron beam. Among the ways of control that recently have been widely discussed, we can mention such approaches as colliding laser pulses [2, 3], varying plasma density along the acceleration path [4-6], ionization control [7] and others. The theoretical models developed at XCELS will be used to plan and analyze the experiments.

One of the most important applications of the interaction of intense laser pulses with matter is the creation of a new generation of electromagnetic light sources in the hardly accessible regions of the electromagnetic spectrum with critical parameters. Possible applications include the study of ultrafast processes in atoms, molecules and solids, new diagnostic methods in medicine, structural studies of complex molecules in biology, organic chemistry, pharmaceuticals, etc. At present, no powerful, compact and efficient light sources are available in this range. There are many mechanisms that lead to efficient

generation of short-wave radiation: the betatron mechanism [8], the Compton effect [9], high harmonic generation due to the interaction of a laser pulse with the surface of a solid target [10], electromagnetic cascades [11]. Note that the creation of theoretical models describing these mechanisms is far from being complete. Certain progress has been achieved by using an asymptotic analysis based on the relativistic self-similarity theory [12]. This approach has permitted to obtain relatively universal spectra of high-order harmonics generated on the target surface [13, 14]. These spectra have been confirmed experimentally [15, 16].

In strongly nonlinear regimes a more accurate model is the model of relativistic electronic spring [17]. This model describes the harmonic generation as a three-stage process: first, the laser energy is transferred into the energy of plasma fields arising from charge separation, then this energy is converted into kinetic energy of electrons emitted towards the radiation, and finally, a beam of accelerated electrons generates a short attosecond burst.

Since the early 1960s numerous calculations of fundamental quantum electrodynamic processes (including the probabilities of emission and absorption of a photon, photon pair production and single-photon annihilation of pairs, splitting of photon, polarization and mass operators - in the magnetic, constant crossed field and in the field of plane monochromatic waves) have been carried out, in which the external field is taken into account nonperturbatively (these studies were initiated in [18-25]). Note that at sufficiently high intensities of laser fields, to obtain correct results when calculating quantum processes it is necessary to take into account the whole set of radiative corrections that arise from inserting an unlimited number of polarization loops, since the expansion parameter of the perturbation theory in these conditions may be more than one [26, 27]. For this reason, the formalism developed to date is actually fundamentally limited by the intensities of the order of 10^{29} W/cm². Unfortunately, the naturally occurring problem of overcoming the above mentioned difficulties has not received adequate attention in the literature.

In the recent paper [28] it was predicted on the basis of simple estimates that at the intensity of the electromagnetic fields of the order of 10^{24} W/cm² and above, "spontaneous" quantum electrodynamic cascades initiated by initially slow seed charged particles should be expected. In this case the laser field plays a dual role. First, it accelerates the charged particles, and then initiates the quantum electrodynamic processes with charged particles that have accumulated energy during acceleration. In this case, the occurrence of the cascades is in principle possible in almost arbitrary

configuration of the laser field. The development of the cascades will continue until the complete expulsion of all charged particles from the focus of the laser field by the ponderomotive potential, or, in more extreme conditions, until the depletion of the laser field due to its absorption by quickly generating electron-positron plasma [29]. To date, the theory of collective quantum-plasma processes have not yet been developed. Therefore, at XCELS much attention will be paid to the development of the theoretical effects of QED processes in intense light fields.

Activity 1.2. Development and implementation of new computer codes

Because of the difficulties in the theoretical description of the interaction of intense laser pulses with plasma, numerical modeling is an important and powerful tool for studying this interaction as well as for verifying the theoretical results, setting up experiments and interpreting of experimental data. Since radiation intensities are so great that any substance that comes into its field of localization becomes almost instantaneously ionized, the main task is to model self-consistent dynamics of the interaction of electromagnetic waves with plasma. To solve this problem, different methods based on different approximations have been applied. In particular, one can mention here the numerical methods based on solving the hydrodynamic and kinetic equations for plasma. At the same time, to solve the kinetic equation (the Vlasov equation) both the Euler methods (based on finite differences, finite volumes, spectral decomposition, etc.) and the Lagrangian methods are used. Among the latter, most popular is the Particle-In-Cell (PIC) method. Based on this method, the vast majority of modern numerical results concerning the interaction of high-intensity laser light with matter have been obtained.

This method is developed for a mathematical model, in which the plasma is represented as an ensemble of negatively charged electrons and positively charged ions created and moving under the influence of electromagnetic fields. The model actually consists in successive integration of the equations of motion for all particles in the plasma and the evolution equations of the electromagnetic field defined on a discrete mesh in a certain part of space. The evolution of the electric and magnetic fields is described in terms of Maxwell's equations that can be solved by the finite difference method (in particular, a popular method is the FDTD method [30]) and by spectroscopic methods, e.g. by Fourier series expansion.

The generic structure of the computational cycle of the PIC method is shown in Fig. 4.1. The computational cycle consists of four main parts, being successively performed at each time iteration. Top and bottom in Fig. 4.1 show the procedure of numerical integration of the

equations of motion for plasma particles and Maxwell's equations for electromagnetic fields at the next iteration, respectively. The left and right parts of the image show the so-called weighting procedures that define the relationship between particles with continuous coordinates and spatial distributions of currents and electromagnetic fields defined on the discrete mesh. The particle weighting consists in determining the matrix of spatial current density by continuous values of coordinates and particle velocities. The weighting of electromagnetic fields consists in determining the electric and magnetic fields at the location of each particle by values of the electromagnetic field defined on the discrete mesh.

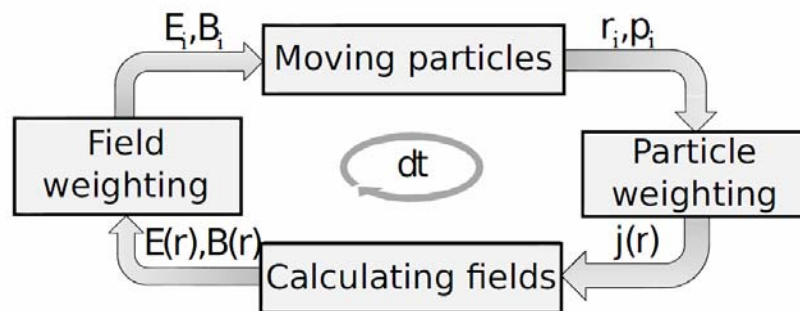


Fig. 4.1. Generic structure of the computational cycle by the PIC method

In a one-dimensional geometry, the plasma simulation technique by the PIC method on modern personal computers, often with the correct implementation of the algorithm, allows one to perform a numerical experiment for times from a few seconds to a few hours. Compared to the one-dimensional geometry simulation, the two- and three-dimensional geometries require larger amounts of computation, making the use of supercomputers for parallel computing extremely important.

In addition to the available standard three-dimensional codes QUILL [31] and ELMIS [32], based on the PIC method, it is expected to develop a line of faster three-dimensional codes for simulating laser-plasma acceleration on large tracks:

1) *A computer code based on the PIC method using the ponderomotive approximation.*

Standard computer programs based on the PIC method even on modern computer systems require too much computing time for simulation of large tracks of acceleration. A numerical algorithm based on the PIC method and the ponderomotive approximation to describe the action of the laser field on a particle can simulate a three-dimensional geometry of the interaction of a relativistically strong laser pulse with plasma, using a larger spatial step of the mesh determined by the plasma wavelength than the step in standard computer programs based on the PIC method determined by the laser wavelength. For gas targets, in turn, this fact will allow this numerical algorithm to simulate large tracks of electron acceleration.

2) *A computer code based on the PIC method using the quasi-static and ponderomotive approximation.*

When simulating electron acceleration on tracks a few meters in length, it is necessary to use faster and more stable numerical schemes. These tracks are possible in case of the interaction of multipetawatt laser pulses with a rarefied gas jet. The numerical scheme that uses the PIC method and the quasi-static approximation to describe the electromagnetic fields has an increased stability and allows simulation of long acceleration tracks.

3) *A computer code based on process modeling in a reference frame moving at a near-light speed relative to the laboratory reference frame [33].* In this case, of interest is the recently discovered problem of numerical instability [34]. This problem may be solved by using the method of parallel Fourier transform to compute the electromagnetic fields, which was developed by our team.

4) *One of the promising directions in the development of modern parallel programs is to use graphics processing units (GPU), which are less expensive and have lower power consumption per unit of performance [35, 36].* Of particular interest is the possibility to create programs that can work on hybrid architectures: using both the traditional processors, as well as graphical ones. At the same time simulation with GPUs poses a number of difficulties associated with the peculiarities of the device for storing and accessing memory in them. In the XCELS Project we plan activities to develop the Picador code designed to work on a hybrid CPU/GPU architecture [37].

To simulate new sources of radiation in the X-ray and gamma-ray bands it is suggested to develop separate modules that describe the radiation and quantum effects, as well as independent programs fully simulating key processes occurring in the sources. It is assumed that the modules can be integrated into existing and new programs describing the interaction of intense electromagnetic radiation with matter.

To study the dynamics of electron-positron plasma formed as a result of the cascade development, it is expected to develop a three-dimensional numerical model based on the PIC method and the Monte Carlo method. A two-dimensional version has been described in [29]. However, this model employs the electrostatic equations to describe the plasma fields, the classical approach to photon radiation and the radiation reaction force in the equations of motion. Our numerical model will use a more general approach: emission of a photon is considered within the framework of the quantum theory, while the dynamics of laser and plasma fields is described in the framework of Maxwell's equations. It is important to note that the characteristic energy of photons in electron-positron plasma

differs by many orders of magnitude. The photon energy of the laser and plasma field is quite low ($\hbar\omega \ll mc^2$), whereas the energy of photons emitted by accelerated electrons and positrons, on the contrary, is very high ($\hbar\omega \gg mc^2$). This fact allows us to consider high-energy photons as particles, calculating their distribution by solving the equations of motion and evolution of the laser and plasma fields – by numerically solving Maxwell's equations. Thus, the dynamics of electrons, positrons and hard photons, as well as the evolution of the plasma and laser fields is calculated using the PIC method, while the emission of hard photons and production of electron-positron pairs will be calculated using the Monte Carlo method.

It is supposed to simulate the photon emission in the following way. At each time step for each electron and positron, the possibility of photon emission with a probability distribution is tested. An emitted photon appears in the simulation region as a new particle. The coordinates of the photon coincide with the coordinates of its electron (positron) emitting this photon. The photon momentum is directed towards the momentum of the electrons (positrons) at the instant of radiation. The value of the electron (positron) momentum is reduced by the value of the photon momentum. A similar algorithm is used to simulate the electron-positron pair production. A new electron and a positron are added to the simulation, while the photon which splits into the pair is removed. In this case, the sum of the energies of the electron and positron is equal to the photon energy and the velocity of the electron-positron pair is directed along the velocity of the photon at the moment of splitting.

The motion of particles and the evolution of the low-frequency electromagnetic field will be calculated using a standard numerical scheme based on the PIC method [31]. In order to prevent memory overflow during simulation owing to the exponential growth in the number of particles in the cascade, the method of particle fusion will be used. If the number of particles in the simulation is too large, randomly selected particles will be removed, while the charge, mass and energy of the remaining particles will be increased by the charge, mass and energy of the removed particles, respectively. A block diagram of the calculation of radiation and quantum effects in laser plasma is shown in Fig. 4.2.

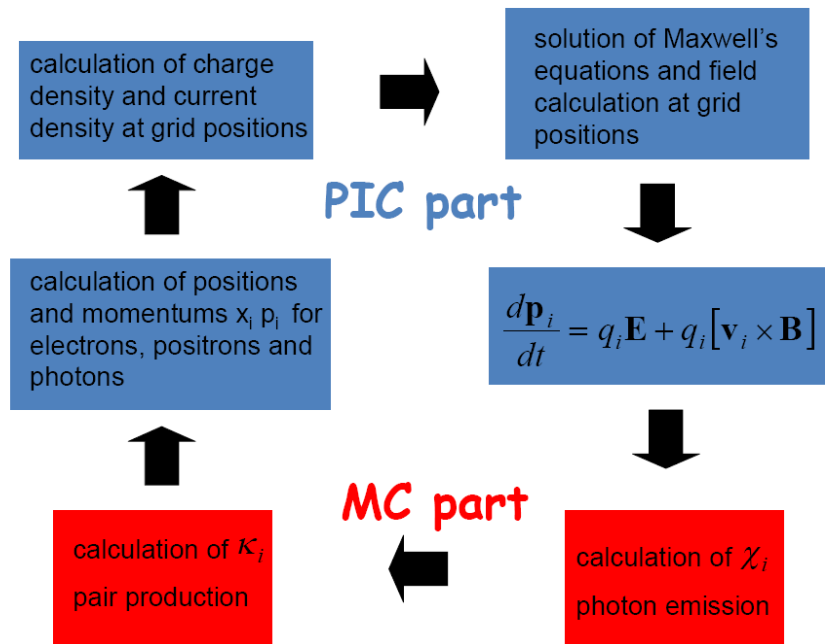


Fig. 4.2. Block diagram of the calculation of radiation and quantum effects in laser-produced plasma by the PIC method

At EXCEL much attention will be paid also to the creation of codes for simulating extreme states of matter under extremely high temperatures and pressures. To describe such states at a micro-level it is supposed to use the techniques of molecular dynamics, while for simulation of conditions on a large scale we plan to employ methods of radiation magnetohydrodynamics.

We intend to develop and debug the three-dimensional codes and to perform a full-scale numerical simulation of the processes in laser fields of realistic configuration taking into account the radiation and quantum effects in the range of parameters corresponding to the planned experiments at the facility. Based on the analytical and numerical calculations we will plan experiments on the observation of new phenomena, and interpret experimental results.

Objective 2. Carrying out experiments on laser-plasma acceleration of charged particles

This objective is aimed at creating compact sources of accelerated charged particles on the basis of laser-plasma interactions. Different mechanisms of electron and ion acceleration in gas, solid and structured targets will be investigated. The rates of laser-plasma acceleration of charged particles 3-4 orders of magnitude higher than in conventional accelerators have been demonstrated by now. It is intended to achieve under the XCELS Project integral characteristics of acceleration and quality of beams in compact devices, which will meet the requirements of experiments on high energy physics. Of particular interest is combined electron acceleration in linear and laser-plasma accelerators, which will give an opportunity to combine high quality of the injected bunches of particles and their high-rate of acceleration. Based on the projected XCELS results, acceleration of electrons up to energies of hundreds of GeV and of ions up to energies of tens of GeV may be realized in relatively small laboratories of academic and university centers, which will expand significantly the research front in high energy physics. Works on this objective will include development of laser targets, experiments on the exawatt complex prototype, including experiments with a small linear accelerator, and 200 PW laser and 100 MeV linear electron accelerator.

Activity 2.1. Laser-plasma electron acceleration up to energies of 10-1000 GeV

Standard modern methods of accelerating charged particles have reached the technological limit at which further increase of accelerating field can lead to destruction of the accelerating structure. The difficulties faced by modern accelerators force us to seek alternative ways of accelerating charged particles that would allow achieving a higher acceleration rate. Recently the most actively discussed alternative schemes with a high rate of charged particles acceleration are based on the use of superintense light fields. Plasma arising as a result of interaction of laser field with a target allows efficient conversion of laser energy into the kinetic energy of charged particles. When a short intense laser pulse is propagating in a plasma, structures with a giant longitudinal electric field with intensity several orders of magnitude exceeding that of accelerating field in modern accelerators are formed. Such structures are moving behind the laser pulse at a velocity close to the speed of light. A charged particle trapped into the plasma structure in the accelerating phase of the longitudinal field can be accelerated to high energies (Fig. 4.3).

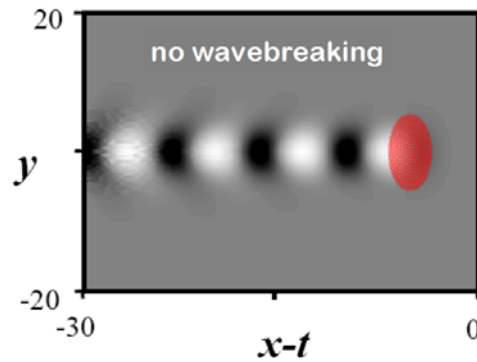


Fig. 4.3. Distribution of electron density behind the laser pulse

In the case of high-intensity laser radiation, which is characteristic of the proposed facility, the pulse-plasma interaction occurs in a strongly nonlinear regime. Ponderomotive force of a relativistically intense laser pulse pushes the plasma electrons out of the high intensity region. As a result, a plasma cavity devoid of electrons is formed behind the laser pulse [38] (Fig. 4.4). A huge unshielded ion charge creates inside the cavity strong accelerating and focusing fields. In addition, a large number of plasma electrons may be captured by the cavity, followed by acceleration to high energies. Recent experiments have shown the possibility of electron trapping and obtaining quasi-monoenergetic electron beams with energy up to 1 GeV [1].

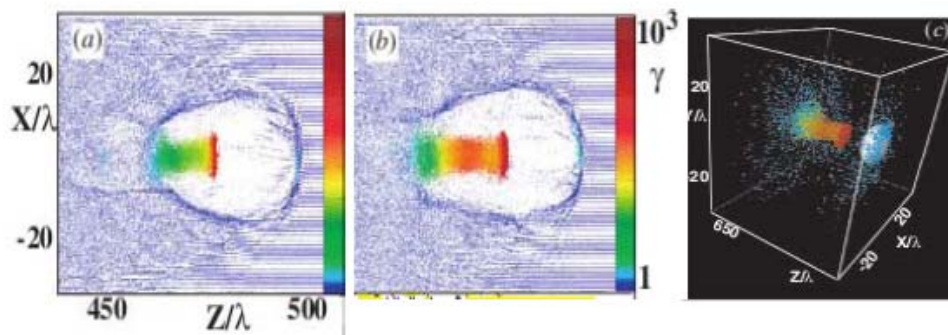


Fig. 4.4. Distribution of electron concentration (a) and fast electrons (b) in the strongly nonlinear regime [38]

In the simplest case, the scheme of electron acceleration by an intense laser pulse is illustrated in Fig. 4.5. A target – a nozzle-produced gas jet – is located in the focus of a parabolic mirror on which an unfocused laser pulse is incident. During the interaction of the laser pulse with gas the latter is ionized by the leading edge of the pulse. The major portion of the pulse generates an accelerating plasma structure. The trapped plasma electrons or the electrons injected from the outside can be accelerated in such a structure to high energies. Gas composition and laser pulse shape can be changed, allowing parameters of the accelerated electrons to be controlled. It is possible to improve this scheme and to use plasma channels, multi-stage acceleration, plasma profiling, etc.

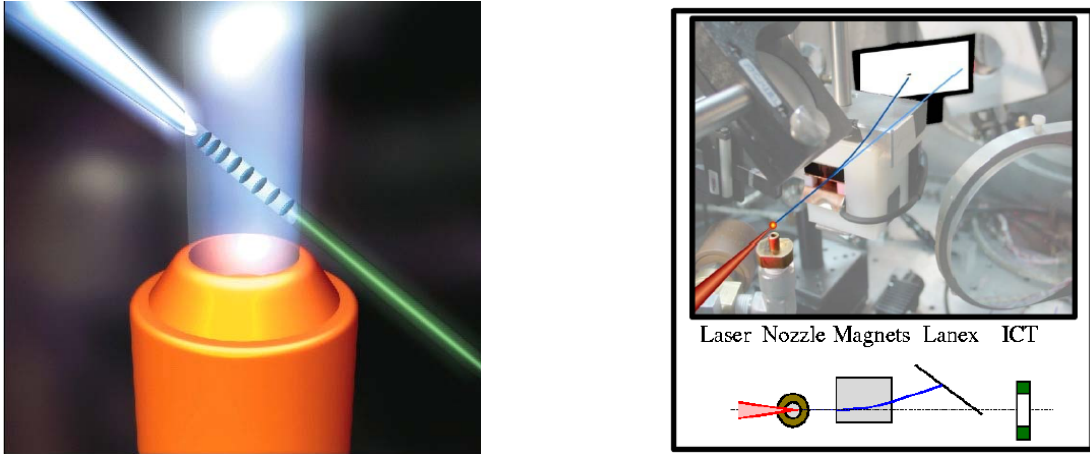


Fig. 4.5. Scheme of the experiment on laser-plasma acceleration of electrons [39]

As follows from the theory of self-focusing [40], for suppression of wave beam diffraction in plasma, its power must be greater than some value known as self-focusing critical power

$$P > P_c = 0.017 \frac{n_c}{n} \quad [\text{TW}] \quad (2.1.1)$$

where n is plasma density, $n_c \approx 1.3 \cdot 10^{21} \text{ cm}^{-3}$ is the critical plasma density for laser radiation with a wavelength of $\lambda = 910 \text{ nm}$. This condition sets a lower limit of plasma density which allows laser pulse self-channeling. For example, for the power of a single beam of 15 PW, $n > 10^{15} \text{ cm}^{-3}$; for the total power of 180 PW, $n > 10^{14} \text{ cm}^{-3}$. It should be noted that this condition is an approximation, since it is obtained for an infinitely long laser pulse. In addition to the laser pulse diffraction, the electron acceleration in laser plasma is also limited by electron dephasing (the electrons moving in a plasma wave can get from the accelerating phase to the decelerating phase of the field) and by energy absorption of the laser field in plasma. The characteristic length at which the electrons get out of phase is defined by [41]

$$l_d \approx \frac{\omega^2}{\omega_p^2} \lambda_p \quad (2.1.2)$$

$$1, \quad a_0^2 \ll 1,$$

$$\frac{2a_0^2}{\pi}, \quad a_0^2 \gg 1,$$

where ω is laser radiation frequency, ω_p is electron plasma frequency, a_0 is the normalized vector potential of laser radiation. The normalized vector potential is related to the laser radiation intensity by

$$a_0 = 8.6 \times 10^{-10} \lambda [\mu\text{m}] \sqrt{I [\text{W}/\text{cm}^2]}. \quad (2.1.3)$$

In the strongly nonlinear regime, which is typical for XCELS experiments, strong electron cavitation occurs. As a result, plasma cavity almost completely free of plasma electrons is

formed behind the laser pulse. In this strongly nonlinear regime, the dephasing length is given by [12]

$$l_p \approx (2/3) \left(\omega^2 / \omega_p^2 \right) R, \quad (2.1.4)$$

where R is the radius of the cavity. The length on which a significant part of the laser pulse energy is lost can be estimated to be [41]

$$l_{pd} \approx \frac{\omega^2}{\omega_p^2} \lambda_p$$

$$a_0^{-2}, \quad a_0^2 \ll 1, \quad (2.1.5)$$

$$a_0 / 3\pi, \quad a_0^2 \gg 1.$$

These estimates were obtained in the one-dimensional approximation. For a real three-dimensional geometry, there are no simple and accurate estimates for l_{pd} .

The similarity theory developed in the works [12, 42] allows relating parameters of the electrons accelerated in plasma to parameters of the laser and the plasma. It follows from the theory that the requirement of effective electron acceleration imposes certain restrictions on the geometry of the laser pulse

$$R < cT, \quad (2.1.6)$$

where R is the transverse size of the laser pulse, and T is its duration. In addition, the plasma density must also be bounded from above [42]

$$n_1 < n_c \sqrt{\frac{P}{P_{rel}}} \frac{1}{\omega T}, \quad (2.1.7)$$

where $P_{rel} = m_e^2 c^5 / e^2 \approx 8.5$ GW is relativistic power. The energy of the accelerated electrons can be estimated from the similarity theory as [42]

$$E_{mono} \approx 0.65 m_e c^2 \sqrt{\frac{P}{P_{rel}}} \frac{cT}{\lambda}. \quad (2.1.8)$$

For the minimum duration of laser pulse of 25 fs and the power of one beam of 15 PW, from (2.1.9) we obtain the electron energy of 3.6 GeV. Summation of the energy of all 12 beams will give the electron energy of 12.5 GeV.

However, this laser pulse duration is not optimal, since in this case $a_0 \gg 1$. Indeed, under the assumption that $R = cT$, formula (8) can be rewritten as

$$E_{mono} \approx 299 a_0^{-1/3} \left(\frac{W}{\lambda} \right)^{2/3} \text{ MeV}. \quad (2.1.9)$$

From this formula it follows that the maximum energy of the accelerated electrons can be obtained at the lowest possible value of the parameter $a_0 \approx 1$. Then, for a single beam with a pulse energy of 370 J the energy of the accelerated electrons may reach 16.6 GeV, and the pulse duration will be 537 fs. The scheme of the XCELS laser facility allows increasing laser pulse duration. Summation of all 12 beams will increase pulse

energy up to 4440 J. Then, the energy of the accelerated electrons may reach 87 GeV, which greatly exceeds the energy achievable in modern linear accelerators.

Finally, hydrogenation of a laser pulse using plasma channels and injection of an external electron beam into laser-plasma accelerating structure can further enhance acceleration efficiency. In this case, according to the estimates made by the UCLA group (see Table 4.1), for the parameters similar to XCELS parameters, the energy of accelerated electrons can exceed 1 TeV, which means advance to the lepton energy level unattainable to the currently available accelerators.

P(PW)	τ(fs)	n_p (cm⁻³)	w_0 (μm)	L(m)	a_0	$\Delta n_c/n_p$	Q(nC)	E(GeV)
0.020	30	1×10^{18}	14	0.016	1.76	60%	0.18	0.99
0.040	30	1.5×10^{18}	14	0.011	2.53	40%	0.25	0.95
0.100	30	2.0×10^{18}	15	0.009	3.78	0%	0.40	1.06
0.200	100	1.0×10^{17}	45	0.52	1.76	60%	0.57	9.9
2.0	100	3.0×10^{17}	47	0.18	5.45	0%	1.8	10.2
2.0	310	1.0×10^{16}	140	16.3	1.76	60%	1.8	99
40	330	4.0×10^{16}	146	4.2	7.6	0%	8	106
20	1000	1.0×10^{15}	450	500	1.76	60%	5.7	999
1000	1000	6.5×10^{15}	460	82	12.1	0%	40	1040

Table 4.1. Maximum energy of accelerated electrons for different values of laser and plasma parameters with and without plasma channel, with self-injection and with external injection.

Channel guiding: 60% and 40%; Self-guiding: 0%; external injection: 60%; self-injection: 40% and 0% $P/P_c = 0.7$ for 60% case, and 2 for 40% case [42, 43].

Activity 2.2. Laser-plasma acceleration of ions to 1–10 GeV energy

In comparison with the laser acceleration of electrons, study of the possibilities of laser acceleration of protons and light ions was initiated relatively recently, a little more than a decade ago. The main reason for this is that, being much heavier particles than electrons, protons are significantly less susceptible to the direct effect of rapidly oscillating laser fields, so they demand for acceleration larger radiation intensities. For example, in experiments on laser acceleration of electrons in a transparent plasma produced by ionization of gas targets, the ions are practically immobile, acting as a background of a positive charge. In the case of interaction with a target in the form of dense (e.g., solid state) plasma on femtosecond time scales, the energy of intense laser radiation converts mainly to the energy of motion of a small surface fraction of the electrons. Because of the acquired high heat, these electrons with a small scattering cross-section scatter within the plasma target almost without collision. Therefore, thermal equilibrium occurs on the temporal and spatial scales greatly exceeding the characteristic values of the durations of currently available ultraintense laser pulses, which on the whole provides dispersal of laser energy, resulting in relatively low ion thermal energies.

Nevertheless, thanks to a number of critical applications, laser acceleration of protons and light ions is now one of the priority researches in the field of high power laser systems. Of special mention among these applications is development of relatively compact and cheap ion accelerators for medical purposes as an alternative to the currently used huge and expensive classical accelerators. Development on the basis of laser technologies of compact sources of proton and ion beams with controlled energies up to several hundred MeV may have revolutionary implications for the development and wide application of hadron therapy for cancer treatment. This therapy, like other forms of radiotherapy, is basically ionizing action on tumor cells. Of major importance is a possibility of spatially localized irradiation, which eliminates the negative impact of radiation on neighboring biological tissues. The advantage of using accelerated light ions over the methods of radiotherapy more commonly used today can be readily seen in Fig. 4.6, which shows the relative dose of absorbed energy as a function of the radiation penetration depth. The plot for the accelerated carbon ions clearly demonstrates the so-called Bragg peak of the absorbed energy, position of which may be controlled by changing the ion energy at the input to the biological tissues. The ion impact on the neighboring biological tissues is much less than in the case of alternative methods. It should be noted, however, that proton therapy makes very significant demands on the quality of the ion beam. In particular, it requires very low energy spread (about 1%).

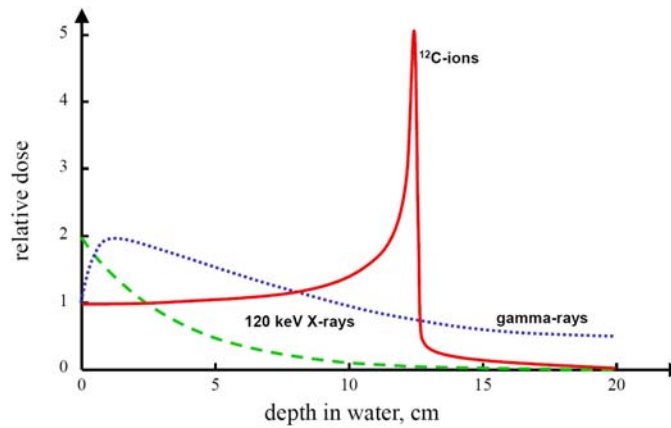


Fig. 4.6. Relative dose of absorbed radiation energy versus penetration depth into water for different methods of radiotherapy

Among other applications of laser acceleration of protons worthy of mention is protonography – the technique of determining internal structure of various objects by recording the protons that have passed through them. Also of interest is the concept of "fast ignition" for controlled thermonuclear fusion using for fuel compression and heating protons accelerated by laser radiation [44].

Due to the increase of laser radiation intensities and stimulation of possible applications, the laser acceleration of protons and light ions has been rapidly developing in the recent ten years. During this time, a variety of theoretical concepts based on the use of different structured targets and strongly nonlinear relativistic effects were developed. In addition, the first experimental studies were conducted that enabled producing protons with energies of several tens of MeV.

Historically, acceleration near the surface layer of hot electrons (Target Normal Sheath Acceleration – TNSA) was the first studied mechanism of acceleration of protons and light ions [45], that is basically the following (see Fig. 4.7). An intense laser pulse is focused onto the surface of a thin metal foil, usually at an angle to increase the degree of laser radiation absorption and to avoid backreflection, which can cause damage to the amplifying medium of the laser system. When interacting with the metal surface the near surface atoms are ionized and the electrons are rapidly (over times of the order of the period of optical radiation) heated and they acquire high energies (from several tens or hundreds of keV to several MeV). Further, these electrons scatter in all directions. Because of high energies the electrons have small scattering cross-sections at target atoms and penetrate almost collisionlessly through the thickness of the foil, reaching the surface opposite to the irradiated one. Due to the high-energy, despite the restraining electrostatic forces of the target ions, the fast electrons mechanically escape from the metal foil, forming near the surface a quasi-stationary electric field of charge separation

directed normally to the surface. This field, in turn, accelerates the ions normally to the target surface. It should be noted that in the first experiments protons and light ions were observed that were contained in the surface layer usually present in natural conditions due to formation of an oxide film and condensation of water vapor.

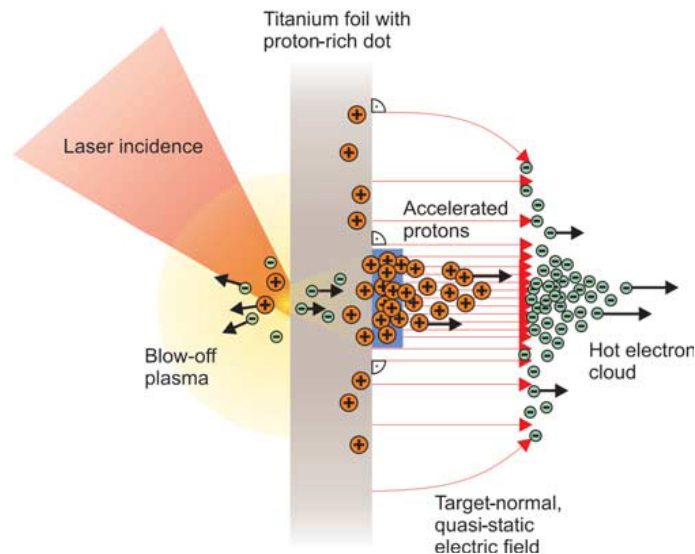


Fig. 4.7. Scheme of ion acceleration by a surface layer of heated electrons (source: [46]). The laser pulse incident from the left heats target electrons which go beyond the target, creating electrostatic field. Light ions and protons on the target surface are accelerated by this field in the direction nearly perpendicular to the target surface

One of the first experiments demonstrating the possibility of ion acceleration in the above process was conducted at the Lawrence Livermore National Laboratory, where a 0.5-5 ps *Nova* pulse with peak intensity over 10^{20} W/cm² generated by a petawatt laser system was focused on the surface of different metal foils. Light ions accelerated from the back surface of the foils, which had quasi-maxwellian energy distribution up to an energy of about 55 MeV were recorded in that experiment. The total of more than 10^{13} particles with average energy of about 1 MeV were accelerated [47].

A possible way of producing ion beams with quasi-monoenergetic spectra, which is required for most applications, is to use a structured target in the form of a metal foil coated with a thin layer containing accelerated light ions [48]. The idea is that after formation of accelerating field near the rear surface, the heavy ions of the foil remain almost stationary for a relatively long time, forming an accelerating field constant in time, whereas the light ions from the surface coating layer are accelerated in this field over relatively small times. If the number of light ions is so small that they do not strongly perturb the accelerating field, and the coating thickness is much smaller than the characteristic scale of the accelerating field decay, the light ions are in equal conditions and acquire almost the same energy during acceleration, forming a quasi-monoenergetic spectrum. This technique has been confirmed by numerical simulations as well as in

experiments [46, 49], in which proton beams with energies of about 1.2 MeV and energy spread of about 25% were obtained.

To increase the efficiency of energy absorption and, consequently, increase the energy of the accelerated ions it is promising to use nanostructured targets. For example, it was shown that with the use of foil with small optimal-size holes the efficiency of laser pulse energy conversion into kinetic energy of ions can reach 17.6% [50]. It was also proposed to use as a target foil with another foil placed against it in the plane of incidence [51]. It is argued that this foil can play the role of an additional source of hot electrons effectively accelerated by the laser pulse propagating along it. An alternative source of hot electrons may be a target in the form of a thin foil and an attached thicker foil having a thin channel propagating in which a laser pulse accelerates electrons from the channel surface in the direction to the thin foil [52].

Under the XCELS Project it is intended to investigate experimentally new methods for more effective acceleration in the TNSA regime, as well as to examine the efficiency of this method at high intensities.

At the same time, despite the relative success of the TNSA scheme, at high intensities, other schemes, most of which cannot be implemented at low intensities, seem to be more effective. Particularly noteworthy of these is the so-called scheme of laser-piston proposed in 2004 [53] (also called light sails scheme or light pressure acceleration scheme). This scheme is based on the idea of acceleration of bodies under the action of light pressure proposed back in the early XX century. In the initially proposed scheme a thin foil consisting of hydrogen is irradiated by a laser pulse having intensity of about 10^{23} W/cm², resulting in extraction of a plasmoid consisting of electrons and ions and in its acceleration as a whole up to proton energies of several GeV (see Fig. 4.8). Also proposed in [53] was a simple model of acceleration of an ion layer which was based on the assumption that the layer as a whole is accelerated by the force of pressure from the laser pulse. It should be taken into consideration that due to the Doppler effect the reflected pulse has a much lower frequency than the incident one, so at relativistic velocities almost 100% of the energy of the incident radiation may be transferred to the layer. The final energy of ions in the layer as a function of the acceleration time for the ultrarelativistic case can be assessed as:

$$E_i^{kin}(t) \approx m_i c^2 \left(\frac{3E_L^2 t}{8\pi n_e l m_i c} \right)^{\frac{1}{3}},$$

where the following notation is used: m_i – ion mass, E_L – electric field amplitude in the laser pulse, n_e – initial electron concentration in the layer, l – initial layer thickness. For typical

values of parameters to be achieved in one channel of XCELS facility (25 fs pulse duration, maximum intensity of 10^{23} W/cm²) the estimation is 30 GeV for 1 micron thick foil and electron density 10^{22} cm⁻³.



Fig. 4.8. Modeling of acceleration of a thin (10 nm) metal foil by light pressure of superintense laser radiation. Left – system at the initial moment of time, right – system during acceleration. The green color depicts electron density, white – the ion density, brown – electromagnetic field

A similar idea can be used to accelerate ions at the front surface [54-58]. In this scheme normal incidence of a circularly polarized pulse on a solid target is employed. The use of circular polarization ensures absence of collisionless heating, and normal incidence leads to a quasi-stationary acceleration pattern: the electrons are pushed away under the action of ponderomotive force and form an accelerating potential, on passing which the ions that were at the front border acquire energy proportional to the amplitude of the laser pulse [59]. Later this scheme was supplemented by the idea of a multiple use of the layer: at the first stage the stationary layer is accelerated; when the pulse reaches its end, it begins to accelerate again the ions that have already been accelerated, thus increasing their energy [60]. For small layer thicknesses, this scheme reduces to the same idea of thin film acceleration by light pressure. However, the use of a circularly polarized pulse is significant, as it allows reducing radiation intensity required in this scheme [61]. A characteristic feature of the scheme is that all the ions acquire the same energy. Other advantages of this scheme have also been shown. These are high efficiency, high-densities of the produced ion bunches, small divergence of the generated beam and its short – femtosecond – duration [62].

The disadvantage of the method of ion acceleration by light pressure is its susceptibility to transverse instabilities of the Rayleigh-Taylor type [63] or smaller scale instabilities [64, 65], which may lead to a transparent layer and to a complete halt of the acceleration process. However, it was shown that these instabilities may be suppressed if the accelerated layer motion is ultrarelativistic (which requires very high radiation intensities) [66]; it is also possible to use a specially profiled laser pulse [67] or target [68]. The layer may also be stabilized due to the boundary effects [69] or by addition of the

initial phase of pulse self-channeling [70]. It was also suggested to use a two-component target [71] consisting of carbon and hydrogen atoms. Worthy of notice is the possibility of cascading the acceleration process in several thin films [72].

The regime of light pressure acceleration mode is currently poorly investigated experimentally, as it requires sufficiently high radiation intensities. Two series of experiments on the subpetawatt facility VULCAN were conducted at the Rutherford Laboratory in 2008 [73]. Laser pulses with energies of 60 and 250 J, duration of 1 and 0.7 ps, respectively, were used. The focus intensities in the 10^{19} - 10^{20} W/cm² range were attained. On irradiation by such pulses, of metal foils of aluminum and copper 2 and 5 microns thick, respectively, accelerated proton beams emitted from the rear of the target were observed. Their specific feature was that the low-energy part of the beam had relatively small divergence and was emitted from a spot of small area. This contradicts the results obtained for TNSA regime before, so it was concluded that in those experiments, the ions were accelerated by the force of light pressure, which was further confirmed by numerical simulations. In 2009, results of the experiments conducted at the Max Born Institute on the 20 TW facility were published [74]. In those experiments, a circularly polarized laser pulse having energy 1.2 J and duration 45 fs with a wavelength of 810 nm was used for the first time. The experimenters used the double plasma mirror technique to attain pulse contrast of order 10^{-11} at times less than 10 ps. This allowed them to implement the interaction of a laser pulse with intact ultra-thin targets; carbon films with a thickness of 2.9 to 40 nm were used in the experiment. The result of the experiment was formation of a monoenergetic beam of carbon ions C⁶⁺ with an energy of 30 MeV. The optimal interaction was attained for the 5.3 nm thick foil (see Fig. 4.9). Both results are in good agreement with the previously developed theory and the conducted numerical simulations.

The acceleration of protons and light ions by light pressure will be one of special foci under the XCELS Project. This will demand solution of a number of technological problems which include the following. First, it is necessary to learn to produce high-intensity pulses with circular polarization. Second, the produced pulses should have high contrast for the interaction to occur without breaking the target. This is particularly important for targets which are thin, nanometer films. It is also necessary to develop production technology of nanostructured targets of arbitrary geometry which allows optimizing the interaction process.

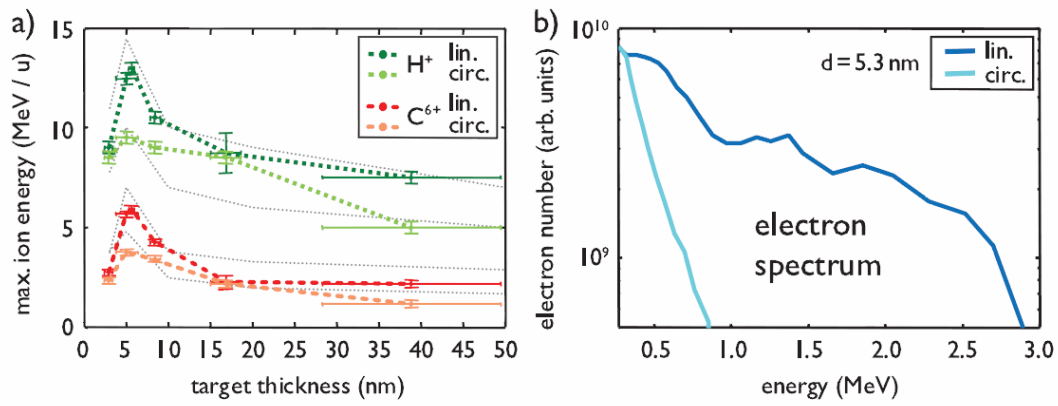


Fig. 4.9. (a) The measured dependence of maximum proton energy (green and light green dotted lines) and carbon ions C^{6+} (red and orange dotted lines) for the irradiation of linearly and circularly polarized pulses. The grey dashed lines correspond to the results obtained by two-dimensional PIC-simulations. (b) Electron spectra measured for the case of optimal target thickness (5.3 nm). It is seen that for the case of circular polarization, electron heating is much weaker. The results are taken from [74]

Other techniques of producing high-energy beams of protons and light ions are also considered in the literature. Of special notice are the following techniques. A possibility of proton acceleration in the cavitation mode of laser pulse propagation in a transparent plasma was considered in [75], but this scheme requires relativistic ion energies; therefore it was proposed to combine it with pre-acceleration by the method of light pressure [76]. Another proposed regime is the so-called BOA regime (Breakout Afterburner) [77]. In this mode, linearly polarized laser radiation interacts with a thin foil heated over the entire volume and destroyed, resulting in pulse propagation in the heated plasma. In this case, relativistic Buneman instability develops [78], which leads to efficient energy transfer from electrons to ions [79, 80].

A pulse with the energy of 80 J and pulse duration of 500–600 fs focused on the target with F/3 off-axis parabola was used in the experiments at the *Trident* facility in the Livermore National Laboratory. Average intensity on the target was about 2×10^{20} W/cm², and peak intensity amounted to 5×10^{20} W/cm². A significant feature was use of special technologies (short-pulse optical parametric amplification) for enhancing radiation contrast. The resulting contrast was $< 2 \times 10^{-12}$ for the pedestal with a duration of 1.2 ns and $< 5 \times 10^{-10}$ for the pedestal of 0.5 ps. This enabled experiments with ultrathin (down to 3 nm) films. Films of diamond-like carbon (DLC), developed at the Kurchatov Institute, were used as targets. An important feature of DLC as compared to other forms of carbon is high mechanical strength of films made of this material.

A specially developed high-resolution Thomson parabola [81] was used as diagnostic equipment. It allowed measuring carbon ion energies up to 2 GeV. A typical ion spectrum obtained for 150 nm foil is shown in Fig. 4.10. Maximum attained carbon ion C^{6+} energy

was 500 MeV; there were almost no ions with smaller charge. Maximum ion energy changed with changing target thickness (see Fig. 4.11) as a result of the transition to other interaction modes. If the foil thickness was too small, the foil rapidly became transparent, whereas the best conditions for ion acceleration were observed in the mode of relativistic plasma transparency. This means that plasma density must be higher than critical in the linear case, but lower than the threshold of self-induced relativistic transparency. For larger plasma thickness, no relativistic transparency occurs, and acceleration occurs in a less efficient TNSA mode.

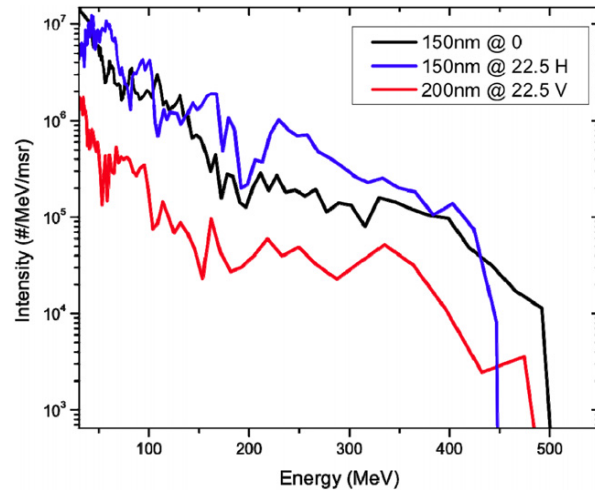


Fig. 4.10. Spectrum of carbon ions accelerated by laser pulse for optimal thickness of DLC-film. The spectra were measured for different angles relative to the propagation direction of laser pulse that was incident normally to the target surface. Black: 0° , red: 22.5° in the vertical plane, blue: 22.5° in the horizontal plane. The results were taken from [80]

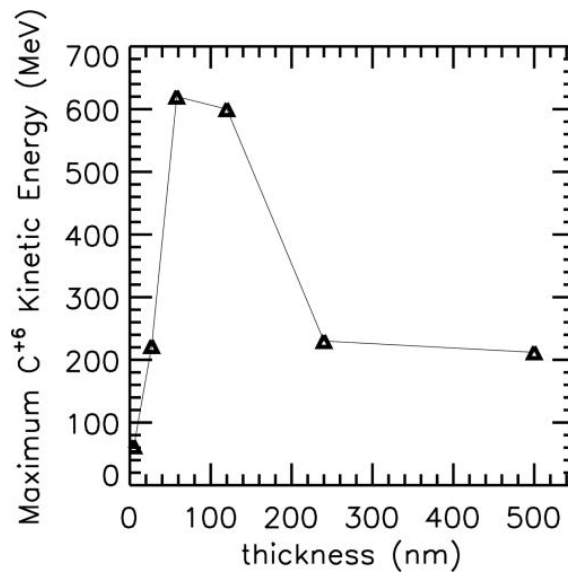


Fig. 4.11. Maximum carbon ion energy *versus* film thickness for parameters of the experiment on *Trident* facility (result of numerical calculation). Taken from [79]

It is expected that the XCELS Project will be carried out in close collaboration with the Livermore National Laboratory aiming at exchanging experience in fabrication and use of ultrathin nanometer targets and on the problems concerned with diagnostics of processes occurring in the experiments. The laser systems constructed under the XCELS Project will be used for conducting experiments analogous to the ones at *Trident*, but with higher radiation energy, which will enable generating still higher energies of accelerated ions.

Activity 2.3. Combined acceleration in linear and laser-plasma particle accelerators

As can be seen from *Activity 2.1*, a promising scheme to achieve maximum energy of accelerated electrons is a scheme which is based on the acceleration of the external electron beam injected into an accelerating plasma structure. Moreover, in recent years such a scheme is considered to be most suitable for achieving high quality beams of accelerated electrons (low energy spread, low emittance, etc.), which is especially important for some applications, such as the creation of X-ray free electron lasers.

A key problem to be solved before the laser-plasma X-ray laser will be built is to reduce the energy spread of accelerated electrons in the beam to values less than 0.1%. Two ways are suggested to solve this problem:

- To analyze and select the most suitable scheme for self-injection of plasma electrons, which would provide the minimum energy spread of electrons in the beam (less than 0.1%). The scheme may utilize different methods: an auxiliary laser pulse, a special spatial profile of the plasma, plasma additives, etc.
- To investigate the external injection based on the injection into a plasma accelerating structure of an electron beam generated in the external photoinjector. The purpose of this investigation is to find a regime in which the initial energy spread is maintained, and an exact synchronization between the photoinjector and the laser pulse that generates a plasma accelerating structure is performed.

The Project envisions construction of a low energy electron accelerator based on standard technology using a photoinjector. A beam produced by such an accelerator will be injected into a plasma accelerating structure formed by a powerful laser pulse. Currently, much interest is given to a scheme of electron beam injection at a small angle to the axis of the laser pulse [82-86] (see Fig. 4.12). This scheme can provide high efficiency of injection, so that the percentage of electrons trapped in the accelerating plasma structure may reach 50% [82].

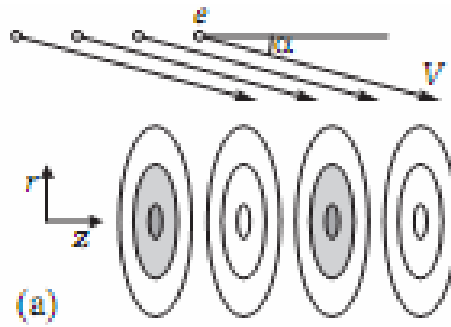


Fig. 4.12. Schematic of angular injection into the accelerating plasma structure [86]

Although part of the electrons may initially fall into the defocusing region of the accelerating plasma structure, thanks to the longitudinal dynamics (deceleration or acceleration along the axis of the laser pulse), the electrons can move to the focusing phase and get accelerated (Fig. 4.13).

Estimates show that the optimal angle for the injection of electrons is [86]

$$\alpha \approx (V_w - V_e) \frac{\sigma^2 \omega_p}{2c^2 r_0}, \quad (2.3.1)$$

where V_w is the phase velocity of the accelerating structure of the plasma, V_e is the initial velocity of the electron beam, ω_p is the electron plasma frequency, c is the speed of light, σ is the size of the focal spot of the laser pulse, and r_0 is the distance of the injection point from the axis.

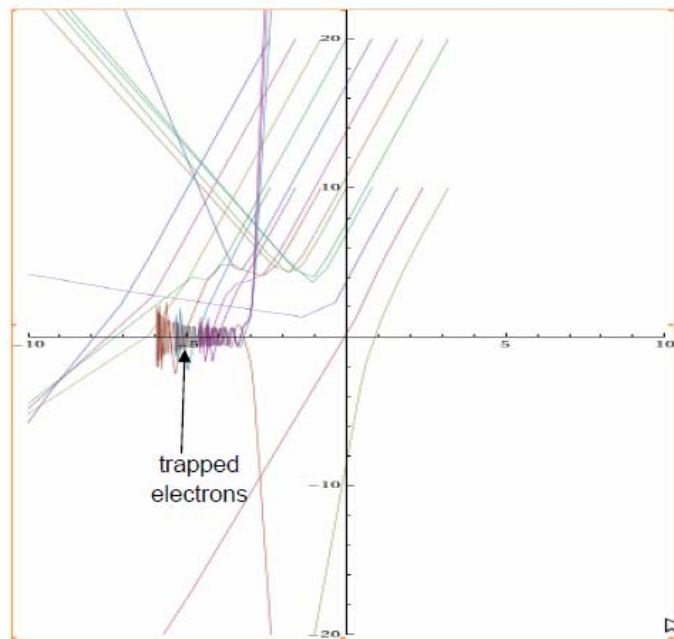


Fig. 4.13. Trajectories of test electrons of an external beam injected into an accelerating plasma structure

Objective 3. Creating new sources of radiation in the hard X-ray and gamma-ray regions

Under this objective, it is supposed to create several classes of unique light sources in the X-ray and gamma-ray bands, including femtosecond sources of incoherent radiation with extremely high brightness, femtosecond sources of coherent radiation – compact X-ray free-electron lasers, attosecond and zeptosecond light sources, and narrow-band gamma-ray sources for photonuclear physics tasks. To create these sources laser targets and wigglers will be developed, special features of energy transformation of high-intensity optical pulses to the X-ray and gamma-ray bands will be studied, experiments on a prototype laser and then on a 200 PW laser will be performed. The new light sources will have great diagnostic potential. Essentially, they will open up opportunities, for the first time, to study objects with picometer spatial and subfemtosecond temporal resolution.

Activity 3.1. Creating hard radiation sources with extremely high brightness

The high rate of acceleration of charged particles in a plasma allows using laser-plasma accelerators in sources of hard electromagnetic radiation such as X-ray free electron lasers. Moreover, large focusing forces in accelerating plasma structures make it possible to use them as plasma wigglers. All this can significantly reduce the size and cost of radiation sources. Compact and bright X-ray sources are now in high demand in medicine for low-dose phase-contrast X-ray tomography, which enables diagnosis of tumors in the body without histology. Creating compact X-ray and gamma-ray sources would introduce the X-ray imaging to routine medical practice and allow the investigation of nanostructures in small laboratories, since modern nanotechnology centers are now built around huge centers of synchrotron radiation.

In the strongly nonlinear regime of interaction of a relativistically strong laser pulse with a plasma, which is typical for the XCELS facility, electrons trapped in the plasma cavity will make transverse betatron oscillations during acceleration (Fig. 4.14). The betatron oscillations lead to the generation of electromagnetic radiation. The Doppler effect makes the radiation frequency of the ultrarelativistic electron many times greater than the frequency of betatron oscillations. For typical parameters of the laser pulse-plasma interaction the frequency of the "betatron" radiation is in the X-ray region of the electromagnetic spectrum [8]. As is shown by calculations [87, 88] and recent experiments [89-93], this mechanism can be used to create a compact and powerful X-ray source for laser plasma diagnostics as well.

The focusing forces acting on an electron in the plasma cavity can be represented as $\mathbf{F}_\perp \approx -m\omega_p^2 \mathbf{r}_\perp / 2$, where \mathbf{r}_\perp is the radius vector from the axis of the cavity to the electron. If the longitudinal momentum of the electron is much greater than the transverse momentum, the equation describing the transverse (betatron) oscillations coincides with the equation of the linear oscillator $\ddot{\mathbf{r}}_\perp + \mathbf{r}_\perp \omega_p^2 / 2\gamma = 0$, where γ is the relativistic gamma factor of the electron. Consequently, the betatron frequency is $\omega_b = \omega_p / (2\gamma)$. The betatron oscillation period $\lambda_b = 2\pi / k_b = 2\pi \sqrt{2\gamma} / k_p$ was measured in experiments [94], where $k_p = \omega_p / c$.

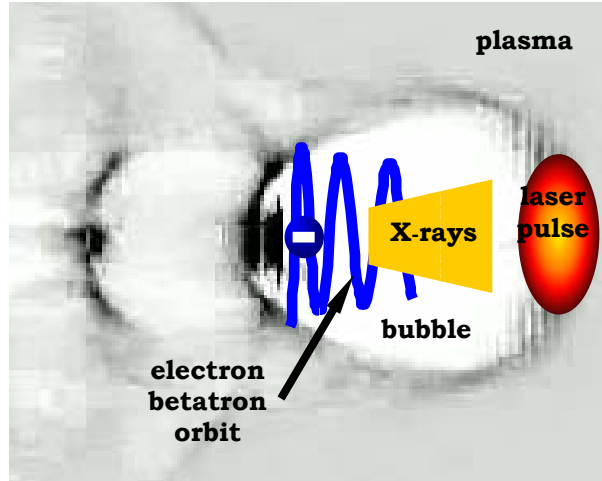


Fig. 4.14. Generation of betatron radiation in the plasma cavity (schematically)

The wavelength emitted by the electron which produces betatron oscillations of low amplitude near the axis of the channel is of the order of $\lambda \approx \lambda_b / (2\gamma^2)$. If the oscillation amplitude increases, the electron radiates high harmonics. If the oscillation amplitude r_0 is so large that the parameter

$$K = \gamma k_b r_0 = 1.33 \cdot 10^{-10} \sqrt{\gamma n_e [\text{cm}^{-3}]} r_0 [\mu\text{m}] \quad (3.1.1)$$

characterizing the intensity of the "ion undulator" becomes large $K \gg 1$, the radiation spectrum becomes broadband and quasi-continuous. In this case, the frequency dependence of the emission spectrum becomes similar to that of the spectrum of synchrotron radiation, which is determined by a universal function (see Fig. 4.15)

$$S(\omega/\omega_c) = (\omega/\omega_c) \int_{\omega/\omega_c}^{\infty} K_{5/3}(x) dx, \quad (3.1.2)$$

where ω_c is the critical frequency [95]. For frequencies much lower than the critical one the radiated energy increases by the law $\sim \omega^{2/3}$, reaches its maximum at $\sim 0.29\omega_c$, and decreases exponentially at $\omega > \omega_c$. The critical frequency for an electron emitting betatron oscillations in the ion channel is given by [88]

$$\hbar\omega_c = \frac{3}{2}\gamma^3\hbar cr_0 k_b^2 \approx 5 \times 10^{-24} \gamma^2 n_e [cm^{-3}] r_0 [\mu m] keV. \quad (3.1.3)$$

Since the particles are ultrarelativistic, the radiation is contained within a small solid angle

$$\theta \approx \frac{K}{\gamma}. \quad (3.1.4)$$

The synchrotron radiation in the ion channel has been observed recently in experiments [89].

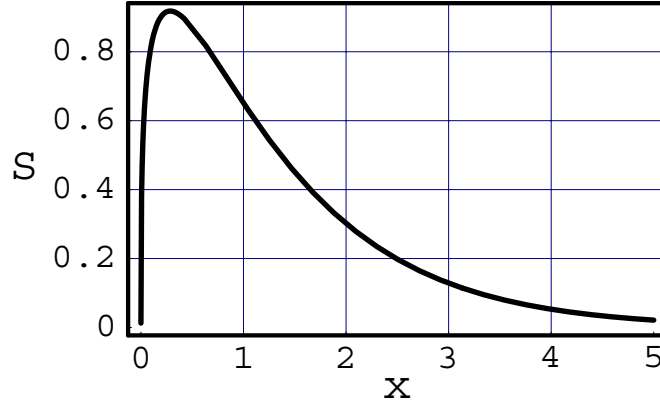


Fig. 4.15. Universal function for the spectrum of synchrotron radiation $S(x)$

The average power emitted in a plasma cavity is defined by [87]

$$\langle P_{total} \rangle \approx \frac{e^2 c}{12} N_b \gamma^2 k_b^4 r_0^2, \quad (3.1.5)$$

where N_b is the number of betatron oscillations excited by an electron. It is also possible to introduce a quantity corresponding to the amount of energy lost by the electron per unit length:

$$Q = \langle P_{total} \rangle / c \approx 1.5 \cdot 10^{-45} \left(\gamma n_e [cm^{-3}] r_0 [\mu m] \right)^2 \frac{MeV}{cm}. \quad (3.1.6)$$

The average number of photons of energy $\hbar\omega_c$ emitted by the electron is [88]

$$\langle N_{ph} \rangle \approx \frac{4\pi e^2}{9 \hbar c} N_b K \approx 1.02 \cdot 10^{-2} N_b K. \quad (3.1.7)$$

It follows from (3.1.7) that the radiated power is proportional to the square of the plasma density, which was confirmed experimentally [94].

The plasma wiggler offers much greater focusing power than the standard magnetic wiggler. Indeed, the ratio of focusing forces in the plasma and magnetic wigglers can be estimated as follows: $F_{\perp,pl}/F_{\perp,m} \approx \omega_p^2 r_0 / (\omega_H c)$, where $\omega_H = eH/(mc)$ is nonrelativistic cyclotron frequency, and H is the characteristic intensity of the wiggler magnetic field. For typical XCELS parameters $n_e = 10^{19} cm^{-3}$, $r_0 = 1 \mu m$, $H = 10^4 G$, the plasma focusing force is 5 orders of magnitude greater than the magnetic one. Thus, for a given electron energy,

the energy of the emitted photon will be 10^5 times higher and the radiated power 10^{10} times greater for the plasma wiggler than for the magnetic wiggler.

The resonant interaction of an electromagnetic (EM) wave and betatron oscillations leads to electron bunching in the beam, which in turn may lead to amplification (or attenuation) of the wave. Such a process can be described by stimulated emission (absorption) of electrons in the ion channel. The increase in the intensity of the betatron radiation observed in recent experiments [92, 93] is associated with the resonant bounce of the betatron oscillations by the laser field.

Equation (3.1.7) can be rewritten as follows [96]

$$\langle N_{ph} \rangle \approx \frac{1}{9} \frac{e^2}{\hbar c} (k_p L) (k_p r_0) \approx \frac{1}{9} \frac{e^2}{\hbar c} (k_p L) \left(\frac{a_0^2}{\gamma} \right)^{1/4}, \quad (3.1.8)$$

where L is the distance at which an electron executes betatron oscillations. We assume that the initial amplitude of the betatron oscillations is about the size of a plasma cavity is $k_p R \approx \sqrt{a_0}$, where a_0 is the dimensionless vector potential of the laser field, and R is the radius of the laser cavity. At acceleration the amplitude of the betatron oscillations decreases $k_p r_0 \approx k_p R \gamma^{-1/4} \approx a_0^{1/2} \gamma^{-1/4}$. However, as the accelerated electrons move inside the plasma cavity, they can enter an area occupied by the laser pulse. As a result of the betatron resonance, the amplitude of betatron oscillations can again grow to the size of the cavity. In this case, the number of emitted photons increases $\gamma^{1/4}$ times. The conversion efficiency of electron energy into the hard radiation can be estimated as

$$\frac{N_{ph} \hbar \omega_c}{\gamma m c^2} \approx \frac{1}{12} \frac{e^2}{\hbar c} \frac{\hbar \omega_p}{m c^2} (k_p L) a_0 \gamma. \quad (3.1.9)$$

It follows from this expression that, in contrast to the acceleration, where the radiation friction plays a negative role, the generation of radiation is most effective in dense plasmas, and for large values a_0 . Estimates show that at plasma density of $n > 10^{18} \text{ cm}^{-3}$ and the energy of accelerated electrons over 10 GeV, a significant part of the beam energy is transferred to the energy of radiation. Since the efficient generation requires high energy of electrons, a two-step plasma profile can be used. At the first stage, where the plasma density is low, the electrons are accelerated to high energies, and at the second stage with the high plasma density the electron energy is converted into radiation.

As follows from (3.1.3), the energy of the photon emitted by an electron in a plasma cavity increases quadratically with the electron energy. When these energies are compared, the classical theory of radiation is not applicable any longer. The quantum effects in the strong electromagnetic field are characterized by the invariants [97]

$\chi = e\hbar/(m^3 c^5) |F_{\mu\nu} p_\nu| \approx \gamma(F_\perp/eE_{cr})$ and $\Upsilon \approx (\hbar\omega/mc^2)(F_\perp/eE_{cr})$, where $F_{\mu\nu}$ is the electromagnetic field tensor, p_μ is the four-vector of the particle, $\hbar\omega$ is the photon energy, and $F_\perp = m\omega_p^2 r$ is the shear force acting on a relativistic electron at a distance r from the axis of the cavity. χ defines the ratio of the electric field intensity in the reference frame connected with the electron to the intensity of the critical field E_{cr} . Υ defines the interaction of photons with the electromagnetic field. The quantum-electrodynamic effects become significant at $\chi \gg 1$ or $\Upsilon \gg 1$. If $\chi \gg 1$, then $\hbar\omega \gg \varepsilon$, and the quantum recoil of the electron associated with the photon emission becomes significant. Invariants can be presented in the form $\chi \approx 10^{-6} \gamma$ and $\Upsilon \approx 10^{-6} (\hbar\omega/mc^2)$ for parameters $n_0 \approx 10^{19} \text{ cm}^{-3}$ and $r = 15 \text{ } \mu\text{m}$. As follows from these expressions, the invariants are close to unity at particle energies of around 500 GeV. At a plasma density of $n_0 = 10^{20} \text{ cm}^{-3}$ the threshold electron energy above which the photon emission is of quantum nature is close to 50 GeV. In Fig. 4.16. different regimes of electron dynamics in a plasma cavity are shown, taking into account the radiation reaction force in the plane of parameters γ_0 (initial electron energy) – r_0 (initial deflection).

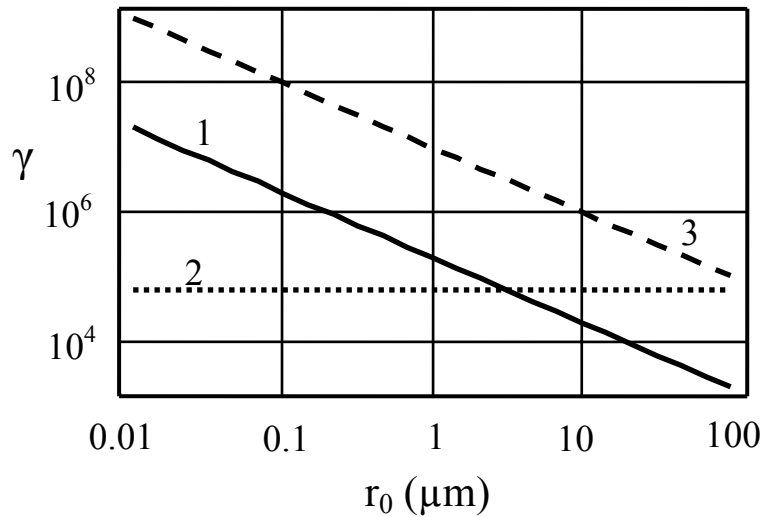


Fig. 4.16. Different regimes of electron dynamics in a plasma cavity, taking into account the radiation reaction force in the plane of parameters γ (initial electron energy) – r_0 (distance from the electron to the cavity axis at the initial time). Line 1 corresponds to the boundary, where the accelerating force is equal to the radiation friction force. Line 2 corresponds to the boundary at which the transit time through the cavity is equal to the period of betatron oscillations. Line 3 corresponds to the boundary that separates the quantum radiation region from the classical one

Let us analyze the one-step scheme for the XCELS parameters. In the experiments [92, 93] the brightness of the betatron X-ray radiation reached $10^{22} \div 10^{23}$ photons/s \times mrad² \times mm² in the 0.1% bandwidth. The spectrum of the radiation reached 7 MeV at 700 MeV accelerated electron energy for the energy of the laser pulse of 2 \div 5 J. This brightness is comparable to that of synchrotron sources of the third generation at a much smaller scale. Assuming that the plasma density is constant $2 \div 8 \cdot 10^{18}$ cm⁻³, and considering the same laser pulse duration ~ 30 fs [92], by using formulas (3.1.1)–(3.1.9) and the similarity theory for the strongly nonlinear regime [12] one can recalculate the parameters of radiation obtained in these experiments to parameters of radiation which will be available at XCELS. The energy of the radiation quanta at XCELS will be $\alpha^{5/4}$ times higher than in the experiments [92, 93] and will reach 2 GeV, where α is the ratio of the laser pulse energy at XCELS (4.4 kJ in the case of addition of 12 beams). In this case, the brightness will be $\alpha^{1/4}$ times higher and will reach 10^{24} photons/s \times mrad² \times mm² in the 0.1% bandwidth. By controlling the plasma density and the size of the focal spot one can dramatically increase the brightness by reducing the characteristic photon energy.

Let us now consider using numerical simulation [8] the two step scheme for XCELS. Let us suppose that at the first stage an electron bunch is obtained with the following parameters: energy 28.5 GeV, diameter $2r_0 = 24.6$ μ m, length $L_b = 82$ μ m, full charge $Q_b = 5.4$ nC. At the second stage the bunch interacts with the plasma cavity formed by a circularly polarized laser pulse with the Gaussian envelope $a(t, r) = a_0 \exp(-r_{\perp}^2/r_L^2 - t^2/T_L^2)$ and the following parameters $r_L = 8.2$ μ m, $T_L = 22$ fs, $a_0 = 10$, where $a = eA/mc^2$. The laser pulse propagates in a plasma with a density of $n_e = 10^{19}$ cm⁻³. The parameters used in this simulation are close to the XCELS parameters. At the beginning of the interaction, the leading edge of the bunch is located approximately in the center of the laser pulse (see Fig. 4.17(a)). The leading edge of the external electron bunch overruns the center of the laser pulse by 46λ during the time $T_{int} = 4500\lambda/c$. The number of betatron oscillations made by the electron bunch is about $N_0 = cT_{int}/\lambda_b \approx 1.1$. As can be seen from Fig. 4.17(b), the laser pulse and the plasma cavity are not destroyed during the whole time of interaction, when focusing of the external bunch occurs.

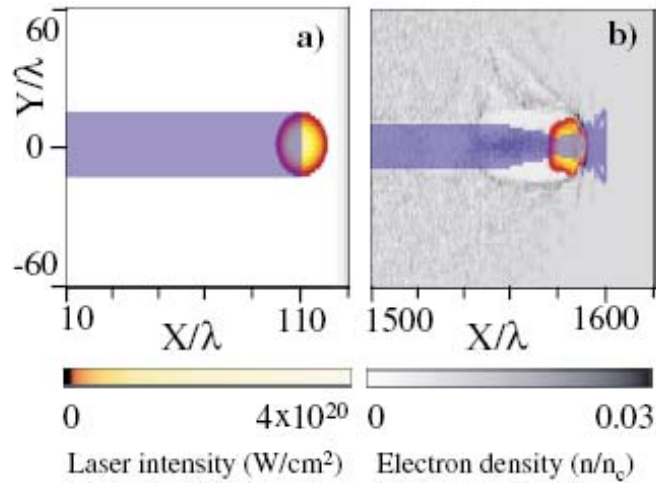


Fig. 4.17. Electronic concentration of a plasma and a beam, and the intensity of the laser pulse: a) at the beginning of interaction and b) at $ct/\lambda = 1500$

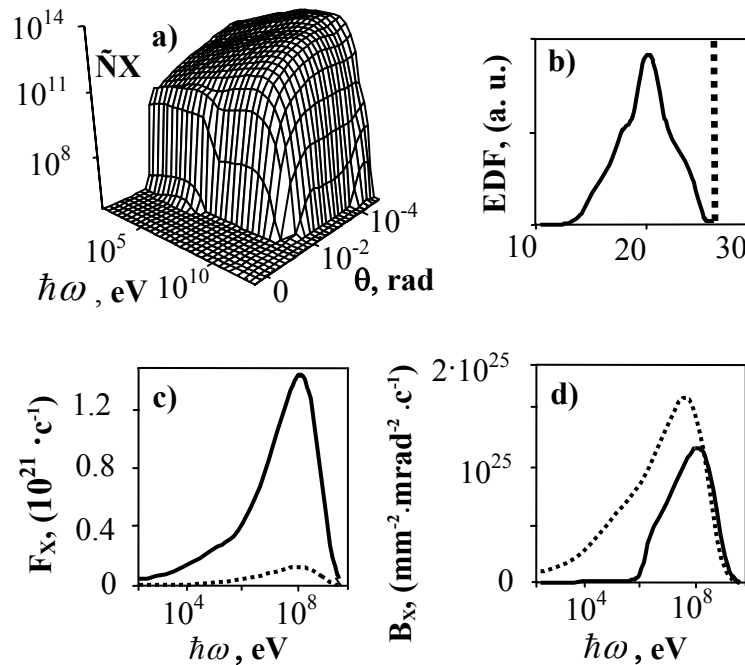


Fig. 4.18. a) The emission spectrum of the external electron beam after the laser pulse has passed the distance $ct/\lambda = 4500$; b) the distribution of the electron beam energy: solid line $ct/\lambda = 4500$, dotted arrow shows the initial monoenergetic distribution of the electron beam c) the photon flux and d) the spectral brightness. The dashed line in Fig. c) and d) corresponds to $ct/\lambda = 500$, solid line – $ct/\lambda = 4500$

The photon distribution by energy and angle for the interaction time $T_{int} = 4500\lambda/c$ is shown in Fig. 4.18(a). At this beam energy the intensity of the plasma undulator is approximately equal to $K \approx 817$. As can be seen from Fig. 4.18(a) the relativistic bunch radiates hard photons in a narrow solid angle. The maximum photon spectrum lies near the energy 210 MeV. The radiation is contained in a narrow angle relative to the axis of the

beam propagation $\theta \approx 10$ mrad, which is close to the estimated value of $K/\gamma \approx 15$ mrad. The total number of photons emitted by the bunch electron is about 2×10^{11} . This means that each photon emits approximately 6 photons. When estimating the number of photons with energy $\hbar\omega_c$, we obtain $N_x \approx N_e \langle N_x \rangle; 1.5 \times 10^{11}$, where N_e is the number of electrons in a bunch. Thus, the estimated value is in good agreement with simulation results. The bunch loses about a third of its energy for radiation. The energy distribution of electrons in the bunch after interaction is shown in Fig. 4.18(b). The photon flux and brightness as a function of photon energy are shown in Fig. 4.18(c, d). The brightness of the radiation at the beginning of interaction is somewhat higher than that at the end of the interaction, since at the beginning of the interaction the bunch is yet insignificantly focused and emits at low angles to the direction of propagation. The peak brightness of such a source exceeds that of synchrotron sources of the third generation.

Activity 3.2. Creation of a compact free-electron laser and wigglers

The creation of compact accelerators and X-ray sources, as well as X-ray lasers is a very topical and critical task facing the scientific and technological community. These compact devices will inevitably win most of the scientific market, competing with the existing individual large-scale facilities and providing new opportunities and new markets. These compact systems are very much in demand in university laboratories, medical and technology centers, and their widespread availability will greatly facilitate the use and access to such tools (Fig. 4.19).

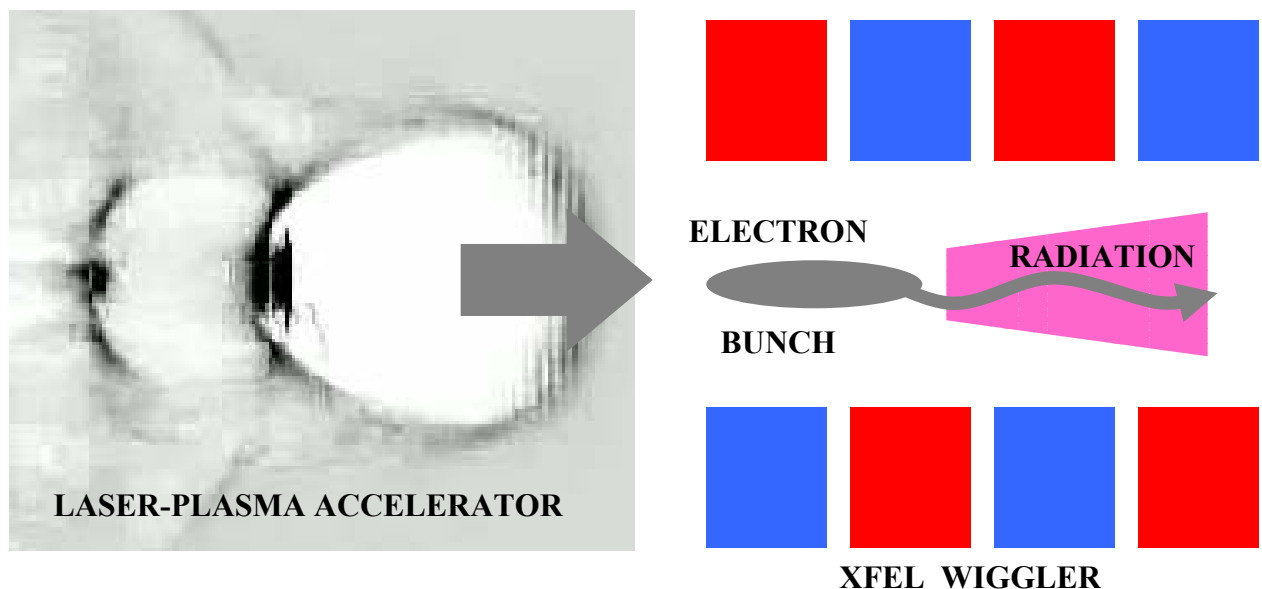


Fig. 4.19. The schematic of a free-electron laser with a laser-plasma accelerator

The advantages of the laser-plasma technology for compact X-ray lasers rely on the following recent achievements:

- Development and creation of high-power laser systems providing a high acceleration gradient in plasma (as high as 1 GeV per centimeter).
- Development of various methods of self-injection and external injection to accelerate electron beams to energies of more than 1 GeV with a small energy spread of electrons in the beam (less than 1% at present), allowing to anticipate that the best approach to achieve the energy spread of less than 0.1% will eventually be found.
- Steady progress in laser technology, making possible the creation of more efficient laser systems capable of generating high-quality electron beams with a high repetition rate.
- Experimentally tested idea of employing, instead of a common magnetic undulator, a plasma wiggler, which provides a several orders of magnitude higher value of the field intensity, deflecting the accelerated electrons. This solution significantly reduces the size of the radiation source.

Provided the above-mentioned scientific issues are resolved, the following technological challenges must be overcome before commercially attractive, technologically prepared samples of X-ray lasers can be created:

- Selection of optimal schemes for generating X-rays, both with the standard magnetic undulators and the plasma wigglers.
- Analysis and optimization of the laser system to improve efficiency and repetition rate, and to reduce the cost of fabrication of the system components, etc.
- In the case of an external photoinjector, the development of an optimal timing scheme between the laser system and the injector, selection of the scheme (magnetron or klystron) and optimization of microwave systems injector.
- If the acceleration scheme in the capillary will be chosen as the best way to maintain a long-term interaction between a laser and an electron bunch, it will be necessary to solve the problem of heat removal from the capillary at the desired high-repetition rate of the x-ray laser.

Activity 3.3. Creating high-brightness narrow-band gamma-ray beams

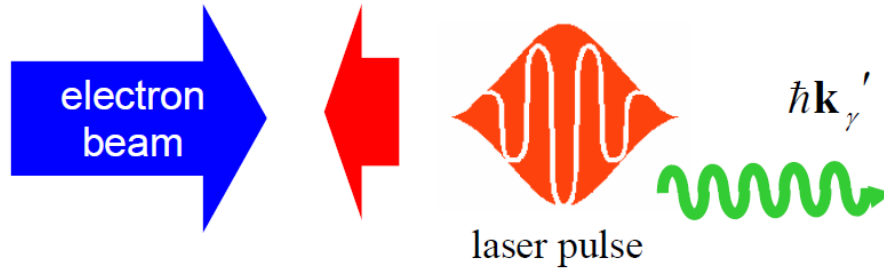


Fig. 4.20. Inverse Compton radiation (schematically)

Another relatively simple way of generating high-energy photons and testing the quantum electrodynamics in a laboratory is the Compton backscattering of an electron beam on a laser pulse (Fig. 4.20). In the case of the nonlinear Compton scattering each electron absorbs several quanta of the laser field with energy $\hbar\omega_L$ and emits a gamma quantum with energy $\hbar\omega$:

$$e + n\hbar\omega_L \rightarrow e' + \hbar\omega \quad (3.3.1)$$

The highest energy of the gamma-quanta is obtained by head-on collisions. In the linear regime, when the intensity of the laser pulse is not very high $a_0 \ll 1$, and the electron beam is relativistic $\gamma \gg 1$, the energy of backscattered photons increases by $4\gamma^2$ times, where $a_0 = |e|E_0/(mc\omega)$, E_0 is the electric field amplitude. In the nonlinear regime, when $a_0 \gg 1$ the Compton radiation spectrum consists of a set of harmonics and can be described by a universe function $S(x)$ defined by expression (3.1.2). The critical frequency in this case is

$$\omega_c = 3\sqrt{2}\gamma^2 a_0 \omega_L. \quad (3.3.2)$$

The number of photons emitted by a single electron can be estimated as follows [98]

$$\begin{aligned} N_{ph} &\approx \alpha a^2 N_{osc}, & a_0 \ll 1, \\ N_{ph} &\approx \alpha a N_{osc}, & a_0 \gg 1, \end{aligned} \quad (3.3.3)$$

where $\alpha = e^2/\hbar c \approx 137$ is the thin structure constant, N_{osc} is the number of periods of the laser field during which the electron interacts with the laser pulse. From these expressions it follows that the number of emitted photons depends only on a_0 , while the energy of the emitted photon increases with increasing a_0 and γ .

The energy of the emitted photon increases as γ^2 . When it becomes comparable to the electron energy γmc^2 , the classical description is no longer valid. In this case, the recoil effect and the spin effect become important. They should be considered in the framework

of quantum electrodynamics. In this case, the emission spectrum is determined by the function $S_q(\delta)$

$$S_q(\delta) = S(\delta) + x \left(\frac{1}{1-x} - x - 1 \right) K_{2/3}(\delta), \quad (3.3.4)$$

where $\delta = 2x/3\chi(1-x)$ and $x = \hbar\omega/\gamma mc^2$. $S_q(\delta) \rightarrow S(\omega/\omega_c)$ in the classical limit $\chi \ll 1$ and $\hbar\omega \ll \gamma mc^2$. The QED parameter χ can also be expressed through the critical frequency ω_c : $\chi = 3\hbar\omega_c\gamma mc^2/2$. In the limit opposite to the classical limit $\chi \gg 1$ the radiation spectrum has a maximum near γmc^2 . The characteristic time between two successive moments of emission of photons by the same electron (photon emission time) can be estimated as the ratio of the characteristic energy of emitted photons to the radiation power. In the classical limit, the average energy of the emitted photons is approximately equal to $\hbar\omega_{em} \approx a_0\gamma^2\hbar\omega$, in the quantum limit to $\hbar\omega_{em} \approx \gamma mc^2$. Using expressions for the radiation power in the classical and quantum limits, for the time of photon emission we obtain:

$$t_{rad} \approx \frac{\hbar c}{e^2} (1 + \chi^{1/3}) t_f,$$

where ct_f is the so-called formation length of radiation, which is equal to the length of the path that an electron travels in the time during which the direction of the electron motion changes at an angle of about $1/\gamma$. The radiation formation length for the problem can be estimated to be $t_f = 1/(2\pi a_0)$.

To generate the narrow-band gamma-ray radiation with high brightness at XCELS we can use an electron beam with energy of 300 MeV and a laser pulse of 50 ps duration with amplitude $a_0 \approx 0.7$. The energy of the emitted gamma quanta in this case is about 2 MeV. Each electron will emit, on the average, about 70 photons. Thus, almost half of the beam energy will be transferred into the hard radiation.

The XCELS facility also allows investigating strongly nonlinear Compton scattering, when the quantum effects will become essential. Prior to that, the only such experiment was carried out at SLAC, where an electron beam with energy 47 GeV collided with a terawatt laser pulse $a_0 \approx 0.4$ [99]. In this case, the nonlinear nature of the Compton scattering was little exhibited. For example, let us consider, using the QUILL numerical simulation code [29], the interaction of a relativistic electron beam with a laser pulse. The laser pulse is linearly polarized $\vec{E}_y = \vec{B}_z = a_0 \exp[-y^2/\sigma_y^2 - (x-t)^2/\sigma_x^2]$, where \vec{E} and \vec{B} the electric and magnetic fields, respectively, σ_x is the pulse duration, and σ_y is the pulse

width. Here, the coordinates are normalized to the wavelength of the laser pulse, and time to the oscillation period of the field. The parameters of the laser pulse and electron beam will be attainable at the XCELS facility and will have the values $\sigma_x=1.6$, $a_0=100$ and $\gamma_0=2 \times 10^4$. For these parameters $\chi \approx 6$, and $t_{rad} \approx 0.2$. The energy spectrum of electrons after the interaction is presented in Fig. 4.21, which shows that the beam has lost much of its initial energy. In addition, some of the emitted photons decayed with the production of electron-positron pairs, thus forming electromagnetic cascades. The electromagnetic cascades are one of the basic phenomena of the strong field physics. In contrast to the classical physics, in the quantum physics a photon can decay in the external electromagnetic field. The photon can decay with the production of an electron-positron pair. If the energy of the resulting electron and positron is high enough, each of them can emit a new photon, which, in turn, can also break up producing new electron-positron pairs. This process is called an electromagnetic cascade or shower.

Another interesting example of the Compton scattering with parameters achievable at the XCELS facility is $\gamma mc^2 = 50$ GeV, $a_0 = 5$, $\sigma_x = 32\lambda_L$, σ_y is much greater than the transverse beam size. For these parameters $\chi \approx 3$, which corresponds to the quantum regime of radiation (i.e., the energy of the emitted photon is of the order of the electron energy and recoil is strong). The spectrum of the emitted photons is shown in Fig. 4.22.

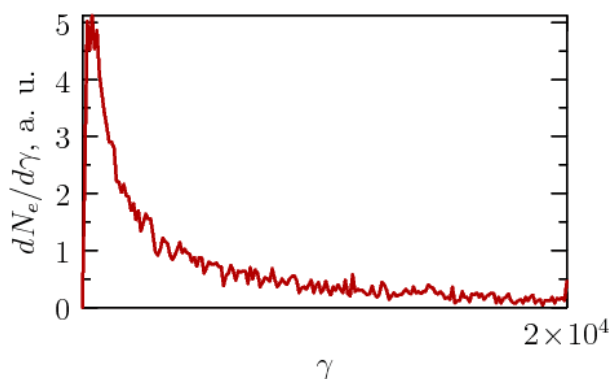


Fig. 4.21. The energy spectrum of an electron beam after a collision with a linearly polarized laser pulse: $a_0 = 100$, $\sigma_x = 1.6$, the initial gamma-factor of the electrons is $2 \cdot 10^4$

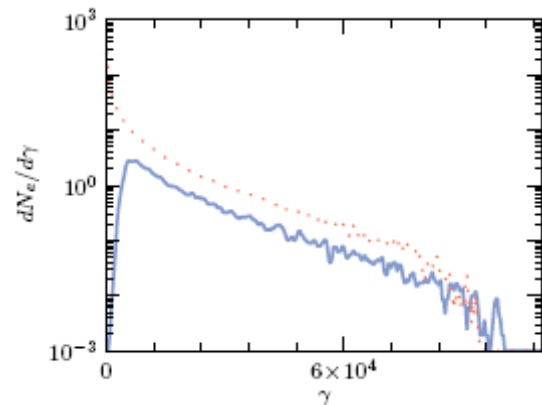


Fig. 4.22. The energy spectrum of emitted photons (dashed line) and beam electrons (solid line), after passing through the laser pulse

The energy of the beam electron and energy of emitted photons is shown as a function of time in Fig. 4.23. As the results of simulation indicate, the electrons have lost 75% of its original energy. Each electron emitted, on an average, 12 photons with average energy of 3 GeV. It is interesting to note that about 1% of the initial beam energy

transferred to the energy of the positrons born as a result of the decay of high-energy photons in the laser field. A similar effect was recently discussed in [11].

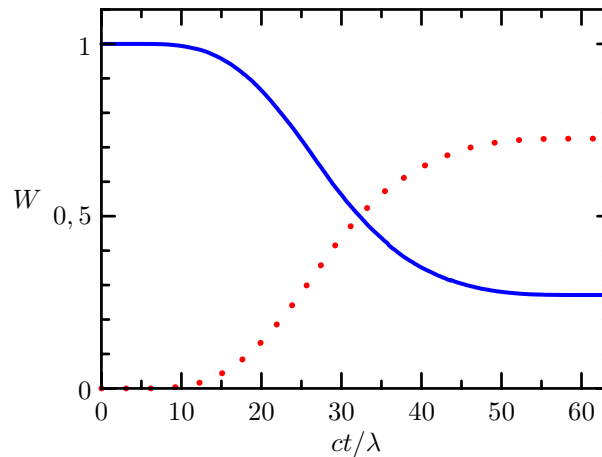


Fig. 4.23. The energy of the electron beam (solid line) and the energy of the emitted photons (dashed line) as a function of time

It is assumed that the electron beam involved in the Compton scattering will be formed by a laser pulse of one of the rays of the system. The remaining beams will collide with the electron beam. Since the generation of the electron beam is also performed by a laser pulse, the time synchronization of the beam and the scattering pulse is simplified.

It is also possible to implement a recently proposed scheme of gamma-ray generation with the Compton effect by the same laser pulse that accelerated electrons in the plasma [100]. In this scheme, the laser pulse intensity of about 10^{22} W/cm² is distributed in a relatively dense plasma (electron density is 10^{20} cm⁻³) and provides acceleration of the electron beam in a bubble mode. According to estimates and the results of numerical simulation, in the selected mode a beam contains about 10^{11} trapped electrons with a quasi-thermal energy spectrum. At a distance of about 200-300 microns the electrons reach the energy of 1 GeV and the pulse with the initial 30 fs duration is almost completely depleted, decreasing to one half-period (see Fig. 4.24 and 4.25). At this moment, a metal plate which fully reflects the laser pulse is placed into the laser pulse path. As a result, the reflected pulse collides with the accelerated electron beam. It should be noted that in this scheme spatial and temporal synchronization of the laser pulse and the electron beam, that is generally not an easy task, is solved automatically. For these pulse parameters estimates show that the gamma-photons emitted due to the nonlinear Compton scattering have an energy of about 200 MeV and their total number will be 10^{10} particles. It is easy to estimate that such a source will have an extremely high peak brightness – 10^{27} photons in 1 s per 1 mm² mrad². The total energy converted into gamma rays will be about 0.1 J.

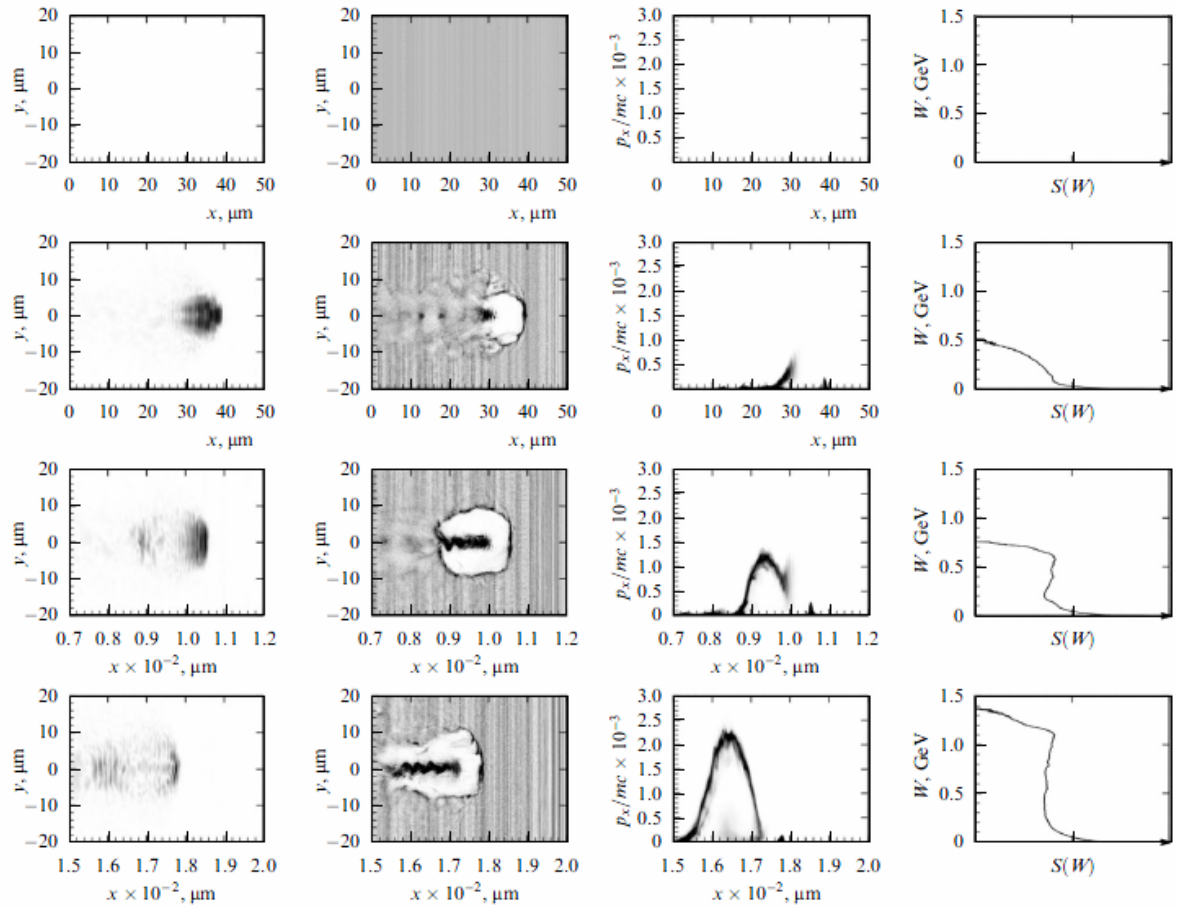


Fig. 4.24. The dynamics of electron acceleration by a laser pulse.
 The first column is the distribution of the transverse electric field.
 The second column is the distribution of electron density.
 The third column is the electron distribution on the phase plane.
 The fourth column is the electron energy distribution on a logarithmic scale

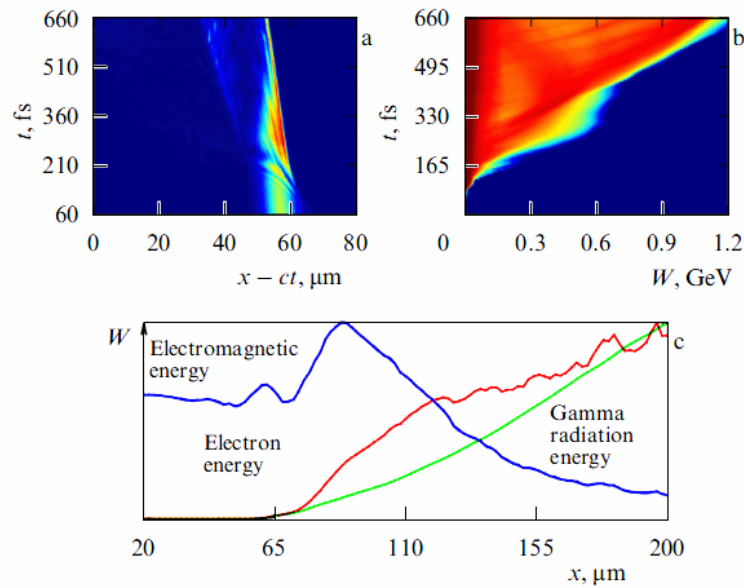


Fig. 4.25. (a) The energy distribution of the electromagnetic field in calculation window, (b) the energy spectrum of accelerated electrons as a function of elapsed time, (c) the relative change in time of electromagnetic energy (blue), electron energy (red) and the total energy of the radiation that would be obtained, if the pulse were reflected at that time (green)

Electromagnetic cascades in the field of two colliding laser pulses are themselves an efficient source of gamma rays [101]. Parameters of the XCELS facility allow us to study the cascades and use them as sources of high energy photons. Let us consider this process in detail using the QUILL simulation code. Let laser pulses be linearly polarized, have a Gaussian envelope and travel towards each other along the axis x . At the initial time $t = 0$ the distance between the centers of the laser pulses is $2\sigma_x$, and the coordinates of the centers are $x = -\sigma_x$ and $x = \sigma_x$. The cascade was initiated by twelve 1 GeV photons in the vicinity of the point $x = -15$, $x = 0$. The parameter values used in the simulation: $\sigma_x = 19$, $\sigma_y = 8$. For a laser pulse propagating from left to right $a_{left} = 2.1 \cdot 10^3$, for a pulse propagating from right to left $a_{right} = 1.4 \cdot 10^3$.

The spatial distribution of the normalized electron and photon densities, as well as the laser field intensity at different time points are shown in Fig. 4.26-4.28. At the initial stage of the cascade, the density of electron-positron plasma quickly reaches values of the relativistic critical density $a_0 n_{cr}$, where $n_{cr} = m\omega^2 / 4\pi e^2$ is the non-relativistic critical density of electron-positron plasma. The characteristic scale along the x -axis formed in the course of cascade development is of the order of the wavelength of the laser pulse. The formation of a dense plasma leads to strong absorption of laser pulses and a decrease in the electric field in the region occupied by the plasma, which drastically reduces the rate of growth in the number of particles. At the later stages, the formed plasma spreads.

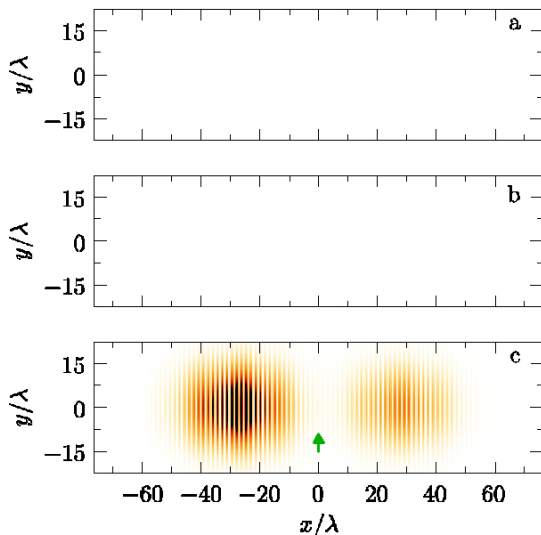


Fig. 4.26. The density distribution of (a) electrons and (b) photons, (c) distribution of the energy density of the electromagnetic field at the initial time $t = 0$. The green arrow shows the position and direction of the photon bunch, initiating the cascade

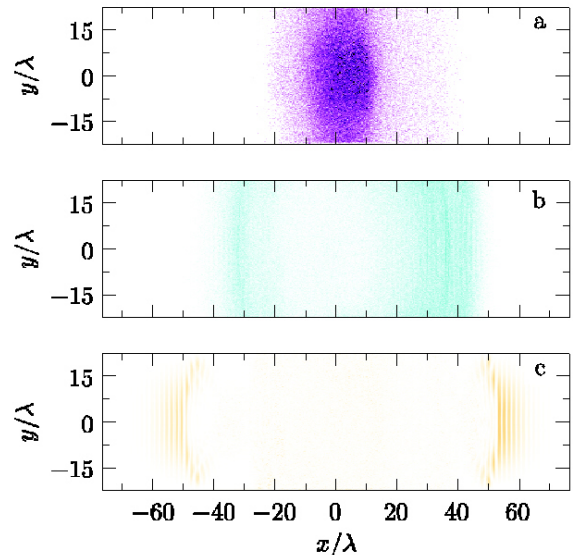


Fig. 4.27. The density distribution of (a) electrons and (b) photons, (c) distribution of the energy density of the electromagnetic field at time $80\lambda_L / c$

Strong absorption of laser pulses is observed starting from the time $t \approx 80\lambda_L/c$ when the plasma density is close to $a_0 n_{cr}$. The asymmetry of the initial distribution of the laser field leads to an asymmetry in the distribution of the emitted high-energy photons. As can be seen from Fig. 4.27 and 4.28, most of the hard photons propagate to the right. The anisotropic distribution of the emitted photons can be used at the XCELS to create bright sources of gamma rays. Using appropriate filters a required narrow frequency band can be cut out of the broadband spectrum.

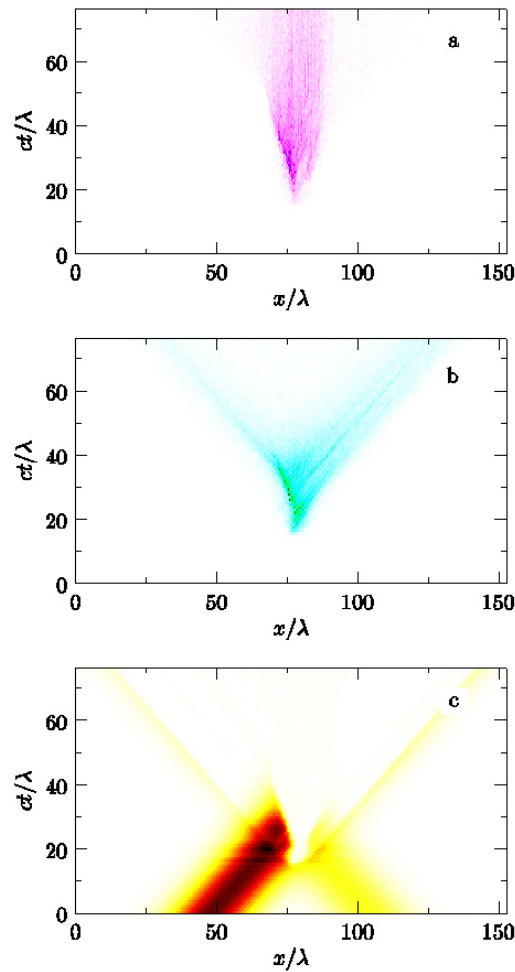


Fig. 4.28. The density distribution of (a) electrons and (b) photons, (c) density distribution of the electromagnetic field in the plane $x - t$ with $y = 0$

Activity 3.4. *Creating sources of electromagnetic waves of attosecond and subattosecond duration*

One of the main directions in the development of lasers since their introduction was to obtain ever shorter electromagnetic pulses. At the end of the XX century the theoretical limit was reached: the duration of optical pulses became equal to one wave period, equal to a few femtoseconds. This gave rise to a number of new diagnostic techniques and, among all, allowed to study the temporal dynamics of vibrational-rotational motion of molecules, as well as the problems of electron transport in large molecules (e.g., proteins), which is especially important for the study of photosynthesis in plant cells. However, the intra-atomic dynamics of electrons is unattainable for such pulses, since the characteristic times of electron rotation in the orbit are tens of attoseconds.

The task of obtaining pulses with such short durations is extremely difficult because it requires an efficient generator of high frequency radiation in the ultraviolet and X-ray ranges, which would be capable to operate in a pulsed mode. At the same time, in the nonlinear regimes of interaction of superintense laser radiation with matter, the energy of optical radiation can be efficiently converted into higher harmonics centered in subfemtosecond pulses.

Historically, the basis for attosecond sources of the first generation was the process of ionization of atoms and molecules interacting with a gas target with an intensity of laser pulses at 10^{14} W/cm². At such intensities, the ionization of each atom can be described by the wave packet dynamics of the electron of an ionizing atom, which is described by the time-dependent Schrödinger equation. During the ionization process, not only the escape from the vicinity of a parent ion is characteristic for the evolution of the electron wave packet, but also the oscillation in the external laser field (in the case of linear polarization). This, as a consequence, may lead, under certain conditions, to the return of part of the wave packet that has left the vicinity of the parent ion. In this process, the dipole moment of the atom and electron system changes with time in a rather complicated way and thus provides a highly nonlinear response of the atomic system as a whole. As a result, the radiation generated by the changing dipole moment of the atomic system has a wide spectrum, which contains rather intense high-order harmonics.

Despite the apparent progress in the generation of attosecond pulses under the action of laser pulses on gas targets, a further increase in the power of laser pulses due to the development of laser technology does not open up any essentially new and more efficient mechanisms, which could provide a greater intensity and shorter duration of the pulses. Today, the intensity of the attosecond pulses generated in gas targets is limited to

the level of 10^{14} W/cm². First of all, the efficiency cannot be improved, because for a single atom the high-order harmonic generation process is actually close to its limit with regard to efficiency, whereas the number of atoms involved in the radiation is limited by gas concentration in the target. An increase in the intensity of the laser pulse leads to an increase in the role of the magnetic field and relativistic effects, which, in general, negatively affect the fulfillment of the task. On the other hand, an increase in the density of the gas target violates the mechanisms underlying the harmonics generation, since electrons accelerated by the laser pulse field begin to feel the influence of neighboring atoms and molecules that perturb their trajectory. This leads to a significant reduction in the efficiency of generation.

Therefore, one of the most natural ways to increase the intensity of attosecond pulses is to find mechanisms of their generation on the surface of a solid target, where due to the high density the collective motion of electrons of the substance can provide coherent radiation of attosecond pulses with an intensity much higher than the pulse intensity with the gas target.

In the early 1980s it was shown that high harmonic generation is possible on solid surfaces as well, but the physics of this process is significantly different from that on individual atoms. In particular, owing to the high density the dominant role is played by the collective effects. Further investigation of this process showed its high efficiency and the possibility to achieve extremely high intensities with this method.

The pioneer studies on the high-order harmonic generation on the solid surface were performed in Los Alamos in 1981 [102]. Solid targets of aluminum, iron, gold, copper, polyethylene and teflon were irradiated by a CO₂-laser with intensities 10^{14} - 10^{16} W/cm² and harmonics up to the 29th order were observed in the reflected signal. The number of harmonics was determined by the target material.

The first idea of how to explain the mechanism of harmonic generation on solid surfaces was as follows. An intense laser pulse causes ionization and subsequent heating and spread of the plasma formed. Although the frequency of the plasma formed by ionization of the substance with solid-state density is about one order of magnitude higher than the frequency of optical radiation, a resonant excitation of plasma oscillations by the incident laser radiation is possible in the region of thermal spread for a plasma with a lower concentration. Further, as a result of an arbitrary quadratic nonlinearity, plasma oscillations can be excited at the doubled frequency in a deeper layer, where the concentration is higher, and so on to the point of oscillation excitation in plasma with the solid-state density and the subsequent emission of electromagnetic radiation at the frequency of plasma

oscillations. Omitting the discussion of specific physical mechanisms, it is possible to make one general conclusion in the framework of this idea: the frequency of generated radiation is limited by the oscillation frequency of plasma, which is formed by ionization of the target material, i.e., for typical materials no more than several tens of harmonics can be generated. Moreover, doubtful is the possibility of obtaining high efficiency of excitation of Langmuir oscillations, which depends on the nonlinearity in the system, thus requiring, for example, laser pulses with relativistic intensity (i.e., with an intensity at which electrons start moving relativistically, providing the non-linearity mechanism). For this reason, there has been almost no interest in the generation of high harmonics in solid targets for a long time until more detailed theoretical and experimental studies of this process were restarted.

The theoretical study of the interaction of intense radiation from the surface of overdense plasma formed by ionization of the material with solid-state density is one of the major problems not only for the generation of high harmonics, but also for many other applications. Numerical simulation of plasma by the PIC method [103] allows very accurate simulation of the behavior of plasma for parameters typical for this problem in a three-dimensional geometry, as indicated by good agreement between the simulation results and experimental findings. In another approach, which is based on the hydrodynamic approximation, a set of partial differential equations permits mathematical description, in a general form, of the process of irradiation of the surface of overdense plasma by relativistically intense radiation [104]. However, a strongly nonlinear behavior of the plasma is characteristic of this process, which greatly complicates the development of analytical approaches for studying this problem and limits the study to a qualitative analysis of the results of numerical simulation and the subsequent development of phenomenological models.

To understand the physics underlying the high harmonic generation in solid targets, we consider the results of numerical calculations of the interaction of a linearly polarized laser radiation with the surface of a dense plasma. Let a laser beam be incident at an angle θ to the surface and the electric field vector lie in the plane of incidence. To account for the effect of thermal spread of the plasma, for the sake of generality, we consider the case of a smooth plasma boundary, so that there is a concentration gradient. Such calculations are conveniently performed in a reference frame moving with the velocity $c\sin\theta$ along the surface. In this reference frame a laser beam is incident normally to the surface and the problem becomes one-dimensional (see Fig. 4.29).

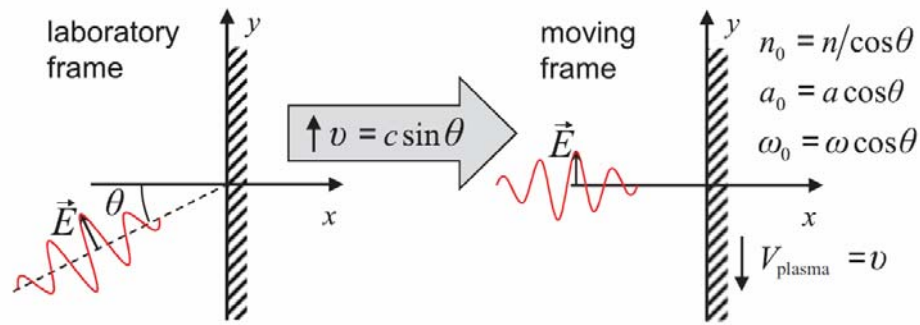


Fig. 4.29. The problem of the inclined irradiation of plasma surface is reduced to the one-dimensional geometry when a moving reference frame is used

Figure 4.30 shows the results of calculations for the following parameters: $\theta = \pi/4$, $N_e = 8 \cdot 10^{22} \text{ cm}^{-3}$, $I = 5 \cdot 10^{17} \text{ W/cm}^2$. A plasma layer was 60 nm thick, on the irradiated side of the layer there was an area with an exponential concentration gradient, which had a characteristic scale of concentration decrease equal to 60 nm, the wavelength of laser light was 1 micron. It is evident that there are two sources of high-order harmonics in the form of attosecond pulses. One source is located directly on plasma surface, and the second is slightly deeper.

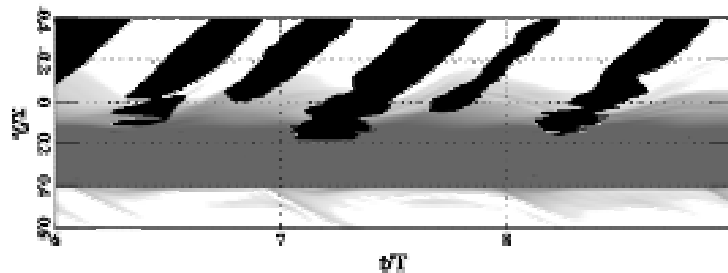


Fig. 4.30. The dynamics of the interaction of laser radiation with the surface of a dense plasma. Light grey gradient shows the electron density on logarithmic scale, the black is the intensity of radiation in the frequency window from the fifth to the ninth harmonic of the laser pulse. The laser pulse propagates in the positive direction of x . Flying beams of Brunel electrons can be seen on the non-irradiated side of the plasma layer

Detailed investigations show that the first source manifests itself only for the relativistically intense fields, i.e., for such laser pulse intensities for which the energy of electron oscillations in its field is comparable with their rest energy. At the same time, the second source dominates for low intensities, but almost disappears in the case of very steep plasma gradients.

At present, it is assumed that the second source is associated with the generation of the so-called Brunel electrons injected at each period of the laser pulse into the plasma. This effect was first described by Brunel in 1987 [105]. He showed that in the interaction of laser radiation with the surface of a dense plasma, part of electrons oscillating in the pulse field are extracted from the plasma and back-injected with the formation of an electron

bunch propagating into the interior of the plasma. This bunch passing through the plasma generates Langmuir oscillations behind. It is known that in an inhomogeneous plasma the Langmuir oscillations can be converted into electromagnetic waves, as observed in the gradient of electron concentration in the form of generated high-order harmonics. This process is called coherent wake emission [106]. It is a special case of linear transformation of plasma waves and to some extent may be regarded as a process that is reverse to resonant absorption.

Already in the mid 1990s it was observed that the harmonic generation can be explained by the Doppler effect [107]. Doppler predicted the generation of harmonics with a frequency proportional to the square of the relativistic factor of electrons, and, importantly, not limited by the plasma density. The model based on this idea is called the oscillating mirror model (OMM) and is as follows. An overdense plasma surface, as in the linear case, fully reflects the incident radiation. However, unlike the case of low-intensity, the mirror surface, i.e., the point of reflection, slightly varies under the influence of radiation pressure. In fact, numerical simulation shows that the distribution of electrons at the plasma boundary does not have any pronounced jump with a position varying in time, but, instead, it exhibits a smooth gradual drop that changes in a quite complicated manner. However, the model actually assumes the existence of an apparent reflection point (ARP) x_{ARP} of the incident radiation, which seems to be a very productive idealization.

Since the idea of a mirror essentially means the reflection of all incident electromagnetic energy from the surface, then for the apparent reflection point one can write the conditions of the equality to zero of electromagnetic energy flux, which is equivalent to a zero tangential component of the electric field that is the sum of the tangential components of incident and reflected waves:

$$E_{\tau}^i(x_{ARP} + ct) + E_{\tau}^r(x_{ARP} - ct) = 0. \quad (3.4.1)$$

Using this condition, from the position of the apparent reflection point as a function of time, one can mathematically express the exact shape of the plasma-generated radiation, for which this point is actually a moving source.

Thus, plasma emission is equal to the incident radiation with a phase that varies in accordance with the movement of the apparent reflection point. In a general case, it is difficult to determine its dynamics, but the asymptotic analysis is sufficient for finding the spectral properties of the plasma-generated radiation. This is due to the fact that the higher harmonics that are of interest for applications are generated at the time of rapid change in phase, i.e., when the apparent reflection point moves as quickly as possible toward the incident radiation. Assuming the quadratic dependence on the time of the

apparent reflection point rate near the maximum value, which is close to the speed of light, one can show in a general form that the plasma-reflected electromagnetic pulse will have a steep drop on a scale $1/\gamma$, where γ is the relativistic factor corresponding to the maximum velocity of the apparent reflection point. Detailed analysis allows formulating the following general statement that does not depend on the parameters of the problem: for the radiation spectrum from the plasma surface and for irradiation with the relativistic intensity there is a universal law of the intensity distribution of harmonics in the form of a power decay with exponent $-8/3$, and the spectrum extends to the cut-off frequency, whose value is proportional to the third degree of the relativistic factor of electrons.

This prediction obtained in [13, 14] is confirmed by numerical simulations and experiments [15, 16, 108]. One of the most intriguing consequences of this theory is the idea not only to obtain intense high harmonics, but also to further coherently focus them in a nanoscale volume, using a spherical plasma surface as a target [109].

It should be emphasized that the oscillating mirror model does not imply that the plasma is effectively represented by the oscillating mirror. In this case, as we know, the radiation reflected from a relativistically quickly forward-moving mirror would have an amplitude significantly greater than the amplitude of the incident radiation. Within the same oscillating mirror model, it is assumed that there is a point at each time moment, at which the energy flux is zero. This is equivalent to the equality of amplitudes of the incident and reflected radiation at this point in the laboratory frame at any moment of time. Therefore, within the oscillating mirror model the amplitude of the reflected radiation cannot exceed the amplitude of the incident radiation. This is directly related to the assumption of local in time energy conservation, i.e., an energy flux equal to the absorbed energy flux is emitted at each time moment. As is shown by numerical simulations and theoretical studies [100], such a situation is characteristic only at $S > 5$, where $S = n/a$ is the ultrarelativistic similarity parameter that is the ratio of the plasma density n dimensionless for the critical density to the amplitude of the incident wave a dimensionless for the relativistic amplitude.

When a pulse back-emitted by the plasma has an amplitude exceeding the amplitude of the exciting radiation, the following scenario is typical for the process of interaction. An electromagnetic wave incident on a layer shifts electrons deeper into the plasma by the ponderomotive force. At a half-period, when the electric field is directed along the y -axis (see Fig. 4.29), the electrons increase their momentum in the direction opposite to the y -axis, and the Lorentz force due to the magnetic field of stripped ions additionally shifts them farther from the border, leading to the formation of a thin electron current layer with a charge density and current density significantly superior to their initial values in the

plasma. As a result of the appearance of the internal fields in the plasma and accelerated motion of part of the plasma electrons, the plasma accumulates energy of the incident wave at this stage. Since for the linear polarization the force of light pressure oscillates in a period of the field, at some point it begins to decrease and under the action of the charge separation force the bunch formed from the shifted electrons breaks away and flies towards the incident wave, thus becoming a source of the attosecond burst. At the same time, the energy accumulated at the first stage is emitted during about several tens of attoseconds. Because of its similarities with the scenario of energy accumulation with a mechanical spring, this three-stage description of the process was called the relativistic electronic spring [100], which implies not local but rather global conservation of energy in each period of the optical radiation. The theory developed for this model is based on the analysis of the nonlinear differential equation describing the dynamics of a thin layer of electrons, which is of the order of several nanometers at ultrarelativistic intensities. The theory agrees well with the simulation results and provides optimal conditions for generating the most intense attosecond pulses:

$$\theta_g \approx 62^\circ, \quad S_g \approx 1/2. \quad (3.4.2)$$

In this case the amplification coefficient, i.e., the ratio of the amplitude of the generated attosecond pulse to the amplitude of the incident radiation, increases with increasing intensity of the incident radiation, and, for example, at the intensity of 10^{23} W/cm² reaches 10.

Under optimal conditions, the plasma boundary acts as an efficient converter of optical radiation in a short and powerful attosecond burst, accumulating the energy of optical radiation in each period and sharply emitting it in the form of a giant pulse. This effect with the subsequent focusing of the giant attosecond pulse in space can be used to obtain intensities of electromagnetic fields previously unavailable in laboratory conditions. The concept of obtaining such fields relies on using a solid object as a target with a surface in the form of a slightly curved groove. The solid target is irradiated at optimal parameters so that the guide groove is located in the plane of incidence (see Fig. 4.31(a)). Numerical simulation by the PIC method shows that by using a 10 PW laser pulse (corresponding to a single channel at the XCELS facility) with focal intensity of 5×10^{22} W/cm², it is possible to achieve intensities of 2×10^{26} W/cm² in the region of several nanometers (see Fig. 4.31(b)).

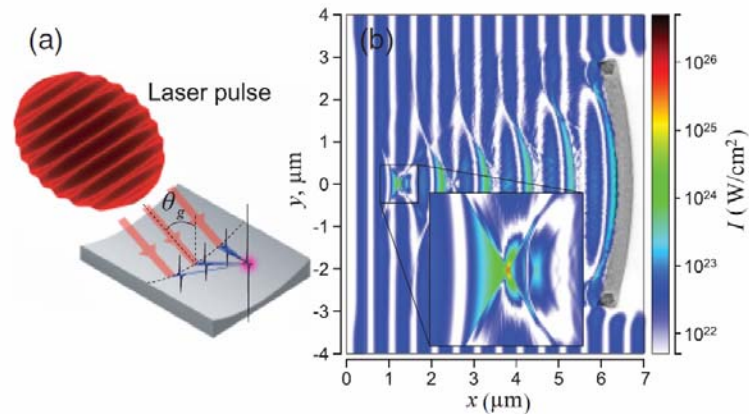


Fig. 4.31. (a) Schematic representation of the grooved-target concept to obtain the intensities required for observing the effects of nonlinearity of vacuum. (b) The distribution of the electric field at the moment of focusing of giant attosecond pulses generated at the target surface, obtained by numerical simulation in a reference frame moving along the guide groove

Activity 3.5. Use of sources for diagnostics of processes and structures with picometer spatial and subfemtosecond temporal resolution

Since its discovery in 1896, the X-ray radiation is one of the most popular imaging tools in science, medicine and industry [110]. Compared with the optical radiation the X-ray radiation has a much shorter wavelength and higher bandwidth. The first provides a high resolution (up to nano- and even picoscales), while the second offers an opportunity to see what is unattainable for the human eye.

The X-ray tomography can be divided into absorption tomography, which is based on the difference in the absorption rates in different materials, and phase-contrast tomography, which relies on the difference in refractive indices [111, 112]. In living organisms, the absorption tomography can image only fairly dense tissues such as the bone. Imaging of soft tissues with the X-ray absorption requires special agents. This either severely restricts the applicability of the method, or requires invasive intervention. The phase-contrast imaging is free of such disadvantages; however, it imposes more stringent conditions to the quality of the X-rays, in particular, requiring a coherent source. In addition, when using the phase-contrast imaging with harder (i.e., short-wavelength) photons having greater penetrating powers, it is possible to greatly reduce the radiation dose absorbed by the body.

Of particular interest is the possibility of imaging with a high (femtosecond) time resolution. This would allow one to study not only the structure of an object, but also its dynamics over time. Such a tool could help to investigate in detail the biomechanics of the movements of insects, the kinetics of biochemical reactions, processes of mass transfer

and signal transmission in biological molecules, etc. At present, the so-called four-dimensional (4D) imaging (i.e., acquisition of three-dimensional images with a time-base sweep) is implemented, for example, by electron tomography [113] and is a rapidly developing branch of modern physics. It should be noted that femtosecond time resolutions require laser technologies to be employed, because only they can provide such a high pulse repetition rate. Thus, in the 4D electron tomography a laser is used to generate electron beams at the photocathode. X-rays obtained by the interaction of superintense laser radiation with matter is a natural tool for the creation of the 4D X-ray tomography.

The absorption [92] and phase-contrast [93, 114, 115] three-dimensional X-ray tomography has been already implemented in the world with the use of high power laser facilities. The basic scheme of such experiments is relatively simple and is shown in Fig. 4.32. A laser pulse is focused on a gas jet to ionize gas and to excite in the formed plasma a wake wave, which is capable of capturing part of the electrons and accelerate them to energies of hundreds of MeV. These electrons, in a kind of an ion channel, make small transverse vibrations called betatron vibrations. The result is the generation of X-rays. At the jet output the electron bunch is deflected by a special magnet, and the generated X-rays are incident on a target that should be imaged. Upon passing through the target, the radiation comes to a detector.

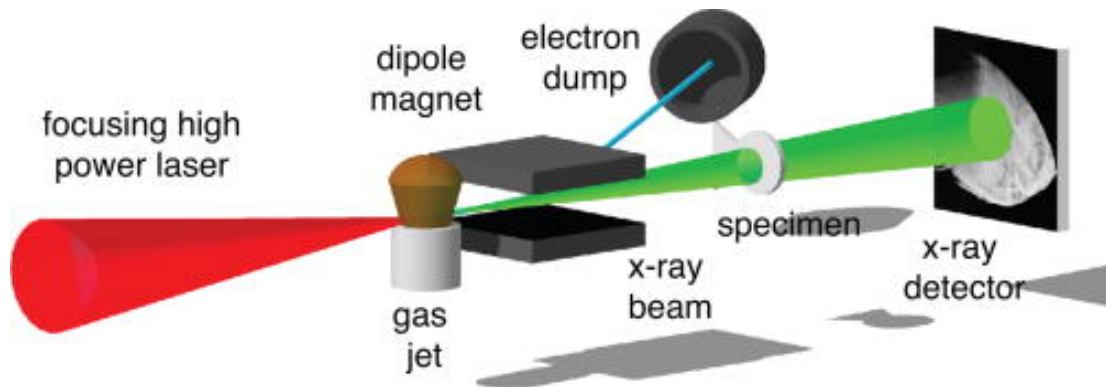


Fig. 4.32. Schematic diagram of the experimental X-ray tomography using high-power laser radiation. Source: [115]

The absorption X-ray tomography provides images of sufficiently dense materials. For example, the result of experiment on obtaining images of metal wires and foils with micron holes is demonstrated in Fig. 4.33 [92].

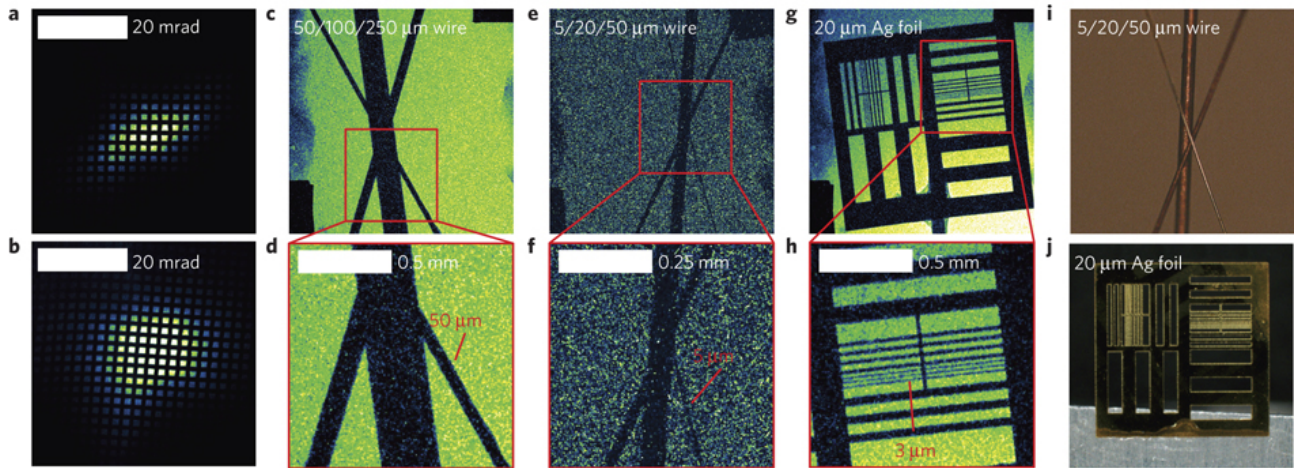


Fig. 4.33. (a) X-ray beam profile in one shot; (b) the overall profile of five beams; (ch) images of three wires and a thin silver foil obtained in one and five shots, respectively; the size of the smallest details in the images is about 3 microns; (i , j) photographs of the same objects obtained in the optical range. Source: [92]

The phase-contrast X-ray imaging requires a high degree of spatial coherence of the source, which can be achieved either by increasing the distance from the radiation source to the object under study, or by decreasing the source size. Both the ways require fairly bright sources. The experimenters succeeded to bring the brightness of the betatron X-ray radiation from laser-plasma sources to the level of synchrotrons of the 3rd generation (10^{22} - 10^{23} photons/second/Mrad²/mm²/0.1% bandwidth) [93, 115]. This allowed obtaining high-resolution images of living tissues. The result of one such experiment is shown in Fig. 4.34. Of particular note is the significantly better quality of the dragonfly image obtained by the phase-contrast method. In particular, due to the use of this method, the contrast of edges has been increased and one can see fine details of the structure of the wing, leg and the external skeleton of the insect.

Despite the relative success in the use of high power lasers as X-rays sources for imaging purposes, there is much room in this area for new research. In particular, the idea of full four-dimensional imaging has not yet been implemented. In addition, of interest is the possibility of increasing the photon energy used for imaging. At present, photons with energies up to several MeV have been obtained in experiments [93], but there is no doubt that the increase in laser power will demonstrate gamma-ray sources with much higher photon energies, which also have a record-breaking high brightness. The development of such sources will become one of the research areas under the XCELS Project.

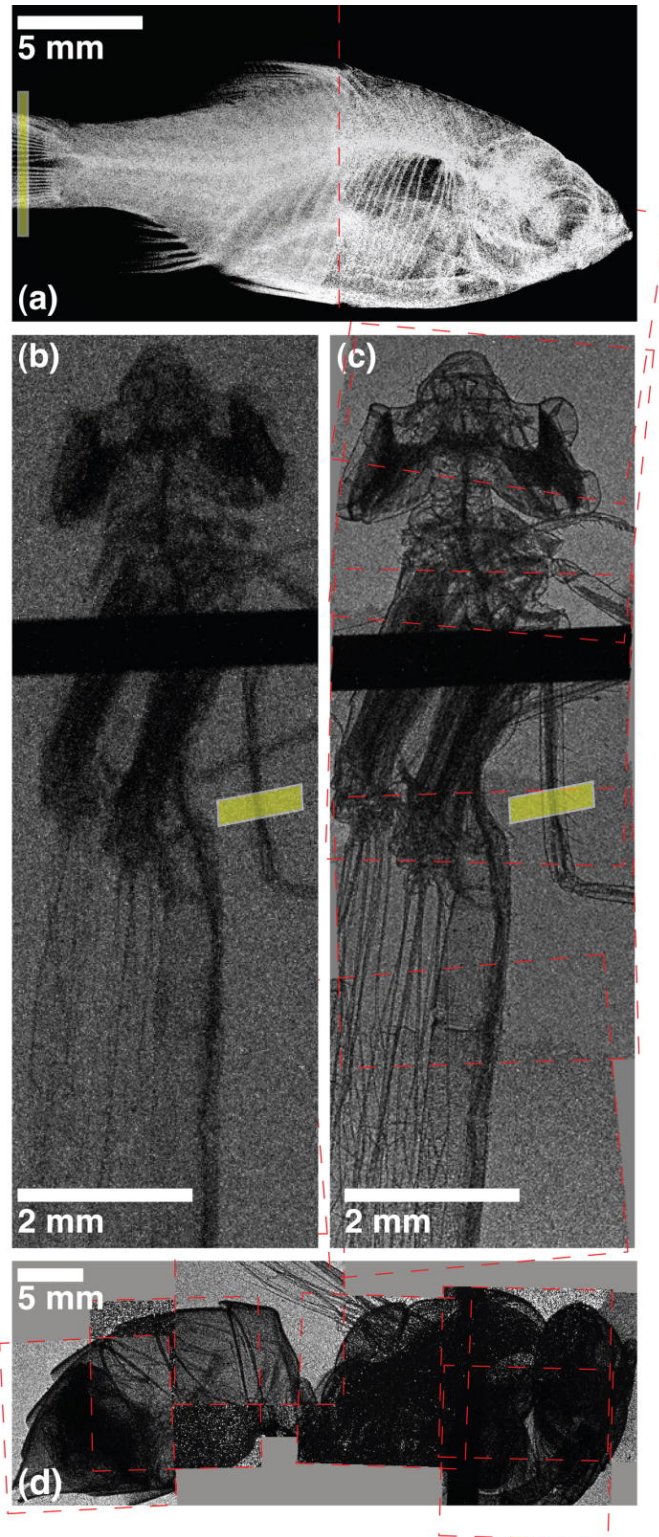


Fig. 4.34. Images of an orange tetra (a) and a dragonfly (b), obtained by the absorption X-ray tomography, and images of the same dragonfly (c) and a wasp (d) obtained by the phase-contrast X-ray tomography. The phase-contrast images were obtained in one shot with a 30 fs exposure. Source: [115]

Objective 4. Study of nonlinear properties of vacuum in extreme light fields

This direction (the so-called "fourth pillar of physics of extreme light") is most fundamental and challenging for experimental studies, because, for the first time, it puts on the agenda the observation of space-time structure and nonlinear properties of vacuum, and, on the other hand, requires the utmost achievable laser beam parameters for experiments. Experiments will be conducted on a 200 PW laser, permitting to obtain, at sharp focusing of optical radiation and coherent summation of all channels, more than 10^{25} W/cm² intensities, and in the mode of generation of attosecond pulses in the X-ray range – up to 10^{27} W/cm². These levels will be sufficient for observation of the effects of the interaction of electromagnetic fields in vacuum, as well as quantum electrodynamic effects, such as electron-positron pair production and particle showers in vacuum.

Activity 4.1. Study of the nonlinear optical properties of vacuum exposed to laser light with an intensity up to 10^{25} W/cm²

Quantum electrodynamics predicts that the vacuum in strong fields behaves like a nonlinear medium with regard to the propagation of photons. This fundamental conclusion has no experimental evidence so far, because it is currently technically impossible to obtain sufficiently strong fields. The study of strong electromagnetic fields is of great importance for astrophysics. For example, the magnetic field intensity around pulsars can be of the order of the Schwinger field intensity (at such intensity, the vacuum can be significantly nonlinear). Many astronomical objects, whose nature is not fully understood now, are assumed to possess high magnetic fields (e.g., quasars). The experimental study of quantum electrodynamics in previously inaccessible areas may probably enrich the science with previously unknown effects.

The Lagrangian, which describes the electromagnetic field, is nonlinear in quantum electrodynamics. However, the Lagrangian depends on field invariants so that the vacuum nonlinearity does not manifest itself for a plane wave. Therefore, it is insufficient to generate high intensities for the detection of this nonlinearity. It is also necessary to develop experimental schemes in which the vacuum nonlinearity could become apparent.

The high field intensities can be obtained by different methods. When a laser with an intensity of about 10^{25} W/cm² is employed, the field intensity is 100 times smaller than the Schwinger intensity. Thus, even in a laser facility with such intense pulses the observation of the vacuum nonlinearity is a difficult experimental problem. Therefore, the development of experimental schemes, which would allow observing the quantum electrodynamic nonlinearity at lowest intensities, is now a topical problem.

In the generation and focusing of laser radiation from a solid surface, the electric field intensity at the focal point can be much greater than the field intensity of the original laser pulse [109], giving us hope to obtain the Schwinger field in the laboratory. Various, often quite complex experimental schemes have been suggested also, in which the nonlinear effects can be observed in vacuum even at not too high intensities [116] (Fig. 4.35). The basis for such schemes is usually the effect of light scattering by light. This effect is basically the following: during the interaction of optical or X-ray radiation part of the photons can change its direction of propagation or polarization. The polarization of the photons can now be measured with very good accuracy. At present, attempts are being made to experimentally detect the nonlinearity of vacuum [117].

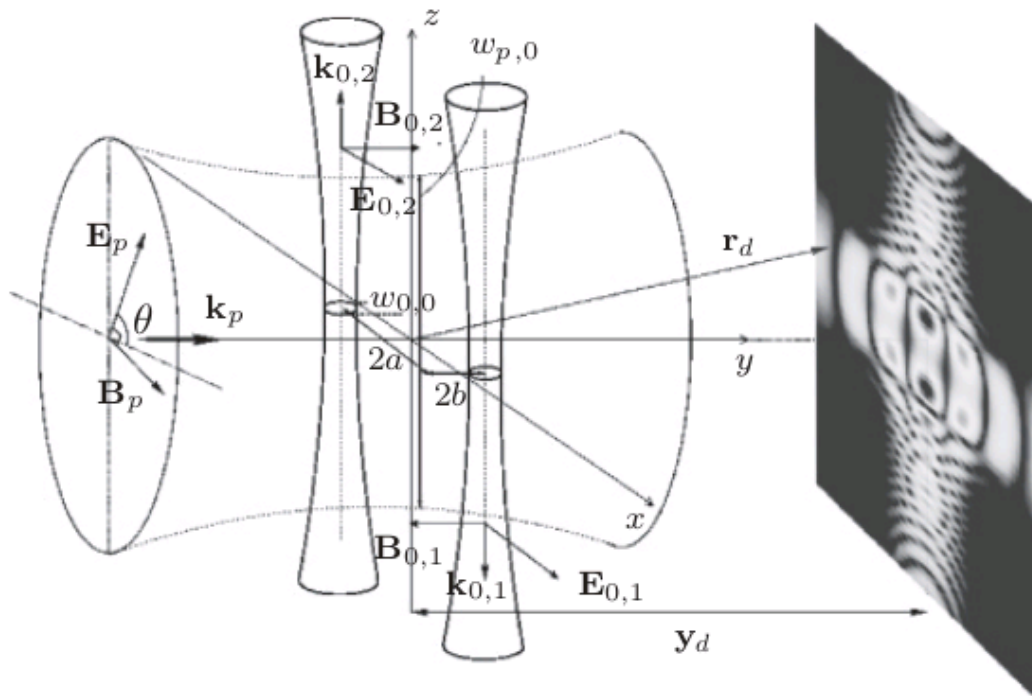


Fig. 4.35. Schematic diagram of the proposed experiment to detect nonlinear properties of vacuum. A linearly polarized low-intensity laser pulse is incident normally to two counter-propagating strongly-focused intense laser pulses. It is proposed to observe the diffraction pattern arising due to changes in the refractive index of the intense laser pulses [116]

Activity 4.2. *Study of the phenomena of quantum electrodynamics in the presence of extremely strong laser fields, including processes of creating matter and antimatter by radiation*

The high-intensity laser radiation, which we intend to achieve at XCELS, will help explore the structure of the physical vacuum and test the foundations of quantum electrodynamics (QED). One of the QED effects currently attracting increased interest is the formation of electron-positron plasma in a superstrong laser field [28, 118]. Such a plasma can be formed as a result of an electromagnetic cascade: a seed charged particle is first accelerated in the laser field to emit a high-energy photon, which decays in the laser field into an electron-positron pair. The produced pair is also accelerated in the laser field to form a next generation of electron-positron pairs and photons (Fig. 4.36). In [118] it was predicted that a significant portion of the laser energy is spent on the production and heating of the electron-positron plasma. Such a process may limit the intensity achievable by a laser in laboratory conditions.

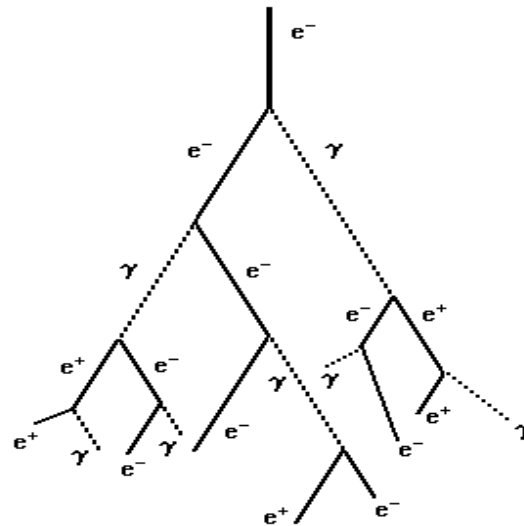


Fig. 4.36. The development of an electromagnetic cascade (shown schematically)

The quantum effects in strong laser fields can be characterized by the dimensionless parameters:

$$\chi_e = e\hbar/(m^3 c^4) |F_{\mu\nu} p_\nu| \approx \gamma(F_\perp/eE_{cr}), \quad (4.2.1)$$

$$\chi_\gamma \approx (\hbar\omega/mc^2)(F_\perp/eE_{cr}), \quad (4.2.2)$$

where $F_{\mu\nu}$ is the tensor of the electromagnetic field, p_μ is particle four-momentum, $\hbar\omega$ is photon energy, γ is the gamma-factor of the particle, F_\perp is the Lorentz force component perpendicular to the direction of instantaneous particle velocity, \hbar is Planck's constant, m is the mass of the electron, c is the speed of light, and the critical field is given by $E_{cr} = m^2 c^3 / (e\hbar) = 10^{16}$ V/cm. The parameter χ_e determines the emission of photons by a

relativistic electron (positron), while χ_γ determines the interaction of a high-energy photon with the electromagnetic field. The quantum effects become significant when $\chi_e \gg 1$ or $\chi_\gamma \gg 1$. If $\chi_e \gg 1$, then $\hbar\omega \approx \gamma mc^2$, and the recoil effect during photon emission by an electron becomes strong. If for some photon $\chi_\gamma > 1$, then the decay process becomes possible for this photon, otherwise, ($\chi_\gamma \ll 1$) the probability of photon decay is exponentially small.

Let us consider the cascade development in the field of two colliding circularly polarized laser pulses [118, 119]. The cascade develops most efficiently in the region of maximum electric field, where there is no magnetic field. Since at $\chi_\gamma < 1$ the probability of the photon decay is small, we can assume that the threshold for the cascade development corresponds to the fact that the average quantum parameter of particles reaches $\chi_\gamma = 1$. In order to assess at which intensity of the external field this occurs, we shall use the following assumptions. First, we assume that the electron stops after emission. Second, we use the semiclassical expressions for the probability of photon emission and decay obtained in the limit $\chi_\gamma \gg 1$. In this limit, the photon decay probability coincides in the order of magnitude with the probability of emission, so the characteristic photon lifetime is of the order of magnitude of the characteristic time between successive processes of photon emission by an electron t_l . Using the expression for the probability of emission of radiation per unit time W , obtained in the semiclassical approach for particles $\chi \gg 1$, we have:

$$t_l \sim \frac{1}{W} \sim \frac{\hbar^2 \gamma}{e^2 mc \chi^{2/3}}. \quad (4.2.3)$$

We introduce a growth rate of the cascade Γ , which characterizes the time required for doubling the number of particles in the cascade, i.e., we assume that the number of particles in the cascade grows as $N \propto \exp \Gamma t$, where Γ may depend on time. Obviously, the lifetime t_l is related to the growth rate of the cascade Γ : $\Gamma \gg 1/t_l$. Another important characteristic time is the time at which the electron is accelerated to energies so that $\chi \sim 1$. We denote it t_χ .

For small values of time $t \ll \omega^{-1}$ and initial electron at rest, we have:

$$eEt / mc, \quad (4.2.4)$$

$$\psi \approx \omega t, \quad (4.2.5)$$

$$\chi \approx \frac{\hbar e \gamma E \psi}{m^2 c^3}, \quad (4.2.6)$$

where ψ is the angle between the vectors \mathbf{E} and \mathbf{p} . Substituting in these solutions $t = t_l$, and using equation (4.2.3), we can find t_l and the average value of the parameter χ in the cascade:

$$\omega t_l \approx \frac{1}{\alpha \mu^{1/4}} \sqrt{\frac{\hbar \omega}{m c^2}}, \quad (4.2.7)$$

$$\langle \chi \rangle \sim \mu^{3/2}, \quad (4.2.8)$$

where $E / \alpha E_{cr}$. Substituting $t = t_\chi$ into equation (4.2.4)–(4.2.5) and equating χ to unity, we find t_χ :

$$\omega t_\chi \approx \frac{1}{\alpha \mu} \sqrt{\frac{\hbar \omega}{m c^2}}, \quad (4.2.9)$$

From these expressions we can make several important conclusions. First, χ can become of the order of unity, if $\mu > 1$ and the conditions under which the estimates were made are fulfilled. There are two such conditions: $\omega t_l \ll 1$ and $t_l / t_\chi \gg 1$, i.e., we assumed that the characteristic lifetime is much shorter than the period (which is used to derive equations (4.2.4)–(4.2.5)) and that a particle during its lifetime acquires $\chi \gg 1$. For $\mu \sim 1$ the estimation of the lifetime gives $\omega t_l \sim 0.21$ for a wavelength of $\lambda_L = 911$ nm, used at XCELS, therefore, the lifetime is much shorter than the rotation period of the field. In addition, it is easy to find that $t_l / t_\chi \sim \mu^{3/4} > 1$ for $\mu > 1$, therefore, the assumption that $\chi \gg 1$ for most of the particles of the cascade also holds. Thus, we conclude that

$$E_{th} \sim \alpha E_{cr}, \quad (4.2.10)$$

$$\Gamma / \omega \sim \alpha \mu^{1/4} \left(\frac{m c^2}{\hbar \omega} \right)^{1/2}, \quad (4.2.11)$$

where E_{th} is the threshold field for the cascade development. However, the determination of the threshold for the cascade development is not entirely unequivocal, and the threshold intensity may depend on focusing, duration, and polarization of the laser pulses used, as well as on other parameters. With the help of the found relations the time dependence of the number of particles in the cascade can be represented as

$$N \approx \exp \left(t \pi \alpha \mu^{1/4} \sqrt{\frac{m c^2}{\hbar \omega}} \right). \quad (4.2.12)$$

Let us make estimations for the XCELS parameters. Let the electromagnetic cascade be initiated by a particle in the field of two colliding linearly polarized laser pulses with energy of 2220 kJ and duration of 25 fs. The pulses are focused in the focal spot of $2\lambda_L \approx 1.8\mu\text{m}$. Then the intensity at the focus will be $4 \cdot 10^{24} \text{W/cm}^2$ ($a_0 \approx 1500$), and $\mu \approx 0.83$. After pulse propagation the number of produced electron-positron pairs is estimated to be 10^{50} . This estimate gives, obviously, a greatly overestimated number of pairs, since it does not take into account energy absorption of the laser pulses. However, this result indicates that a very dense electron-positron plasma can be obtained at the XCELS facility.

The cascade development is over when all energy of the laser pulse converts into the energy of particles and plasma fields. Then the characteristic density of the produced electron-positron plasma can be estimated from the balance of energies of the laser pulse and particles. For simplicity, we assume that the gamma factor of electrons and positrons is equal to $\gamma \approx a_0$. Then, from the energy balance

$$W_{laser} = \frac{E^2}{4\pi} V = \frac{a_0^2 m^2 c^2 \omega^2}{4\pi e^2} \approx N m c^2 a_0 \quad (4.2.13)$$

we find the characteristic density of the electron-positron plasma

$$n = \frac{N}{V} = \frac{a_0 m^2 \omega^2}{4\pi e^2} \approx n_{cr} a_0. \quad (4.2.14)$$

As can be seen from this expression, it is close to the relativistic critical density.

A more precise determination of the cascade dynamics can be obtained by numerical simulation. Let us consider the formation of an electron-positron plasma as a result of an electromagnetic cascade initiated by one electron situated in the field of two colliding laser pulses [29]. The laser pulses have a Gaussian envelope and propagate along the x -axis. The components of the laser field at the time $t = 0$ are as follows:

$$E_y, B_z = a \exp\left[ix + i\Psi - \frac{y^2}{\sigma_r^2}\right] \left[e^{-(x+x_0)^2/\sigma_x^2} \pm e^{-(x-x_0)^2/\sigma_x^2} \right] \quad (4.2.15)$$

Here, the field intensities are normalized to $mc\omega_L/|e|$ where ω_L is the angular frequency of the laser pulse. The coordinates are normalized to c/ω_L , time is normalized to $1/\omega_L$. $a = |e| E_0/(mc\omega_L)$, where E_0 is the electric field amplitude of a single laser pulse. $2x_0$ is the initial distance between the laser pulses, and Ψ is the phase shift describing, among all, the focusing of pulses.

We choose parameters close to the XCELS parameters: the energy of each of the two pulses (consisting of six beams at the XCELS facility) is 2220 J, pulse duration is 25 fs, and the focal spot size is $2\lambda_L \approx 1.8\mu\text{m}$. The cascade is initiated by one electron located at $t = 0$ at a point $x = y = 0$ with a zero initial momentum, when the laser pulses

are close to each other (σ_x is the distance between the centers of the pulse at $t = 0$). The cascade development at the initial time $t = 0$ and at a later stage $t = 9\lambda/c$ is presented in Figs. 4.37 and 4.38, showing the density distribution of electrons (the density distribution of positrons almost coincides with that for electrons), the density distribution of photons and the intensity distribution of laser radiation. As shown in Fig. 4.38, a super-dense electron-positron plasma cluster of micron size is formed.

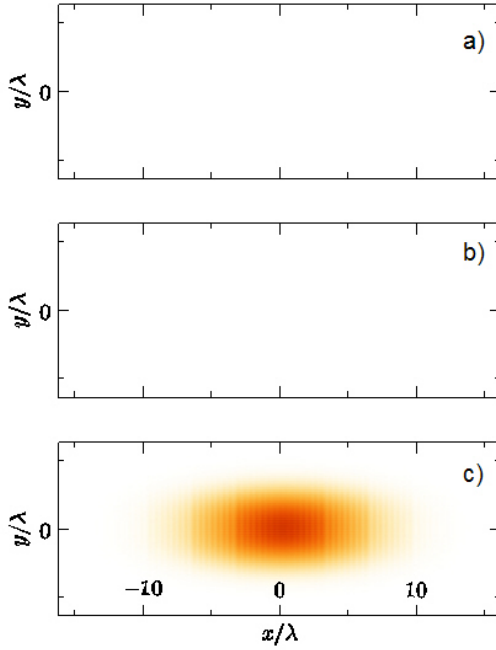


Fig. 4.37. Normalized electron density $\rho_e = 50n_e/(a_0n_{cr})$, normalized photon density $\rho_\gamma = 50n_\gamma/(a_0n_{cr})$ (b) and laser intensity, normalized to the maximum initial intensity ρ_I (c) during the collision of two linearly polarized laser pulses at the initial time $t = 0$

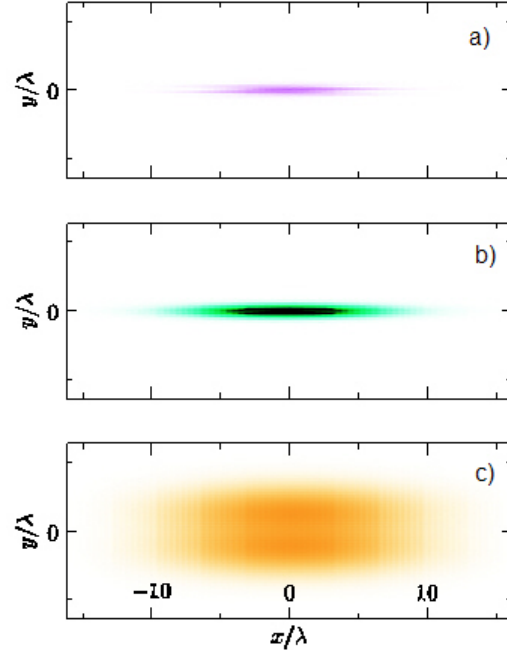


Fig. 4.38. Normalized electron density $\rho_e = 50n_e/(a_0n_{cr})$, normalized photon density $\rho_\gamma = 50n_\gamma/(a_0n_{cr})$ (b) and laser intensity, normalized to the maximum initial intensity ρ_I (c) during the collision of two linearly polarized laser pulses at the moment $t = 9/c$

The temporal evolution of the number of electrons in the cascade is shown in Fig. 4.39. Prior to $ct < 7\lambda$ the number of electrons grows exponentially. After pulse centers have passed through each other, the growth becomes slower, since the total amplitude of the laser field at the center decreases. The number of electron-positron pairs reaches 10^{10} . The number of photons is an order of magnitude greater. As is evident from Fig. 4.38, there is a slight absorption of laser energy by the formed electron-positron gamma-ray plasma in the central part of the laser pulse near the horizontal axis. According to calculations, about 1% of the laser energy transfers to the energy of particles. Moreover, the total energy of the photons is about 3.5 times greater than the total energy of the electron-positron pairs. The average energy of the electron (positron) is about 600 MeV.

Thus, the numerical calculations also show that the XCELS parameters will allow achieving, for the first time, a dense and hot electron-positron-gamma-ray plasma and investigating, for the first time, the collective high energy QED effects in laboratory conditions.

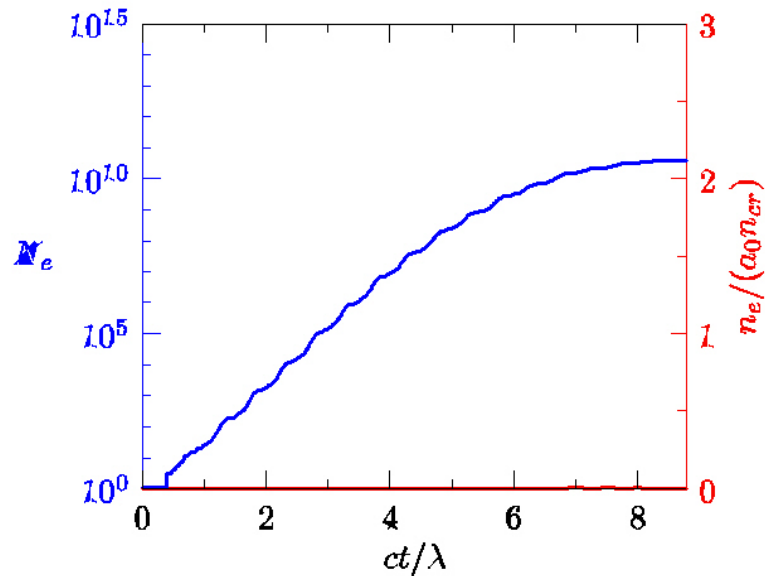


Fig. 4.39. The number of electrons formed by a cascade as a function of time

Activity 4.3. Study of the space-time structure of vacuum irradiated by X-rays and gamma-rays with intensity up to 10^{27} W/cm²

One of the most important problems of modern physics is the problem of combining quantum mechanics and gravity theory. However, its solution is difficult due to the unavailability of laboratory sources of photons or particles needed for energy research. Indeed, the quantum nature of gravity must be manifested at distances of the order of the Planck length, which requires particles with energies of the order of the Planck energy (about 10^{18} eV). At the same time there is an assumption that the space-time structure of the vacuum caused by the quantum nature of gravity (see Fig. 4.40) should manifest itself as a reduced speed of photons of sufficiently high energies [120, 121]. There are also other theories that predict high-energy photon deceleration [122-124].

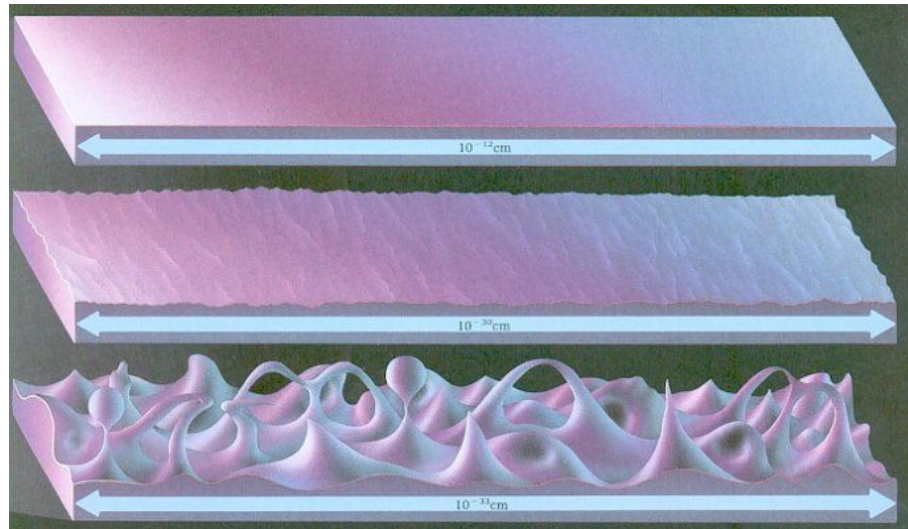


Fig. 4.40. The structure of vacuum (the so-called quantum foam) according to the theory of loop quantum gravity. On the scale of the order of 10^{-30} m the inhomogeneity of this structure becomes evident, which may result in a slower rate of high-energy photon propagation. Source: [125]

The question of whether this high-energy photon deceleration does exist is therefore of fundamental importance. Among all, it is important not only for the development of the theory of quantum gravity, but also for verification of the postulates of special theory of relativity and for possible modification of this theory.

To register any significant deviations of the photon speed from the speed of light, photons with energies of about hundreds of TeV are required. Sources of such photons currently accessible for observation are active galactic nuclei [126, 127] and gamma-ray bursts [128, 129]. Being far from the Earth, these sources cannot be controlled, so their study involves certain difficulties. Despite this, a study of the most distant gamma-ray bursts showed that there is a delay in the time of registration of the high energy photons. Of course, this delay is not necessarily associated with the difference in propagation velocity, and could be explained, for example, by the specific mechanism of gamma-radiation.

Thus, a controlled experiment in the laboratory is the only way to definitely answer the question of whether the speed of a photon depends on its energy, and whether this dependence is related to the structure of vacuum, and if it does, then how. At the same time, the use of traditional accelerators for this purpose is extremely difficult. The PeV-level accelerator proposed by Enrico Fermi would require construction of a synchrotron with a radius equal to the Earth's radius, which is obviously almost impossible from an economic point of view. An alternative is to use accelerators based on high-intensity lasers.

Recent evaluations made by T. Tajima et al. [130] have shown that the required energy level can be achieved on lasers with characteristics which are only slightly higher than in lasers that have been recently constructed or are planned for construction in the near future. Despite the fact that the characteristics of the laser system that we plan to create at the XCELS are far from those required for laser acceleration of electrons up to the PeV level (according to estimates, a laser pulse with power of about 42 PW and energy of about 4.1 kJ is required, provided there are 1000 acceleration cascades [130]), we can expect that with an X-ray and/or gamma-ray source with intensity of 10^{27} W/cm² (a source that is planned to be created at XCELS) conditions (for example, the interaction of radiation with a bunch of high-energy electrons) can be provided to generate photons with energies above TeV. This perspective will be studied in detail under the XCELS Project, resulting in a model experiment on high-energy photon generation with measurements of the dependence of the photon speed on photon energy.

Objective 5. Research on photonuclear physics

Just like the creation of coherent optical sources has led to the development of atomic optics, the creation of high-brightness narrow-band gamma-ray sources will form, in the near future, the basis for nuclear optics or photonuclear physics. These sources under the XCELS Project will be obtained in different modes of interaction of multipetawatt laser pulses with relativistic electron beams. The narrow-band gamma-ray sources will be one of the foundations of photonuclear physics tools. Another foundation will be adaptation of traditional methods and tools of nuclear physics to this scientific direction. The research part of this objective will include the study of intranuclear processes initiated by secondary sources of radiation, the creation of exotic nuclear structures and the development of methods for laser control of intranuclear processes.

Activity 5.1. Development of diagnostic methods and tools of photonuclear physics

High-power laser systems will allow generating high-brightness gamma-ray beams, for example, by Compton backscattering of laser pulse photons by electrons. The use of a powerful laser pulse and a dense short electron bunch (which can be obtained, for example, by means of laser-plasma acceleration methods) may make it possible to obtain gamma-ray beams with ultrahigh brightness and very small durations (tens of femtoseconds), opening up new opportunities for the study of nuclear physics. Perhaps, employing a relativistic plasma mirror will help create a source of gamma rays with even greater intensities. Estimates show that for photons with energies of MeV (typical excitation energy of the nuclei is 100 keV - 1 MeV), up to 10^{14} photons per shot for an area of about $1 \mu\text{m}^2$ can be expected. This will allow pioneer experiments on double excitation of nuclei, and will provide the possibility for measurements using the pump-probe technique (pump and measuring pulse). New sources of gamma rays may also provide for a deeper investigation of the resonance fluorescence of the nuclei. This phenomenon can be used not only for diagnostics but also for remote monitoring of nuclear emissions, as it allows easy detection of isotopes of heavy elements.

Activity 5.2. The study of intranuclear processes initiated by secondary sources of radiation

The primary processes include the acceleration of electrons, protons and nuclei of the target. The accelerated electrons can produce photons by scattering on nuclei, and these photons can initiate nuclear reactions. Also, ions accelerated by a laser pulse may participate in the nuclear reactions. These reactions and collisions may lead to the generation of a variety of secondary particles, gamma-ray quanta, neutrons, etc.

A separate task here is the diagnostics of the secondary particles. Low-energy levels of many metastable isotopes are studied insufficiently [131] (Fig. 4.41). Excitation of nuclei in a dense hot laser plasma (including by the secondary sources) can provide new methods for studying them, and new experimental data can stimulate the development of the theory.

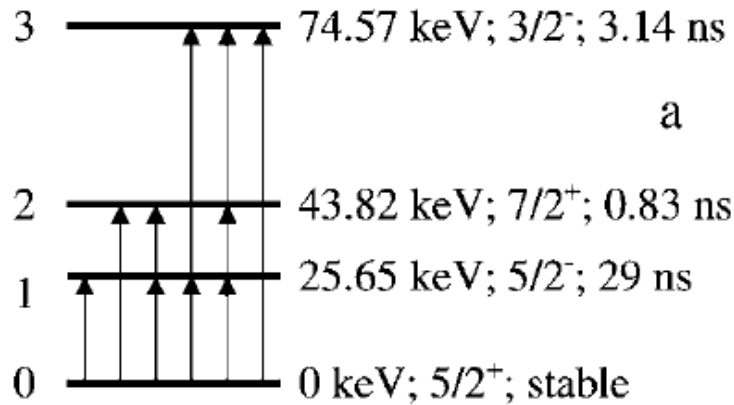


Fig. 4.41. Energy levels of dysprosium-161 and their lifetimes; arrows show various ways of excitation of levels (see [131])

Activity 5.3. Studying methods for control of intranuclear processes and creation of exotic nuclear structures

Ion acceleration by intense laser pulses will produce ion beams that are up to 10^{15} times denser than those achievable in modern classical accelerators. As a result, the cascade reactions of nuclear fission and fusion may allow one for the first time to obtain heavy nuclei with a very high proportion of neutrons. Also, it will open up opportunities for studying fusion reactions of heavy nuclei, which might help solve the problem of the origin of heavy elements in the universe.

The excited states of nuclei with low excitation energies are now well studied, as low-energy gamma-ray sources are largely available. Such states are usually associated with rotational and vibrational degrees of freedom of nuclei. High excitation levels associated with more chaotic dynamics of the nuclei can be investigated using beams of gamma-ray quanta produced by high-intensity laser systems. Currently, the random matrix theory is applied to describe the chaotic excited states, and new ways of excitation of the nuclei will provide the opportunity to test this theory [132]. By using powerful laser systems it is planned to obtain beams of gamma rays with a narrower spectrum than with the use of standard methods. Thanks to a narrower spectrum width, better resolution of the upper excited levels of nuclei can be achieved, thus allowing conducting experiments to test the theory of symmetry breaking in the quantum chromodynamics [133].

Objective 6. Experimental simulation of astrophysical phenomena

The basis for the simulation of astrophysical phenomena using high power lasers is the record-breaking values of pressure, acceleration, and electro-magnetic field strength obtained under the action of laser radiation on matter. Thus, in a laboratory experiment conditions may be realized that occur in large-scale astrophysical phenomena, including the interiors of stars or in the vicinity of black holes, as well as some features of the particles interaction at the early stages of the evolution of the universe.

Activity 6.1. Laboratory modeling of processes in the interiors of stars and planets

In the interaction of a 200-petawatt laser pulse with a variety of targets, temperatures ranging from many thousands to millions of Kelvin degrees can be achieved in macroscopic samples with dimensions greater than a cubic micron in a short time compared with the time of the so-called hydrodynamic expansion of the sample. This makes it possible to study the properties of matter at huge pressures typical for the internal layers of the planets, brown dwarfs, and different stars, as well as the surface layers of white dwarfs and neutron stars. However, there is quite a long quasiadiabatic hydrodynamic expansion of the sample with the laws of the temperature and pressure drop controlled to some extent by profiling geometry, chemical composition and density of the original target. As a result, by properly diagnosing the current state of the target material by means of simultaneous transmission by probing radiation and particle beams, and detection of photons and particles emitted by the target itself, it can be expected that some problems concerning the internal structure of planets and stars may be solved and a number of their dynamical properties may be explained.

For instance, the elucidation of the rheological, electrical and microstructural properties of the inner layers of the terrestrial planets is important for the study of continental drift and analysis of the existence conditions and dynamics of planetary magnetic fields. For gas giant planets, such experiments will advance solution of the problems of the existence and determination of the properties of a dense core (in particular, the question of metallic hydrogen in the Jupiter core). For brown and white dwarfs, these experiments will help to understand the turbulent structure of their surface layers and features of the generated magnetic field that drives the flare activity of these stars. For neutron stars, one can expect to determine details of the structure of the upper layers of the cortex responsible for starquakes and, in particular, the phenomenon of magnetars – X-ray bursts arising from the restructuring of the crust of neutron stars with superstrong magnetic fields. The experiments will be undoubtedly useful for the analysis of

outbursts of Type I and II supernovae, which are associated, respectively, with thermonuclear explosions of white dwarf surface layers and with the collapse of the cores of burnt-out stars, whose initial mass was about ten or more solar masses.

Many of these and other similar astrophysical phenomena are readily available for astronomical observations (see, for example, in Fig. 4.42), but because of their complexity, still do not have any detailed and reasonable interpretation. It is unlikely that this interpretation could be made in the foreseeable future by analytical or numerical analysis, even with the constantly increasing power of computers, without the use of the results of the proposed laboratory modeling.



Fig. 4.42. Supernova 1987A, a core-collapse supernova, exploded in 1987 in the Large Magellanic Cloud.
The image was taken by the Hubble Space Telescope in 1999

Activity 6.2. Laboratory modeling of gravitational effects

Objects with the strongest gravitational fields are neutron stars and black holes. In the presence of an accretion flow of surrounding matter around them, for example, from a companion star in a binary star system, hot accretion disks are formed in the equatorial region, and relativistic jets, the tightly collimated outflows of hot plasma (see the diagram in Fig. 4.43), escape from the poles area. Astronomical observations provide very rich information about such structures, which owe their existence to plasma flows and radiation in a strongly inhomogeneous gravitational field. However, because of the variety of radiation-plasma phenomena in the accretion disks and jets, there is still no satisfactory theoretical description of these structures. The ponderomotive force of a strong laser field under certain conditions can model the nonuniform gravitational field, and hence an

experimental study of laser plasma behavior will enable us to understand many phenomena inherent in astrophysical plasmas in these structures.

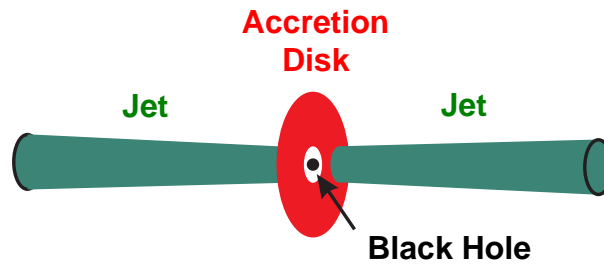


Fig. 4.43.

Of considerable interest is the effect of black hole “quantum evaporation” theoretically substantiated by Hawking, which is basically as follows. In a very strong gravitational field near a black hole, there is a non-zero probability for the birth of particle-antiparticle pairs of different fields since pairs of such virtual particles constantly arising and disappearing in vacuum can gain during their “existence” a sufficiently high energy required for the pair breakdown. The resulting radiation in the form of real particles and photons coming from space near the black hole has a characteristic temperature $T \sim \hbar a / kc$, where \hbar is the Planck’s constant, k is the Boltzmann constant, and a is the acceleration at a distance equal to the Schwarzschild radius for this black hole. Because of the constant irradiation energy loss the mass of the black hole decreases. Experimental verification of this effect is a fundamental physical problem, which can be solved using the following circumstance. One of the basic principles of general relativity is the equivalence principle, which states that the gravitational field can locally be reduced to zero by choosing an appropriate non-inertial reference system. This implies that the effects observed in a strong gravitational field can be observed in a non-inertial (accelerating) reference frame. Thus, an accelerated particle also “sees” the Hawking radiation, which in the case of the non-inertial reference frame is often called the Unruh radiation [134] (Fig. 4.44).

R. S., G. Schaller, and D. Habs, *Phys. Rev. Lett.* **97**, 121302 (2006).

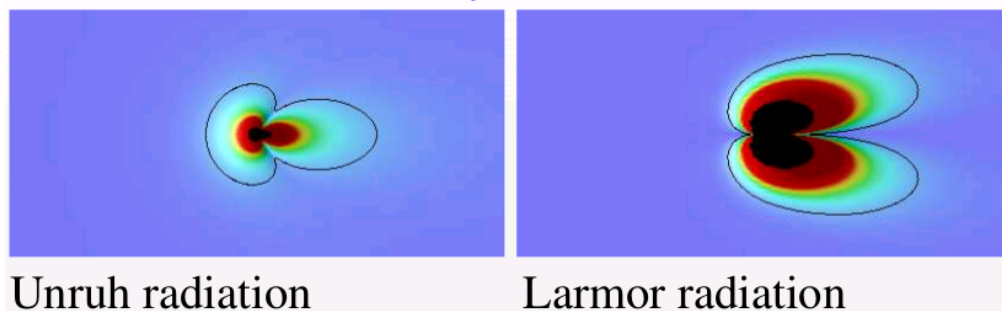


Fig. 4.44. The Unruh radiation pattern (left) and the Larmor radiation pattern (right) for electrons accelerated in a straight trajectory [135]

It can be easily estimated that for the radiation temperature to be equal to one Kelvin in the non-inertial reference frame, its acceleration should be equal to $10^{20}g$, where g is the acceleration of gravity at the Earth's surface. At the same time, for an electron accelerated in the Schwinger field the acceleration is $10^{28}g$. Since the intensity corresponding to the Schwinger field is $\sim 10^{29} \text{ W/cm}^2$ and is proportional to the square of the field, then for a 10^{25} W/cm^2 intensity, we get $a \sim 10^{26}g$ and $T \sim 10^6 \text{ K}$. Thus, at a laser facility with the 10^{25} W/cm^2 intensity one can try to detect a weak signal from thermal photons scattered by the accelerated electron (with a spectrum corresponding to $T \sim 10^6 \text{ K}$), which are present in the non-inertial reference frame associated with the electron. The main difficulty here is that in addition to the Unruh radiation, there are other mechanisms that lead to the emission of photons by the accelerated electron, so it is not so simple to identify the weak Unruh radiation on the general background, especially for the rapidly varying in time electron acceleration (corresponding to a strongly nonuniform gravitational field) when the character of the Unruh radiation changes dramatically.

Various schemes have been proposed to observe the Unruh effect. For example, an electron scattered in the crystal, in addition to the bremsstrahlung radiation, emits the Unruh radiation. The Unruh radiation spectrum differs significantly from the bremsstrahlung spectrum. However, for the Unruh radiation power to become comparable with that of the bremsstrahlung radiation, it is necessary to use electrons with energies of about 100 TeV [136], which are 1000 times higher than the electron energies achieved so far in electron accelerators (about 100 GeV) (Fig. 4.45).

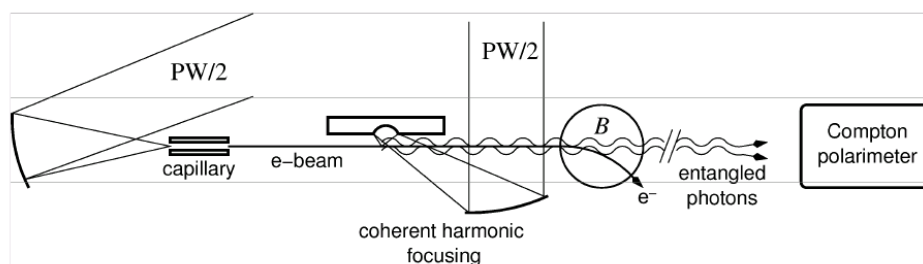


Fig. 4.45. Experimental layout for the detection of the Unruh radiation, which is based on the use of powerful laser pulses and requires no external particle accelerators [135][D. Habs]

More interesting is the method of detecting the Unruh radiation at electron acceleration in a strong laser field [137]. In addition to the large value of acceleration, the laser field has also the advantage that the electron can be accelerated along a straight path (when the bremsstrahlung radiation is simpler and is not related to the curvature of the trajectory.) Thus, besides the Unruh radiation, only the Larmor radiation should be

present, whose directional pattern has a "blind zone". This means that there is a direction in which the Larmor radiation intensity is zero, while the intensity of the Unruh radiation in this direction is non-zero. In addition, the Unruh radiation has a "sharper" temporal structure than the Larmor radiation, which may also facilitate detection [136]. Besides, it was shown that the photons of the Unruh radiation are emitted in pairs with clearly coupled polarizations [135]. Therefore, it is reasonable to try to separate the Unruh radiation from the Larmor radiation by using the polarization statistics of photons received by detectors.

By means of generation and focusing of laser radiation harmonics from a solid surface it is possible to obtain field intensities far surpassing laser field intensities. In such fields, the observation of the Unruh radiation may be simpler. One can also use pre-accelerated electrons, because field intensities are even higher in their reference frames. At the same time, the accelerated electrons can be produced in a laser-plasma accelerator. In general, the proposed experiments offer wide opportunities for the study of such fundamental effects as the Unruh effect and the effect of quantum black hole evaporation.

Activity 6.3. Laboratory modeling of early cosmological phenomena

The foregoing statement is even more true for the study of early cosmological phenomena. First of all, these are phenomena occurring in a high temperature plasma (thousands of Kelvin degrees and higher) of the universe younger than 0.4 million years (the lepton era, before the epoch of recombination and the formation of neutral hydrogen) - quasi-homogeneous, but non-stationary and non-equilibrium due to cosmological expansion. Although the properties of some particles of this era are well studied in accelerators, collective phenomena in such a multicomponent plasma with an intense photon field are still very mysterious and require laboratory modeling in experiments with a laser plasma.

Such modeling will help understand the features of the formation and evolution of different classes of metal-rich stars in the conditions formed after the emergence of the first massive hydrogen-helium stars and massive outbursts of associated supernovae, when the universe was about 1 billion years and its reionization occurred. The study of the parameters of the expected laser plasma is necessary also to elucidate details of evolution of massive stars (especially the third-generation), including the elucidation of the mechanisms of Type II supernovae outbursts, associated with the collapse of the star core from burnt-out thermonuclear fuel of the star. The problem of theoretical description of such supernovae is still unresolved both at the stage of collapse and at the stage of

formation of a diverging shock wave, leading to disruption and expansion of most of the outer layers of the star (Fig. 4.46).

From a physical point of view, we speak about the study of the kinetics of extreme plasma of early universe and dense astrophysical objects under conditions of multiple production and interconversion of high-energy photons and light fermions, as well as the study of the spectral and dynamical peculiarities of the emission of non-equilibrium relativistic plasma bunches characteristic of explosive astrophysical processes and shock waves.



Fig. 4.46. The data from Hubble Space Telescope:
Two supernova remnants DEM L316.
Left – type Ia, Right – type II.
The image is in the optical range

Objective 7. Study of the feasibility of creating exawatt and zettawatt light sources

Further progress in laser power to the exawatt-zettawatt range by direct scaling of parameters of laser channels, or by simply increasing their number is impossible because of fundamental technical limitations (for example, the dimensions of amplifying elements, stability of refraction gratings of the compressor) or difficulties in operating a laser complex. Therefore, a challenging XCELS task is to develop new concepts for obtaining pulses with more than 1 exawatt power. The most interesting concept in this sense is to abandon the traditional grating-based compressors of laser pulses and to employ instead Raman amplification and compression of multipetawatt pulses in plasma in the presence of a relatively long (tens of picoseconds) pump pulse. It is planned to start this experiment after the XCELS 200 PW laser has been launched. The development of this and other approaches for increasing radiation power will be accompanied by the development of appropriate components.

Using backward Raman (combined) scattering it is possible to obtain in plasma output unfocused intensity 10^4 - 10^5 times higher [138, 139] compared to that provided by the conventional technique of amplification of frequency modulated pulses.

The mechanism of using the backward Raman scattering for pulse compression is the following. In a nonlinear medium (plasma), two pulses with a frequency difference equal to the resonant frequency of the medium (plasma frequency) are delivered towards each other. One pulse (pump) has a longer duration, but relatively low intensity. The second pulse (amplified) with a lower frequency should be as short as possible and have a good phase and amplitude profile, but its intensity may be very small. As the amplified pulse passes through the pump, there occurs the backward Raman scattering with excitation of a plasma wave in the medium. Moreover, the plasma wave is excited in such a way that the phase profile of the amplified pulse is not changed, and the plasma wave takes on all the transverse phase inhomogeneities of the pump. This allows one to use almost arbitrary laser pulses as a pump, neglecting their shape and phase profile. Furthermore, this mechanism permits using a pump consisting of many pulses. At the same time, to avoid the appearance of the transverse diffraction structure, each pump pulse can amplify in a particular area in the cross section. Since the amplified pulse does not change its phase profile during amplification, this scheme allows focusing of a pulse amplified by several pulses not synchronized to within a phase.

This Project involves extremely high intensities at which no other material except plasma can be used at the final stage of amplification because of the exceeded breakdown threshold (at technically reasonable transverse scales). As part of the idea of using the

above described mechanism of Raman compression, the so-called C^3 scheme (Cascaded Conversion Compression) has been developed, which is based on three basic methods of compression: chirped pulse amplification (CPA), optical parametric chirped pulse amplification (OPCPA) and Raman compression in the plasma [140].

To achieve the exawatt power level, it is required to have pulse compression with an energy of at least about 10 kJ up to times of the order of 10 fs. None of the existing methods of compression can do it alone. For example, if we start with the energy level of the pump pulse of 10 kJ at 5 ns duration, and we want to achieve compression up to 10 fs using the CPA or OPCPA technique, we encounter serious problems with the breakdown of diffraction gratings. Because of the extremely short duration it is necessary to use broadband diffraction gratings with metal coating (thickness of 200 nm). Such gratings [141] have a low breakdown threshold of about 100 mJ/cm^2 . Therefore, in this case, the standard CPA / OPCPA scheme will require ten fairly expensive diffraction gratings with a size of about 100 m^2 , and each of the gratings may be composed of hundreds of gratings with an area of 1 m^2 . When using solely the plasma compression technique, an unrealistically large area of uniform plasma will be needed, the length of which, as can be easily understood, is determined by the product of pulse duration and the speed of light. This corresponds to 75 cm for a 5 ns pump pulse, which is not feasible from a technical point of view.

The idea of the C^3 method is to separate the process of compression into three stages, including the CPA, OPCPA and compression based on the backward Raman scattering. To illustrate this concept, let us take as an example a laser system at LIL in the center of CEA (France), consisting of eight beams, each having an energy of 10 kJ, duration of 5 ns and a wavelength of 1.05 μm . Due to a small frequency modulation with a shift $\Delta t = 1 / (20 \text{ ps})$ compression may be made up to about 20 ps.

At the first stage of compression, the CPA technique, aimed at transforming the initial pulses into pulses with 10 kJ energies and 20 ps durations, implies a sufficiently narrow-band signal at the output. Therefore, dielectric diffraction gratings may be employed for this purpose instead of metal-coated gratings. The dielectric gratings have three important advantages. First, for a narrow-band signal, they have high efficiency of about 99%. Second, the breakdown threshold for the dielectric used for the 20 ps duration is at the level of 5 J/cm^2 , whereas for the metal-coated gratings it is only about 0.1 J/cm^2 for 10-20 fs. Third, such gratings are commercially available with an area of 1 m^2 . At this intermediate step, gratings with an area of about 0.2 m^2 only will be needed for operating 10 kJ beams.

At the second stage, by using the OPCPA technique it is expected to generate a powerful femtosecond pulse at a wavelength of 1250 nm, which later (at the third stage) will be used as a seed pulse for the Raman compression. A relatively high intensity and quality of the generated pulse, as well as small prepulse provided by this technique are of importance because at the third stage the seed pulse must be repeatedly amplified, competing with a number of undesirable effects: the backward Raman scattering (BRS), due to scattering of Langmuir waves along the path of pump pulse propagation before interaction with the main seed pulse [142], the depletion of the pump pulse due to prepulse amplification [143], scattering by plasma inhomogeneities [144], and resonant side-scattering caused by large values of transverse scales [145]. The influence of these negative processes can be significantly reduced by introducing a plasma density gradient and a corresponding linear frequency modulation in the pump pulse (e.g., as described in [142]). Note that this idea can be realized also for several pump pulses matched appropriately [146]. In case of suppression by one or another way of all the above effects, the seed pulse will be resonantly amplified, absorbing much of the pump energy. In general, this can be achieved because all the unwanted effects are usually more sensitive to frequency detuning than the process of amplification of the seed pulse. The OPCPA method is perfectly suitable for generation of the seed pulse required at this stage. At the IAP RAS the possibility of obtaining pulses with energy of 50 J and duration of 20 fs with an adjustable wavelength of 1250 nm has been demonstrated at the PEARL facility.

At the third stage, it is suggested to use the effect of backward Raman scattering to compress the pulse obtained by the CPA technique from 20 ps to 10 fs. This effect leads to increased radiation with a frequency equal to the difference between the pump frequency and the plasma frequency. For the condition of resonance amplification of the seed with a wavelength of 1250 nm all pump pulses with a wavelength of 1050 nm will require plasma with concentration of 10^{19} cm^{-3} and the size of the interaction region of about 3 mm. The peak intensity after amplification is limited by the manifestation of relativistic effects at the level of 10^{17} W/cm^2 , which corresponds to the transverse diameter of the interaction region of about 3 cm for a pump energy of 10 kJ. Note that in comparison with the crystal the plasma as an amplifying medium is less sensitive to the directions of the pump pulse because of the lack of any selected axes, and therefore allows the use of multiple pump pulses. On the other hand, various nonlinear effects occurring in plasma during the amplification process at high intensities may reduce the efficiency. However, as is shown by numerical experiments with the PIC method, the seed pulse under certain

conditions may be quite stably amplified to the intensities of the order of 4×10^{17} W/cm² with the efficiency of energy transfer from the pump of about 50% [147].

It should be noted that the idea of Raman amplification of laser pulses is being developed in a number of other experimental teams. In particular, besides the above-mentioned laser facility at LIL, France, experiments on Raman amplification are being planned at the Trident facility, Los Alamos National laboratory, USA. At this facility, experiments on the combined stimulated Raman scattering have been already performed (jointly with the LULI, France). In the XCELS Project, we plan to establish close collaboration with the Los Alamos National laboratory to exchange experience and conduct collaborative research on this problem. In the framework of this collaborative activity, an exchange, on a mutually beneficial basis, of diagnostic and other experimental equipment may also be possible.

References to Section 4

- [1] Leemans, W.P., et al., *Nature Physics*, **2**, 696 (2002).
- [2] Esarey, E., et al., *Phys. Rev. Lett.*, **79**, 2682 (1997).
- [3] Faure, J., et al., *Nature (London)*, **444**, 737 (2006).
- [4] Bulanov, S., et al., *Phys. Rev. E*, **58**, R5257 (1998).
- [5] Esirkepov, T., et al., *Phys. Rev. Lett.*, **96**, 014803 (2006).
- [6] Suk, H., et al., *Phys. Rev. Lett.*, **86**, 1011 (2001).
- [7] Oz, E., et al., *Phys. Rev. Lett.*, **98**, 084801 (2007).
- [8] Kiselev, S., et al., *Phys. Rev. Lett.*, **93**, 1350041 (2004).
- [9] Weller, H.R., et al., *Prog. Part. Nucl. Phys.*, **62**, 257 (2009).
- [10] Pukhov, A., *Nature Phys.*, **2**, 439 (2006).
- [11] Nerush, E.N., et al., *NIMA*, **653**(1), 7 (2011).
- [12] Gordienko, S., et al., *Phys. Plasmas*, **12**, 043109 (2005).
- [13] Gordienko, S., et al., *Phys. Rev. Lett.*, **93**(11), 115002 (2004).
- [14] Baeva, T., et al., *Phys. Rev. E*, **74**(4), 046404 (2006).
- [15] Dromey, B., et al., *Nature Phys.*, **2**, 456 (2006).
- [16] Dromey, B., et al., *Phys. Rev. Lett.*, **99**(8), 085001 (2007).
- [17] Gonoskov, A.A., et al., *Phys. Rev. E*, **84**, 046403 (2011).
- [18] Reiss, H.R., et al., *J. Math. Phys.*, **3**, 59 (1962).
- [19] Brown, L.S., et al., *Phys. Rev.*, **133**, A705 (1964).
- [20] Goldman, I.I., *Sov. Phys. JETP*, **19**, 954 (1964).
- [21] Goldman, I.I., *Phys. Lett.*, **8**, 103 (1964).
- [22] Nikishov, A.I., et al., *Sov. Phys. JETP*, **19**, 529 (1964).
- [23] Nikishov, A.I., et al., *Sov. Phys. JETP*, **19**, 1191 (1964).
- [24] Nikishov, A.I., et al., *Sov. Phys. JETP*, **20**, 757 (1965).
- [25] Narozhnyi, N.B., et al., *Sov. Phys. JETP*, **20**, 622 (1965).
- [26] Narozhny, N.B., *Phys. Rev. D*, **20**, 1313 (1979).
- [27] Narozhny, N.B., *Phys. Rev. D*, **21**, 1176 (1980).
- [28] Bell, A.R., et al., *Phys. Rev. Lett.*, **101**, 200403 (2008).
- [29] Nerush, E.N., et al., *Phys. Rev. Lett.*, **106**, 035001 (2011).
- [30] Yee, K., *IEEE Trans. Ant. Prop.*, **14**, 302 (1966).
- [31] Nerush, E.N., et al., *Phys. Rev. Lett.*, **103**, 035001 (2009).
- [32] Korzhimanov, A.V., et al., in *Proc. of the 22nd Int. Conf. On Numerical Simulations of Plasma*, (2011).
- [33] Martins, S.F., et al., *Nature Phys.*, **6**, 311 (2010).
- [34] Martins, S.F., et al., *Comp. Phys. Comm.*, **181**, 869 (2010).
- [35] Burau, H., et al., *IEEE Trans. Plasma Science*, **38**, 2831 (2010).
- [36] Decyk, V.K., et al., *Comp. Phys. Comm.*, **182**, 641 (2010).
- [37] Meyerov, I., et al., in *Proc. of the 22nd Int. Conf. On Numerical Simulations of Plasma*, (2011).
- [38] Pukhov, A., et al., *Appl. Phys. B*, **74**, 355 (2002).
- [39] Malka, V., in *Dream Beam Conference*, Garching, (2007).
- [40] Litvak, A.G., *JETP*, **57**, 629 (1969).
- [41] Esarey, E., et al., *IEEE Trans. Plasma Sci.*, **24**, 252 (1996).
- [42] Lu, W., et al., *Phys. Rev. ST Accel. Beams*, **10**, 061301 (2007).
- [43] Lu, W., et al., in *UCLA, Dream Beam Conference*, (2007).
- [44] Roth, M., et al., *Phys. Rev. Lett.*, **86**, 436 (2001).
- [45] Wilks, S., et al., *Physics of Plasmas*, **8**, 542 (2001).
- [46] Schwoerer, H., et al., *Nature*, **439**, 445 (2006).
- [47] Hatchett, S., et al., *Physics of Plasmas*, **7**, 2076 (2000).
- [48] Esirkepov, T., et al., *Phys. Rev. Lett.*, **89**, 175003 (2002).
- [49] Hegelich, B.M., et al., *Nature*, **439**, 441 (2006).
- [50] Takahashi, K., et al., *Physics of Plasmas*, **17**, 093102 (2010).
- [51] Wang, F., et al., *Physics of Plasmas*, **16**, 093112 (2009).
- [52] Pae, K., et al., *Physics of Plasmas*, **16**, 073106 (2009).
- [53] Esirkepov, T., et al., *Phys. Rev. Lett.*, **92**, 175003 (2004).

- [54] Macchi, A., et al., *Phys. Rev. Lett.*, **94**, 165003 (2005).
- [55] He, F., et al., *Physics of Plasmas*, **13**, 073102 (2006).
- [56] Korzhimanov, A.V., et al., *JETP Letters*, **86**(9), 577 (2007).
- [57] Yan, X.Q., et al., *Phys. Rev. Lett.*, **100**, 135003 (2008).
- [58] Davis, J., et al., *Physics of Plasmas*, **16**, 023105 (2009).
- [59] He, M.-Q., et al., *Phys. Rev. E*, **76**, 035402 (2007).
- [60] Zhang, X., et al., *Physics of Plasmas*, **14**, 073101 (2007).
- [61] Zhang, X., et al., *Physics of Plasmas*, **14**, 123108 (2007).
- [62] Liseikina, T.V., et al., *Appl. Phys. Lett.*, **91**, 171502 (2007).
- [63] Pegoraro, F., et al., *Phys. Rev. Lett.*, **99**, 065002 (2007).
- [64] Robinson, A.P.L., et al., *New Journal of Physics*, **10**, 013021 (2008).
- [65] Klimo, O., et al., *Phys. Rev. ST Accel. Beams*, **11**, 031301 (2008).
- [66] Pegoraro, F., et al., *Eur. Phys. J. D*, **55**, 399 (2009).
- [67] Chen, M., et al., *Physics of Plasmas*, **15**, 113103 (2007).
- [68] Chen, M., et al., *Phys. Rev. Lett.*, **103**, 024801 (2008).
- [69] Yan, X.Q., et al., *Phys. Rev. Lett.*, **103**, 135001 (2009).
- [70] Qiao, B., et al., *Phys. Rev. Lett.*, **102**, 145002 (2009).
- [71] Yu, T.-P., et al., *Phys. Rev. Lett.*, **105**, 065002 (2010).
- [72] Gonoskov, A.A., et al., *Phys. Rev. Lett.*, **102**, 184801 (2009).
- [73] Kar, S., et al., *Phys. Rev. Lett.*, **100**, 225004 (2008).
- [74] Henig, A., et al., *Phys. Rev. Lett.*, **103**, 245003 (2009).
- [75] Shen, B., et al., *Phys. Rev. E*, **76**, 055402 (2007).
- [76] Shen, B., et al., *Phys. Rev. ST Accel. Beams*, **12**, 121301 (2009).
- [77] Yin, L., et al., *Physics of Plasmas*, **14**, 056706 (2007).
- [78] Albright, B.J., et al., *Physics of Plasmas*, **14**, 094502 (2007).
- [79] Yin, L., et al., *Phys. Plasmas*, **18**, 063103 (2011).
- [80] Hegelich, B.M., et al., *Nucl. Fusion*, **51**, 083011 (2011).
- [81] Jung, D., et al., *Rev. Sci. Instrum.*, **82**, 013306 (2011).
- [82] Kalmykov, S.Y., et al., *Phys. Plasmas*, **13**, 113102 (2006).
- [83] Luttkhof, M.J.H., et al., *Phys. Plasmas*, **14**, 083101 (2007).
- [84] Luttkhof, M.J.H., et al., *Laser and Particle Beams*, **27**, 69 (2009).
- [85] Pukhov, A., et al., *Phys. Rev. Lett.*, **107**(14), 145003 (2011).
- [86] Lotov, K.V., *Plasma Physics*, arXiv:1109.6081, (2011).
- [87] Esarey, E., et al., *Phys. Rev. E*, **65**, 056505 (2002).
- [88] Kostyukov, I., et al., *Phys. Plasmas*, **10**, 4818 (2003).
- [89] Rousse, A., et al., *Phys. Rev. Lett.*, **93**, 135005 (2004).
- [90] Ta Phuoc, K., et al., *Phys. Plasmas*, **14**, 080701 (2007).
- [91] Shah, R., et al., *Journal De Physique IV*, **133**, 473 (2006).
- [92] Kneip, S., et al., *Nature Physics*, **6**, 980 (2010).
- [93] Cipiccia, S., et al., *Nature Physics*, DOI: 10.1038/nphys2090 (2011).
- [94] Clayton, C.E., et al., *Phys. Rev. Lett.*, **88**, 154801 (2002).
- [95] Jackson, J.D., *Classical Electrodynamics* (Wiley, New York, 1975).
- [96] Pukhov, A., et al., *Plasma Phys. Control Fusion*, **52**, 124039 (2010).
- [97] Berestetskii, V.B., et al., *"Quantum Electrodynamics"*. 1982, New York: Pergamon Press.
- [98] Kostyukov, I.Y., et al., *Proc. of SPIE*, **8075**, 807504 (2011).
- [99] Bamber, C., et al., *Phys. Rev. D*, **60**, 092004 (1999).
- [100] Korzhimanov, A.V., et al., *Phys. Usp.*, **54**, 9 (2011).
- [101] Sokolov, I.V., et al., *Phys. Rev. Lett.*, **105**, 195005 (2010).
- [102] Carman, R.L., et al., *Phys. Rev. Lett.*, **46**(1), 29 (1981).
- [103] Badsell, C., et al., *Plasma Physics and Simulation* (Énergoatomizdat, Moscow, 1989).
- [104] Akhiezer, A.I., et al., *Sov. Phys. JETP*, **3**, 696 (1956).
- [105] Brunel, F., *Phys. Rev. Lett.*, **59**(1), 52 (1987).
- [106] Quéré, F., et al., *Phys. Rev. Lett.*, **96**(12), 125004 (2006).
- [107] Bulanov, S.V., et al., *Phys. Plasmas*, **1**(1), 745 (1994).
- [108] Nomura, Y., et al., *Nat. Phys.*, **5**, 124 (2009).
- [109] Gordienko, S., et al., *Phys. Rev. Lett.*, **94**(10), 103903 (2005).
- [110] Roentgen, W.C., *Nature*, **53**, 274 (1986).

- [111] Bonse, U., et al., *Appl. Phys. Lett.*, **6**, 155 (1965).
- [112] Momose, A., et al., *Med. Phys.*, **22**, 375 (1995).
- [113] Kwon, O.H., et al., *Science*, **328**, 1668 (2010).
- [114] Fourmaux, S., et al., *Opt. Lett.*, **36**, 2426 (2011).
- [115] Kneip, S., et al., *Appl. Phys. Lett.*, **99**, 093701 (2011).
- [116] King, B., et al., *Phys. Rev. A*, **82**, 032114 (2010).
- [117] Zavattini, E., et al., *Phys. Rev. Lett.*, **96**, 110406 (2006).
- [118] Fedotov, A.M., et al., *Phys. Rev. Lett.*, **105**, 080402 (2010).
- [119] Nerush, E.N., et al., *Phys. Plasmas*, **18**, 083107 (2011).
- [120] Ellis, J., et al., *Phys. Lett. B*, **665**, 412 (2008).
- [121] Amelino-Camelia, G., et al., *Nature*, **393**, 763 (1998).
- [122] Sato, H., et al., *Prog. Theor. Phys.*, **47**, 1788 (1972).
- [123] Coleman, S., et al., *Phys. Lett. B*, **405**, 249 (1997).
- [124] Coleman, S., et al., *Phys. Rev. D*, **59**, 116008 (1999).
- [125] <http://www.aei.mpg.de>.
- [126] MAGIC Collaboration: Albert, J., et al., *Phys. Lett. B*, **668**(4), 253 (2008).
- [127] Aharonian, F., et al., *Phys. Rev. Lett.*, **101**, 170402 (2008).
- [128] Gonzalez, M.M., et al., *Nature*, **424**, 749 (2003).
- [129] Abdo, A.A., et al., *Astrophys. J.*, **706**, L138 (2009).
- [130] Tajima, T., et al., *Prog. Theor. Phys.*, **125**, 617 (2010).
- [131] Andreev, A.V., et al., *Hyperfine Interactions*, **143**, 23 (2002).
- [132] Dietz, B., et al., *Phys. Lett. B*, **693**, 316 (2010).
- [133] Finelli, P., et al., *Nucl. Phys. A*, **735**, 449 (2004).
- [134] Unruh, W.G., *Phys. Rev. D*, **14**, 870 (1976).
- [135] Schützhold, R., et al., *Phys. Rev. Lett.*, **97**, 121302 (2006).
- [136] Rosu, H., in *"Quantum Aspects of Beam Physics"*, P. Chen, Editor (World Scientific, 2004).
- [137] Chen, P., et al., *Phys. Rev. Lett.*, **83**, 256 (1999).
- [138] Malkin, V.M., et al., *Phys. Rev. Lett.*, **82**, 4448 (1999).
- [139] Malkin, V.M., et al., *Phys. Plasmas*, **7**, 2232 (2000).
- [140] Mourou, G.A., et al., *v1 [physics.optics]*, arXiv:1108.2116 (2011).
- [141] Stuart, B.C., et al., *Phys. Rev. Lett.*, **74**, 2249 (1995).
- [142] Malkin, V.M., et al., *Phys. Rev. Lett.*, **84**, 1208 (2000).
- [143] Tsidulko, Y.A., et al., *Phys. Rev. Lett.*, **88**, 235004 (2002).
- [144] Solodov, A., et al., *Physics of Plasma*, **10**, 2540 (2003).
- [145] Solodov, A.A., et al., *Physical Review E*, **69**, 066413 (2004).
- [146] Balakin, A.A., et al., *Physics of Plasma*, **10**, 4856 (2003).
- [147] Trines, R.M.G.M., et al., *Nature Physics*, **7**, 87 (2011).

Innovative Research (Goal 3 and Objectives to Achieve this Goal)

The third goal of the Project is to implement innovative solutions using the established XCELS infrastructure. This goal includes three objectives for the development and prototyping of accelerators, diagnostic and metrological systems, as well as laser sources with high peak and average powers.

Objective 1. Design and prototyping of accelerators of new generation

Activities under this objective include the development of prototypes of compact laser-plasma electron accelerators, combined systems of conventional and laser-plasma electron accelerators, as well as compact laser-plasma ion accelerators. The development of appropriate prototypes will be based on the results of basic research in the framework of [Objective 2](#), **Goal 2** of the Project.

Objective 2. Prototyping of diagnostic and metrological systems with record-breaking resolution

Activities here will include the development of prototype diagnostic systems for monitoring processes with attosecond temporal resolution, studying materials with picometer spatial and attosecond temporal resolution, as well as for probing materials and media with the combined use of light and corpuscular pulses of femtosecond duration. The development of appropriate prototypes will be based on the results of basic research in the framework of [Objective 3](#), **Goal 2** of the Project.

Objective 3. New technologies for creating laser sources with high peak and average power

Activities under this objective include the development and prototyping of a new generation of laser sources for industrial, medical, nuclear, and hybrid power purposes. In each of these areas, new concepts and technical solutions will be created and patented, key laser, optical and electronic components will be developed, and relevant technologies will be transferred for production. The development of appropriate prototypes will be based on the research results obtained under [Objective 4](#), **Goal 1** of the Project.

5. Conclusion

Results expected in all parts of the XCELS program will provide a breakthrough, acquiring utterly new knowledge and development of new technologies. A unique world-class research infrastructure will be created, which will enable conducting experimental investigation of the properties of matter and vacuum in the conditions that were unattainable before. They will be determined by a giant peak power of optical radiation 2-3 orders of magnitude higher than those achieved to date, ultrarelativistic intensity of radiation 4-5 orders of magnitude higher than the current record values, and ultrashort duration of radiation allowing resolving intraatomic and intranuclear processes. Secondary sources of radiation and fast particles will be developed that may make a revolution in accelerator technologies and make research in high energy physics accessible to a broad class of laboratories, including academic and university ones. Novel methods of diagnosing matter with unprecedented precision will be created, thereby greatly expanding the horizons of fundamental metrology. The space-time structure of vacuum will be studied for the first time and methods of producing matter and antimatter in vacuum in the presence of ultrahigh intensity fields will be developed.

Along with the unique challenges of basic science, the significance of results of establishing XCELS will be determined by numerous applications that will be developed during exploitation of the complex. These include, in particular, development of new sources of radiation and particles for clinical diagnostics and treatment, new metrology complexes for diagnostics of materials with picometer spatial and attosecond temporal resolution. An important innovation and economic impact can be achieved due to significant reduction of the cost of accelerator technology working on new principles for creation of new research centers of high energy physics. New technologies for creating laser sources with high peak and average power will be developed, which provides adoption of the applied research at XCELS in prospective areas of industry, medicine, nuclear and hybrid power engineering.

XCELS will be a truly international research establishment providing efficient collaboration of scientists of many countries in the area of extreme light physics and applications. It will provide space for equipping laboratories and time for using the main laser source and secondary sources of radiation for conducting research within the framework of international agreements. An international steering committee will be formed to define the importance and priority of the research programs at XCELS. XCELS will closely cooperate with world leading centers in laser, accelerator, and nuclear research, first of all with those performing related research programs, like ELI, CEA, CERN, KEK, RAL, LANL, and others.

Appendices

Appendix 1: Roadmap

Summary

Appendix 1		Cost, mln RUB																																																		
Goals, Objectives and Activities	Description of works	Funds requested from federal budget	Expected extra-budgetary funds from national sources	Expected contribution from foreign partners	2012				2013				2014				2015				2016				2017				2018				2019				2020				2021											
					I	II	III	IV	I	II	III	IV	I	II	III	IV	I	II	III	IV	I	II	III	IV	I	II	III	IV	I	II	III	IV	I	II	III	IV	I	II	III	IV	I	II	III	IV								
Goal 1. Establishment and operation of mega-project infrastructure		28 900	1 600	4 700	35200 mln																																															
Objective 1. Creating two prototype 15 PW laser modules		5 300	500		5800 mln																																															
Objective 2. Construction of buildings and utilities		4 200	600		4800 mln																																															
Objective 3. Creating a 200 PW laser		12 000	200	2 000	14200 mln																																															
Objective 4. Creation of powerful high-average-power femtosecond lasers for innovative applications		900	100	100	1100 mln																																															
Objective 5. Creation of an electron source with 100 MeV energy based on a photocathode and microwave resonators		550			550 mln																																															
Objective 6. Creating the main target chamber		420			420 mln																																															
Objective 7. Establishing and equipping research laboratories		2 880		2 600	5480 mln																																															
Objective 8. Radiation safety		400			400 mln																																															
Objective 9. Constructing a computer and communication center		600			600 mln																																															
Objective 10. Equipping engineering and supporting workshops		350			350 mln																																															
Objective 11. Maintenance of the MEGA facility		1 300	200		1500 mln																																															
Goal 2. Carrying out fundamental research in the established infrastructure		1 400	100	600	2100 mln																																															
Objective 1. Simulation of interaction of extreme light with matter and vacuum		100			100 mln																																															
Objective 2. Carrying out experiments on laser-plasma acceleration of charged particles		230	100	100	430 mln																																															
Objective 3. Creating new sources of radiation in the hard X-ray and gamma-ray regions		310		100	410 mln																																															
Objective 4. Study of nonlinear properties of vacuum in extreme light fields		230		100	330 mln																																															
Objective 5. Research on photonuclear physics		190		100	290 mln																																															
Objective 6. Experimental simulation of astrophysical phenomena		240		100	340 mln																																															
Objective 7. Study of the feasibility of creating exawatt and zettawatt light sources		100		100	200 mln																																															
Goal 3. Implementation of innovative developments using the infrastructure		1900	300	800	3000 mln																																															
Objective 1. Design and prototyping of accelerators of new generation		600		250	850 mln																																															
Objective 2. Prototyping of diagnostic and metrological systems with record-breaking resolution		400		100	500 mln																																															
Objective 3. New technologies for creating laser sources with high peak and average power		900	300	450	1650 mln																																															
SUB-TOTAL		32 200	2 000	6 100																																																
TOTAL		40 300																																																		

Appendix 1

List of Executors

Short title	Full title
IAP	Institute of Applied Physics RAS
VNIIEF	Russian Federal Nuclear Center - All-Russian Research Institute of Experimental Physics (RFNC-VNIIEF)
ILIT	Institute of Laser and Information Technologies RAS
JINR	Joint Institute for Nuclear Research
INP	Institute of Nuclear Physics SB RAS
GOI	Vavilov State Optical Institute
NSU	Novosibirsk State University
INJECT	JSC "Scientific-Production Enterprise" INJECT "
ILP	Institute of Laser Physics SB RAS
GPI	AM Prokhorov General Physics Institute RAS
UNN	Nizhny Novgorod State University
MEPhI	National Nuclear Research University "MEPhI"
LPI	PN Lebedev Physics Institute RAS
NIIKI	Research Institute of Complex Testing of Optoelectronic Devices and Systems (NIIKI OEP)
VNIITF	Russian Federal Nuclear Center - All-Russian Research Institute of Technical Physics (VNIITF)
IGM	Institute of Geology and Mineralogy SB RAS
JIHT	Joint Institute for High Temperatures RAS
MSU	Moscow State University
NNRG	Nizhny Novgorod Regional Government
INRP	Institute of Nuclear and Radiation Physics RFNC-VNIIEF
Presidium RAS	Presidium RAS
RRC KI	Russian Research Center "Kurchatov Institute"
IAM	MV Keldysh Institute of Applied Mathematics RAS
IZEST	International Center for Zettawatt-Exawatt Science and Technology (France)
LANL	Los Alamos National Laboratory (USA)
MPIK	Max-Planck-Institut für Kernphysik (Germany)
KEK	High Energy Acceleration Research Organization - KEK (Japan)
RAL	Rutherford Appleton Laboratory (UK)
JAI	John Adams Institute for Accelerator Science (UK)
ELI-NP	Extreme Light Infrastructure site in Romania
CEA	Commissariat à l'énergie atomique (France)
IN2P3	National Institute of Nuclear Physics and Particle Physics (France)
CERN	European Organization for Nuclear Research
ELI-ALPS	Extreme Light Infrastructure site in Hungary
DESY	Deutsches Elektronen-Synchrotron
TBD	To be determined

Appendix 2

List of international organizations planning to participate in the mega-science project "Exawatt Center for Extreme Light Studies," and officials to address for negotiations

Country	Organization	Responsible person involved in negotiations
France	CEA – Commissariat à l'énergie atomique (The Ministry of Nuclear Energy)	Thierry Massard Director of Science thierry.massard@cea.fr
United Kingdom	RAL – Rutherford Appleton Laboratory	John Collier Director, Central Laser Facility john.collier@stfc.ac.uk
United Kingdom	John Adams Institute for Accelerator Science	Andrei. Seryi Director andrei.seryi@adams-institute.ac.uk
USA	LANL – Los Alamos National Laboratory	Susan Seestrom Deputy Director seestrom@lanl.gov
USA	Fermi National Accelerator Laboratory	Young-Kee Kim Deputy Director ykkim@fnal.gov
Japan	KEK – High Energy Accelerator Research Organization	Atsuto Suzuki Director General atsuto.suzuki@kek.jp
Japan	JAEA – Japan Atomic Energy Agency	Paul Bolton Deputy Director General, Kansai Photon Science Institute, Japan Atomic Energy Agency bolton.paul@jaea.go.jp
Germany	FAIR – Facility for Antiproton and Ion Research	Boris Sharkov Scientific Director b.sharkov@gsi.de
Switzerland	CERN – European Organization for Nuclear Research	Rolf Heuer Director General rolf.heuer@cern.ch
Canada	Institut National de la Recherche Scientifique (National Institute for Scientific Research)	Jean-Claude Kieffer Director, Centre for Energy, Materials and Telecommunications, National Institute for Scientific Research kieffer@emt.inrs.ca

Appendix 3

Letters of Support



Sept. 28, 2011

Professor Alexander Litvak
 Director, Institute for Applied Physics
 Nizhny Novgorod, Russia

www.ICUIL.org

ICUIL Board

Chair

Toshiki Tajima

Co-Chairs

Chris Barty

Wolfgang Sandner

Secretary

Terry Kessler

Treasurer

Tsuneyuki Ozaki

Re: Support Letter of XCELS

Dear Professor Litvak:

I am writing to you to express my respect for your initiative of XCELS (Exawatt Center on Extreme Light Studies) in Russia and my strongest support of this project from the point of view of the Chairman of the International Committee for Ultrahigh Intensity Lasers (ICUIL) under the commission of the International Union of Pure and Applied Physics (IUPAP).

ICUIL represents all world's research institutes that hold intense lasers that can deliver intensities more than 10^{19} W/cm², which now amount hundred of institutions. ICUIL promotes the research of intense lasers and their applications to science, industrial usages, medical and other societal merits. It also aspires to advance the frontier of high field science.

Thus the initiative by the Russian scientists headed by Professor Alexander Litvak of the Institute of Applied Physics at Nizhny Novgorod for the Mega Science Project toward exawatt laser at XCELS is an extraordinary example of what ICUIL espouses to push the frontier of intense lasers. Many world's intense lasers have exceeded the level of PW now. However, seldom do the 10PW level. XCELS, on the other hand, not only exceeds 10PW threshold, but not only 100PW, it would go toward 1000PW, in another word, 1EW. This is an endeavor unprecedented in the world and what the ICUIL community covets. I am so enthused by this research initiated and thus I express my strongest support and my willingness to actively participate in its research proceedings along the way. We also would like to congratulate their far-sighted vision of the EW class laser and its applications.

I also mention that as Chairman of Extreme Light Infrastructure Preparatory Phase (ELI-PP) Science Advisory Chair, I have advanced the science of the world most intense lasers at ELI. There are three pillars to ELI now (attosecond, photonuclear, and laser-driven beam pillars) and we are anticipating the fourth and final pillar of high field science pillar. The Russian initiative might fit this aspiration of ELI fourth pillar in its scope.

Among the research arena it opens up, I consider the following can be seen: Fundamental High Energy Physics (HEP) has been mainly driven by the high energy fermionic colliding beam paradigm. Today the possibility to amplify laser to extreme energy and peak power offers, in addition to possibly more compact and cheaper ways to help HEP, a suit of complementary new alternatives underpinned by single shot, large field laser pulse, that together we could call Laser-based High Field Fundamental Physics. Thus, Professor Mourou and I started form the International Center for Zetta-Exawatt Science Technology (IZEST) this September. The main mission of the IZEST is to muster the scientific community behind this new concept. The XCELS is the most essential part of this effort. In other words, the Russian initiative of XCELS has the world support by the leading scientists



who are engaged in high field scientist and blessed by their scientific wisdom. It is a world-wide effort already.

As an example, it could provide the avenue to use the laser field to probe the nonlinearity of vacuum due to nonlinearities and light-mass weak coupling fields such as Heisenberg-Euler QED, dark matter and dark energy. We envision that seeking the non-collider paradigm without large luminosity substantially shorten our time-line;. The accelerated research on the non-collider paradigm in TeV and beyond could, however stimulate innovation in collider thinking such as lower luminosity paths, novel radiation cooling, and gamma-gamma colliders. The advancement of intense short-pulsed laser energy by 2-3 orders of magnitude empowers us a tremendous potential of unprecedented discoveries. These include: TeV physics, physics beyond TeV, new light-mass weak-coupling field discovery potential, nonlinear QED and QCD fields, radiation physics in the vicinity of the Schwinger field, and zeptosecond dynamical spectroscopy of vacuum. In addition, we want to take advantage of the ultrashort particle or radiation pulses produced in the femto, atto, and zeptosecond timescale to perform a new type of particle/radiation precision metrology that would help to remove the uncertainty around the neutrino speed. Finally, the TeV particles that can be produced on demand could offer a new tool to TeV Astrophysics.

Hereby, once again I would like to voice my appreciation for and fullest support of XCELS project. The Russian Government's strongest support will further mankind's quest in high field science and the world will benefit from it. We are fully behind your XCELS effort.

Sincerely yours,

A handwritten signature in black ink, appearing to read 'Tajima', is written over the typed name. The signature is fluid and cursive, with a long horizontal stroke extending to the right.

Toshiaki Tajima
Chair, ICUIL

Chair Professor, Faculty of Physics, Ludwig Maximilian University of Munich



The John Adams Institute for Accelerator Science

Prof. Andrei Seryi, Director
Denys Wilkinson Building
Keble Road, Oxford
OX1 3RH, UK

Mobile: [+44][0] 7722 474701

Tel: [+44][0] 1865 273595

Fax: [+44][0] 1865 273601

e-mail: Andrei.Seryi@adams-institute.ac.uk

29 September 2011

Prof Alexander Litvak
Director, Institute for Applied Physics,
Nizhny Novgorod, Russia

Dear Alexander,

With this letter I would like to express our strongest support for your efforts to promote and create the International Center for Extreme Light Studies (XCELS) proposed to be built in Nizhny Novgorod, Russia, within the framework of the Mega-Science Projects.

Lasers of extreme power, in synergy with accelerator and plasma science, have the potential and great promise to revolutionise the entire scientific landscape. In particular, the laser-plasma acceleration, enabled by novel lasers, is now on the verge of breaking through towards applications, for compact light sources, medical applications, and other scientific and technical fields. The XCELS project, due to its exawatt capabilities, has also the potential to redefine the contours of high energy physics, and open new possibilities for investigations of nonlinear quantum electrodynamics.

Realisation of this potential and creation of XCELS will require coherent efforts of many scientists. The laser-plasma acceleration is a major direction of the John Adams Institute, and we will be happy to become a part of the international collaboration supporting your efforts for development of XCELS, for participation in the joint research and for possible in-kind contribution of accelerator and other components to XCELS.

I am also very delighted that collaboration on the XCELS project is coherent with the ongoing joint efforts of the Institute for Applied Physics and of the John Adams Institute towards development of compact laser-plasma acceleration based X-ray sources. I am happy that these joint plans received attention at the highest level of the governments, and that the UK Prime Minister David Cameron briefly mentioned these plans during his speech in Moscow State University on September 12, 2011, and that these plans were also highlighted in the press release of the Science and Technology Section of UK Embassy in Russia. Collaboration in this area will significantly boost both projects.

I would like to assure you that the JAI we will do its best to support you in this endeavour to create the International Center for Extreme Light Studies (XCELS) in Nizhny Novgorod.

Sincerely,

Andrei Seryi

The John Adams Institute for Accelerator Science is jointly hosted by the Departments of Physics of the University of Oxford and the Royal Holloway University of London



**Science & Technology
Facilities Council**

Professor John Collier
Director, Central Laser Facility
Central Laser Facility
Science and Technology Facilities Council
Rutherford Appleton Laboratory
Harwell Oxford
Didcot, Oxfordshire OX11 0QX
Tel: +44 (0)1235 446728 Fax: -44 (0)1235 445888
Email: john.collier@stfc.ac.uk www.stfc.ac.uk

Prof. Alexander Litvak
Director, Institute of Applied Physics
Russian Academy of Sciences

7th October 2011

Dear Professor Litvak,

Letter of Support for the International Centre for Extreme Light Studies

I write in support of establishing the International Centre for Extreme Light Studies (XCELS) at the Institute of Applied Physics in Nizhny Novgorod that is aimed at increasing laser power to unprecedented levels and promoting new fundamental science and compelling applications. Unique opportunities will be created with XCELS to gain insight into the space-time structure of vacuum. Laser-matter interaction at highest intensity levels provided by XCELS will open new routes to particle and ultra brilliant gamma-ray sources. Accelerators could become compact, more versatile, and available by many university and academic laboratories, which in turn will result in significant impact on many branches of science, spurring new applications, including those in medical, industrial, and other sectors.

I believe that the proposal to build the international centre at the Russian Academy of Sciences is a very timely and fascinating initiative that I strongly support. The Institute of Applied Physics is an ideal place in Russia where this establishment will surely be a success. I have been acquainted with the outstanding results of the Institute in ultra intense laser physics, especially in creating a Petawatt laser facility and demonstrating electron acceleration to the multi-hundred MeV energy level.

The XCELS project and its promise of science are compelling. It will be a facility of revolutionary capability which would create new science and a new scientific community. To make this possible a multidisciplinary joint effort is required and we would hope to participate in research activities under this project. RAL looks forward to collaborating with XCELS, for example through assisting (via mutual agreement) in the construction of the exawatt laser facility and performing advanced research at this infrastructure. We understand that an international steering committee for XCELS will be necessary and we stand ready to participate in this, and to assist in other agreed activities, together with other major research establishments.

Finally, we believe that the proposed XCELS infrastructure is highly promising and could ensure advanced science not only in Russia but well beyond its borders.

Yours sincerely

Professor John Collier
Director Central Laser Facility



INTER-UNIVERSITY RESEARCH INSTITUTE CORPORATION
HIGH ENERGY ACCELERATOR RESEARCH ORGANIZATION

1-1.OHO.TSUKUBA-SHI
IBARAKI-KEN.305-0801 JAPAN
<http://www.kek.jp/>
e-mail: atsuto.suzuki@kek.jp

October 20, 2011

Letter of interest for IZEST and its activities by KEK

Dear Professor Gerard Mourou and Professor Alexander Litvak,

It is our intention for KEK to support your efforts of and participate in the joint research activities of promoting the highest intensity frontier of lasers and high field science associated with such lasers and in particular for laser plasma accelerators and in forming an international team and network of scientists under the International Center for Zettawatt-Exawatt Science and Technology (IZEST) and its reach of activities including the LIL and XCELS, as explained in your letter dated Sept. 1, 2011.

I am of opinion that revolutionary ideas are essential for future advanced ultra-high energy and ultra-high power accelerators. Such accelerators open up not only the new paradigms of fundamental physics, but also widespread application-fields. The laser-plasma accelerator is the most challenging and prospective area for future high energy accelerators. I seriously feel the requirement of technological advances will come from the current proof-of-principle one-shot laser-plasma acceleration to multi-shots with high repetition acceleration, that is, the laser-plasma accelerator of practical importance. Noting this, your IZEST to increase the laser power and capabilities much beyond the current level and form a team of international scientific talents is one of keys for achieving this goal.

But we need to forge the effort of the accelerator physics community and laser physics community in a positive collaborative framework. This is why I promoted as Chair of ICFA to closely collaborate with ICUIL. I am glad that the joint activities of ICFA-ICUIL are fostering the necessary research and environment. I am also aware that a lot more is necessary to meet the new challenges to realize laser accelerators. This is why I am so impressed with the activities of IZEST and whose goals to erect the exawatt lasers that can drive particle accelerators with energies of TeV and beyond and we at KEK would participate in this process.

We understand that IZEST will assist and promote the world-wide efforts, for example, that of French LIL Exawatt, that of Russian Mega Science laser project (XCELS), and possibly the deliberated Japanese Exawatt Laser among others. KEK is glad to closely collaborate in these research activities by bringing in its research capabilities and resources in trained personnel, accelerator and detector components, high energy physics expertise, and related technologies contributions as becoming necessary. By introducing the "Laser-based high energy and fundamental physics" paradigm, IZEST has the potential to redefine the contours of high energy physics. I admire the leading role that France with the Ecole Polytechnique and the Commissariat al Energie Atomique is taking in this matter. At KEK we want to assure you that we will do our utmost to second you in this endeavor to reshape and reenergize high energy physics around the ultra high intensity laser. KEK will also collaborate with IZEST by assisting the world-wide initiatives.

Sincerely yours,

A handwritten signature in black ink, appearing to read "A. Suzuki". The signature is fluid and cursive, with a large initial "A" and a long, sweeping tail.

Atsuto Suzuki
Director General of KEK
High Energy Accelerator Research Organization



Fermilab
Fermi National Accelerator Laboratory
P.O. Box 500
Batavia, IL 60510-0-500

September 16, 2011

Subject: Letter of interest for IZEST and its activities by Fermi National Accelerator Laboratory

Dear Professor Mourou:

I am writing to express Fermilab's support for your efforts to establish joint research activities to extend the capability and applicability of the highest intensity lasers to the fields of particle physics and high field science, and in particular for the development of laser plasma accelerators for high-energy physics. I would like to express our intention to participate in these joint research activities through the newly formed International Center for Zettawatt-Exawatt Science and Technology (IZEST).

I believe that innovative ideas are essential for future advanced ultra-high energy and ultra-high power accelerators. Such accelerators open up not only new paradigms of fundamental physics, but also widespread application in a variety of scientific fields. The laser-plasma accelerator is one of the most challenging and interesting areas for future high-energy accelerators. I believe that the required technological advances will only be realized through a dedicated effort focused on proof-of-principle demonstration, which is an essential element of the IZEST mission. Noting this, the mission of IZEST to increase the laser power and capabilities far beyond the current level by forming a team of international scientific talent is one of the keys for achieving these long-term goals.

Reaching these goals will require forging the effort of the accelerator physics community and laser physics community in a positive collaborative framework. That is why I directed our staff, as Deputy Director of Fermilab, to look into such research possibilities and to participate in the ICFA-ICUIL collaboration on related efforts. I am also aware that much more is necessary to meet these new challenges to realize practical laser accelerators and the associated laser technology that is required. That is why Fermilab is already a participating member of the International Coherent Amplification Network (ICAN) consortium that you head. I am very impressed with the activities and goals of IZEST to erect exawatt lasers that can drive particle accelerators with energies of a TeV and beyond. Fermilab has expertise which will be useful in realizing these goals.

We understand that IZEST will assist and promote the world-wide efforts, for example, at the French LIL exawatt, the Russian Mega Science laser project (XCELS), and possibly the Japanese Exawatt Laser, among others. Fermilab looks forward to closely collaborating in these research activities by bringing in its research capabilities and resources in terms of trained personnel, accelerator and detector components, high energy physics expertise, and expertise in related technologies. By introducing the "Laser-based high-energy and fundamental physics" paradigm, IZEST has the potential to redefine the contours of high-energy physics. I applaud the leading role that France, with the Ecole Polytechnique and the Commissariat à l'Energie Atomique, is taking in this matter. At Fermilab we want to assure you that we will do our utmost to support you in this endeavor to reshape and reenergize high-energy physics based on the development of ultra-high intensity lasers for particle acceleration.

Sincerely,

Young-Kee Kim
Deputy Director, Fermilab
Professor of Physics, the University of Chicago



ORGANISATION EUROPÉENNE POUR LA RECHERCHE NUCLÉAIRE
EUROPEAN ORGANIZATION FOR NUCLEAR RESEARCH

Laboratoire Européen pour la Physique des Particules
European Laboratory for Particle Physics

Professor Rolf HEUER
Director-General
CERN
CH - 1211 GENEVA 23, Switzerland

To Whom It May Concern

Telephone:

Direct + 41 22 767 2300
Secretariat + 41 22 767 4054/1240

Telefax:

Direct + 41 22 767 8995

Electronic mail: Rolf.Heuer@cern.ch

Our reference: DG/2011-325

Geneva, 19 October 2011

Support Letter for IZEST

CERN has been informed by Prof. Mourou and Prof. Tajima about the intended creation of an International center on Zetta-Exawatt Science and Technology, abbreviated IZEST. This initiative aims at investigating the use of ultra-intense lasers for so-called "(Laser-based) High Field Fundamental Physics", essentially the study of fundamental physics questions in a regime of very high energy (TeV and beyond) but low luminosity. The theoretical IZEST studies are complemented by an experimental program relying on the French LIL laser.

The creation of such high energy events is of strong interest for the development of future high energy physics accelerators with ultra-intense lasers. Lasers have seen a dramatic progress in recent years and they are expected to progress further, not only in peak and average power but also in stability and efficiency.

CERN believes that IZEST will provide useful insights into the feasibility and physics potential of accelerators with high energies and low luminosity. The IZEST activity will feed efficiently into the European work towards novel accelerators with high beam brightness and high luminosity, as recently discussed at the EuroNNAC (European Network on Novel Accelerators) workshop at CERN. IZEST will be able to cover an additional and potentially promising regime of future accelerators.

In summary, CERN believes that the regime addressed by IZEST is very interesting and therefore supports the further studies and discussions towards IZEST.

Yours sincerely,

Rolf Heuer

Appendix 4

From:

Phone:

Sept., 23 2011 16:20 Page 1

Ministry of Investment Policy of Nizhny Novgorod Region



**Министерство
инвестиционной политики
Нижегородской области**

Кремль, корп. 2, г. Нижний Новгород, 603082
тел. 411-82-16, факс 411-83-27
e-mail: official@invest.krcml.nnov.ru

22.09.2011 № 307-01 - 9222/11

на № _____ от _____

О рассмотрении обращения

Director
Institute of Applied Physics
St. Ulyanov, 46,
Nizhny Novgorod, 603950

Dear Alexander Grigorievich,

As requested by D.V. Svatkovsky, the Deputy Governor of the Nizhny Novgorod region, ref. PR-001-41/11-0-0 dated 11 August, 2011, the Ministry of Investment Policy of the Nizhny Novgorod region, together with concerned executive authorities and local authorities of Nizhny Novgorod Region, have considered your application for the selection of a land site for the project aimed at establishing the Exawatt Center for Extreme Light Studies in the Nizhny Novgorod region.

Based on the results of thorough consideration and taking into account a plot of land that belongs to the IAP RAS in the Kstovo area along the Kazanskoe road in close proximity to Nizhny Novgorod's borders, we suggest you consider hosting the Exawatt Center for Extreme Light Studies on the following land sites in the Kstovo area:

1. A land site along the Kazanskoe road, eastward to the land site of the IAP RAS. Allocation of this land for the project's purposes is possible, provided third-party rights on this land are waived, and the land has changed its category of agricultural land. The site is located along a hill slope, so engineering works to prepare the territory for construction activities will be needed.

From:

Phone:

Sept., 23 2011 16:20 Page 2

2. A land site along the Kazanskoe road, southward to the IAP RAS land. Allocation of this land for the project's purposes is possible, provided third-party rights on this land are waived (part of this land is the property of "Stage" Ltd. meant for housing development), and the land has changed its category of agricultural land. In addition, a pressure sewer collection pipe D = 3000 with a buffer area of 50 meters runs along the land site (the land site has been considered at the suggestion of the applicant).

3. A land site in the Kstovo area, approximately 1,100 m south-east from Opaliha settlement. The site is immediately adjacent to the highway M-7 "Volga". In accordance with the planning and surveying project of Bolshelninskogo settlement, it belongs to industrial and municipal storage area of IV-V class of danger. The site is recommended by the administration of the Kstovo area as a promising investment area.

4. A land site located in the Prioksky district of N. Novgorod, on the south side of the Starokstovskaya road. Allocation of this land for the project's purposes is possible, provided third-party rights on this land are waived (this land is in federal ownership).

Please inform the Ministry of Investment Policy of the Nizhny Novgorod region of your decision no later than 30.09.2011.

Appendix: layouts of land sites on 3 pages, 1 copy.

N.V. Kazachkova

Minister

Министр

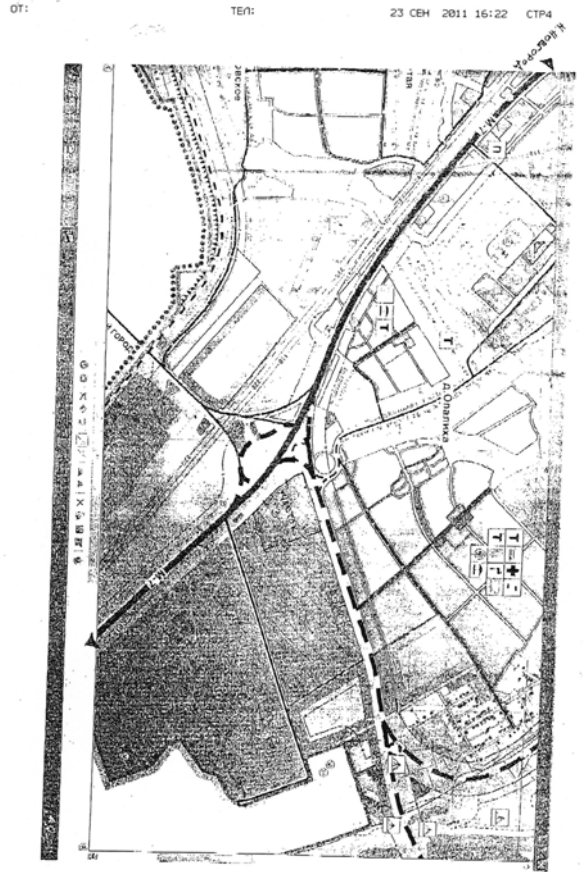
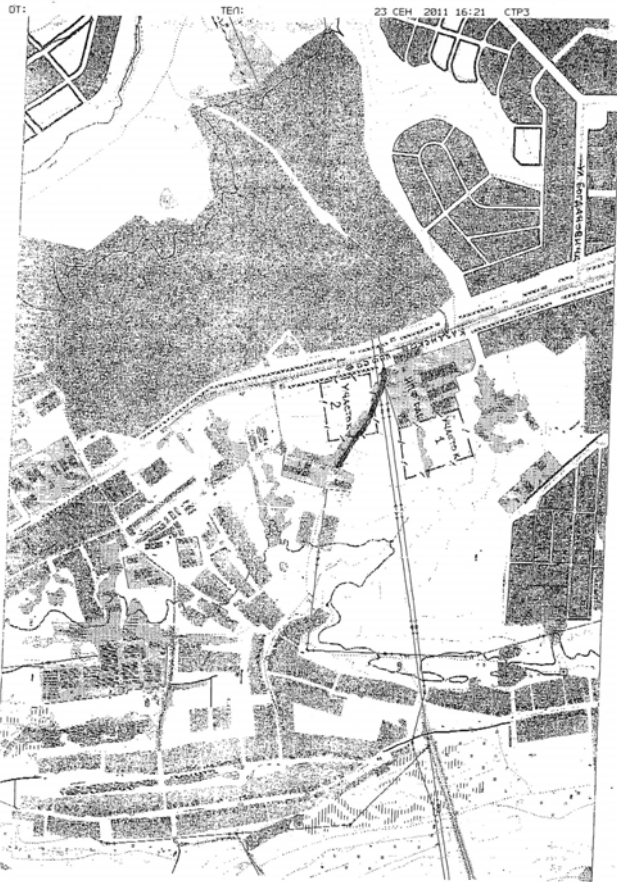


Н.В.Казачкова

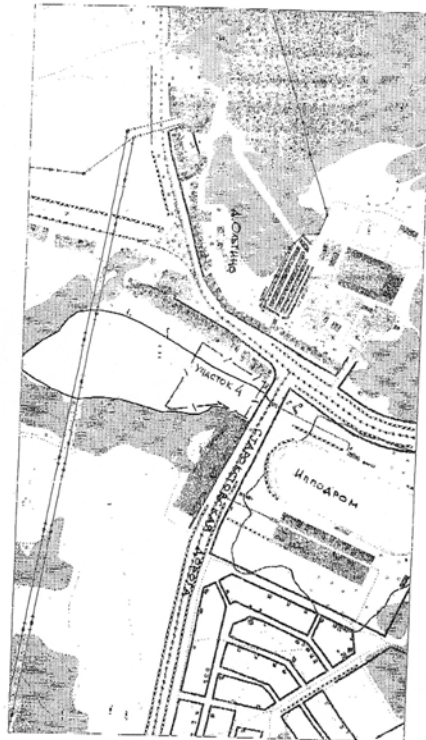
Номерта
419-68-84

Ponomarev

419-68-84



OT: ТЕП: 23 СЕН 2011 16:22 СТП5



МИНОБРНАУКИ РОССИИ
 Федеральное государственное
 бюджетное образовательное
 учреждение высшего
 профессионального образования
 «Нижегородский
 государственный
 университет
 им. Н.И. Лобачевского»
 (ННГУ)
 г. Гagarина, 23, г. Нижний Новгород,
 ГСП-20, 603950
 Тел.: (831) 462-30-90 факс: (831) 462-30-86
 e-mail: univ@nnu.ru
 ОКПО 603950403 ОГРН 102603720510
 ИНН /КПП 5260304042 /5260305001

29.09.2014 1927/0416

На № _____ от _____

Director of the Institute
 of Applied Physics
 A.G. Litvak
 603950, Nizhny Novgorod,
 st. Ulyanov, 46

Dear Alexander Grigorievich,

In connection with the plans of the Lobachevsky State University of Nizhny Novgorod to participate in the project for establishing the Exawatt Center for Extreme Light Studies, we would suggest that you consider placing the future center on the land area, cadastral number 52:18:080136:0003, Nizhny Novgorod, Prioksky district, that is now in use of the Lobachevsky State University.

Yu. V. Chuprunov
 Rector

Ректор



Е.В. Чупрунов

Appendix 5

Interview with Professor Toshiki Tajima

Chair Professor, Faculty of Physics, Ludwig Maximilian University of Munich,
Chairman of the International Committee on Ultra-high Intensity Lasers (ICUIL)

http://www.strf.ru/material.aspx?CatalogId=358&d_no=40863

05/07/11

Sterligov Ivan



05.07.11
I Sterligov Ivan
Государственная политика: Госполитика

Сверхмощный лазер как интегратор науки

В числе **мега-научных проектов**, которые будут реализованы на территории России, – Международный центр исследований экстремальных световых полей на основе сверхмощности лазерного комплекса в Нижнем Новгороде. Руководит центром всемирно известный физик, Жерар Муру при поддержке Минобрнауки России. STRF.ru подробно рассказывал об этой работе в статье «**Российские ученые строят сверхмощный лазер**». Насколько значим этот проект для мировой науки, мы выяснили у **Тосики Тадзимы**, заведующего кафедрой физического факультета Университета Людвиг Максимилиана в Мюнхене, председателя Международного комитета по сверхмощным лазерам (International Committee on Ultra-High Intensity Lasers, ICUIL).



Страна STRF.ru
Международный комитет по сверхмощным лазерам – подразделение Международного союза фундаментальной и прикладной физики, основанное в 2003 году. Лазеры ICUIL – продолжение науки и технологии сверхмощных лазеров и координация исследований и разработки в этой области. Под сверхмощными лазерами в комитете понимают лазеры с интенсивностью 10^{18} ватт на см² и мощностью около 10 тераватт.

На Ваш взгляд, что примечательного произошло в области сверхмощных лазеров в последние времена?

– Прошлый год стал эпохальным для нас благодаря решению Бароскоза о запуске проекта **Extreme Light Infrastructure (ELI)**, включает целый ряд сверхмощных лазеров в нескольких регионах Европы], а также началу реальной работы **National Ignition Facility** в США – альтернативной токамак проект термоядерной энергетики, основанный на лазерном нагреве и инерционном удержании плазмы. Мы предполагаем, что развитие сверхмощных лазеров и сопутствующих областей науки значительно ускорится, и стараясь способствовать этому процессу во всем мире. Очень воодушевляет участие новых стран и регионов в развитии сверхмощных лазеров: Венгрия, Чехия и Румыния (в составе ELI), Китай и, конечно, Россия.

Наблюдая эти тенденции, я верю, что физика сверхмощных лазеров в скором времени откроет новые области: ускорение сверхвысоких энергий, еще более короткие импульсы излучения, ядерную фотонику и даже исследования природы вакуума.

Как Вы оцениваете амбиции России стать одним из ключевых игроков в физике сверхмощных лазеров с помощью проекта в Нижнем Новгороде?

– Я считаю, что это смелая и дальновидная инициатива, и очень уважаю принятое решение. Для меня здесь важны три момента. Во-первых, наука за последнее столетие продвинулась столь далеко вперед, что перед ней стоят все еще исключительно сложные задачи. Поэтому требуется значительная воля и концентрация ресурсов, чтобы получить ответы на ныне стоящие перед нами важные вопросы.

Во-вторых, эти оставшиеся нерешенными сложные проблемы важны для науки и технологий в целом и способны повлиять на жизнь людей не только в стране-спонсоре, но и во всем мире. Поэтому для их решения требуется международное сотрудничество, плоды которого будут разделены соответствующим образом. Другими словами, сам мир и стоящие перед ним научные проблемы сейчас гораздо более взаимосвязаны, чем раньше, и требуют более глобального подхода к исследованиям.

Наконец – и это особенно очевидно для исследований с помощью эксаваттных (10^{18} ватт) лазеров – сверхмощные лазеры способны оказать влияние на очень широкий спектр дисциплин. Например, они могут придать второе дыхание физике высоких энергий, а также сделать более доступными компактные установки для лучевой терапии рака. В то же время сверхбыстрая метрология и кристаллография атто (10^{-18} секунда) и зептосекунда (10^{-21} секунда) позволят нам непосредственно наблюдать ход химических и биологических процессов. Эксаваттные лазеры станут интеграторами науки XXI века, противостоять тенденциям к узкой специализации науки, характерным для XX века.

Какова может быть роль Международного центра исследований экстремальных световых полей в мировой науке и есть ли ICUIL и Вас лично желание непосредственно поддержать его?

– Число лабораторий, стремящихся заниматься лазерами сверхвысокой интенсивности, в последнее время в мире растет экспоненциально. Но если мы говорим о действительно переднем крае, требуется самый мощный лазер с самыми короткими импульсами. Как мы с Жераром Муру недавно установили (см. [сообщение](#) в журнале Science. – STRF.ru), исторически длина импульсов прямо связана с мощностью лазерных установок. Необходим по меньшей мере один мировой центр с лазером сверхвысокой мощности для действительно прорывных открытий.

Российский центр – именно то, что нужно.

Ни один другой проект не готов превзойти эксаваттный рубеж. В числе возможных применений – новый и наиболее привлекательный принцип работы коллайдеров, требующий лазерных импульсов уровня 10^{18} ватт/см², а также исследования темной материи и темной энергии, для которого необходим значительный объем фотонов, чтобы надежно отделять важные сигналы из шума. Зептосекундное временное разрешение также требует наибольшей интенсивности лазера.

Потому благодаря мощности лазера центр сразу станет основой точной притяжения науки и технологий экстремально сильных полей, в которой ученые со всего мира будут двигать вперед целый блок научных дисциплин. Установка подобного уровня неминуемо породит массу производных технологий и инновационных технологических компаний вокруг центра. Оптика, физика плазмы, ядерная физика, физика высоких энергий, нелинейная наука, атомная физика, материаловедение, химия, биология, медицина, ядерные технологии, астрономия, геофизика и геология – все эти дисциплины получат импульс к развитию. Сверхмощный лазер способен предоставить совершенно новые возможности решения целого ряда разнообразных принципиальных научных проблем.

У ICUIL есть полномочия содействовать подобному центру и сотрудничать с ним. Его миссия и цели, отраженные в нашем уставе, прекрасно сочетаются. Любо и настолько полон энтузиазма, что хотел бы сам участвовать в проекте.

Добавлю, для того чтобы привлечь лучших мировых ученых-лазерщиков, необходима среда, способствующая свободным академическим поискам. Кроме того, нельзя недооценивать качество и комфорт социально-бытовой инфраструктуры для ученых и их семей.

Ultra-high intensity laser as an integrator of science

Among mega-science projects to be implemented in Russia is the Exawatt Center for Extreme Light Studies based on an ultra-high intensity laser facility in Nizhny Novgorod. The center is directed by the world famous physicist Gerard Mourou, with the support of Russian Ministry of Education and Science. STRF.ru wrote about this work in detail in the article "Russian scientists are building an ultra-high intensity laser." How relevant is this project to the world of science? We asked Toshiki Tajima, Chair Professor of Faculty of Physics at the Ludwig Maximilian University of Munich, and Chairman of the International Committee on Ultra-high Intensity Lasers (ICUIL).

STRF.ru Reference:

The International Committee on Ultra-high Intensity Lasers (ICUIL) is a division of the International Union of Pure and Applied Physics, founded in 2003. The ICUIL mission is to promote science and technology of ultra-high intensity lasers and to coordinate research and development activities in this area. An ultra-high intensity laser, according to the committee, is a laser with intensity of 10^{19} watts per cm², and power of about 10 terawatt

Photo caption:

Toshiki Tajima is eager to take part in Russia's megaproject for constructing an ultra-high intensity laser

In your opinion, what was remarkable in the field of high intensity lasers in recent years?

- Last year was a milestone for us because of the EU's decision to launch the Extreme Light Infrastructure project [ELI, which includes a number of ultra-high intensity lasers in several regions of Europe], as well as the beginning of real operation of the National Ignition Facility in the United States - an alternative fusion energy project to tokamaks, based on laser heating and inertial confinement of plasma. We assume that the development of ultra-high intensity lasers and related areas of science will be significantly accelerated, and we try to contribute to this process throughout the world. Very encouraging is the participation of new countries and regions in the development of ultra-high intensity lasers: Hungary, the Czech Republic and Romania (in the ELI), China and, of course, Russia.

Observing these trends, I believe that the physics of ultra-high intensity lasers in the near future will open new areas such as acceleration of ultra-high energies, even shorter pulses, nuclear photonics, and even research on the nature of vacuum.

How do you assess Russia's ambitions to become one of the key players in physics of high intensity lasers with the project in Nizhny Novgorod?

- I think this is a challenging and forward-looking initiative, and I have great respect for this decision. For me, there are three important issues here. First, science has advanced so far ahead over the last century that it has now great challenges in front. Therefore, significant commitment and concentration of resources are required to answer the challenges that we face today.

Second, these unsolved problems are important for science and technology in general and could affect people's lives not only in the sponsoring country, but also throughout the world. Therefore, solving these problems requires international cooperation, and the fruits of this cooperation will be shared accordingly. In other words, the world itself and the scientific challenges it confronts now are interconnected to a greater degree than ever before, requiring a more global approach to research.

Finally, and this is particularly evident for studies using exawatt (10¹⁸ watt) lasers, ultra-high intensity lasers are capable of affecting a broad range of disciplines. For example, they may give a new impetus to high-energy physics, as well as make more affordable compact systems for radiation therapy of cancer. At the same time, ultrafast metrology, and crystallography at atto (10⁻¹⁸ seconds) and zepto (10⁻²¹ seconds) levels will allow us to directly observe the course of chemical and biological processes. Exawatt lasers will become integrators of the XXI century science, as opposed to the tendency toward narrow specialization of science that was characteristic of the XX century.

What could be the role of the Exawatt Center for Extreme Light Studies in the world of science and would ICUIL and you personally like to support it directly?

- The number of laboratories seeking to work with ultra-high intensity lasers is growing exponentially throughout the world. But if we're talking about a real cutting edge of science, the most powerful laser with shortest pulses is required. As Gerard Mourou and I have recently shown (see report in the Science journal. - STRF.ru), historically pulse duration is directly related to power of laser systems. At least one world center with an ultra-high intensity laser is needed to provide truly breakthrough discoveries.

The Russian Centre is just what you need.

No other project is ready to exceed the exawatt level. Among possible applications is a new and most attractive principle of colliders, which requires laser pulses of 10 kilojoules, as well as studies of dark matter and dark energy, which requires a significant amount of photons to reliably separate important signals from noise. Zeptosecond temporal resolution also calls for the highest laser intensity.

So, thanks to the high laser power, the center will immediately become the main point of attraction of science and technology of extremely strong fields, in which scientists from around the world will advance a whole set of scientific disciplines. Such a facility will inevitably generate a lot of derived technologies and innovative technology companies around the center. Optics, plasma physics, nuclear physics, high energy physics, nonlinear science, nuclear physics, material science, chemistry, biology, medicine, nuclear technology, astronomy, geophysics and geology - all these disciplines will get an impetus for development. The ultra-high intensity laser can provide completely new opportunities for solving a number of different fundamental scientific problems.

ICUIL has the authority to promote such a center and co-operate with it. Its mission and goals, as reflected in our charter, match perfectly. Personally, I'm so enthusiastic that I would like to participate in the project.

I should add that in order to attract world's best laser scientists it is necessary to provide an environment that would promote free academic research. In addition, one should not underestimate the quality and comfort of social infrastructure for researchers and their families.

Appendix 6

AGREEMENT ON THE ESTABLISHMENT OF THE INTERNATIONAL SCIENTIFIC ASSOCIATION (ISA)

«Extreme Light Infrastructure Support Activities»

ELISA

RUSSIAN ACADEMY OF SCIENCES, a self-governing organization with public status, hereinafter referred to as RAS, legal address: Leninsky Prospekt, 14, 119991-71, Moscow, Russia, represented by Vice President, Academician Alexander Fedorovich Andreev, acting for and on behalf of:

- Institute of Applied Physics RAS, Nizhny Novgorod
- Lebedev Physical Institute RAS, Moscow
- Prokhorov General Physics Institute RAS, Moscow
- Institute of Laser Physics SB RAS, Novosibirsk
- Joint Institute for High Temperatures RAS, Moscow
- Institute of Laser and Information Technologies RAS, Moscow
- Keldysh Institute of Applied Mathematics, Moscow
- Sobolev Institute of Mineralogy and Petrology SB RAS, Novosibirsk

RUSSIAN FOUNDATION FOR BASIC RESEARCH, a public self-governing non-profit organization existing in the form of a federal institution under the jurisdiction of the Government of the Russian Federation, hereinafter referred to as the RFBR, legal address: 117 334 Russia, Moscow, Leninsky Prospekt 32a, represented by the Chairman of the Board of the Foundation, Academician Vladislav Yakovljevic PANCHENKO

LOMONOSOV MOSCOW STATE UNIVERSITY, a public institution of a scientific and professional nature, hereinafter referred to as MSU, legal address: 119991, Moscow, GSP-1, Vorob'evy Gory, represented by its Rector, Academician Viktor Antonovich Sadovnichy, acting for and on behalf of:

- International Laser Center

MOSCOW ENGINEERING PHYSICS INSTITUTE (STATE UNIVERSITY), a public institution of an academic and professional nature, hereinafter referred to as MEPI, legal address: 115409 Moscow, Kashirskoe highway, 31, represented by Rector Prof. Mikhail N. Strikhanov

VAVILOV STATE OPTICAL INSTITUTE, the Federal State Unitary Enterprise, Scientific-Production Corporation, hereinafter referred to as SOI, legal address: 199034, St. Petersburg, Exchange line 12, represented by Director, Professor Vladimir Alekseevich Tupikov,

on the one part,

AND

NATIONAL CENTER FOR SCIENTIFIC RESEARCH, a public institution of a scientific and technological nature, hereinafter referred to as CNRS, legal address: 3 rue Michel Ange, 75 794 Paris, cedex 16, represented by Director General, Professor Arnold MIGUS acting for and on behalf of:

- Laboratory of Applied Optics (LOA UMR 7639),
- Laboratory for the use of intense lasers (LULI UMR 7605),
- Laboratory of X-ray interaction with matter (LIXAM UMR8624),
- Charles Fabry Laboratory of the Institute of Optics (LCFIO UMR8501),
- Leprince Ringuet Laboratory (LLR UMR 7638),
- Center for Theoretical Physics (CPhT UMR 7644),
- Irradiated Solids Laboratory (LSI UMR 7642),
- Gas and Plasma Physics Laboratory (LPGP UMR 8578),
- Linear Accelerator Laboratory (LAL UMR 8607)
- Center for Intense Lasers and Applications (CELIA UMR5107)
- Institute of Extreme Light (ILE UMS3205)

ATOMIC ENERGY COMMISSION, a public institution of a scientific, technological and industrial nature, hereinafter referred to as "CEA", legal address: sis Batiment 447, 91 191, Gif-sur-Yvette cedex, France, represented by General Administrator, Professor Bernard Bigot, acting for and on behalf of:

- Laser-Matter Interaction Laboratory (LILM)
- Department of Research on condensed matter, atoms and molecules (DRECAM)
- Laboratory for the use of intense lasers (LULI UMR 7605),
- Laboratory of radiation physics of solids (LSI UMR 7642)
- Center for Intense Lasers and Applications (CELIA UMR5107)

POLYTECHNIC SCHOOL, an establishment of administrative nature, hereinafter referred to as PS, legal address: sis Route de Saclay 91 128 Palaiseau Cedex, represented by Director General, General Xavier Michel, acting for and on behalf of:

- Laboratory of Applied Optics (LOA UMR 7639),
- Laboratory for the use of intense lasers (LULI UMR 7605),
- Leprince Ringuet Laboratory (LLR UMR 7638),
- Center for Theoretical Physics (CPhT UMR 7644),
- Irradiated Solids Laboratory (LSI UMR 7642)
- Institute of Extreme Light (ILE)

UNIVERSITY OF PARIS-SUD, a public institution of a scientific, cultural and professional nature, hereinafter referred to as Paris 11, legal address: sis 15 rue George Clémenceau, 91 405 Orsay Cedex, represented by President Prof. M. Guy Couarraze, acting for and on behalf of:

- Laboratory of Applied Optics (LOA UMR 7639),
- Laboratory of X-ray interaction with matter (LIXAM UMR8624),
- Charles Fabry Laboratory of the Institute of Optics (LCFIO UMR8501),
- Laboratory of Gas and Plasma (LPGP UMR 8578),
- Linear Accelerator Laboratory (LAL UMR 8607)
- Institute of Extreme light (ILE)

HIGHER NATIONAL SCHOOL OF ADVANCED TECHNOLOGIES, a public institution of an administrative nature, hereinafter referred to as ENSTA, legal address: sis 32 Boulevard Victor, 75 739 Paris cedex 15, represented by Director, Professor Yves Demay, acting for and on behalf of:

- Laboratory of Applied Optics (LOA UMR 7639),
- Institute of Extreme Light (ILE)

INSTITUTE OF OPTICS GRADUATE SCHOOL, a private institution recognized to be of public benefit, hereinafter referred to as IOGS, legal address: Sampus Polytechnique, RD 128,91127 Palaiseau Cedex, represented by Director General Prof. Jean-Louis MARTIN, acting for and on behalf of:

- Charles Fabry Laboratory of the Institute of Optics (LCFIO UMR8501),
- Institute of Extreme Light (ILE)

PIERRE AND MARIE CURIE UNIVERSITY, a public institution of a scientific, cultural and professional nature, hereinafter referred to as UPMC, legal address: sis 4, place Jussieu 75005 Paris, represented by President Prof. Jean-Charles POMEROL, acting for and on behalf of:

- Laboratory for the use of intense lasers (LULI UMR 7605)

UNIVERSITY OF BORDEAUX 1 SCIENCE AND TECHNOLOGY, a public institution of a scientific, cultural and professional nature, hereinafter referred to as USTB, legal address: sis 351 cours de la Libération, 33 405 Talence Cedex, represented by President Prof. Alain BOUDOU, acting for and on behalf of:

- Center for Intense Lasers and Applications (CELIA UMR5107)

on the other part,

hereinafter collectively referred to as the "Parties" or individually as the "Party",

WITH REFERENCE TO:

- *Agreement on Cultural Cooperation between the Government of the Russian Federation and the Government of the French Republic, signed at Paris on February 6, 1992,*
- *Agreement on Scientific and Technological Cooperation between the Government of the Russian Federation and the Government of the French Republic, signed at Moscow on July 28, 1992,*
- *Agreement on scientific cooperation between the Russian Academy of Sciences and the CNRS, signed at Moscow on March 12, 2002, extended at Paris July 4, 2006,*
- *Agreement on scientific cooperation between the Russian Foundation for Basic Research and the CNRS, signed at Paris on March 6, 2003,*
- *Memorandum of Understanding between the Russian Foundation for Basic Research and National Center for Scientific Research, signed at Paris on October 10, 2008*

PREAMBLE

It is possible today to envision laser delivering extremely high peak power in the exawatt range. This power focused over dimensions limited by the wavelength of light will make available intensities in the 1025 W/cm² regime well beyond what is today accessible. This is three orders of magnitude above what is attainable today and become the gateway to a regime of light-matter interaction fundamentally novel: the ultrarelativistic regime.

Two new facilities susceptible to provide ultrarelativistic intensities are built. One in France called Apollon , housed in the Institute of Extreme Light (Institut de la Lumière Extrême, ILE) delivering 10PW. It will mirror a 5-10 PW laser, built in the Nizhny Novgorod Institute of Applied Physics (IAP). Both systems will give access to the ultra relativistic regime. It will afford new investigations in particle physics, nuclear physics, nonlinear field theory, ultrahigh-pressure physics, attoscience, plasma and beam physics, laboratory astrophysics and cosmology. Apollon will be the forerunner of ELI, composed of 10 Apollon beams, all in phase. One of the fundamental missions of ILE will be to validate the Apollon technology for ELI. Apollon will provide ultra-short energetic particles (10-100 GeV) and radiation (up to few MeV) beams produced from compact laser plasma accelerators.

The French (ILE) and the Nizhny Novgorod ultrarelativistic facilities will mate their scientific, engineering and medical missions for the benefit of industry and society. For instance, the secondary sources expected in the project will provide X-ray technologies to clarify the complete time history of reactions such as protein activity and protein folding, radiolysis, monitoring of chemical bonds and catalysis processes. This will lead to a better understanding and control of key events during chemical bond formation and destruction. A high impact on society and on new technologies for industry is then expected.

The International Scientific Association (ISA), composed of French and Russian scientists, will foster the interaction in this emerging field both on technological and scientific grounds. This ISA would be the first step towards a Laboratoire International Associé, with well defined objectives.

IT IS HEREBY AGREED AS FOLLOWS:

ARTICLE 1 – ESTABLISHMENT AND DURATION

The International Scientific Association «ELISA» in the area of basic and applied research of extreme light, hereinafter referred to as the "Area", having neither legal personality nor legal capacity, hereinafter referred to as ISA, is established by the Parties as of January 1, 2010 for a period of 4 (four) years.

The agreement on the establishment of the ISA (hereinafter referred to as the "Agreement") may be extended by signing an additional agreement.

The decision to extend the agreement will be made by the parties, upon notice to the Scientific Council and the Board of ISA.

ARTICLE 2 - MISSION

The ISA mission is to ensure support and coordination of scientific activities described in Annex 1, which is an integral part of this Agreement.

For this purpose, the ISA aims at the following:

- to facilitate contacts and exchange between researchers;
- to encourage cooperation both within the scientific community, and with third parties;
- to coordinate and structure partnership research programs aimed at supporting scientific research within the frameworks of national, European or international programs for support of research and technological development;
- to seek harmonization and complementarity of programs of conferences and congresses held on associated scientific topics;
- to promote educational activities;

ARTICLE 3 - COMPOSITION

The ISA consists of laboratories or groups listed in Annex 2, which is an integral part of this Agreement.

The staff assigned to work in the ISA remains under full administrative control of the organizations in which they are employed.

A list of staff at the time of ISA establishment is included in Annex 2.

ARTICLE 4 - ORGANIZATION

4.1. COORDINATORS

The parties jointly appoint one person responsible for the coordination of ISA activities from the French side and one responsible person from the Russian side. The ISA coordinators, as presented in Annex 3, shall be appointed by the parties for a period of four (4) years.

To help the coordinators, a bureau is created whose members are appointed jointly by the parties on the initiative of the coordinators for a period of four (4) years. Information about the members of the Bureau is presented in Annex 3. The ISA coordinators prepare

an annual budget and make a scientific report and annual financial report, the latter to be then transmitted to the parties upon approval by the ISA Board.

4.2. THE BOARD

The ISA Board consists of representatives of laboratories or groups enlisted in Annex 2, one representative for each laboratory.

The Board is headed by the ISA coordinators.

The Board monitors the progress of ISA activities, evaluates proposed international projects, determines the necessary budget and human resources in the ISA, and approves the annual financial report.

The coordinators advise the Board on all other issues related to the ISA.

The Board Meeting is held at least once a year, or at the initiative of the coordinators or of one third of its members. If necessary, provided there is a single consent of the Board, the meeting may be held by conference call.

In case a board member fails to participate in the meeting in person, he may grant a proxy to represent him at the meeting to another board member. One member of the Board can have no more than one proxy.

At the initiative of the coordinators, the Board may invite any expert to attend meetings on a confidential basis, if required by the aims and objectives of the ISA.

4.3. SCIENTIFIC COUNCIL

To coordinate the ISA scientific program, the parties have established the Scientific Council. The Scientific Council is composed of:

- One representative from RAS
- One representative from MSU
- One representative from RFBR
- One representative from CNRS
- One representative from CEA
- One representative from ENSTA

The Scientific Council of the ISA shall:

- evaluate the financial management of the ISA, the ISA scientific program worked out by the coordinators, as well as progress of activities, suggesting, if necessary, new directions;
- decide on the acceptance of new laboratories to ISA, upon prior consultations with the Board;
- make suggestions about changes to the present Agreement.

Meetings of the Scientific Council shall be held at least once every two years as initiated by one quarter of its members. The Scientific Council shall be chaired alternately by one of its members, who shall choose a secretary to keep minutes of the meetings. The minutes of the meeting, approved by the Scientific Council members, will be addressed to all parties to the ISA.

Decisions of the Scientific Council shall be taken by a qualified majority (3/4) vote of the Parties or their representatives. Each member of the Scientific Council may be represented by another member, provided that one member represents no more than one member absent from the meeting.

The ISA coordinators shall attend the meetings of the Scientific Council with advisory vote.

ARTICLE 5 - FINANCIAL PROVISIONS

At the beginning of each calendar year, each party shall inform the coordinators of the ISA on proposed amount of funds intended for ISA laboratories or groups to achieve the ISA objectives (Annex 4). Each Party shall independently manage allocated funds.

ARTICLE 6. INTELLECTUAL PROPERTY RIGHTS

6.1. Publications

The publications regarding the results of activities jointly conducted within the ISA framework should include reference to the institutions - the ISA founders. The publication of scientific results is carried out in accordance with the rules existing in the scientific community after the approval of the results by all relevant partners.

6.2. Information disclosure - Confidentiality

Each laboratory shall transfer to other participants to the ISA all the information necessary for the ISA activities. Information resulting from work performed beyond the ISA scope is the property of the Parties.

With regard to any information clearly identified as "confidential" and disclosed under this Agreement by one party to another party, the receiving party or parties shall be responsible within five (5) years from the date of disclosure not to disclose said information to third parties without the disclosing party, as well as not to disclose information that is private intellectual property of other party and is identified as "confidential".

All the above should not prevent from presenting theses to members of the dissertation jury in accordance with the rules and usual practices of each Party; in extreme cases, the jury members shall have the same strict obligations of confidentiality as those formulated above.

In case of confidential information, the ISA participants may provide this information as a confidential report for internal use only.

6.3. Ownership and use of the results

Each Party shall retain full ownership of any result, patented or not, received either beyond the scopes of the joint research conducted under this Agreement during the period preceding this Agreement or simultaneously with it, or independently. Other parties have no right to claim ownership for the above results.

The results, patented or not, obtained under this Agreement, are the common property of the Parties and the Parties agree on a contract basis to clarify the rules for distribution and use of the jointly obtained results.

Each Party shall enjoy the right of free and non-transferable use of the results jointly obtained under this Agreement, except for any activity of industrial or commercial nature.

ARTICLE 7 - MISCELLANEOUS

7.1. New membership

Any new laboratory or group of one of the parties or a new party may join the ISA by the decision of the Scientific Council.

The joining of new parties will require signing an additional agreement, which shall enter into force upon signature. The RAS and the CNRS have the right to sign the additional agreement on behalf of all ISA parties by a unanimous decision of the ISA Board.

The additional agreement in no way alters the provisions of this Agreement, except for Annexes 2 and 4. All parties are informed in writing of any entry of a new team to the ISA and receive a copy of the additional agreement on accession to the ISA.

7.2. Withdrawal

Withdrawal of any ISA laboratory or group from this Agreement is carried out at the request of the Party(s) upon prior notice to coordinators. Parties shall be notified 6 months before the intended withdrawal of the laboratory(s).

7.3. Responsibility

None of the Parties shall be responsible to other Parties or third parties regarding compliance, importance or completeness of information, as well as misuse or misunderstanding by the Party or any third party of information obtained under this Agreement.

Each Party is responsible, under the common law, for damages that their personnel may cause to third parties or personnel of other Parties in connection with this Agreement, including damages during use of equipment belonging to other parties and made available for said personnel.

Each Party shall retain responsibility (except for the heavy and deliberate damages incurred by other Party) to correct the damage caused to its private property under this Agreement.

7.4. Termination

This Agreement may be terminated for exceptional and justified reasons prior to the end of its duration as prescribed in Article 1 with prior notice sent six (6) months before the intended date of termination. In this case, the parties will endeavor to complete the already initiated joint activities.

The decision to terminate the Agreement shall be made by the parties upon receiving a conclusion from the coordinators and the Board.

In case of termination or withdrawal of one of the Parties from the ISA, provisions of Articles 6 and 7.3 remain valid.

7.5. Disputes

In case of difficulties in the interpretation or execution of this Agreement, the Parties shall seek to resolve all disputes through negotiations.

If the parties cannot settle the disputes in such a way, all disputes shall be resolved in accordance with the provisions of international law. Otherwise, the decision will be made in accordance with the provisions of the UN Commission on International Trade Law (UNCITRAL).

This Agreement is made in twenty-six (26) copies, including thirteen (13) copies in Russian and thirteen (13) copies in French, both texts being equally authentic. Annexes are written in English.

Executed in Moscow on December 21, 2009.

For the Russian Academy of Sciences Academician A.F. Andreev Vice-President	For the National Center for Scientific Research Professor A. MIGUS Director General
For the Russian Foundation for Basic Research Academician V.Ya. Panchenko Chairman of the Board	For the Atomic Energy Commission Professor B. Bigot General Administrator
For the Lomonosov Moscow State University Academician V.A. Sadovnichy Rector	For the Polytechnic School Professor, X. Michel Director General
For the Moscow Engineering Physics Institute Professor M.N. Strikhanov Rector	For the University of Paris-Sud Professor G. Couarraze President
For the Vavilov State Optical Institute Professor V.A. Tupikov Director	For the Higher National School of Advanced Technologies Professor Y. DEMAY Director
For the University of Bordeaux 1 Science and Technology Professor A. BOUDOU President	For Optics Institute Graduate School Professor J.L. Martin Director General
	For the Pierre and Marie Curie University Professor J.C. POMEROL President